Characterisation of groundwater and surface water interaction in the eThekwini Metropolitan District, KwaZulu-Natal, South Africa

by

Sphindile Mtshali

Submitted in fulfilment of the academic requirement for Master of Science

In Hydrogeology

Discipline of Geological Sciences

School of Agricultural, Earth and Environmental Sciences,

University of KwaZulu-Natal,

Durban, South Africa

August 2021

Supervisor: Professor Molla Demlie

ABSTRACT

The expansion of the city of Durban is proceeding rapidly due to rural to urban population migration and economic development. The urban development has been changing the mode of groundwater-surface water interactions, groundwater recharge, and water quality. These impacts of urbanization on groundwater-surface water interaction in the eThekwini Metropolitan District including the impact on groundwater-dependent ecosystems are not well understood. This study aims to contribute towards an improved understanding of groundwater-surface water interaction in the greater eThekwini district and understand the impact of urbanization thereof. The study was conducted by collecting primary data through a serious of field measurements and sampling of rivers, wetlands, springs and groundwater and complemented by secondary data obtained from Umgeni Water, eThekwini Municipality, the Groundwater Resource Information Projects (KZN-GRIP) database of the Department of Water and Sanitation (DWS), National Groundwater Archives (NGA) and consulting reports. The web-based hydrograph analysis tool (WHAT) was used to separate baseflow components from river discharge. The hydrochemical and environmental isotope data were analysed via diagnostic plots and multivariate statistical analyses. Kriging was used to interpolate groundwater level and generate groundwater flow directions. The results of data analyses indicate that groundwater in the study area occurs mainly in intergranular and fractured aquifers. Groundwater flows from west to east, towards the Indian Ocean, following the topographic gradient. The groundwater flow converges at rivers and wetlands, indicating that groundwater discharge contributes to the flow of streams and sustains wetlands in riparian areas. The groundwater contribution to stream flow is confirmed by baseflows separated from the river discharge. However, due to variation in hydraulic heads and aquifer properties, rivers also loose water to groundwater at some reaches, recharging the groundwater. Major ion hydrochemical data indicates that groundwater samples are dominated by Na-Cl-HCO_3 facies, while surface water samples are mainly Na-Mg-Ca-HCO_3 water type. Durov diagram of major ion hydrochemical data shows that the hydrochemical composition of groundwater in the area is influenced by dissolution and mixing processes. The Schoeller diagram plots the hydrochemical data of groundwater, rivers, springs, and wetlands parallel to each other indicating similar origin and appears to indicate groundwater and surface water interactions. The hydrochemistry of the study area is influenced by urban land uses, where an overall increase in the concentration of Na^+, Cl^- and Electrical Conductivity (EC) noted from suburban headwaters towards the developed urban areas in surface waters. The groundwater hydrochemistry also shows increased concentration of EC, Na^+, Cl^-, Si^{+4}, NO_3^- and SO_4^{2-}, likely related to recharge from domestic wastewater leakage, industrial waste leakage and related land uses. Groundwater - surface water interaction in the area means that there is a pollutant transfer from surface water to groundwater and vice versa. The stable environmental isotope signatures of water samples in the study area averages to −8.78 ‰ for Deuterium (D), and ranges from -4.18 ‰ to 2.22 ‰ for ^{18}O. Groundwater samples have relatively depleted heavy isotopic signal indicating direct recharge from precipitation. While surface water and some groundwater samples plots towards the heavy isotopic enriched signatures. The presence of groundwater samples with enriched heavy isotopic signal indicates that these samples may have undergone evaporation before infiltration and hence recharged from surface water sources. Urbanization in the greater Durban region has modified the natural landscape, by converting most of the natural land to impervious surfaces, reducing infiltration and consequently reducing groundwater recharge and shrinking of groundwater fed wetlands. These results are organized in the form of groundwater - surface water interaction conceptual model based on integrating the geology, hydrology, geomorphology, hydrogeology and climatic variables of the area.

Key words/Phrases: Environmental isotopes, Groundwater - surface water interaction, hydrochemistry, Land use changes, eThekwini, South Africa.

PREFACE

The research contained in this dissertation was completed by the candidate while based in the Discipline of Geological Sciences, School of Agricultural, Earth and Environmental Sciences in the College of Agriculture, Engineering and Science, University of KwaZulu-Natal, Westville Campus, South Africa. The research was financially supported by the eThekwini Municipality through the Durban Research Action Partnership and UKZN.

The contents of this work have not been submitted in any form to another university and, except where the work of others is acknowledged in the text, the results reported are due to investigations by the candidate.

Signed: [redacted] Date: 25 August 2021

DECLARATION -PLAGIARISM

I, Sphindile Mtshali declare that:

I. The research reported in this dissertation, except where otherwise indicated, is my original research.

II. This dissertation has not been submitted for any degree or examination at any other university.

III. This dissertation does not contain other persons' data, pictures, graphs or other information, unless specifically acknowledged as being sourced from other persons.

IV. This dissertation does not contain other persons' writing, unless specifically acknowledged as being sourced from other researchers. Where other sources have been quoted, then:

   a. Their words have been re-written, but the general information attributed to them has been referenced.

   b. Where their exact words have been used, then their writing has been placed in italics and inside quotation marks and referenced.

V. This dissertation does not contain text, graphics or tables copied and pasted from the internet, unless specifically acknowledged, and the source being detailed in the thesis and in the references section.

[redacted]

....

Signed: Sphindile Mtshali

Date. 25 August 2021

TABLE OF CONTENTS

TABLE OF FIGURES

LIST OF TABLES

LIST OF ACRONYMS

amsl: Above mean sea level

bmsl: Below mean sea level

C: Runoff Coefficient

Cl_p: Chloride concentration in precipitation (mg/l)

Cl_{gw}: Chloride concentration in groundwater (mg/l)

CMB: Chloride Mass Balance

DEM: Digital Elevation Model

DO: Dissolve Oxygen (mg/l)

DAEA & RD: Department of Agriculture, Environmental Affairs and Rural Development

DWS: Department of water Affairs

DWS: Department of Water and Sanitation

EC: Electrical Conductivity (µS/m)

Eh: Reduction Potential (mV)

EIA: Environmental Impact Assessment

EMA: eThekwini Municipality Area

ETo: Reference Crop Evapotranspiration

ETc: Crop evapotranspiration under standard condition (mm/day)

G: Soil heat flux

GMWL: Global Meteoric Water Line

GRIP: Groundwater Resource Information Project

I: Thermal Index

IC: Ion Chromatograph

ICP-MS: Inductive Coupled Plasma Mass Spectrometry

ITCZ: Inter-Tropical Convergence Zone

ISCW: Institute of Soil Climate and Weather

LMWL: Local Meteoric Water Line

LULC: land use, and land cover

NEMA: National Environmental Management

NGA: National Groundwater Archives

NMP: Natal Metamorphic Province

Nm: Latitude correlation factor

N: Actual duration of sunshine in a day (hourly)

Ma: Million years

ORP: Oxygen Reduction Potential (mV)

P: Precipitation (mm/a)

PET: Potential evapotranspiration

Q: Peak runoff rate (m^3/s)

Q: Yield (l/s or m^3/d)

Q: Monthly runoff (mm)

SAWS: South African Weather Services

SWSA-gw: Strategic water resources for groundwater

SWSA-sw: Strategic water resources for surface water

T: Air Temperature (^{O}C)

TDS: Total Dissolved Solids

UEP: Urban Environmental Profile

V-SMOW: Vienna Standard Mean Ocean Water

WHAT: WEB based Hydrograph Analysis Tool

ACKNOWLEDGEMENTS

I would first like to thank my Father in heaven for blessing me with this opportunity and giving me the strength, wisdom and perseverance to complete this Research Project.

To my Supervisor, Professor Molla Demlie, words cannot express the gratitude I have for all you did. Thank you for creating an environment that encouraged not only my academic growth but with my personal growth too. Thank you for challenging me and pushing me to my limits. Your guidance, patience, wisdom have taught me many valuable lessons that is engraved in my brain.

I express my sincerest gratitude to the Durban Research Action Partnership (DRAP) for affording me the opportunity to further my studies by proving financial funding.

I would like to express my gratitude towards different discipline within the eThekwini Municipality for providing relevant data and for consultations.

The South African Weather Services (SAWS) is acknowledged for providing the necessary climatic data.

To my parents, Mbekiseni Fakude, Zanele Mtshali and Kwanele khumalo, thank you for being the pillar of strength, thank you for the sacrifices that you had to make. Your inspiration, drive support and encouraging me to always remember the power that lies within me.

To my sisters Nokulunga Mtshali, Nomonde Radebe, Nomndeni Zikhali and Zinhle Mabusela for being my biggest cheerleaders.

To Nqobile Nkomo, Ntobeko Ngema, Thandolwethu Mteshana, I could not have asked for better friends and companions to walk this journey with.

Sphesihle Ndlovu, Moneri Modiba and Michael Jacobs are acknowledged for always willing to lend their time and knowledge

CHAPTER ONE: INTRODUCTION

1.1 Background and rationale

The increase in population since the 1960s has increased water supply demand for domestic, industrial and agricultural uses (United Nations, 1992). It is estimated that about 90% of population growth and urbanization will be concentrated in Africa and Asia, which would increase the world's urban population by 2.5 billion people by 2050 (United Nations, 2014). More than 60% of the continent in Africa is characterized by spatial and temporal variability of water resources availability as it is dominated by an arid climate (Braune and Xu, 2009). Urbanization in Africa is increasing rapidly, as more than 50% population resides in cities, town and urban settlement (Kometa et al., 2017). Future urbanization means that approximately more than 70% of the population will be living in cities by 2050 (Bello-Schünemann and Aucoin, 2016). The population growth increases the challenges of urban areas to become sustainable and healthy place to live. However, the African water vision envisages to have an Africa that is an equitable, sustainable and manages water resources for poverty alleviation, socio-economic development and regional cooperation (Economic Commission for Africa, 2000).

South Africa is one of the 20th water-scarce countries in the world, which is characterized by a semi-arid climate, constraining future social and economic development (Nel et al., 2011). The country receives an average annual rainfall of about 450 mm/a, which is below the world average of about 860 mm/a (Botai et al., 2016). The western provinces of South Africa are dominated by semi-arid condition resulting in low groundwater recharge rate. Surface water resources are mostly ephemeral, and most perennial rivers in these areas receive their recharge from humid up catchment areas. The eastern part of South Africa is characterized by a relatively wet and humid tropical climate. South Africa has been experiencing a decrease in the duration of the rainy season and prolonged periods of droughts (Phaduli, 2018). This overall reduction in the duration of rainy periods and increase in the length of dry periods along with increase in population, economic and agricultural development resulted a reduction of freshwater aquifer recharge, particularly in the province of KwaZulu-Natal (eThekwini Municipality, 2008). South Africa's water supply schemes are dependent on surface water sources due to its easy accessibility (DWA, 2010). However, surface water resources are excessively utilized, putting pressure on groundwater resources. According to the National Water Act of South Africa (Act 36 of 1998), water resources cannot be managed in isolation, as all surface water, groundwater and unconventional water resources are sourced from one entity. Groundwater management is vital as it supports groundwater-dependent ecosystems and agricultural development and water supply in rural communities and small towns. Therefore, groundwater resources must be valued and utilized sustainably to achieve water security and alleviate poverty issues (Braune and Xu, 2009).

Further urban development and climatic changes have impacted the hydrological cycle affecting both the quantity and quality of surface and groundwater resources (Changnon, 1976). Urbanization has transformed pervious surfaces into impervious surfaces. This has a negative impact on groundwater recharge as infiltration rate is decreased. However, engineered pipes that collect large amount storm drainage contribute to increased recharge through various form of leaks (Stephenson and Barta, 2005). This is also the case in the eThekwini Metropolitan District, especially in the urban and peri-urban areas.

Urbanization in the city of Durban is proceeding rapidly, as population migrate from rural to urban centres. The migration is promoted by social, industrial, economic development. These developments include changes in land use/ land cover such as deforestation, paving more surfaces to accommodate the busy transportation networks and continuous building to accommodate the growing population. Rechannelling, distorting and removal of some surface water bodies put strain on city’s ecology including groundwater resources and groundwater dependent ecosystems. These impacts of urbanization on groundwater-surface water interaction in the eThekwini Metropolitan District including the impact on groundwater-dependent ecosystems are not well understood. Therefore, understanding water resources, their interaction and conceptual understanding of the impacts of urbanization on the occurrence and circulation of water resources is very important to manage the resource in an urban setting. These urban and peri-urban water resources management help to ensure water security and healthy ecosystems that support development. This M.Sc. research envisages to better understand the elements of the hydrological cycle in the Durban (eThekwini) Metropolitan region through a thorough understanding of the hydrology, hydrogeology and hydrochemistry of both groundwater and surface water.

1.2 Statement of the research problem

Rapid urbanization and consequent infrastructure development are changing the mode of groundwater - surface water interaction and threatening groundwater dependent ecosystems. These impacts of urbanization on groundwater - surface water interaction in the eThekwini Metropolitan District including the impact on groundwater dependent ecosystems is not well understood.

1.3 Hypothesis

- Groundwater interacts with surface water within the greater eThekwini Metropolitan District where groundwater sustain wetlands, contributes to the baseflow of rivers along riparian areas and surface water in some areas replenish groundwater reservoirs.
- Urbanization has impacted the mode of groundwater – surface water interaction in the Metropolitan region.

1.4 Research aims and objectives

The main aim of this research is to understand groundwater-surface water interaction in the greater eThekwini region and understand the impact of urbanization thereof.

Specific Objectives

- To characterize groundwater-surface water interconnection in the greater eThekwini Metropolitan region.
- To identify and map areas characterised by groundwater dependent wetlands in the Metropolitan region.
- To develop a conceptual model for groundwater-surface water interaction in the greater eThekwini Metropolitan region.

CHAPTER TWO: DESCRIPTION OF THE STUDY AREA

2.1. Location of the study area

The eThekwini Metropolitan District is located in the east coast of South Africa in the Province of KwaZulu-Natal (Figure 2.1). The eThekwini Metropolitan District covers a total area of about 2555 km^2, with a population of 3.8 million people, making it the second most populated area in the country (eThekwini Municipality, 2018). This urban region consists of a diverse society that faces various challenges, including economic and environmental problems (eThekwini Municipality, 2018). Surface water serves as a primary source of water supply to the region. The fact that relatively better urban economic development means that people are forced to migrate from rural to urban areas, these uncontrolled rural to urban migration creates housing shortages creating informal settlements, invading unauthorized land and causing a negative impact on water resources and the general environment.

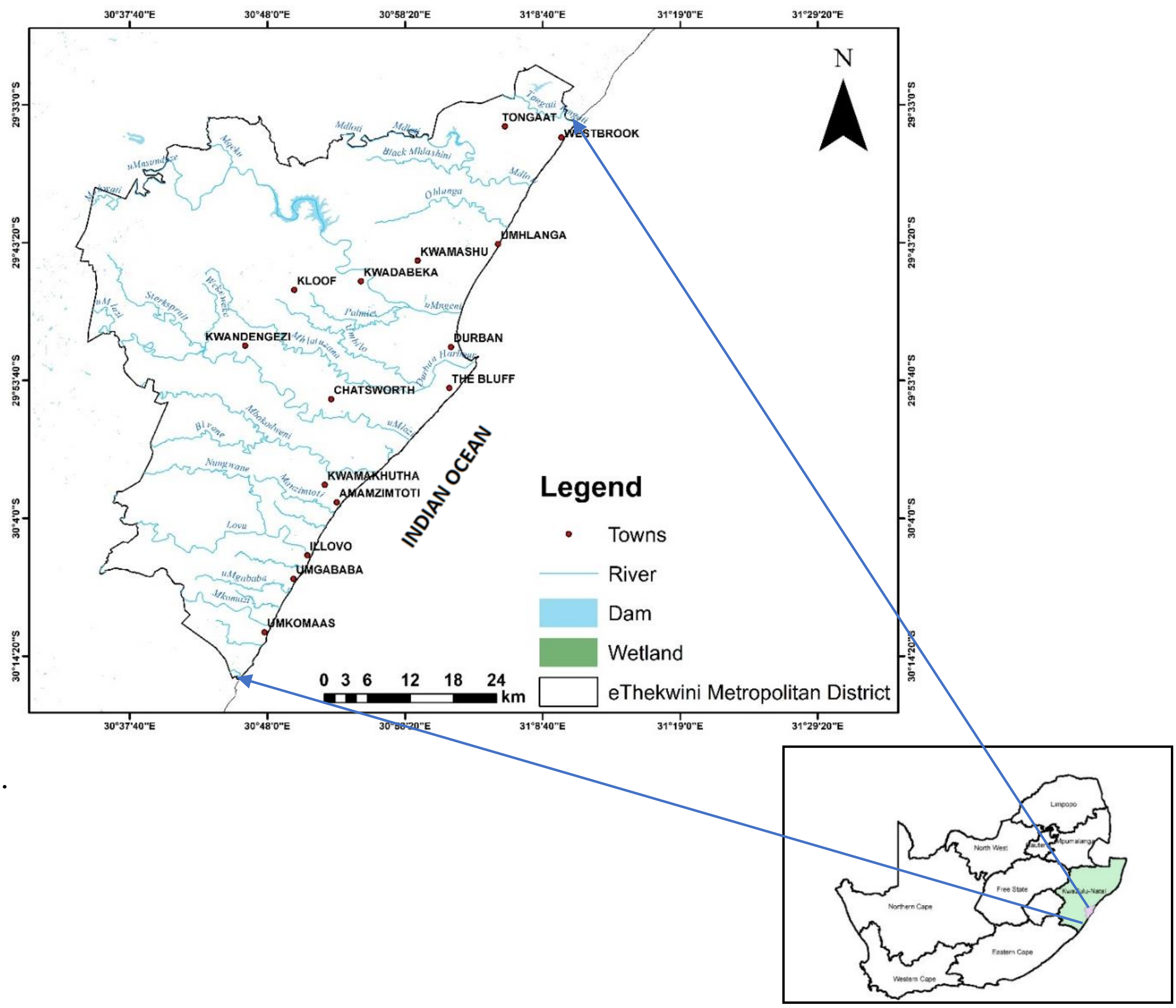

.

Figure 2. 1. Location map of the eThekwini Metropolitan District along with the drainage systems**.**

2.2. Climate, topography and drainage

The study area experiences a warm subtropical climate with hot, wet summers and dry, mild winters due to the warm Indian Ocean influences. The mean temperature varies seasonally with a minimum average of 16.79°C and a maximum average of 25.07°C (SAWS, 2019). The rainfall is driven by the coastal and ocean influence, it varies from summer to winter with an average rainfall of 996 mm/a. The wind direction is northeasterly in the morning and southeasterly in the evening, as the east coast experience warm and moist south-moving air (SAWS, 2019). The topography of the study area includes steep escarpment caused by weathering of ancient deposits in the west to a narrow and flat coastal plain in the east (eThekwini Municipality, 2008). The study area's elevation vary from 1200 m above mean sea leve (amsl) in the west to narrow flat plain along the coast (Figure 2.2).

The study area is drained by 12 main rivers, covering a catchment area of about 4000 km^2 and 16 estuaries (Plan, 2019). The perennial rivers that drain the study area from north to south are: uTongati, uMdloti, ohlanga, uMngeni, Palmiet, uMbilo, Sterkspruit, uMlazi, Mbokodweni, Nungwane, Lovu and uMkomazi (Figure 2.2). The study area has active private and public owned wetlands. The privately-owned wetlands include Mount Moreland Wetland System, Plantation wetland, Harrison Flats N3 Wetland park wetland system and infracombe wetland system. The spatial distribution of wetlands in the eThekwini Metropolitan District varies from dense to sparse due to development.

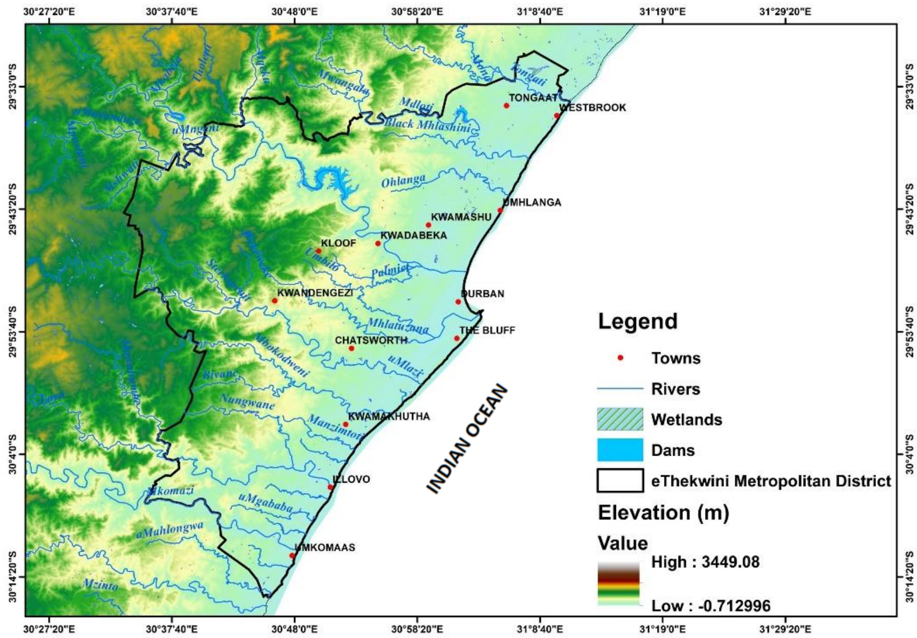

Figure 2. 2. Digital elevation model and Drainage map of the eThekwini Metropolitan District.

2.3. Soil, land use and land cover

Soil characteristics are primarily influenced by parent material, i.e., the underlying geology. According to King (1997), geomorphology, physiography, vegetation, and climate affect the soil type. Soil thickness, nature of soil cover, amount of soil moisture taken up by vegetation have an important influence on the amount of groundwater recharge (Bell & Maud, 2000). In general, the deeper the soil cover the less rainfall penetrates through the soil column, and the more clayey the soil, the more impermeable it becomes (Bell & Maud, 2000).

The study area is dominated by leptosols which are known as rocky soils that are found in hard rock and erosional surfaces that has kept pace with soil formation in very shallow areas (Figure 2.3). They are limited at shallow depths of less than 10 cm to 50 cm of the soil surface (King, 1997).

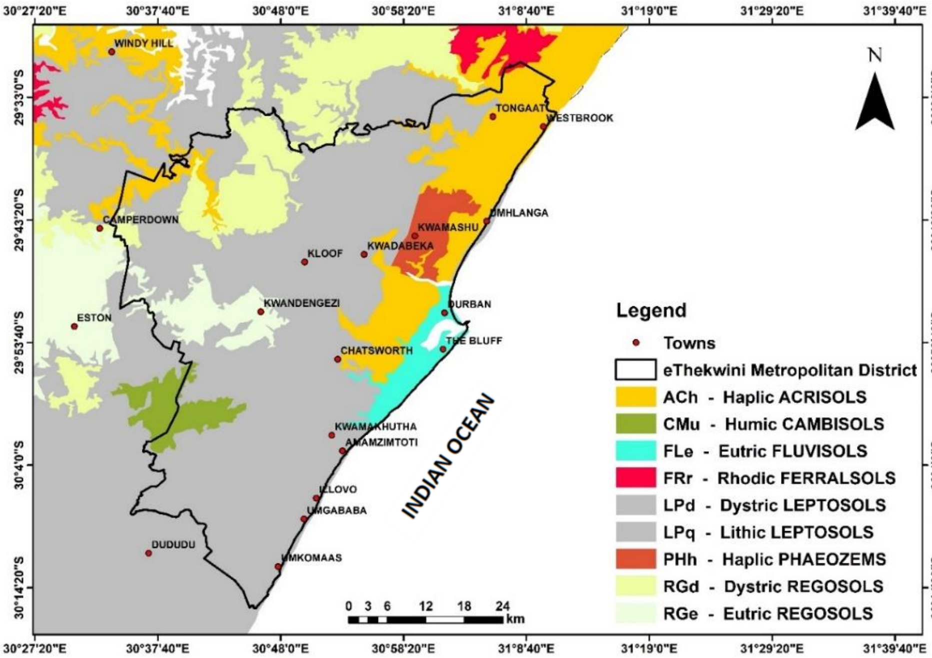

Figure 2. 3. Soil type distribution map of the eThekwini Metropolitan District (adapted from ISCW, 2014).

The eThekwini Metropolitan Area (EMA) is made up of Durban, which is the third largest city in South Africa and adjacent smaller towns (eThekwini Municipality, 2013). The EMA's central urban core is the most densely populated area accounting for about 35% of human population in the Durban city (Otunga et al., 2014). However, Durban accomodates 33% of the province (eThekwini Municipality, 2013). The population spread is concentrated in the central region, which is the most urbanized area (Figure 2.4). The Metropolitan region is dominated by residential, commercial and industrial use activities (Figure 2.4) (eThekwini Municipality, 2017). The main economic activities include light and substantial industrial activities, agricultural, commercial and tourism.

The eThekwini Municipality covers 68% of rural areas, with a group of dense settlement. Rural areas in the eThekwini Municipality is undergoing rapid change as the existing rural settlement are sprawling and transforming to peri-urban settlements (Plan, 2019). The warm and humid climate with a relatively high rainfall has created good condition for dense vegetation growth in the region. The Landsat images show built-up area's size increase with increased urbanization, transforming terrestrial habitat significantly. Bio-physical transformation increase pressure on urban green space resulting in changing land use and land cover types (Otunga et al., 2014). Natural vegetation is mostly replaced by sugarcane-farming, industries and commercial forestry (Gillson and Suthers, 2012; Otunga et al., 2014). Furthermore, invasive alien plants species increased by 14% per annum, driven by development (Gillson and Suthers, 2012).

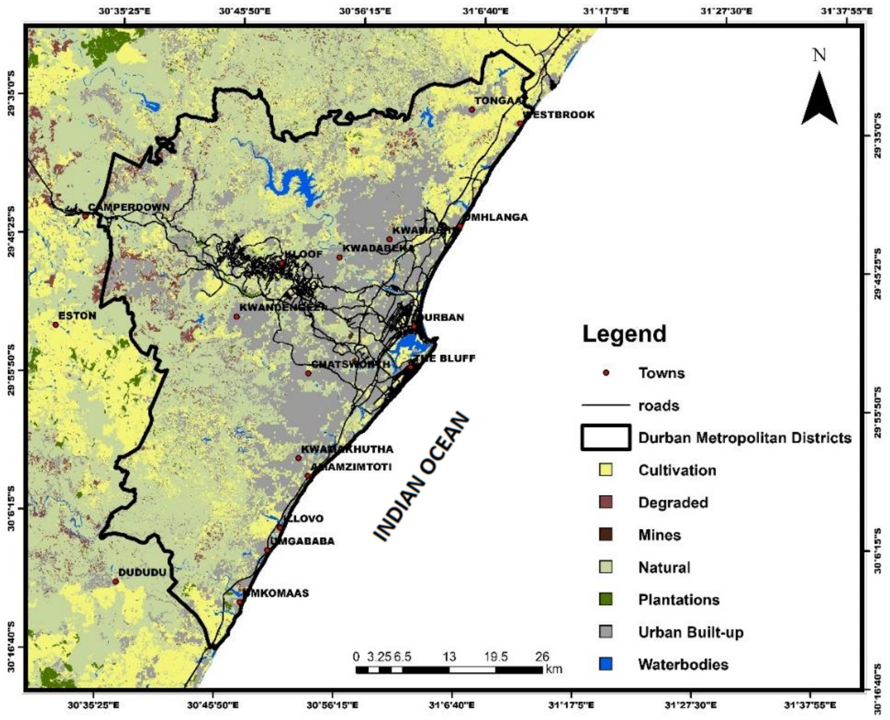

Figure 2. 4. Land cover and land use map of the eThekwini Metropolitan District (modified from KZN-PPC, 2016).

2.4. Geological Setting

2.4.1 Regional Geology

The geological history of the eThekwini Metropolitan region extends back to approximately 1200 Million years (Ma). The late Proterozoic crystalline basement of the Natal Metamorphic Province (NMP) comprising of granite-gneisses is unconformably overlain by the Phanerozoic sandstone-dominated siltstones and subordinate conglomerates of the Natal Group (Marshall, 2006). The Natal Group is in turn unconformably overlain by the late phanerozoic to Mesozoic clastic sedimentary rocks of the Karoo Supergroup, namely, the Dwyka Group and Ecca Group. The Ecca Group in the study area comprises of the argillaceous Pietermaritzburg Formation and the arenaceous-argillaceous Vryheid Formation. These rocks are heavily intruded by Jurassic dolerite dykes and sills, which is related to igneous activities of the rifting and break-up of Gondwana. The Cenozoic Maputaland Group succession includes a variety of aeolian, lacustrine, littoral and fluvial deposits. These rocks form the youngest units completing the geological sequence of the Durban region (Clarke, 2008).

2.4.2. Geology of the Thekwini Metropolitan District

Natal Metarmophic Province (NMP)

The NMP forms the granite basement unit in the study area (Figure 2.5). The NMP comprises three distinct tectonostratigraphic terranes, namely, from north to south, the Tugela, Mzumbe and Margate terranes (Matthews, 1972). Each terrane differs in the type of metarmophic grade, resulting into different rock types. The tectonostratigraphic terrane present in the study area is the Mzumbe Terrane bounded by the Lilani-Matigulu shear zone and Mellville shear zone in the north and south, respectively (Clarke, 2008). This terrane is made up of high-grade supracrustal gneisses of the Mzimkulu Group intruded by a distinctive suite of pre, syn- and late tectonic granite suites. The Mzumbe Terrane is also characterized in the south by several suites of sheet-like, gneissic granites and granitoids (Thomas, 1988). These include Mkomazi, Mzimlilo and Mahlonga Suites (Clarke, 2008). The older gneisses of the Mzumbe terrane collectively known as Mapumulo Group comprises of amphibolite grade gneiss of the basement complex and instrusive granitoids suits. The Mapumulo Group is over 1.1 Ba old comprises of two units, Quha and Ndonyane Formation occuring as a relatively thin belt and discountinuous septa between the later granitoid intrusion (Bell and Maud, 2000; Cornell et al., 1996).

Natal Group

The early Palaeozoic Natal Group in the study area unconformably overlies the basement complex (Bell and Maud, 2000). The Natal Group comprises reddish-brown arenaceous rocks with interbedded mudrock, medium to coarse-grained arkosic sandstones, siltstones and conglomerate (Bell and Maud, 2000; Marshall, 2006). Most of the sediments of the Natal Group are fluviatile, and they were deposited by an extensive braided river system with a northeast trending lowland trough or rift basin (Marshall, 1994; Bell and Lindsay, 1999; Liu, 2000; Shone and Booth, 2005). The Natal Group is divided into two Formations which are the Durban and Marianhill Formations (Marshall, 2006). The Durban Formation within the study area is further divided into the kranskloof Member which consists mainly of silicified quartz arenite and subarkose, with interbedded mudrock attaining a thickness of 51 m. The Situndu Member overlies the kranskloof Member conformably and consists of coarse arkosic sandstone with a maximum thickness of 84 m. The Dassenhoek Member with resistant silicified quartz arenite unit of 42 m thickness rest conformably on the Situndu Member (Marshall, 2006). The Marianhill Formation within the study area is found in Westville Member constisting of matrix-supported polymict conglomerate with sparse, well-rounded clasts of quartz, chert, jasper and quartziter up to 5 cm in diameter and a maximum thickness of 30 m.

Karoo Supergroup

The lowermost lithostratigraphic unit of the Karoo Supergroup is the Dwyka Group which is unconformably overlain by the Ecca Group with a gradational contact (Africa, 2017). The Ecca Group comprises 16 Formations that reflects lateral facies changes that characterize the succession. Among these, the Pietermaritzburg and Vryheid Formations occur in the study area. The Ecca Group is some 350 m thick in the Durban area, consisting of shale and mudstone (Bell and Maud, 2000). The Vryheid Formation conformably overlies the Pietermaritzburg Formation, which is made up of medium to coarse-grained sandstone, grey micaceous shale and coal seams (Botha et al., 1998). The Pietermaritzburg Formation generally overlies the Dwyka Group with a sharp contact. The Dwyka Group rocks consist of dark colored, well-laminated shales and mudstone, with interlayers of fine-grained sandstone (King, 2002). The Dwyka Group forms the basal rocks of the Karoo Supergroup.

Maputaland Group

The Quaternary coastal deposits are the youngest within geological units of the study area (Figure 2.5). It is characterized mainly by the Bluff, Isipingo, Berea and Harbour Beds Formations (Botha *et al*., 2003). The Pleistocene Berea Formation is the weathered product of the Bluff Formation and as a result of marine transgression. The late Pleistocene Berea Formation extends up to 100 m in thickness, occupies the upper and inner part of the Durban Bluff, as well as the Berea Ridge (Bell and Maud, 2000). The Berea Ridge runs parallel to the coast immediately to the west of the central city and harbour area (Bell and Maud, 2000). This late to middle Pleistocene to Holocene Formation incorporates basal aeolianites truncated locally by the late interglacial age calcified beach and dune deposits at 4-5 m above mean sea level (Ramsay and Cooper, 2002). The Isipingo Formation replaces the poorly constrained Bluff Formation and can be subdivided into genetically significant shallow marine, beach and various dune lithological units recording sea-level changes. These cemented deposits are readily distinguished from the non-calcareous Kosi Bay Formation sands in areas where they occur in proximity (Maud, 1986). The Bluff Formation also is late Pleistocene in age, and it extends to approximately 100 m below present sea level and rests unconformably on siltstone of the St Lucia Formation of the Zululand Group (Bell and Maud, 2000). The Durban Harbour Beds comprises of unconsolidated sediments ranging in texture from sands to silty clays, resting unconformably on siltstones of the St. Lucia Formation.

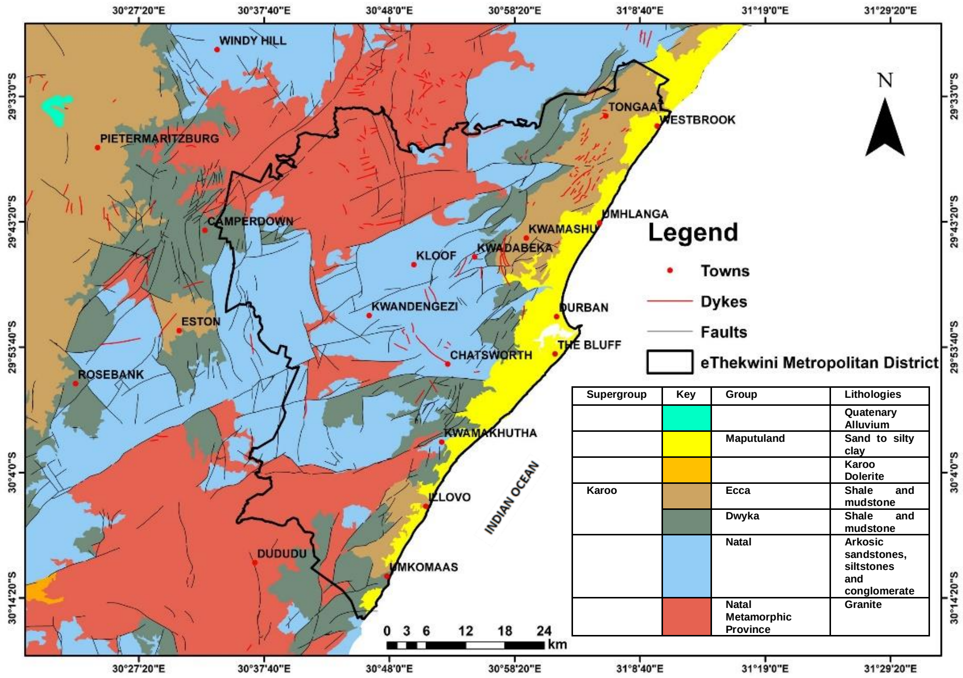

Figure 2. 5. Geological Map of the eThekwini Metropolitan District (modified from the Council for Geosciences, 1988a).

Table 2.1. Table of Lithostratigraphic succession in the eThekwini Metropolitan District (modified from Johnson et al., 2006).

Era	**Supergroup**	**Group**	**Formation**	**Lithology**
Quaternary		Maputuland		Stratified sand to clayey alluvium
Jurassic				Fine-grained(porphyritic) to coarse-grained(gabbroic) dolerite
Permian	Karoo	Ecca	Vryheid	Inter-laminated or interbedded siltstone and coarse to medium grained sandstone.
			Pietermaritzburg	Massive to laminated carboniferous siltstone and shale,
Carboniferous		Dwyka	Elandsvlei	Tillite and diamactite
Ordovician		Natal	Marianhill	Clast supported Conglomerate and arkosic sandstone
			Durban	Flat or cross bedded coarse grained arkosic sandstone and granulestone
Namaquan		Natal Metamorphic Province	Ndonyane	Quartz-felspar gneiss
			Quha	Biotite gneiss, biotite-hornblende gneiss and amphibolite.

2.5. Hydrogeological Setting

Groundwater in the Greater eThekwini region occurs in primary and secondary aquifers that are associated with Intergranular and fractured formations, respectively (Figure 2.6). Primary aquifers contain groundwater in void spaces between particles, while the secondary aquifer contains water in discontinuities such as joints, fractures and bedding planes. Eight hydro-geologically relevant lithologies can be identified in the greater Durban region. These include: the dune, alluvial and estruarine deposits, sandstones, dolerites, tillite, granite-gneiss and mudstone-shale. The hydro-stratigraphic units are divided into primary aquifers (dune, alluvial, estuarine deposits) and secondary aquifers (sandstone, dolerite, tillite, granite-gneiss, and mudstone/shale) due to their fractured and weathered nature (Bell and Maud, 2000). The secondary aquifers are classified into fractured and intergranular and fractured aquifers (King, 2002). Faulting and fracturing in the region contribute significantly to groundwater storage, circulation, and overall groundwater resource potential in otherwise massive rocks (Bell and Maud, 2000).

Generally, groundwater rest-levels in boreholes of the study area tend to be less than 25 m below the ground surface and rarely exceed 75 m. However, in the low-lying areas, the groundwater rest-level is much nearer to the ground surface, especially in the alluvial and estuarine deposits along the coast. Usually, the deeper groundwater rest-levels are found in hard rock aquifers of the granite-gneisses of the Basement Complex. Groundwater exploitation takes place in secondary aquifers, while it is limited in primary aquifers.

According to Bell and Maud (2000), the Department of Water Affairs and Forestry recognises four categories of borehole yields, namely:

- High borehole yields over 3 l/s that support medium to large water supply scheme.
- Moderate borehole yields that range between 0.5 and 2 l/s and supplies villages, clinics and schools with reticulation schemes.
- Low borehole yield ranging between 0.1 and 0.5 l/s, which can supply small communities and domestic stock watering with a hand pump or wind pump of a non-reticulating water supply scheme (Bell and Maud, 2000).
- Meagre borehole yields that are less than 0.1 l/s and only provides a limited supply.

Primary aquifers in the Durban area consist of unconsolidated sediments of the alluvial and estuarine deposits locally known as Harbour Beds and the Bluff and Berea Formations (Bell and Maud, 2000). The average hydraulic conductivity of these intergranular aquifers is about 5 m/day with a storativity value of approximately 0.18 and borehole yield of 5 l/s (King, 2002). Depth to groundwater is typically low, between 2 m and 7 m below ground level (bgl) and sometimes artesian. The sedimentary depositional environment, proximity to the coast and industrial activity all influence groundwater quality in the area. Sodium-chloride type of water is commonly present in the primary aquifers with average electrical conductivity (EC) of 100 mS/m (King, 2002).

The Natal Group and Dwyka Group are fractured aquifers in the study area where groundwater is stored and transmitted in interconnected faults, joints and bedding planes (Bell and Maud, 2000). The Natal Group represent productive secondary aquifer in the area (Bell and Maud, 2000). The high quartz content in the Natal Group results in the brittle behaviour leading to the formation of well-developed interconnected joints and faults (Marshall, 2006). Hence, the aquifer has relatively high yielding boreholes, hydraulic conductivity ranging from 0.4 to 7.7 m/day and estimated storativity of 0.005 (King, 2002). The groundwater quality is good and alkali-chloride to mixed type groundwater are commonly encountered.

On the other hand, due to massive and structureless nature and its muddy matrix, the Dwyka Group is the poorest secondary groundwater aquifer in the greater Durban region (Bell and Maud, 2000). However, reasonable yield is sometimes obtained from a borehole drilled in favourable locations, particularly near the coast on faults and major joints (Bell and Maud, 2000). In areas where the diamictite has undergone large-scale fracturing, it provides boreholes yields of up to 10 l/s locally, but the average expected yield is 0.13 l/s (Bell and Maud, 2000). Its storativity is about 0.0001 and its hydraulic conductivity ranges between 0.8 and 1.2 m/day (King, 2002).

The groundwater occurrence in the Ecca Group is within intergranular and fractured aquifers that have a yield range between 0.5 and 2.0 l/s (DWAF, 1998). Boreholes that intersect fractured rocks produce a yield of 0.9 l/s in argillaceous rocks and 1.2 l/s for boreholes in the Vryheid Formation aquifer. The hydraulic conductivity ranges from 0.05 m/day in unfractured rocks to 0.5 m/day in fractured rocks. The transmissivity of the aquifers in the area range between 0.05 and 0.5 m^2/day, and the storativity vary between 0.0001 and 0.001 (DWAF, 1998). The average porosity of shale in the Pietermaritzburg Formation is 2-11 % (Woodford and Chevallier, 2002). Groundwater occurrence in the Pietermaritzburg Formation is associated with the intrusion of dolerites dykes which cause fracturing and weathering of the secondary aquifer (Bell and Maud, 2000).

The NMP rocks are classified as an intergranular and fractured aquifer. Boreholes that intersect the interconnected fractures have average yields of about 0.4 l/s (King, 2002). The occurrence of groundwater in the crystalline rocks of the NMP is associated with fracturing, near-surface weathering processes and dolerite intrusions (King, 2002). The expected borehole yields within the weathered zones are typically between 0.1 and 0.4 l/s (King, 2002).

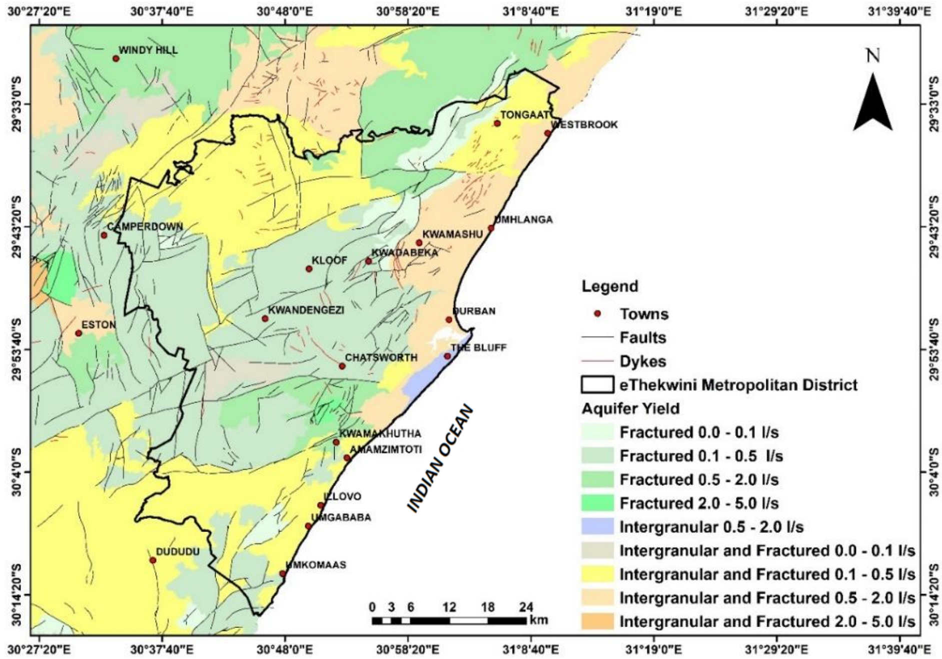

Figure 2. 6. Hydrogeological Map of the eThekwini Metropolitan District for different aquifer type (modified from DWAF, 1998).

CHAPTER THREE: LITERATURE REVIEW

3.1 Elements of hydrological cycle and their interconnection

The hydrological processes of surface water bodies are sustained by geological settings, climate, vegetation and landscape. The interaction is vital for both physical and chemical fluxes in the hydrologic cycle (Anwari, 2018). The transition between groundwater and surface water is critical as it governs the exchange of water, nutrients and filters pollutants (Kalbus et al., 2006; Buss et al., 2009). The main developed human population clusters around surface water resources along the rivers, lakes, and coastal plain. Which in turn, impact the hydrologic cycle through changes in land-use, climatic, overuse of water, redirection of watercourses and water quality. The understanding of groundwater and surface interaction improves the management of water resources and provide insight into both natural dynamics and global change.

3.2 The impact of land use change

Land use is the purposes or activities in which the land is utilized including agriculture, grazing and forest. While land cover is a physical characteristic that occurs on the Earth surface such as vegetation, water bodies, soil and artificial surfaces (Kercival, 2015; Anwari, 2018). Political, technological, economic, environmental and cultural practices drive land use and land cover (LULC) changes. However, urbanization is the key contributing factor responsible for LULC changes (Jansen and Di Gregorio, 2003; Kercival, 2015). These changes of replacing natural land with impervious surfaces affect habitat, ecosystem and water quality (Jabareen, 2006). These impervious surfaces change the infiltration, evapotranspiration and runoff characteristics of the area (Ried et al., 2009). Thus, land use change may result in a rise of the water table, increase land and river salinization, change flood frequency and flow regime, which in turn affect the hydrological balance between surface water and groundwater flow. Similarly, the province of KwaZulu-Natal, particularly the eThekwini Metropolitan region has been experiencing urban growth and rapid development. These improved infrastructure, better social and economic services have encouraged rural to urban migration, creating a large swath of informal settlements in the peri-urban and urban areas of the region.

3.3 Impact of urbanization

Many Metropolitan regions including the eThekwini Municipality have been experiencing high rates of in-migration from rural areas and small-town. The net in-migration results in urbanization and population increase that will make planning and projection of the need for residence requirements including housing and services (eThekwini Municipality, 2017). It is expected that the water demand will outstrip the supply due to the continual increase in population and industrial growth, placing more stress on the water quality and the ecosystem.

The urban water cycle is modified by the presence of engineered water systems, where water is transferred via pipe networks and artificial routing into subsurface drainage networks (Mcgrane, 2016). The urban landscape has an impact on meteorological and hydrological dynamics. As a result, surface runoff increases where it is collected by artificial drains due to increased impervious surfaces. These impervious surfaces change the dynamics of natural water infiltration to the subsurface. Impervious surfaces also change the magnitude, pathway and timing of runoff resulting in a contrasting impact on baseflow behaviour, effectively increasing the overall runoff volume (Arnold and Gibbons, 1996; Walsh, 2005; Mcgrane, 2016). The construction of buildings and roads require a change in gradient by removing soil and vegetation cover in elevated areas. The removal of these features simplifies drainage structure for water transfer in urban surfaces. However, the gentle slope alters catchment drainage, affecting how rainfall is captured, stored and released in the hydrological system. This has a negative impact in the aquatic ecosystem as the degradation of the urban streams through geomorphological and chemical changes.

Additionally, climate change impact in Metropolitan regions causes several challenges such as increased temperature, unusual floods and drought conditions. For example, temperatures are predicted to rise between 1.5 ºC and 2 ºC by 2065 and between 3.0 ºC to 5.0 ºC by 2100 in the eThekwini Municipality (Plan, 2017). The annual rainfall changes are projected to increase by 2065. These climatic changes will result in extreme rainfall events and streamflow intensity across the municipality (Plan, 2017). These seasonal and inter-annual variations in precipitation, surface run-off, interflow, groundwater flow, pumped inflows and outflows have a substantial effect on river discharge and subsequently on the concentration of pollutants in river water (Vega et al., 1998). Climatic changes such as increase in temperature and decrease in precipitation pattern reduce groundwater recharge and groundwater level in urban setting (Kaandorp et al., 2018).

3.4 Groundwater - surface water interactions

Proper understanding of the interaction between groundwater and surface water is vital for the sustainable management of water resources in semi-arid areas (Guggenmos et al., 2011). The interaction between groundwater and surface water describes the exchange between two water bodies. Surface water bodies includes lakes, rivers, stream and wetlands. While groundwater occurs in subsurface geological formations called aquifers. Generally, groundwater is recharged from upstream areas and then flows through aquifers controlled by the prevailing hydraulic gradient. It moves downstream where it discharges into rivers and ocean as baseflow. The exchange of groundwater and surface water is complex and dynamic (McLachlan *et al.*, 2017). Geomorphological features, underlying geology, depth to groundwater and position of the surface water body in relation to the groundwater flow system and climatic settings influence groundwater-surface water exchange (Elliot and Brooks, 1997; Boone et al., 2009). These two water resources cannot be isolated as they are closely related, making it one hydrologic system (Mazvimavi, 2017). Identifying locations and understanding mechanisms of groundwater-surface water interaction is vital for effective environmental management (Dahm et al., 1998).

The interaction between groundwater and surface water proceeds in two ways: 1) groundwater flows into the lake or stream forming a gaining stream; 2) stream water infiltrates through the sediments into the groundwater, effectively recharging it and forming a losing stream (Kalbus *et al.*, 2006). This interaction has an important implication for water quality and quantity management, including ecological health (McLachlan *et al.*, 2017). The interaction may occur either way, including groundwater feeding streams and wetlands when groundwater level is above the surface water level and when stream losses water to groundwater usually during floods when stream stage is above groundwater levels. It is noted that groundwater sustains surface water especially during drought seasons in the form of baseflow or low flow of rivers.

Heterogeneity in geology, hydrological and geochemical components of groundwater-surface water interface, make it difficult to characterise with direct observation. The inability to characterise the subsurface heterogeneity exacerbates the upscaling problem and leads to significant uncertainties in data interpretation (Sophocleous, 2002). Nevertheless, understanding the basic principles of groundwater - surface water interaction processes is crucial in the hydrological cycle and for effective water resources management (Winter, 1995). The interactions can be studied by monitoring groundwater levels, hydrochemistry and environmental isotopes of both groundwater and surface water. Baseflow will give a clue to how much groundwater feeds surface waters. Based on understanding these components, a hydrological model can be developed which will show how groundwater and surface water interacts in urban areas.

3.4.1 Main drivers of groundwater - surface water interactions

Groundwater recharge is influenced by many factors which include the type and rate of precipitation, saturation level and the infiltration capacity of the soil, the underlying geology of the area, the density of vegetation cover, depth from the surface to water table and the topography of the landscape (Fetter, 2014). Changes that take place in precipitation affect recharge to aquifers and possibly nearby surface water that rely on groundwater discharge (Ford, 2016). Groundwater level decreases when precipitation decreases which then affect surface water that receives water from groundwater or surface water lose water back to the subsurface to make up the lost recharge (Ponce, 1989).

The movement of groundwater is determined by various characteristics of the aquifer medium including hydraulic head, hydraulic conductivity, transmissivity and porosity (Fetter, 2014). The hydraulic heads are influenced by topography, the depth to groundwater level and the local pumping regime (Rukundo and Doğan, 2019). Groundwater and surface water are interconnected, the rise in water table above the ground result in water discharging into the surface becoming surface water. Conversely, when water tables drop, surface water recharges the groundwater.

The mode of interaction between groundwater and surface water takes place in different forms. This interaction depends on the physiographic and climatic setting of the landscape. Small streams receive groundwater inflow primarily from local flow systems, which usually have a limited extent and are highly variables seasonally. The stream in a wet climate might receive groundwater inflow. But streams in an identical physiographic setting in an arid climate might lose water to groundwater. The type of rock type underlying soils may be highly weathered or fractured and may transmit a significant additional amount of flow through the subsurface. During intense storms, most water reaches the stream very rapidly by partially saturating and flowing through the highly conductive soil. Whereas in the lower part of hillslopes, the water table rises to the land surface during storms, resulting in overland flow. Surface runoff from precipitation falling on the landscape accumulates in the depression, results in the presence of lakes and wetlands. The groundwater contribution keeps the stream flowing between precipitation events. The movement of water between groundwater and surface water system leads to the mixing of their water qualities.

3.4.2 Groundwater - stream interaction

Groundwater plays a vital role in sustaining perennial rivers through groundwater discharge into rivers, making it the source of all rivers and maintain the flow during the dry season (Le Maitre et al., 2018). However, when the groundwater level is close to the surface, it is prone to evapotranspiration, especially in riparian zones (Tanner and Hughes, 2015). Hydraulic gradient, topography, and geological structures influence groundwater flow to streams (Fan et al., 2017). According to Ried et al. (2009), groundwater is commonly hydraulically connected to surface water. The interaction takes place in all types of landscapes and geological setting. Gaining and losing streams are easily detected by the type of interaction they have with groundwater. The interaction occurs in three primary ways (Winter et al., 1998). These are; 1) Stream gaining water from an inflow of groundwater through the stream bed; 2) Stream losing water to groundwater by infiltration through the streambed; 3) The stream that does both, gaining in some part and losing in others depending on periodic changes in relative stream and groundwater levels.

Gaining streams

The streams gain water when water moves from an aquifer to a stream controlled by the prevailing hydraulic head difference between the surface water and groundwater levels (Figure 3.1). This takes place when the hydraulic head in the adjacent aquifer is higher than the height of the stream surface, thereby the stream receiving water via seepage from the connected aquifer (Winter et al., 1998). This groundwater discharges in the form of the Baseflow of gaining streams, which helps to sustain streamflow between rainfall events (Winter et al., 1998).

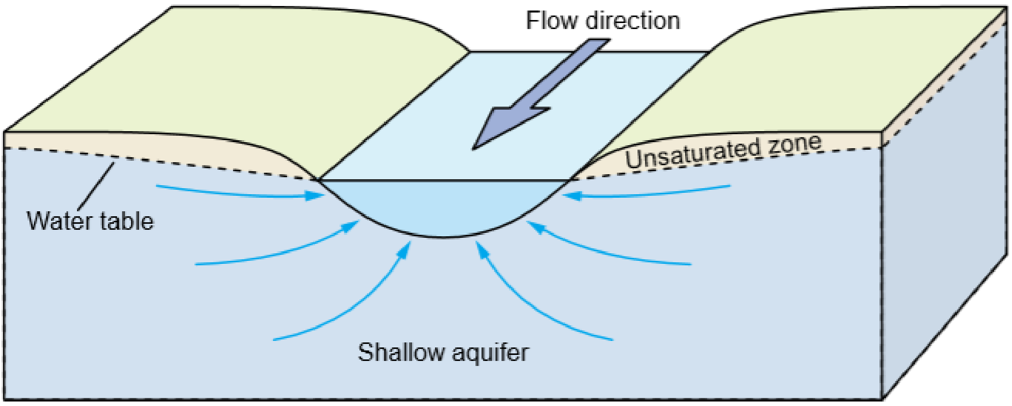

Figure 3. 1. Schematic representation of stream-aquifer interaction for a gaining stream with (adapted Winter et al., 1998).

Loosing streams

Losing streams occur when water filtrates from the stream into aquifers. According to Winter et al. (1998), this groundwater recharge from streams takes place in two ways:

a) When the stream is directly connected to the aquifer via a saturated zone and when the adjacent water table height of the aquifer somewhere between the stream surface and the base of the stream bed (Figure 3.2). The stream contributes some of its flow to the aquifer via seepage as the hydraulic head in the adjacent aquifer is lower than the height of the stream stage.

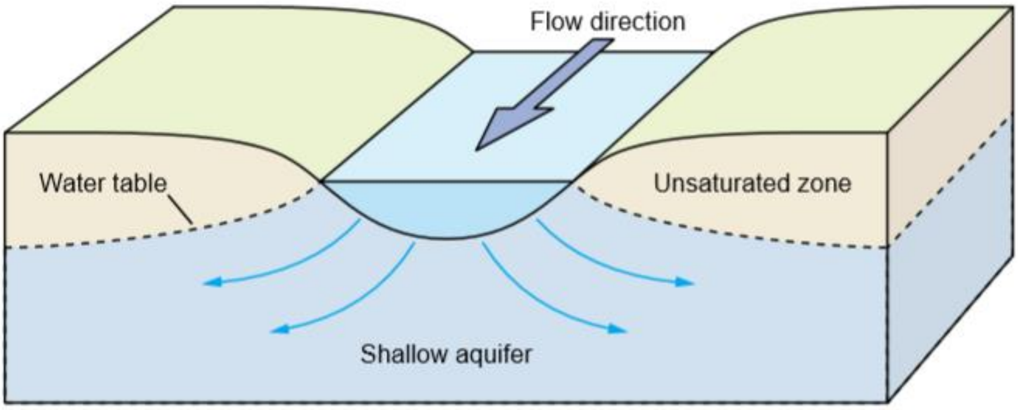

Figure 3. 2. Schematic representation of stream-aquifer interaction for a losing stream with saturated connection (adapted from Winter et al., 1998).

b) The stream is connected to the aquifer via an unsaturated zone and the hydraulic head in the aquifer is below the base of the stream bed (Figure 3.3) (Winter et al., 1998). The table forms a mound at the bottom of the unsaturated zone below the stream. The mound size depends on the rate of stream loss through the unsaturated zone and the hydraulic properties of the aquifer.

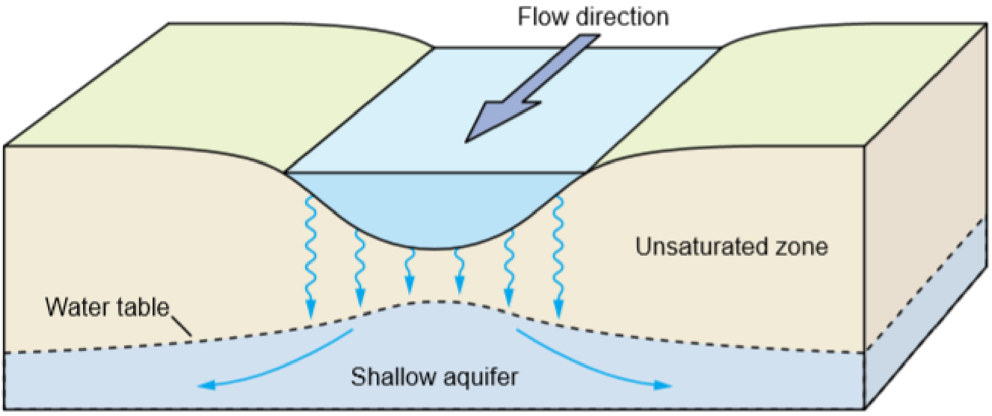

Figure 3. 3. Schematic representation of stream-aquifer interaction for a losing stream with saturated connection (adapted from Winter et al., 1998).

3.4.2.1 Surface runoff estimation and river flow hydrograph separation

In many catchments, groundwater and surface water are interconnected systems and as such they should be regarded as a single water resource (Farvolden, 1963; Prince, 2011). Basin characteristics that influence the interaction include climate, topography, land cover, soil, and geology (Farvolden, 1963; Prince, 2011). The climatic factors such as temperature and precipitation influence baseflow by altering rates of evapotranspiration, infiltration, and recharge in the basin (Winograd et al., 1998; Brutsaert, 2005; Tague and Grant, 2009). Topography controls how water moves across the surface and in the subsurface, thereby influencing infiltration, flow processes, and rate of water transmission. Whereas, the soil and geology of the catchment influence the rate of infiltration, groundwater recharge, hydraulic conductivity (Farvolden, 1963; Prince, 2011; Price et al., 2011; Pirastru and Niedda, 2013). Water balance quantifies all the input and output parameters within the system by using directly measured and calculated parameters. These include precipitation, recharge, evaporation, evapotranspiration, runoff, baseflow, the rate of abstraction and the change in storage (Fetter, 2014).

Surface runoff is a crucial component of the water balance. Whereby excess precipitation flows overland as surface water along streams, rivers and impervious surfaces opposed to being absorbed into the subsurface to be added to the groundwater storage (Khosravi et al., 2013). The rainfall is transmitted as surface runoff when the soil has reached its field capacity. The magnitude of runoff depends on the rainfall intensity, type of land surface, soil type and structure and the catchment slope. In urban watersheds, impervious surfaces dominate, resulting in increased runoff and decreased infiltration (SCS, 1986). Two methods are mostly used to estimate runoff namely, rational method and empirical method.

Rational Method

Tripathi and Singh (1998) developed a rational method that is quick and most widely used to estimate the peak surface runoff rate for a catchment. The runoff is estimated using the following equation:

$$Q = \frac{1}{360} \times C \times I_r \times Ah_a \quad (1)$$

Where Q is the peak rate of runoff (m^3/s) for given rainfall frequency; C is the runoff coefficient; Aha is the area of the basin [ha], and Ir is the intensity of rainfall [mm/h] for the design frequency for a duration equal to the time of concentration.

Empirical Method

The Soil Conservation Service Curve Number (SCS-CN) is a simple method used to predict the volume of direct runoff due to the complexity of the land surface. The CN method requires a limited number of parameters for runoff estimation (Bhuyan et al., 2003). These parameters include values for different hydrologic soil group (HSG), type of land cover and land management conditions and the overall hydrologic conditions (Soulis & Valiantzas, 2012).

The SCS-CN method is given by (SCS, 1986):

$$Q = (\mathrm{P} - 0.1\mathrm{S})^2/(\mathrm{P} - 0.8\mathrm{S}) \quad (2)$$

Where Q is the runoff (mm), P is the rainfall (mm) and S is the potential maximum retention after runoff begins (mm).

The potential retention is expressed in terms of CN by:

$$S = 25400/\mathrm{CN} - 254 \quad (3)$$

Where S is related to soil and cover conditions of the watershed and CN is a dimensionless number, ranging from 0 to 100.

Baseflow

Baseflow is an integrated groundwater coming from multiple flow paths of varying scale, from deep regional groundwater to shallow near-stream flow paths (Price et al., 2011; Miller et al., 2014). Hence, understanding the temporal and spatial variability of groundwater contribution to streamflow is essential for water resources management and development (Farvolden, 1963; Prince, 2011). Baseflow originates as precipitation infiltrating to the subsurface and eventually discharging to streams (Farvolden, 1963; Prince, 2011). Baseflow is considerable in watershed areas where there are high rates of infiltration, recharge, and groundwater storage (Brutsaert, 2005; Gardner et al., 2010; Prince, 2011). In contrast, baseflow is low in watershed areas, where evapotranspiration and runoff dominate (Brutsaert, 2005; Gardner et al., 2013; Prince, 2011).

Several methods of baseflow estimation have been developed. These include graphical hydrograph separation approaches, recession curve analysis, and isotope and chemical mass balance methods (Talleksen, 1995; Stewart et al., 2007; Miller et al., 2014). Stream flow hydrograph recession curve expresses the theoretical relationship between aquifer structure and groundwater outflow to a stream channel (Thomas et al., 2015). Hydrograph recession curve analysis helps in characterizing the relationship between groundwater and surface water during low flow periods (Rumsey *et al.*, 2015). The stream hydrograph is divided into a rising limb, which reflects the increase in discharge resulting from precipitation events and a recession limb that represents dry periods when stream flow is maintained at least in part by discharge from watershed aquifer storage as baseflow (Figure 3.6). Baseflow exists without the contribution of direct runoff from the rainfall. Baseflow can be differentiated from a total streamflow hydrograph by using a recession model based on the following relationship:

$$Q = \mathrm{Qo}^{\mathrm{kt}} \tag{4}$$

Where Q_t is the baseflow at any time, Q_o is the initial baseflow at the beginning of the recession, **t** is time since the begging of the recession and k is the exponential decay constant.

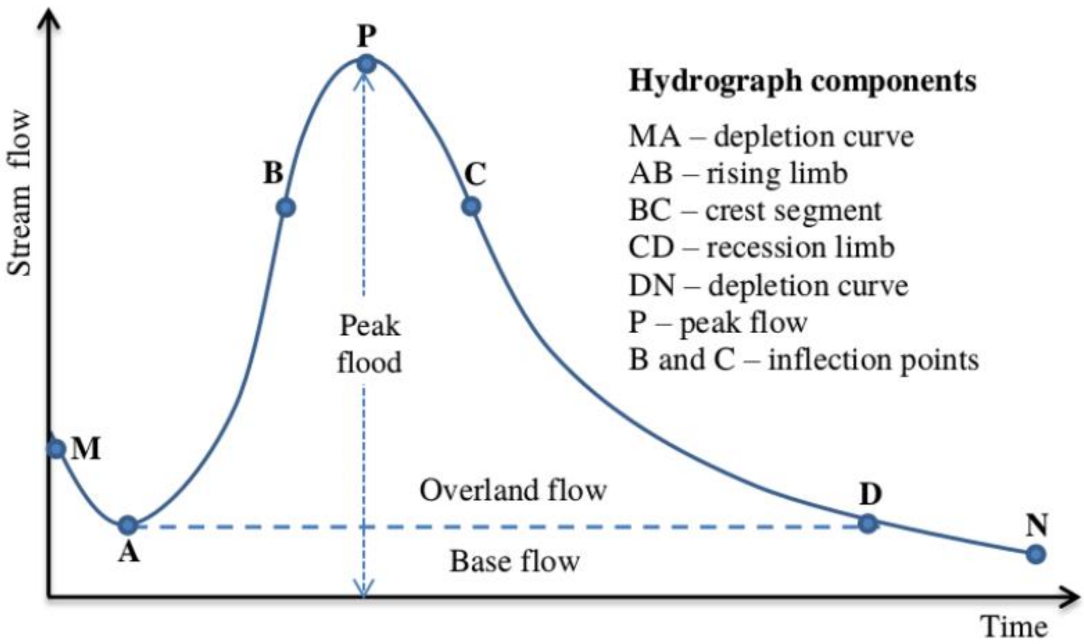

Figure 3. 4. Element of a stream discharge hydrograph (adapted from Subramanyanna, 2008).

3.4.3 Groundwater - wetlands interaction

Urban transformation disconnects the connection between groundwater and surface water. The interaction between groundwater and surface water is controlled by the relative surface water and groundwater heads which can vary significantly over time (Mcewan et al., 2006). As both the engineered channelling of surface water and rerouting of groundwater flow direction result in the two resources not meeting at point of interest. Wetlands are present in landscape that cause groundwater to discharge to land surface or that prevent rapid drainage of water from the land surface. Wetland can receive groundwater inflow, or recharge groundwater or do both depending on the elevation. Wetlands occupy depression on the surface and interact with adjacent upland groundwater. Groundwater-surface water interaction constitute an important link between wetlands and the surrounding catchment. The interaction takes place between wetlands and adjacent upland groundwater level. In areas of steep terrain, the water table sometimes intersects the land surface, resulting in groundwater discharge directly to the land surface in the urban context (Mcewan et al., 2006).

3.4.4 Groundwater-dependent wetlands in an urban setting

Groundwater-dependent wetlands source water derived partly or exclusively from groundwater (Custodio, 2000). Groundwater-fed wetlands occur in all main aquifer type settings in South Africa. It depends on groundwater as the interaction plays a role in ecological processes to maintain their environmental structure and functioning. Groundwater dependent wetlands are essential for both physical and chemical fluxes in the hydrologic cycle (Toran, 2017). Groundwater-dependent wetlands usually grade into lagoon, lakes and river courses as they present a large variety of patterns, circumstances and salinity (Custodio, 2000). They can be classified as groundwater discharge areas that correspond to local, intermediate and regional flow systems (Custodio, 2000). They are frequent in flat areas, coastal zones and lowlands (Custodio, 2000). Groundwater dependency can be direct where some species require immediate access to groundwater in-order to survive, and indirect dependence on species that can access groundwater to sustain species that cannot (Colvin *et al.*, 2007).

3.4.5. Shrinkage of wetland due to urbanization

Historically, wetlands have been known to be affected by development. They were drained and restored for other purposes. Recently it has been shown that they have a unique value for habitat, water quality improvement and flood attenuation. This shift continues to grow, with an average rate of 1.6% per annum worldwide. However, urbanization requires more space for the development of tall buildings (Faller *et al.*, 2010). Therefore, natural surface shrinks in size with time (Faller *et al.*, 2010), resulting in a significant decline in biodiversity worldwide (Plan, 2019). Landscape changes impact, the eThekwini District’s natural environment as a result of vegetation removal, urban development and stream channelization. Application of agricultural pesticides and fertilizers, industries and mines produce waste containing harmful chemicals that directly discharges to sewers, rivers and wetlands (Faller *et al.*, 2010). Pollution, habitat degradation and changes in hydrology results in wetland shrinkage (Boyer and Polasky, 2004; Zhoa and Song, 2004). Groundwater recharge in urban centres is reduced as infiltration is discouraged by storm drains.

Wetland ecosystem has been predominantly drained for cultivation in urban areas; they are frequently transformed by infrastructural development (Paul and Meyer, 2001). The loss of natural ecosystem is driven by urbanization where deforestation takes place (Zedler and Leach 1998; Tockner and Stanford 2002). Extraction of groundwater consequentially leads to overall water-level decline, saltwater intrusion and land subsidence in coastal areas (Ting et al., 1998). Social and economic pressure have resulted in widespread degradation of a freshwater ecosystem. Impact on wetlands results in 37% of freshwater fish species and 30% of all amphibian species to be threatened with extinction (Paul and Meyer, 2001). Value of wetland varies with the nature of the wetland and the needs of the population it interacts with. In more developed areas, dependency on natural wetland resources decreases.

3.5 Wetlands and their ecological services

Wetlands are a diverse ecosystem that links wildlife and environment in a unique way through the essential life-support functions of water (Maltby and Barker, 2009). Wetlands transitions between terrestrial and aquatic systems, where the water level is near the surface or on the ground level (SANBI, 2009). Wetlands are classified as being marine, estuarine, lacustrine and riverine (Mazvimavi, 2017). Wetlands can be natural or artificial, with water that is static or flowing, fresh, brackish or salt (Ramsar Convention, 2007). They are periodically covered with shallow water supporting vegetation that is adapted to live in saturated soil. The extent of wetlands in the world is about 5% to 8 % of the earth land surface (Mitsch and Gosselink, 2007). However, its support 20% of all living organisms, proving an essential source of biodiversity (Zhoa and Song, 2004).

Wetlands are characterized by rainfall-driven water level, tidal and riparian floodplain (Anderson and Davis, 2013). They are also identified by wet soil-forming anaerobic condition as there is a low solubility of oxygen in water, slow rate of advection and slow diffusion rate of oxygen through water (States, 2008). These anaerobic conditions affect vegetation root survival and growth (U.S. EPA. 2008). Yet, despite these anaerobic conditions, wetlands are the most biologically productive ecosystems in the landscape (U.S. EPA. 2008).

Wetland are observed in many parts of the world including both in the boreal and tropical regions of the world (Mitsch and Gosselink, 2007). African wetlands are mostly found in sub-Saharan Africa, including the Inner Niger Delta of Mali (320 000 km^2, when flooded), Congolian Swamp Forest (190 000 km^2), the Sudd of the Upper Nile (30 000 km^2 when flooded) and Okavango in Botswana (28 000 km^2). According to Nel et al. (2011), over half of South Africa's rivers, wetlands and estuary ecosystem types are threatened. South Africa wetlands have been destroyed at an alarming rate in urban areas and extensively in cultivated fields. A different perspective has been recognized, regarding their conservation and protection (Mitsch and Gosselink, 2007). Hence, the Ramsar Convention was adopted to encourage countries to perform national wetland inventories (Mitsch and Gosselink, 2007). Urban wetlands survived historical development around which urbanization gradually took place (Kotze et al., 2005).

The interest in understanding the relationship between groundwater and wetlands has increased in recent years due to the loss of ecosystem to development (Winter, 1995). Wetlands receive groundwater inflow and can also recharge groundwater. This takes place as wetlands and groundwater are interconnected, wetlands receive a continuous supply of chemical constituent of dissolved salt from groundwater.

3.5.1 Wetlands geomorphological settings

Wetland hydrology is dependent on the position of landscape, geology, precipitation and anthropogenic factors (Acremen and Miller, 2007). Generally, wetlands form in flat areas or near the land surface, where it accumulates within a topographic depression (U.S. EPA. 2008). Wetlands depressions are formed when water moves along the surface, erodes, transport sediments downslope. These depressions are classified using principles of hydrogeomorphic wetland types, namely, Hill seep, Unchanneled valley-bottom, Channelled valley-bottom, floodplain, flat and depression (Figure 3.1) (SANBI, 2009). However, wetlands experience changes in water elevation, flow and physiochemistry associated with groundwater input and periodic rainfall events (Dussaillant et al., 2009). In the undulating nature of the EMA, common wetlands are valley bottom both with and without channel (Plan, 2019).

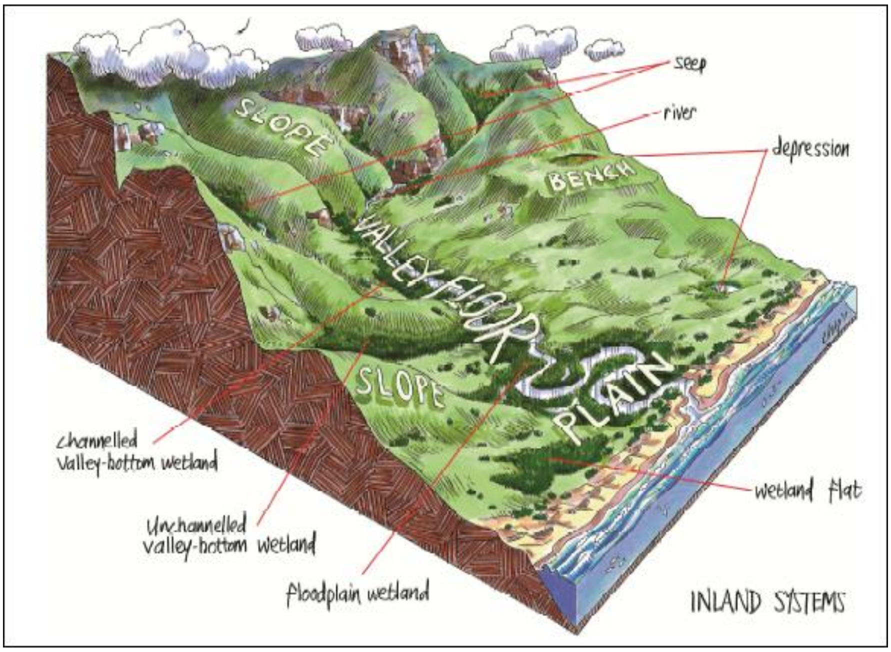

Figure 3. 5. The geomorphic position of different type of wetlands (Deventer et al., 2018).

3.5.2 Type of soil and vegetation in wetlands

Wetlands have dense vegetation and hydrophytes plants that have broad leaves, thus intercepting more precipitation, which is later evaporated (Renault et al., 2000). Evapotranspiration is a vital wetland process (Mazvimavi, 2017). This account for 100% of annual water loss in wetlands (Souch et al., 1998). Wetland soils are divided into Minerals, and organic soil (Mitsch and Gosselink, 2015), with greying and mottles morphological features (Collins, 2005). They help in understanding the hydrological processes of wetlands and their interaction with catchment (Mazvimavi, 2017). As they are saturated for a more extended period with a higher concentration of clay and low organic carbon.

3.5.3 Groundwater-Wetlands ecological services

Wetlands in South Africa are protected by the National Water Act (No.36 of 1998), where extraction of water in any form of use and diverting or obstructing the flow of a waterway requires a specific license. The National Environmental Management Act 107 of 1998 (NEMA) and the Environmental Impact Assessment regulation state that no disturbance of more than 50 m^2 can occur within 32 m of a watercourse without environmental approval from the Department of Agriculture, Environmental Affairs and Rural Development (Botes, 2011). Wetlands provide sustainable opportunities for recreation and tourism (Oumou et al., 2006). As they contribute to aesthetic, cultural and educational purposes (Faller *et al.*, 2010). The floodplain wetlands in the EMA are associated with large rivers such as uMdloti, uMngeni and uMlazi.

Wetlands are recognized as environmental kidneys as they assimilate excess nutrients, especially in temperate areas (Mitsch and Gosselink, 2007; Kometa et al., 2017). Wetlands are also referred to as ecological supermarket as they support extensive food chains and rich biodiversity (Mitsch and Gosselink, 2007). They provide good fertile soil where crops are grown, suitable for recreation and tourist attraction as birding and fishing take place (Mazvimavi, 2017). Wetlands store and improve water quality, recharge groundwater and control flooding and erosion (Mazvimavi, 2017).

Direct services provided by wetlands include the use of reed to build and craft materials. Indirect services, wetlands filter pollutants and excess nutrient from the water, thus improving the quality of water. Wetlands are also used as spawning and nursery habitat by transient fishes widely in both freshwater and marine systems (Lewis and Gilmore, 2007). Wetland conservation and maintenance is crucial as they act as a sponge soaking up water in flood periods and releasing it during dry periods (Bucher et al., 1993). They stabilize water supplies, thus ameliorating floods and drought (Mitsch and Gosselink, 2007). They clean polluted water, protect shorelines and recharge groundwater aquifers (Mitsch and Gosselink, 2007). Wetlands provide habitat for a wide variety of flora and fauna (Mitsch and Gosselink, 2007). They are essential carbon sink (Mitsch and Gosselink, 2007), serve as a source, drain and transformers of nutrient and deep-water aquatic system (Mitsch and Gosselink, 2007). Potential greenhouse gases are trapped within wetlands as overtime, permanent soil trap carbon through the formation of peat. Urban wetlands absorb excess rainfall, reduces flooding and minimize damage to infrastructure, moderate extreme city temperatures, provides habitat for aquatic species, thus conserving the biodiversity. Wetland is useful in the regulation of global cycles, including nitrogen, Sulphur, methane and carbon dioxide (Mitsh and Gosselink, 1986).

3.5.4 Inventory of Wetlands using Remote Sensing

In the classification of wetlands, it is vital to map its location, extent and describe the type of wetland in the area of study. Remote platforms or satellite produced images can be used to document wetlands geographic location and boundaries. Satellite imagery is rapidly becoming a norm of mapping wetlands (Mitsch and Gosselink, 2007). These images are later overlain on the topographical map to produce wetland maps. The commonly used satellite system includes Landsat Multispectral Scanner (MSS), Landsat Thematic Mapper and Systėme Pour I'Observation de la Terre (SPOT). They offer repeated coverage that allows seasonal monitoring of wetlands as well as providing data on the surrounding landscape in a GIS format (Ozesmi and Bauer, 2002). The platform used depends on the resolution needed, the area covered, and the cost of data collection (Mitsch and Gosselink, 2007).

3.6 Conceptual hydrogeological models

Conceptual hydrogeological models are simplification of real-world hydrological problems, which represent systems that conform to hydrogeological principles. The principles are based on geological, geophysical, hydrological, hydrogeochemical and related aspects (Anderson et al., 1990). It characterises the site to integrate relevant local and regional hydrogeological information using simplifying assumptions and qualitative interpretation of site-specific flow and transport processes (Zheng and Bennett, 2002). Hydrogeological Conceptualisation assists in the understanding of the system, particularly for representing the interaction between groundwater and surface water across the landscape.

According to Kolm (1996), nine data sources are necessary to design a conceptual model. These data source includes geomorphology, geology, geophysics, climate, vegetation, soil, hydrology, hydrochemistry and anthropogenic aspects. The critical components of a conceptual model include system boundaries, hydro-stratigraphy, hydrogeological parameters, general direction of groundwater flow and sources and sinks of water (Anderson et al., 1990). These components are represented in a series of diagrammatic, cross-section, fence diagram, tables and workflow (Figure 3.6). It is essential to look at the regional settings in order to understand how regional geology influences groundwater flow in the study area. In the development of a conceptual model, it is important to understand information about the rate of recharge, pumping, evapotranspiration, baseflow, spring flow and other boundary flows along with information on the non-permanent and spatial variability of recharge and discharge conditions (Anderson et al., 2015). The resulting conceptual model is used to define hydrological boundaries, aquifer unit, and water level and flow direction and hydro-chemical evolution processes of the system.

In summary, the critical element of a groundwater and surface water interaction conceptual model are (Brodie et al., 2007):

- Catchment framework: defining the study area boundaries in terms of groundwater and surface water divides.
- Geological framework: the geological structure and composition of the area, as well as the geomorphology.
- Hydrogeological framework: the distribution, configuration and properties of the aquifers and aquitards making up the catchment area.
- Surface water framework: the type and configuration of streams, together with associated floodplains and wetlands.
- Hydrological framework: the key factors and processes defining the movement of water throughout the landscape, including rainfall, evapotranspiration, climate pattern, runoff, stream flow and groundwater flow.
- Ecosystem framework: the vital environmental assets that have a dependency on the study area's surface water and groundwater features, such as wetland ecosystems, endangered aquatic species or the relevant vegetation communities.
- Anthropogenic framework: the human-induced factors that can influence groundwater-stream interaction in terms of water quantity and quality, such as groundwater pumping, land clearing, intensive agriculture, drainage, flood mitigation works, stream diversion and mining. It also includes the social dependencies of the connected water resource such as heritage and cultural values.

3.6.1 Hydrostratigraphic units and their hydraulic properties

Groundwater systems are characterised by aquifers which are geological units that store and transmit significant amount of groundwater. These aquifer systems may be confined, unconfined or a combination of both. These aquifers are classified into hydrostratigraphic units based on their physical characteristics such as nature and connectivity of the rocks, mineralogy, lateral extent and their hydraulic characteristics (Fetter, 2014). The void spaces in a rock are characterised by porosity and permeability, which determines transmission and storage properties. Whereas fractures, conduits and faults are hydro-structural units that act as water flow paths. Isopach maps and borehole logs can show hydro-stratigraphic unit thickness. These properties of the hydro-stratigraphic units are displayed in stratigraphic columns, cross-sections, fence diagrams and block diagrams. In the development of a conceptual model, depositional setting, geological history and the general hydraulic properties of hydro-stratigraphic units and hydro-facies should be determined.

3.6.2 Groundwater levels and Groundwater flow directions

Groundwater flow direction through an aquifer is primarily influenced and controlled by the geology and geometry of the aquifer, including hydraulically connected surface water components. The scale and extent of groundwater flow are determined by geology and surface topography (Reid *et al.*, 2009). The groundwater flow rate through a porous medium is governed by Darcy's Law (Freeze and Cherry, 1979), where groundwater flows from high hydraulic head to low hydraulic head. The flow rate is mainly depended on the hydraulic conductivity of the media and hydraulic pressure gradient. The areas of the high hydraulic head often coincide with high surface topography allowing recharge to enter the aquifer. Whereas the lowest hydraulic head may coincide with surface water bodies discharging to wetlands, lake and streams. The flow direction is determined from a contour map of the water table and potentiometric surface (Anderson et al., 2015). The flow rate is given by:

$$v = Ki \qquad (5)$$

Where v is flow velocity (m/day), K is hydraulic conductivity of the porous media (m/day) and i is hydraulic pressure gradient (difference in head over difference in distance).

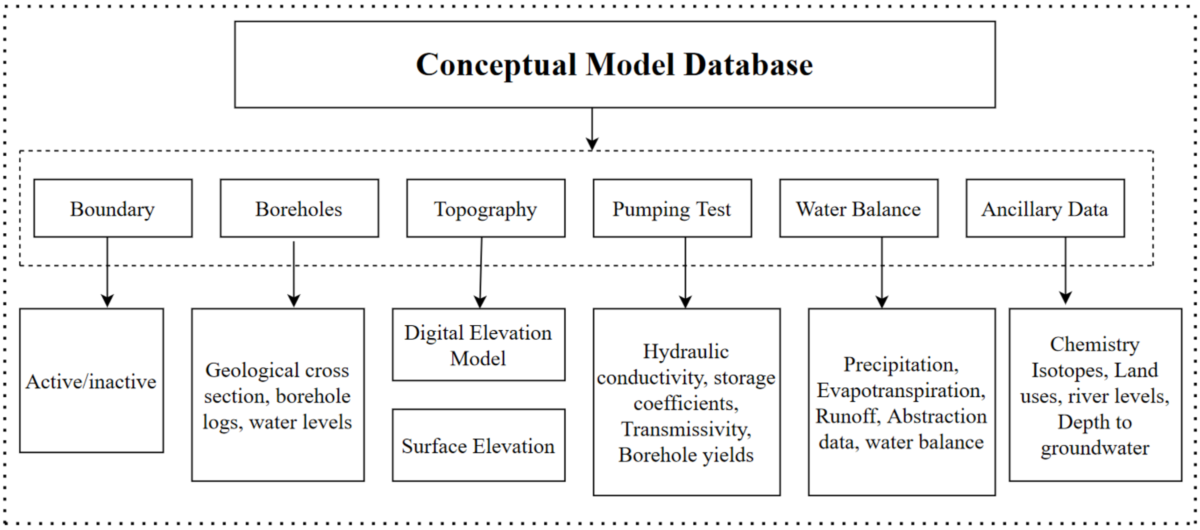

Figure 3. 6. Conceptual model database (adapted from Ndlovu et al., 2019).

3.6.3 Groundwater recharge and its estimation methods

Groundwater recharge is the infiltration of water down to the water table in excess of soil moisture deficit or the percolation of adjacent water bodies to the aquifer which contributes to replenishment of the groundwater reservoir (de Vries and Simmers, 2002; Rukundo and Doğan, 2019). Various mechanisms of groundwater recharge are recognized, namely, 1) Diffuse percolation through unsaturated zone as a saturated front (piston-type flow). 2) Macro-pore flow through root channels, desiccation cracks and fissures. 3) Preferential flow caused by unstable wetting front and differentiated soil physical characteristics within the soil, between sand and clayey sediments (de Vries and Simmers, 2002). These flows take place laterally and vertically from rainfall, surface water bodies such as lakes, rivers and artificial recharge from injection borehole or man-made infiltration ponds (Xu and Beekman, 2003). Natural rainfall recharge is the most important source of groundwater recharge. The interaction between climate, geology, morphology, soil condition and vegetation determine the recharge process (de Vries and Simmers, 2002). The combination of reliable local data, remote sensing, and GIS technology offer a better understanding and quantification of recharge over large areas (de Vries and Simmers, 2002).

Quantifying groundwater recharge is a prerequisite for sustainable groundwater resources management. There are a number of groundwater recharge estimation methods namely, soil water balance, catchment water budget, Water Table Fluctuation (WTF) and Chloride Mass Balance (CMB) to mention few.

Soil Water Budget method

The Soil Water Budget (SWB) method is one of the groundwater recharge estimation techniques. Data requirements include hydro-meteorological parameters such as precipitation, maximum and minimum temperature, relative humidity, radiation and wind speed, soils characteristics, slope of the area and land cover. The SWB method analyses water moving through the unsaturated zone, towards the water table (Fetter, 2014). The method tracks the balance between the inflow of water from precipitation and the outflow of water from evapotranspiration, soil moisture storage, surface runoff and drainage (potential groundwater recharge) (Thornwaitte and Mather, 1955; 1957). The SWB method of groundwater recharge estimation for a catchment is applied using equation 6:

$$P = ET + Q + D + \Delta SW \qquad (6)$$

Where, P is precipitation (mm), ET is Evapotranspiration (mm), Q is surface runoff (mm), D is drainage below the root zone of the plants (mm), and ΔSW is soil water change over the time step.

Water Budget Method

The Water Budget Method (WBM) of groundwater recharge estimation for a groundwater system is undertaken by calculating the major inputs of water from rainfall, irrigation return flow and seepage of rivers and output groundwater system from evapotranspiration, base flow to rivers and groundwater pumping of water and lastly the storage changes of the groundwater system for in a defined aquifer (Thornwaitte and Mather, 1955; 1957). Changes in groundwater storage can vary between the inflow and outflow of water over a specific time. The equation is given by (Thornwaitte and Mather, 1955):

Inflows – outflows = Change in storage (ΔS) (7)

The equation is rewritten in explicit form as follows:

R_{rain}+ RF + Q_{on}+ Q $_{river}$ = ET + PG + Q_{off} + Q_{bf} + ΔS $R_{\mathrm{rain}} + RF + Q_{\mathrm{on}} + Q_{\mathrm{river}} = ET + PG + Q_{\mathrm{o}}\mathrm{ff} + \mathrm{Q}$

(8)

Where, R_{rain} is rainfall recharge (m^3); RF is irrigation return flow (m^3); Q_{on} and Q_{off} are lateral groundwater flows into and out of the groundwater system (m^3); Q_{river} is river seepage recharge (m^3); ET is evapotranspiration (m^3); PG is extraction of groundwater by pumping (m^3); Q_{bf} is baseflow (groundwater discharge to streams, wetland or springs) (m^3); and ΔS is change in groundwater storage (m^3) in the study area.

Water Table Fluctuation (WTF)

The Water Table Fluctuation (WTF) method uses groundwater level fluctuations in observation wells to estimate groundwater recharge. A rise in water table elevation is expected to be caused by the addition of recharge across the water table, lateral inflows or inter-aquifer leakage. The water level measured at an observation well represent only the point of the aquifer where it is measured. The WTF method can be viewed as an integrated approach and less of a point measurement (Thornwaite and Mather, 1955). The equation used in the WTF method is given by:

$$A \times \Delta h \times S_y = \Delta S \qquad (9)$$

Where, A is the surface area of the aquifer (m^2), Δh is water level rise in observation wells at a defined time interval (t_0 to t_1) (m); S_y is the specific yield of the aquifer and ΔS is change in groundwater storage in a defined time interval (m^3) which is assumed to be the recharge.

Chloride Mass Balance (CMB)

The Chloride Mass Balance (CMB) method was developed by Eriksson and Khunakasem (1969). The method uses both wet and dry chloride deposition at the surface and compares it with the chloride concentration in groundwater. This method evaluates recharge processes in a wide range of environments because of the conservative nature of chloride and the availability of precipitation data (Subyani and Sen, 2005). The method is simple, and it is based on the knowledge of annual precipitation and chloride concentration in the rainfall and groundwater. For the application of the CMB method, some assumptions must be considered. These are, 1) a piston flow regime is assumed but may not be always the case as multiple types of moisture transport vertically and horizontally can occur, 2) preferential flow paths need to be attended to, as the soil moisture and solutes may be transported through the unsaturated zone by these pathways, 3) Chloride in the groundwater originates only from precipitation directly on the aquifer, 4) Chloride is conservative in the system, 5) Steady- state conditions are maintained with respect to long term precipitation and chloride concentration in precipitation, 6) No evaporation of groundwater occur upgradient from the groundwater sampling points (Mutoti, 2015). Equation 6 showns the CMB method of groundwater recharge.

$$R = P\,(Cl_p/Cl_{gw}) \qquad (10)$$

Where, R is the recharge flux, P is the average annual Precipitation, Cl_p is the weighted average Cl^- concentration in rainfall, and Cl_{gw} is the average Cl^- concentration in groundwater.

3.7 Hydrochemical and environmental isotope application in groundwater-surface water interaction studies

3.7.1 Hydrochemical application in groundwater-surface water studies

Studying hydrogeochemical processes has been an area of interest in the past few decades as the chemical variation of groundwater and surface water is known to influence water quality (Guggenmos et al., 2011). The study helps to understand the changes in water quality due to rock-water interaction or any anthropogenic influences (Sadashivaiah et al., 2008). Water quality analysis is one of the essential aspects of groundwater studies as it is crucial for effective environmental management (Sadashivaiah et al., 2008). It is widely acknowledged that groundwater and surface waters interact at a variety of spatial and temporal scales (Winter et al., 1998). As indicated in preceding sections, the degree of groundwater – surface water interaction or aquifer-stream water and nutrient exchanges is largely influenced by meteorological, fluvial, topography and geological processes (Guggenmos et al., 2011; Winter et al., 1998). Such water transfers play a significant role in determining the quantity and hydrochemical composition of water bodies at both local and regional scales (Guggenmos et al., 2011). These transfers are quantified by measuring changes in water temperature, stream stage and discharge, water chemistry and using hydrograph separation methods (Sophocleous, 2002; Kalbus et al., 2006). These methods generally assume that a change in one or more of these measured parameters is caused or influenced by the transfer of water across the aquifer-stream boundary (Guggenmos et al., 2011). Subsequently, giving an insight into the various flow pathways, geological settings, physical and chemical processes which the water was subjected to (Freeze and Cherry, 1979; Güler and Thyne, 2004; Kumar et al., 2009).

Numerous studies suggest that similarities in water composition between nearby groundwater and surface water bodies, such as ion ratios or the specific electrical conductivity or the total dissolved solids (TDS), can be used to qualitatively infer potential groundwater-surface water interaction (Burden, 1982; Taylor et al., 1989; Kumar et al., 2009). Furthermore, understanding hydrochemical processes helps to identify the relationship between geochemical processes and water quality and the hydrochemical evolution of the water resources under consideration, which is vital for sustainable water resources management (Xinyan et al., 2018). Kumar et al., (2009) have identified that simple dissolution, mixing, weathering of carbonate and silicate minerals, ion exchange, and interaction with surface water are the critical hydrogeochemical processes that control groundwater quality (Xinyan et al., 2018).

Chemical classification gives clarity on the concentration of various predominant cations, anions and their interrelationships (Sadashivaiah et al., 2008). Several techniques have been developed to interpret chemical data (Sadashivaiah et al., 2008). Presentation of chemical analysis in graphical form makes the understanding of complex groundwater and surface system simpler and quicker (Sadashivaiah et al., 2008). Graphical procedures have been devised to help detect and identify the mixing of waters of different composition and to identify some chemical processes that may take place as natural waters circulate (Hem, 1985). The Piper trilinear diagram (Piper, 1944), which illustrates hydrochemical facies is used to understand the sources of the dissolved constituent in water. The diagram displays the relative concentrations of the major cations and anions on two separate trilinear plots, together with a central diamond plot where the points from the two trilinear plots are projected. The central diamond-shaped field shows the overall chemical character of the water (Hill, 1940; Piper, 1944). The Schoeller semi-logarithmic diagram show relative concentration of anion and cation and allows the major ions of many samples to be plotted on a single graph (Schoeller 1955, 1965). Durov diagram is based on the percentage of major ion milli-equivalents. The cation and anion values are plotted on two separate triangular plots, and the data points are projected onto a square grid at the base of each triangle.

3.7.2 Environmental isotope in groundwater-surface water interaction studies

Environmental isotopes have become a powerful tool for tracing the water cycle including the history of groundwater recharge and groundwater contamination (Clark and Fritz, 1997). These water isotopes have been used in the investigation of groundwater and surface water interaction and are useful in determining the source of water in wetlands (Mazvimavi, 2017).

They provide means to investigate the hydraulic relationship between rivers and aquifers (McCarthy et al., 1992). Where the stable isotope falls into a distinct group, providing information on the secondary processes acting on the water as it travels from precipitation to groundwater or surface water (Baskaran et al., 2009). Where groundwater samples are mainly depleted due to recharge that takes place without evaporation and surface water samples are enriched as water is exposed to climatic variability including heat that increases evapotranspiration (Baskaran et al., 2009). However, groundwater samples may be enriched to some extent when they evaporate before infiltration. The stable isotope composition for groundwater samples close to the river is different from the isotopic composition of the groundwater that is farthest from the river (Baskaran et al., 2009). The near stream groundwater samples have a relatively enriched isotopic signature, similar to that of river water. This indicates that infiltrating river water is the main source of groundwater close to the stream (Baskaran et al., 2009). This indicates that groundwater and stream are hydraulically connected.

There are two stable isotopes of hydrogen, i.e., ^{1}H and ^{2}H (deuterium) and three stable isotopes of oxygen (^{16}O, ^{17}O, ^{18}O). Their combination makes stable water molecules with atomic mass ranging from 18 to 22. These combinations produce light isotopes (^{1}H, ^{16}O) having much higher vapour pressure than the heavy isotopes (^{2}H, ^{18}O) (Freeze and cherry, 1979). Oxygen-18 (^{18}O) and deuterium (^{2}H) are known as heavy isotopes of water that are conservative in nature (Kendall and McDonell, 1998).

Environmental isotopes (^{2}H, ^{18}O) undergo fractionation as they move through the hydrological cycle (Rugel et al., 2016). When water undergoes phase changes between liquid and gas, the various isotopic molecules present in water distribute themselves between the phases (Clark and Fritz, 1997; Fetter, 2014). The heavy water molecules are concentrated in a liquid phase as they have low vapour pressure (Allison et al., 1984; Fetter, 2014). Kinematic fractionation is the change of the isotopic content of a substance as a result of evaporation, condensation, freezing, melting and chemical reaction (Freeze and cherry, 1979). These changes will cause the isotope ratio to vary between localities within the area as they separate into a light and heavy fraction (Fetter, 2014). The higher the temperature, the more evaporation will take place, causing enrichment of ^{18}O and ^{2}H in the remaining water (Kendall and McDonell., 1998). The light isotope evaporates, and heavy isotopes are enriched in water. Condensation takes place leading to precipitation to be more enriched or depleted in isotopic content depending on the storm origin, direction, season, duration of rainfall and altitude (Rugel et al., 2016).

The evaporated water from the ocean produces water vapour that is depleted in ^{18}O and ^{2}H relative to ocean water by 12-15‰ in ^{18}O and 80-120‰ for ^{2}H (Freeze and Cherry, 1979). The atmospheric moisture from the ocean move inland, condensation takes place, followed by precipitation in the form of rainfall that is characterized by denser isotopic signals (Dansgaard, 1964). The rain produced from the condensed water vapour has a higher concentration of ^{18}O and ^{2}H compared to the remaining water vapour (Freeze and Cherry, 1979). However, as the water vapour moves further inland as part of the regional atmospheric circulation system, the process of condensation and precipitation is repeated. The rain is then characterized by low concentration of the heavy isotopes ^{18}O and ^{2}H (Freeze and Cherry 1979).

Some of the factors that affect variations in the isotopic content of precipitation at any given location include temperature, altitude, the timing of rainfall and condensation parent vapour (Kendall and McDonell, 1998, Clark and Fritz, 1997). It is observed that during periods of high rainfall intensity, its isotopic content is depleted with heavy isotopes due to the amount effect (Kendall and McDonell, 1998).

The ^{18}O and ^{2}H isotopes composition of global precipitation correlates according to the relationship given in equation 18 (Craig, 1961) and it is known as the global meteoric water line (Kendall and McDonell, 1998) by:

$$\delta^{2}H‰ = 8\delta^{18}O‰ + 10 \qquad (11)$$

Continental precipitation plot along the meteoric water line, while ocean waters plot below the meteoric water line as it is isotopically enriched (Freeze and cherry, 1979). The deviation from the meteoric water line is caused by a number of processes including evaporation, geochemical changes (Craig, 1961). The stable isotopes of groundwater obtained in urban areas lie along the mixing line between the water supply and meteoric line (Kendall and McDonell., 1998).

D-excess (D-excess = $\delta^{2}H$ -8 $\delta^{18}O$) is widely used in understanding climate condition in the moisture source region, where global average d-excess in precipitation is about 10 (Craig, 1961; Dansgaard, 1964; Pfahl and Sodemann, 2014; Bershaw, 2018). According to Craig (1961) and Craig et al. (1963), a major cause of the d-excess is the relations between the isotope fractionation factors of Oxygen (^{18}O)

and hydrogen (^{2}H) in liquid/vapour equilibrium and in vapour diffusion in air. Thus, the d-excess is largely determined by sea surface temperature (SST), relative humidity (RH) and wind speed at the site of evaporation (Kopec, 2018). An excess of deuterium relative to ^{18}O in vapour occurs when water molecule diffuses across a density gradient during evaporation (Bershaw, 2018). The more kinetic fractionation, the higher the deuterium excess observed in the remaining water (Bershaw, 2018). This is attributed to evaporation from an average ocean surface with SST of 25°C and RH of 80 % (Merlivat and Jouzel, 1979; Guan *et al.*, 2013). The vapour of d-excess at the ocean surface is negatively correlated with RH and slightly positively correlated with SST (Pfahl and Wernli, 2008; Guan *et al.*, 2013). In most high-latitude location, the annual cycle of d-excess has a maximum in winter and a minimum in summer, opposite in phase to $\delta^{2}H$ and $\delta^{18}O$ annual cycles (Kopec, 2018).

CHAPTER FOUR: METHODS AND MATERIALS

4.1. Desktop Study

The research project has been undertaken by reviewing historical data, and literature on the geology, hydrology, and hydrogeology of the area including maps of hydro-stratigraphic units. A 30-year Hydro-meteorological data including rainfall, temperature, relative humidity, wind speed, sunshine duration, and radiation were collected from the South African Weather Service (SAWS) to analyse climatic conditions of the study area (Figure 4.1 and Table 4.1). Secondary hydrogeological information was collected from the Groundwater Resource Information Projects (KZN-GRIP) database of the Department of Water and Sanitation (DWS), National Groundwater Archives (NGA) and from various consultant reports. These include borehole logs, location of monitoring sites, depth to groundwater, pumping test data and hydrochemistry data. Surface water data is obtained from the Umgeni Water, eThekwini Municipality, and Ezemvelo wildlife. A systematic hydrogeological and hydrological database has been developed for the study area, where primary and secondary data collected is analyzed using various software and tools.

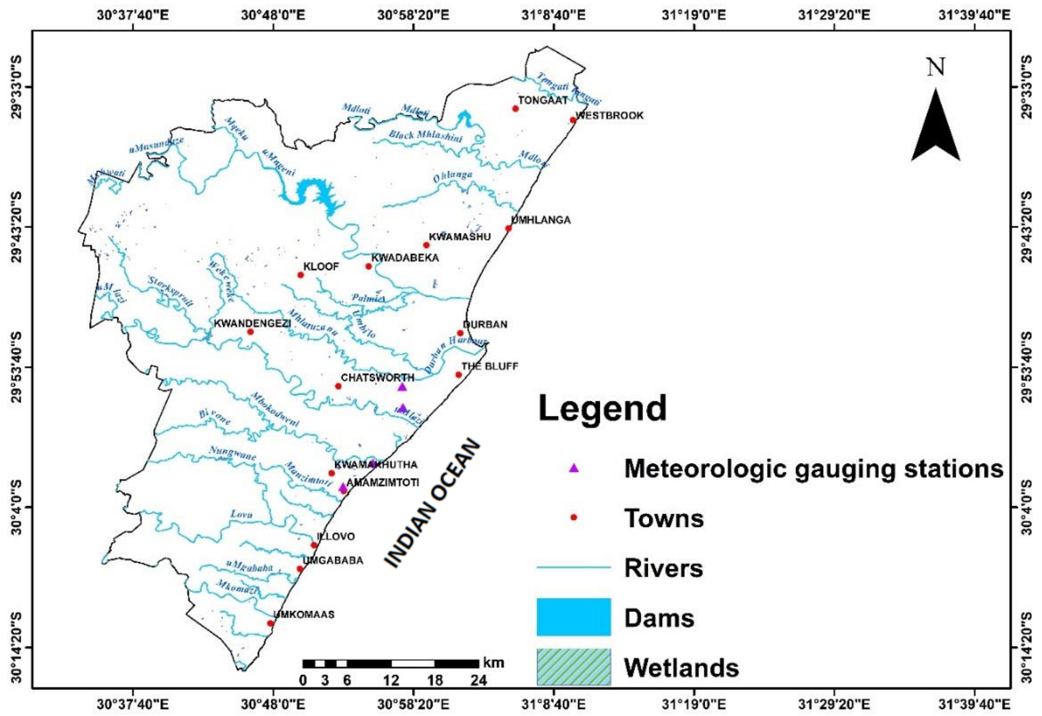

Figure 4. 1. Distribution of meteorological stations within the study area.

Table 4. 1. Hydrometeorological stations.

Station Name	Latitude	Longitude	Time range
Louis Botha -WK	-30.04128	30.88572	1988-1992
Durban South AWS	-29.91807	30.95822	1992-2014
Durban South Merebank	-29.9439	30.959137	2014-2018
Durban SouthAthlone	-30.01205	30.92221	2018

4.2 Hydrometeorological data analysis

4.2.1 Precipitation

Rainfall data for the study area have been sourced from the South African Weather services (SAWS, 2019). For this study, four meteorological stations, namely, Durban South, Athlone park, Durban South Merebank, Durban south AWS, Louis botha WK stations are used to understand the distribution of annual rainfall. The distribution of rainfall over the area is calculated using the isohyetal method. The rainfall gauging stations locations are plotted and the contours that joined the points of equal depth of rainfall are drawn based on the steps discussed in 3.9.2.3. This method is considered as the most accurate method for computing aerial rainfall and area weighted mean rainfall. The mean rainfall, P, is calculated using equation 20 (Linsley et al., 1975):

$$P = \frac{\sum [\mathrm{An}(\mathrm{Pn}+\mathrm{Pn}+1)/2]}{\sum \mathrm{An}} \qquad (12)$$

Where, Pn is the isohyet values and An is the area between two isohyets.

The isohyetal rainfall map is shown in Figure 4.2 and indicates that rainfall decreases from the coast towards the central region, then increases from the central region towards the west. The average annual rainfall is 996 mm/a.

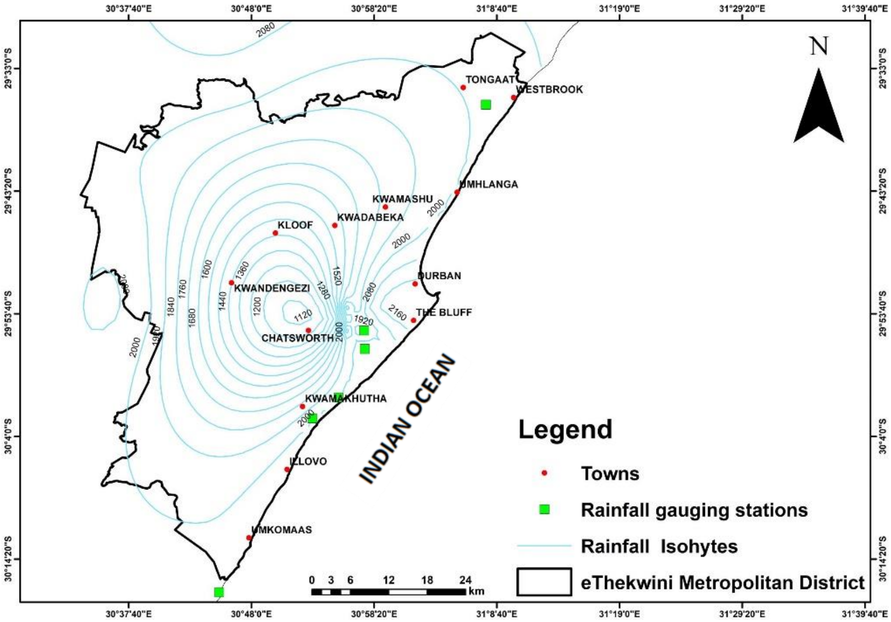

Figure 4. 2. Spatial distribution of rainfall across the study area.

4.2.2 Evapotranspiration

The mean annual potential evapotranspiration (PET) estimated using equation 13 of the FAO56 Penman-Motheith method (Allen et al., 1998) is 983.03 mm/a. Figure 4.3 shows that the highest evapotranspiration occurs in December as a result of high temperatures. The winter evapotranspiration exceeds the amount of rainfall received. The mean annual actual evapotranspiration estimated using equation 14 and 15 for the Turc Method is 748 mm/a. The FAO56 Penman-Motheith method estimated high evapotranspiration as large input data were used without any adjustment of input parameters compared to Turc which used the empirical method by underestimating the mean daily evapotranspiration in dry season and overestimating it in wet season (Diouf et al., 2016).

$$ETo = \left(\frac{0.408\Delta(\mathrm{Rn}-\mathrm{G}) + \gamma\frac{900}{\mathrm{T}+273}\mathrm{u2}(\mathrm{es}-\mathrm{ea})}{\Delta+\gamma\,(1+0.34\mathrm{U}\mathbf{2})} \right) \quad (13)$$

Where, ETo is the reference evapotranspiration [mm day^{-1}], Rn the net radiation at the crop surface [MJ/m2 day^{-1}], G the soil heat flux density [MJ m^{-2} day^{-1}], T represents the mean daily air temperature at 2 m height [°C], U2 is the wind speed at 2 m height [m s^{-1}], es is the saturation vapour pressure [kPa], ea is the actual vapour pressure [kPa], es-ea is the saturation vapour pressure deficit [kPa], Δ is the slope of the vapour pressure curve [kPa °C^{-1}] and γ is the psychometric constant [kPa°C^{-1}]. The reference crop evapotranspiration represents the evapotranspiration from a standardized vegetated surface.

The actual evapotranspiration was calculated using the Turc method (equation 14 and 15) which depends on the relative humidity (RH) (Trajkovic & Kolakovic, 2009; Fisher & Pringle III, 2013):

For RH>50% $\mathrm{ETo} = 0.0133\left(\frac{Tmean}{Tmean+15}\right)*(\mathrm{Rs} + 50)$ (14)

For RH<50% ETo = 0.0133 $\left(\frac{Tmean}{Tmean+15}\right)$*(Rs + 50) * $\left(1+\frac{50-RH}{70}\right)$ (15)

Where ETo is reference evapotranspiration (mm·mon^{-1}), Tmean is the average air temperature (°C) calculated as (Tmax + Tmin)/2 and Rs is the solar radiation (MJ·m^{-2}), and RH is the relative humidity (%).

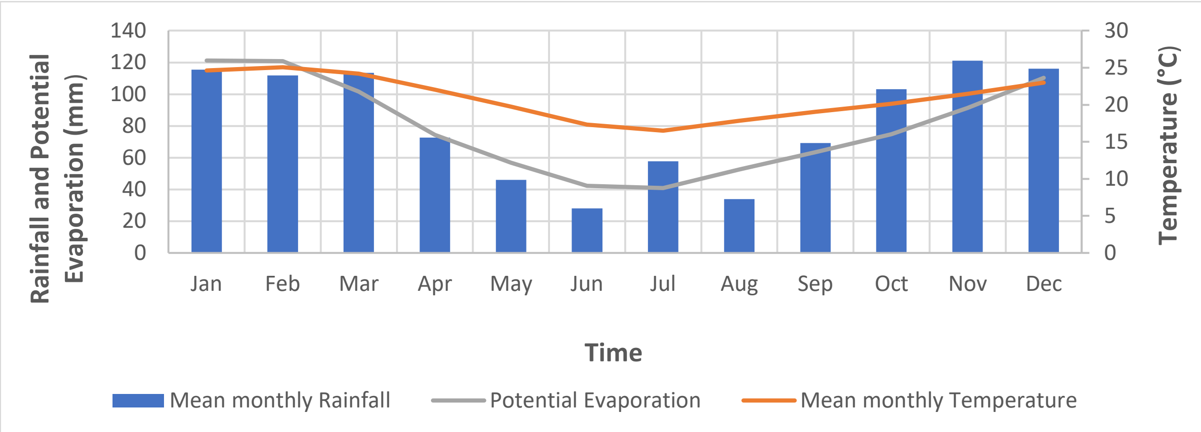

Figure 4. 3. Spatial distribution of mean monthly rainfall, evaporation and temperature across the study area.

4.2.3 Surface runoff and River discharge hydrograph analysis

Water budget forms the basis for investigating a hydrogeological system and in the development of a conceptual model. The water budget is used to determine the hydrological behaviour of a catchment area, by assessing the rate of change in groundwater and surface water system. The various inputs and outputs in the water budget are precipitation, recharge, evaporation, evapotranspiration, runoff, baseflow, the rate of abstraction and the change in storage (Fetter, 2014). The runoff within the study area is estimated using the SCS Runoff Curve Number (CN) method which considers land use and its basis. All the methods used to calculate and estimate the various hydrological parameters of the water balance have been described in the literature review. The simplified water balance of equation 16 is applied in the study area:

$$P - (Et + Rs + W + \mathrm{Rn}) = \pm \Delta S \quad (16)$$

Where, P is the precipitation, Rs is the recharge, Et is the actual evapotranspiration, W is groundwater abstraction rates, Rn Runoff and ΔS is the change in aquifer storage.

The Web GIS-based Hydrograph Analysis Tool

The WEB based Hydrograph Analysis Tool (WHAT) which incorporates digital filtering methods (Lim et al., 2006) was used for baseflow separation from river discharge data monitored at selected discharge measuring stations (Figure 4.4). WHAT is a web interface for baseflow separation using a local minimum method, the BDLOW digital filter method, and the Eckhardt filter method (Lim et al., 2006). The method used for baseflow separation is one parameter digital filter- parameter 0.925. Recursive Digital Filter, the aquifer type used is for perennial streams with porous aquifers, Eckhardt Filter parameter of 0.98 and BFI max value of 0.80 was used for this study. The gauging stations (Figure 4.4) used are those within the boundary along the Umngeni River and one along the umngeni river outside the boundary. The results obtained based on the averaged daily discharge (m^3/s) are presented in Figure 5.5. The data is input in the form of spreadsheet, which is then displayed in the form of a hydrograph as daily stream discharge vs time. In the hydrograph analysis the starting and ending point of direct runoff is noted (Lim et al., 2006). The direct runoff starts when the flow begins to increase, whereas the ending pointing identifies when the plot of log flow rate against time becomes a straight line (Chapman, 1999).

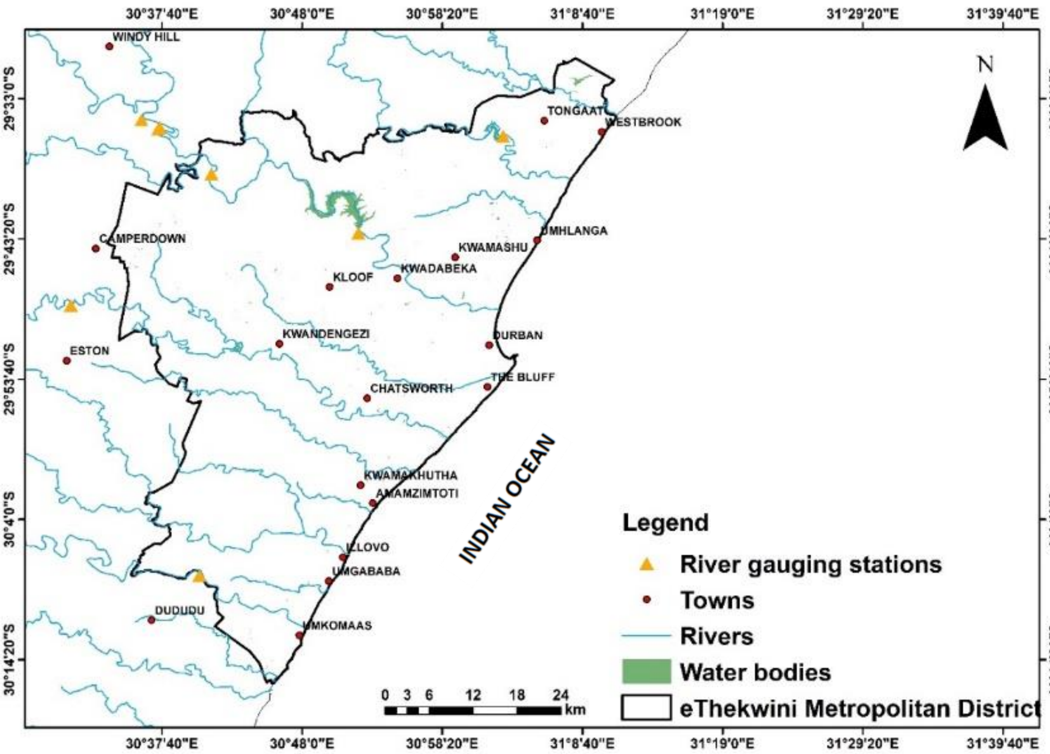

Figure 4. 4. Drainage Map with the river gauging stations.

4.3. Field data collection

4.3.1 Groundwater and surface water sampling procedure

A field sampling and testing have been undertaken across the study area as shown in Figure 4.5. Groundwater levels were measured using Solinist model Temperature, Level and Conductivity (TLC) dip meter. Groundwater samples were collected using a bailer in polyethylene bottles that are rinsed three times with sample water to avoid cross contamination and each sample is clearly labelled. Wetland water sampling was undertaken following MPCA (2007) sampling protocols, using a long-handled dipper to collect water at 5-10 cm below the water surface preferably where bottom sediments have not been disturbed.

Onsite measurements of electrical conductivity (EC), total dissolved solids (TDS), hydrogen ion activity (pH), redox potential (Eh), oxidation reduction potential (ORP), dissolved oxygen (DO), and temperature were undertaken using a Hanna multi-parameter pH/ORP/EC/DO water quality probe (Model H19828) at various representative measurement points (Figure 4.6). Samples undergoing cation and anion analyses are filtered using a 0.45µm membrane filter to remove colloids and suspended material. Major cation samples undergo acidification to pH below 2 using ultrapure nitric acid. All samples were kept in cooler boxes in the field and later transferred to the laboratory for hydrochemical and environmental isotope analyses. Analysis for major ions, minor ions, trace elements and environmental isotopes ($\delta^{18}O$, $\delta^{2}H$) was undertaken according to standard procedures. Total alkalinity, bicarbonate (HCO_3^-) and carbonate (CO_3^{2-}) content of water samples were determined onsite through titration of water samples with a 0.02 M hydrochloric acid.

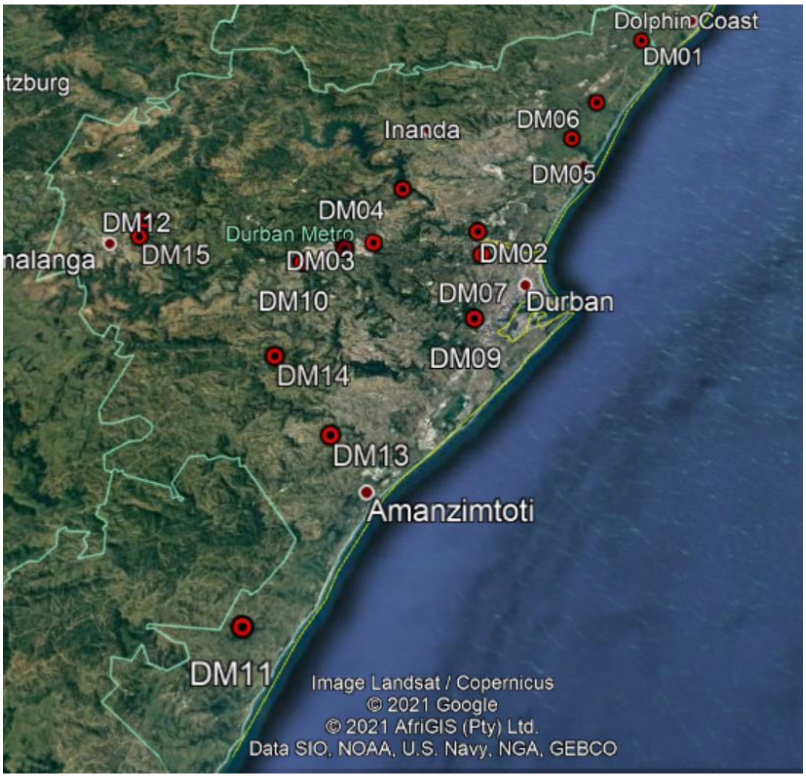

Figure 4. 5. Map showing the spatial distribution of groundwater and surface water sampling point across the eThekwini Metropolitan Districts.

Figure 4. 6. Primary field data collection from (a) Umbilo River, (b) Umbilo Wetland and (c) Inwabi Spring.

4.4. Laboratory Analysis

Hydrochemical parameters such as major cation and anion were analysed at the Talbot &Talbot laboratoris in Pretoria. The environmental isotope samples are analysed at iThemba Environmental Isotope Laboratory in Johannesburg, South Africa following standard methods.

4.5. Data analysis and interpretation

4.5.1 Groundwater level interpolation and analysis

The collected primary and secondary groundwater level data were analysed using ArcGIS and Surfer 14 software to generate groundwater level contour maps and flow directions. The Kriging spatial analyst interpolating tool from Arc-Map is used to create water level surface maps from a set of groundwater sample points. The groundwater flow direction and its relationship with rivers and streams was interpreted in terms of groundwater recharge mechanism and groundwater-surface water interactions and identifying the zones of interaction.

4.5.2 Hydrochemical and Environmental isotope data analyses

Hydrochemical data use various software and present them in the form of tables and various diagnostic diagrams to understand the hydrochemistry of groundwater and surface water and their interaction. EC contour map was interpolated in ArcGIS using Kriging spatial analyst interpolating tool to observe the distribution of EC across the eThekwini Metropolitan District. AquaChem software was used to present the hydrochemistry of the study area in the form of Piper trilinear plot, Durov and Scholler plots. From these plot, hydrochemical facies for groundwater and surface water were determined to understand the hydrochemical evolution of groundwater and surface water from recharge to discharge areas. The SPSS statistical software is used for multivariate statistical analysis of hydrochemical data. The stable environmental isotope data are plotted along the Local Meteoric Water Lines (LMWL) and Global Meteoric Water Lines (GMWL) to interpret the isotopic composition variability and understand the origin and interaction of groundwater and surface water.

4.5.3 Hydrological conceptual modelling of groundwater-surface water interaction

The desktop compiled data and the data generated during field work were integrated, processed, analysed and interpreted using various tools and approaches in order to develop conceptual hydrogeological model of groundwater-surface water interactions in the eThekwini Metropolitan District. All the data analyzed and interpreted have been used to develop hydrogeological conceptual model of the study area which describes the interaction of groundwater and surface water in the region. The procedures followed during the construction of the conceptual hydrogeological model is indicated in Figure 4.7.

The conceptual model was developed based on the understanding of different information that includes all the different types of aquifers and their hydraulic characteristics (thickness and extent, hydraulic conductivity, transmissivity, storativity), groundwater levels, hydrochemical facies, hydrometeorological parameters such as precipitation, runoff and evapotranspiration, groundwater abstraction volume and surface water bodies. This information defines hydrological boundaries, aquifer characteristics, water level and flow direction, surface water parameters and hydro-chemical evolution of the system. The analysed information includes pumping test analysis, aquifer boundaries; hydro-stratigraphic units and their hydrogeological properties, groundwater flow directions and source (recharge and sinks discharge).

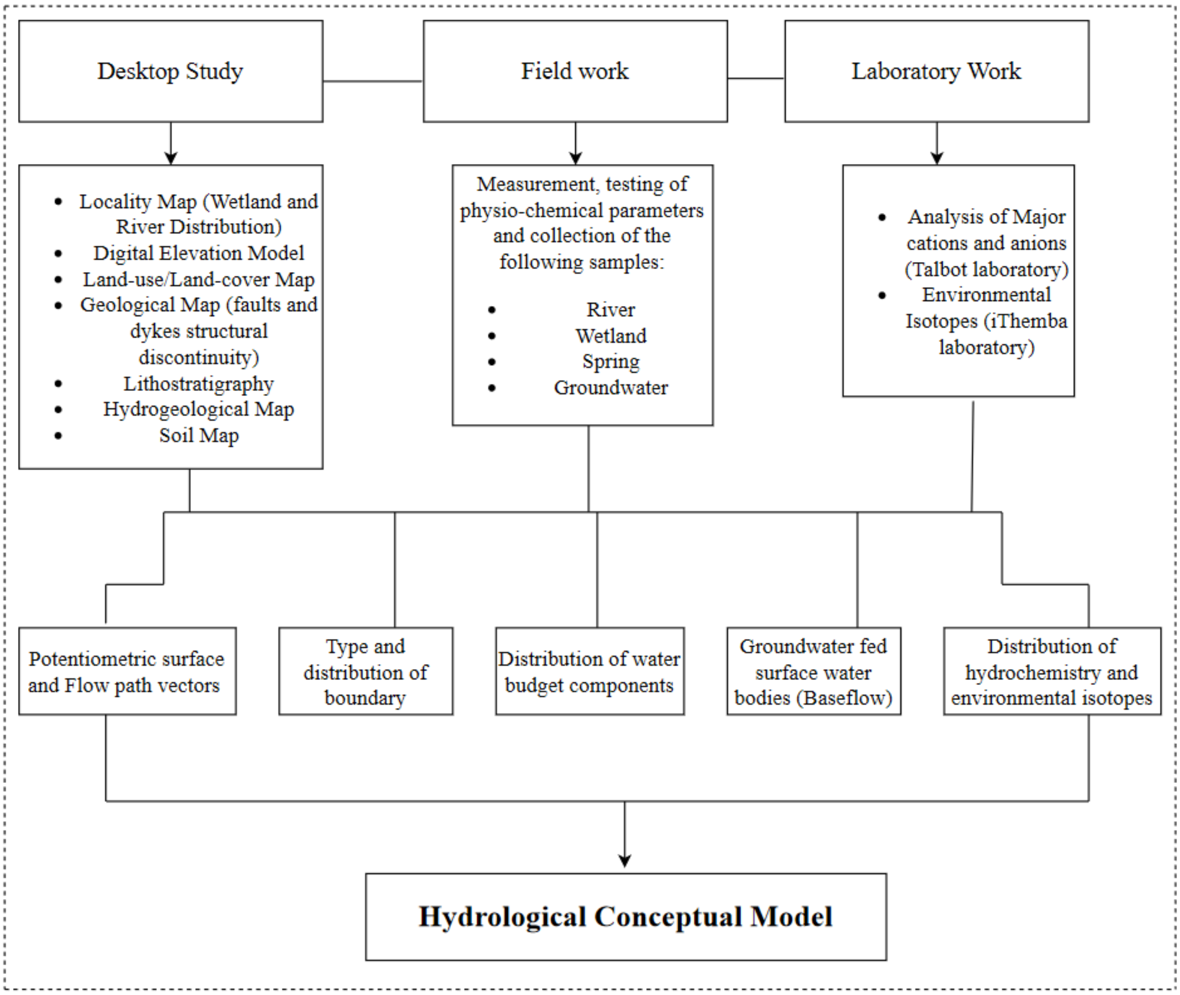

Figure 4. 7. Data and analyses leading to a hydrological conceptual.

CHAPTER FIVE: RESULT AND DISCUSSIONS

5.1 Hydrological Characteristics of the study area

5.1.1 Precipitation and Evapotranspiration

The rainfall in the region is mainly controlled by coastal and ocean influence. The average annual rainfall calculated based on a 30-year meteorological record (1989-2019) from four weather stations, namely, Durban South Athlone Park, Durban South Merebank, Durban South AWS, Louis Botha WK stations vary from summer to winter with an average of 995.7 mm/a (Figure 5.1). Most of the rains occur in summer (October to March), although there are occasional winter showers. The peak rainfall months are December to February in the inland areas and November to March along the coast. The prevailing precipitation are predominately orographic, where warm moist air moves in over the continent from the Indian ocean, rises up the escarpment, cools down and creates rainfall (Umngeni, 2016). This is indicated by isohyetal rainfall map shown in Figure 5.2 where rainfall decreases from the coast towards the central region, then increases from the central region towards the west. The mean annual potential evapotranspiration (PET), estimated using the FAO56 Penman-Motheith method (Allen et al., 1998), is 983 mm. Figure 5.1 shows that the highest evapotranspiration occurs in December as a result of the high temperature conditions and winter evapotranspiration exceeds the amount of rainfall received, creating moisture deficits in the region. The mean annual actual evapotranspiration estimated using the Turc Method is 748 mm/a.

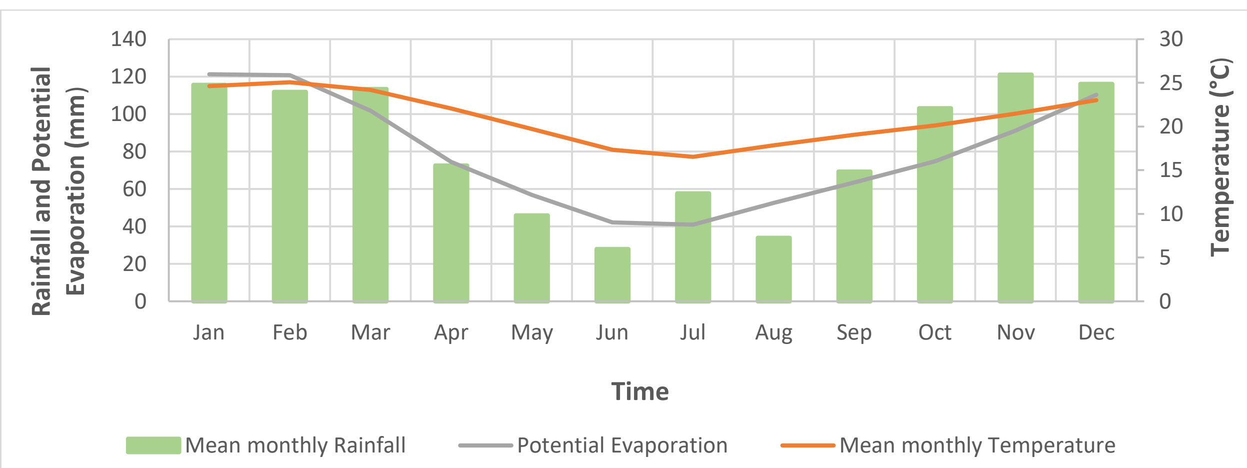

Figure 5. 1. Mean monthly rainfall, potential evapotranspiration and mean monthly temperature for the study area (rainfall data from Louis Botha -WK station sourced from SAWS, 2019).

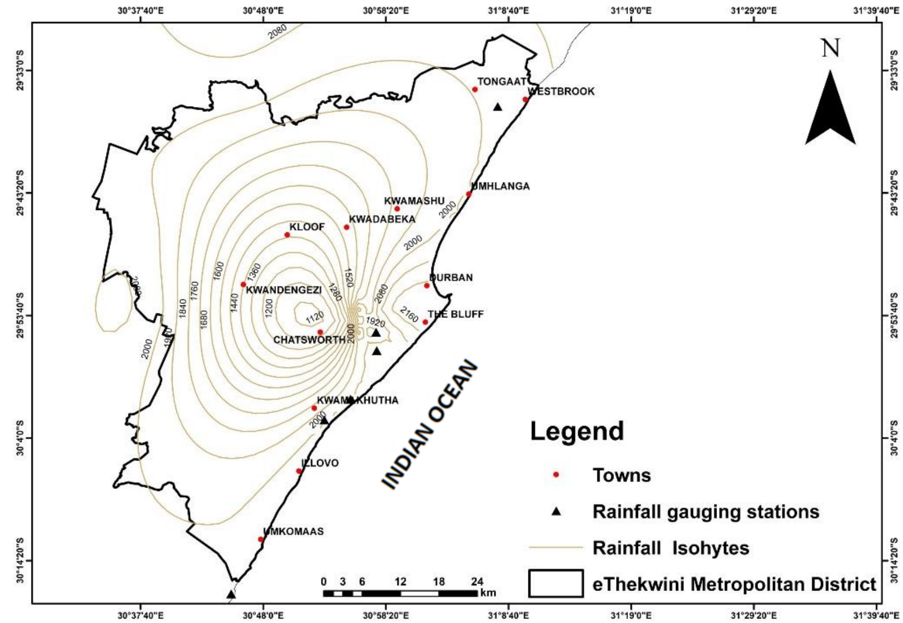

Figure 5. 2. Spatial distribution of rainfall across the study area.

5.1.2 Surface Runoff

The Soil Conservation Service Curve Number (SCS-CN) method as described in the preceding chapter was used to estimate surface runoff in this study. Surface runoff, an important element of the hydrological cycle, is functions of rainfall intensity and duration, soil type, soil moisture, land use/cover and slope. The SCS Runoff Curve Number (CN) (SCS, 1986) was assigned based on hydraulic conditions for each land use and hydrologic soil group (HSG). The estimated mean monthly runoff for the study area is presented in Table 5.1 and the mean annual estimated runoff rate is 198.88 mm/a or 14.2% of mean annual precipitation (MAP) (Figure 5.3). Highest runoff occurs in built up areas due to the presence of impervious surfaces which make up 80% of the land use, whereas low runoff occurs in grassland and forest. The highest runoff occurs during the rainy season from October to March and low during the dry season between April and September. The estimated direct runoff separated using WHAT methods from the total river discharge measured at the river gauging stations indicate that runoff decreases from north to south along the Umngeni River. The decreased may be attributed to evapotranspiration, infiltration and upstream diversions for various uses.

Table 5. 1: Summarized monthly runoff (mm) estimated using the SCS curve number method.

Month	JAN	FEB	MAR	APR	MAY	JUN	JUL	AUG	SEP	OCT	NOV	DEC
Runoff (mm)	32.43	28.44	24.61	3.05	2.75	0.16	1.70	0.08	7.90	25.99	30.08	41.69

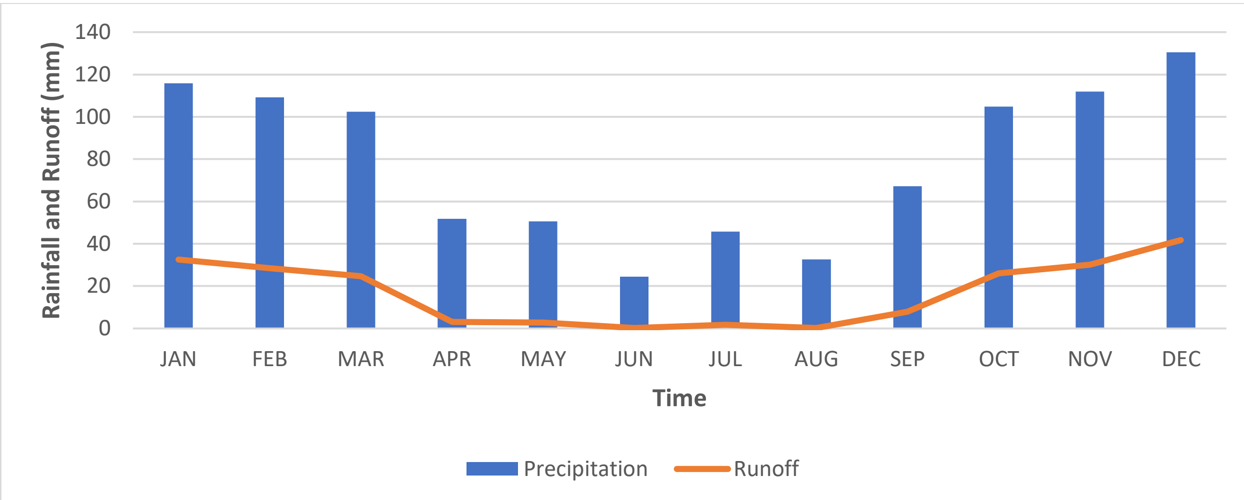

Figure 5. 3. Graph showing average monthly rainfall and average monthly runoff estimated using the Curve Number Method.

5.1.3 Groundwater contribution to baseflow

Baseflow is critical for sustaining stream and river flows during dry seasons and as such responsible for the low flow of rivers. In a groundwater-surface water connected systems, groundwater recharges streams and rivers in some reaches, while in others surface water loose water to recharge the groundwater (Kuusisto, 1996). Baseflows were analysed in the study area along the uMngeni River. The uMngeni River drains partly in urban areas that are dominated by impervious surfaces and densely populated settlements. Furthermore, the uMngeni River is regulated by a number of dams in the upstream reaches, namely, the Spring Grove, Midmar, Albert Falls, Nagle and Inanda Dams (Dickens, 2016). Part of flow is stored in the reservoirs and carried via water supply pipes and the river flow changes from upstream to downstream due to these human interventions. Consequently, less in-stream infiltration takes place, reducing groundwater recharge.

The difference between stream flow components is observed. Three gauging stations, namely, U2HO52, U2HO54 and U2HO55 (Figure 5.4) located along the uMngeni River were used to analyse the variability of stream flow. Total stream flows were separated into direct runoff and baseflow using a web-based hydrograph analysis tool (WHAT) to understand the variability of groundwater contribution to streamflow and consequently understand the interaction between groundwater and surface water in the study area. The gauging station 1 (U2HO52) located upstream close to the Nagle dam has a low base flow rate of 78.6 m^3/s. Baseflow increases downstream with a discharge rate of 320 m^3/s at gauging station 2 (U2HO55). The base flow further decreases to 10.3 m^3/s downstream in gauging station 3 located close to Inanda dam (U2HO54) towards the eastern side of the study area. The low discharge rate observed in gauging station 1 and 3 are influenced by the close proximity to the dams. Thus, as expected the regulated discharge rates have affected the stream flow components. Since the baseflows are relatively low, the groundwater contribution to stream flow is relatively low especially during rainy seasons. Stream hydrograph (Figure 5.5) shows how the stream flow contribution of direct runoff and baseflow vary. Urbanization has altered the natural hydrologic regime, where the amount and timing of water flow through streams vary greatly. These variations are also attributed to climate, topography, surface water, groundwater and human activities (Prince, 2011). The LULC have substantially changed the landscape, gradually shift from forested areas to agricultural and urban landscape, where impervious surfaces have dominated that promote rapid runoff and decreases infiltration to groundwater, therefore limiting the amount of baseflow to the stream.

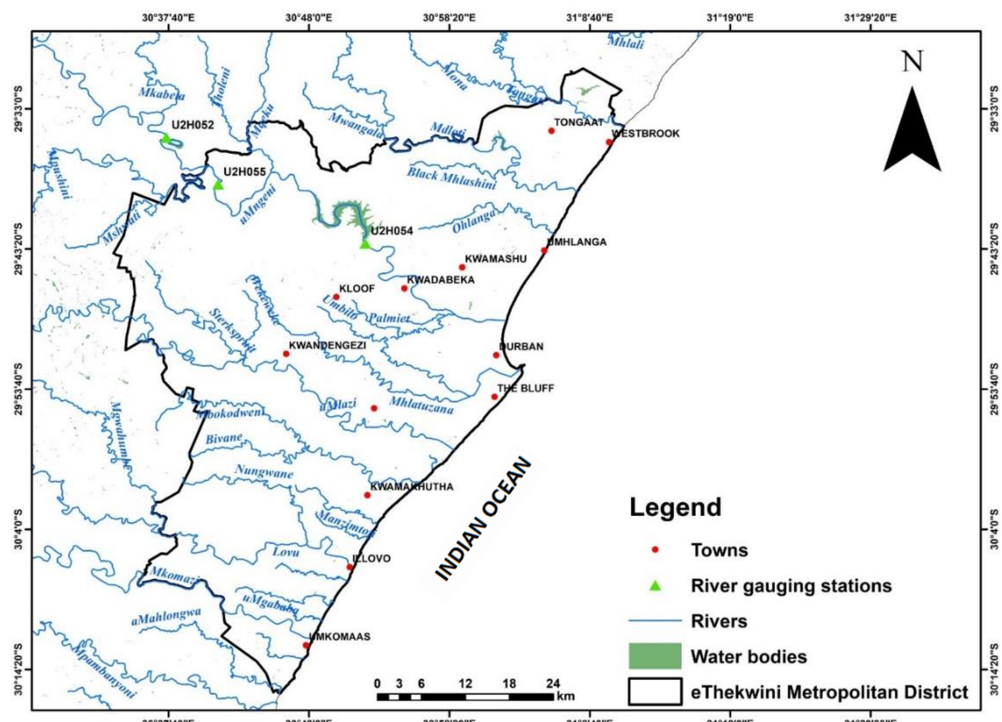

Figure 5. 4. Distribution of Gauging stations across a drainage map.

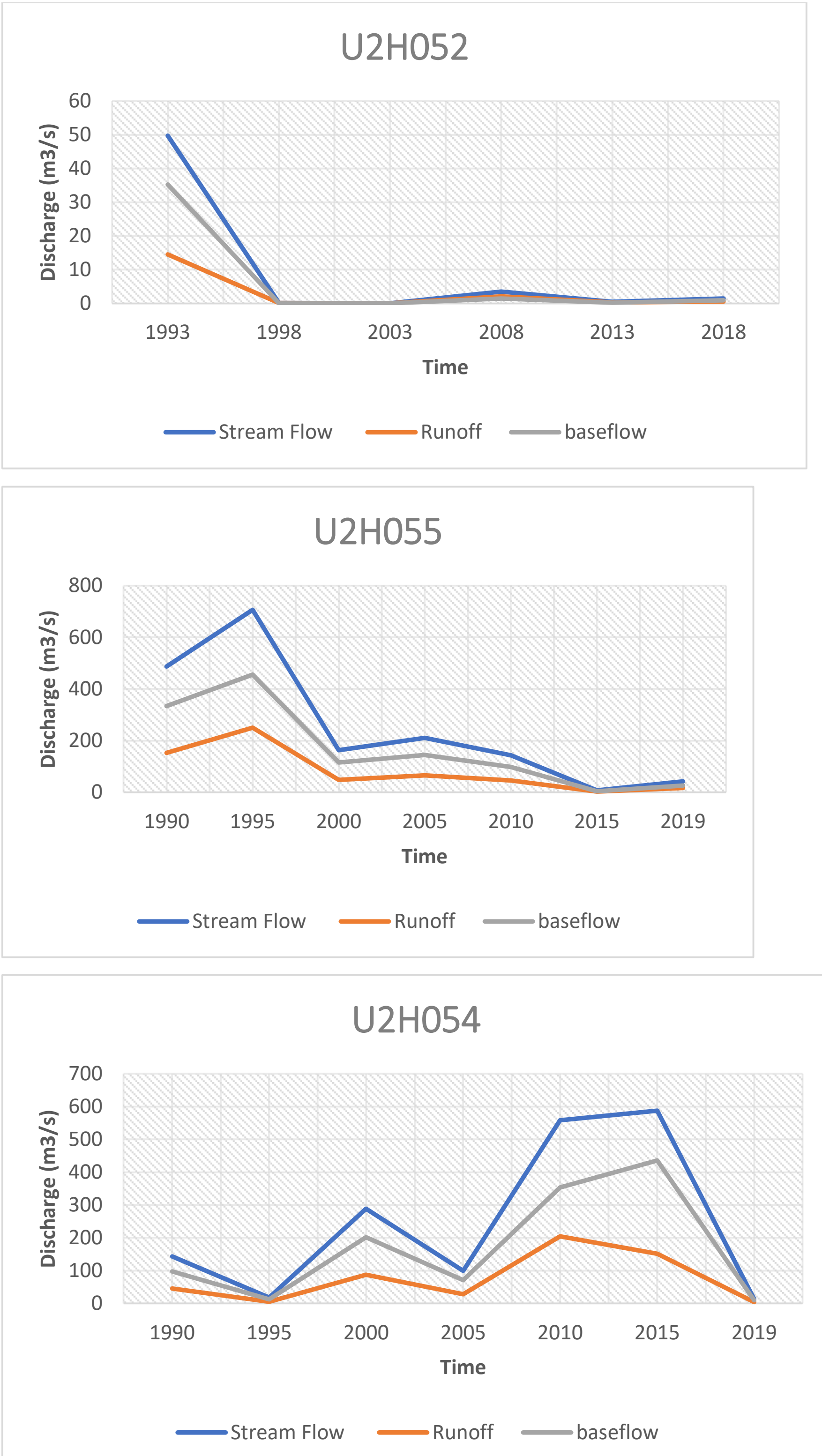

Figure 5. 5. Stream hydrograph in three gauging stations along the Umngeni River (modified from Lim and Engel, 2004).

5.2 Hydrogeological characteristics of the eThekwini Metropolitan District

5.2.1 Characterisation of the eThekwini Metropolitan District aquifers

The study area is part of the Lower uThukela Groundwater Region, which is part of the larger Kwazulu-Natal Coastal Foreland Hydrogeological Region (IMP, 2012). The Lower uThukela Groundwater Region is characterised by basement rocks, largely impermeable granites of the Basement Complex and is overlain by the Natal Group Sandstone (NGS), which form a secondary/fractured aquifer. Furthermore, the NGS is unconformably overlain by the Karoo Supergroup deposits which form a secondary (weathered and fractured) aquifers (IMP, 2012). Figure 5.6 shows the study area's groundwater occurrence, which is dominated by fractured aquifers with yields ranging between 0.1 and 0.5 l/s in the central region, with weathered and fractured aquifer with a yield range between 0.5 and 2.0 l/s along the north-eastern part of the study area and weathered and fractured aquifer with a yield range between 0.1 and 0.5 l/s in the northern and southern section of the study area. These aquifer yields are indicative of typical poor to moderate productivity aquifers in the study area. The Natal Group and Dwyka Group are fractured aquifers in the study area, where the former contributes significantly to groundwater storage, circulation via interconnected faults, joints and bedding planes (Bell and Maud, 2000). The mean aquifer characteristics (Table 5.2), including the transmissivity and hydraulic conductivity vary greatly due to the heterogeneity of the lithologies.

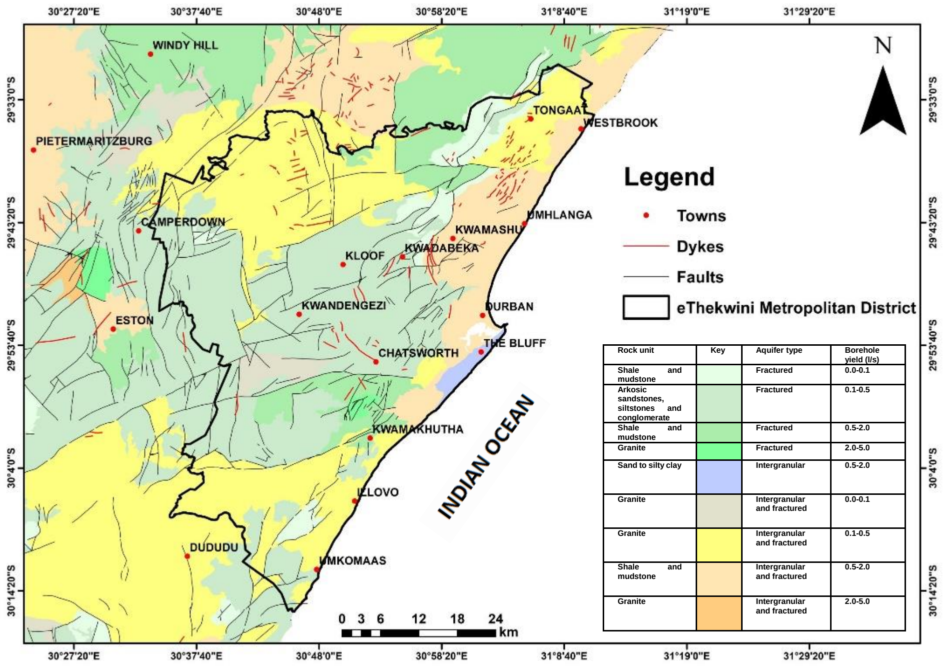

Rock unit	Key	Aquifer type	Borehole yield (l/s)
Shale and mudstone		Fractured	0.0-0.1
Arkosic sandstones, siltstones and conglomerate		Fractured	0.1-0.5
Shale and mudstone		Fractured	0.5-2.0
Granite		Fractured	2.0-5.0
Sand to silty clay		Intergranular	0.5-2.0
Granite		Intergranular and fractured	0.0-0.1
Granite		Intergranular and fractured	0.1-0.5
Shale and mudstone		Intergranular and fractured	0.5-2.0
Granite		Intergranular and fractured	2.0-5.0

Figure 5. 6. Hydrogeological Map of the eThekwini Metropolitan District (modified from DWAF, 1998).

Table 5. 2. Mean aquifer characteristics in the study area (modified from Ndlovu et al., 2019).

Time Period	**Geological Unit**		**Aquifer type**	**Thickness (m)**		**Hydraulic Conductivity (m/day)**	**Transmittivity (m^2/day)**	**Storativity**	**Borehole Yield (l/s)**
	Group/Suite	**Rock type/ Formation**							
Permian	Maputuland Group	Alluvium and Estuarine deposits	Intergranular	2-73		6.5	32	0.18	6-36
		Berea Formation		0.5-45		5	4.06		2.5-45
		Bluff Formation		10-78		3.2	9.6		0.1-26
	Ecca Group	Pietermaritzburg shale	Intergranular and Fractured	15-105		0.03	0.28	0.0001- 0.001	0.02-2.4
		Vryheid Sandstone	Fractured			0.17	6.3	0.0001- 0.001.	0.01-16
	Dwyka Group	Diamictite and Tillite	Fractured	5-135		0.8	1.3	0.0005 -0.005	0.1-3.2
Ordovician	Natal Group	Sandstone and siltstone	Fractured	20-350		2.8	8.32	-	0.2-18
Proterozoic	Natal Metamorphic Province	Carbonate	Karstic	-		-	0.05 - 0.5	-	0.5 - 2
	Mapumulo, Oribi and Mzumbe suite	Granitic Basement	Intergranular and Fractured	-		0.56	3.9	-	0.02-8.3

5.2.2 Depth to groundwater, groundwater levels and groundwater flow directions

The study area is characterised by undulating topography with hills and ridges which has a direct influence on the depth to water. The depth to groundwater map interpolated from data measured in the field and complimented with secondary data is shown in Figure 5.7. The depth and shape of the first impermeable layer below the water table strongly affect the depth to groundwater variation (Heeren *et al.*, 2014). Additionally, the variability of the depth to groundwater is influenced by heterogeneity and anisotropic properties of geological units, and topography (Clark *et al.*, 2015). These influences are observed in the study area as depth to groundwater level becomes deep in high elevated areas including in granitic rock units, while it is shallow in flat and low-lying areas and in sedimentary rocks and alluvial deposits. The presence of faults and dykes in the study area not only affect the rate of recharge but also the depth to groundwater. These geological structures are preferential groundwater flow paths and conduits for groundwater recharge and movement.

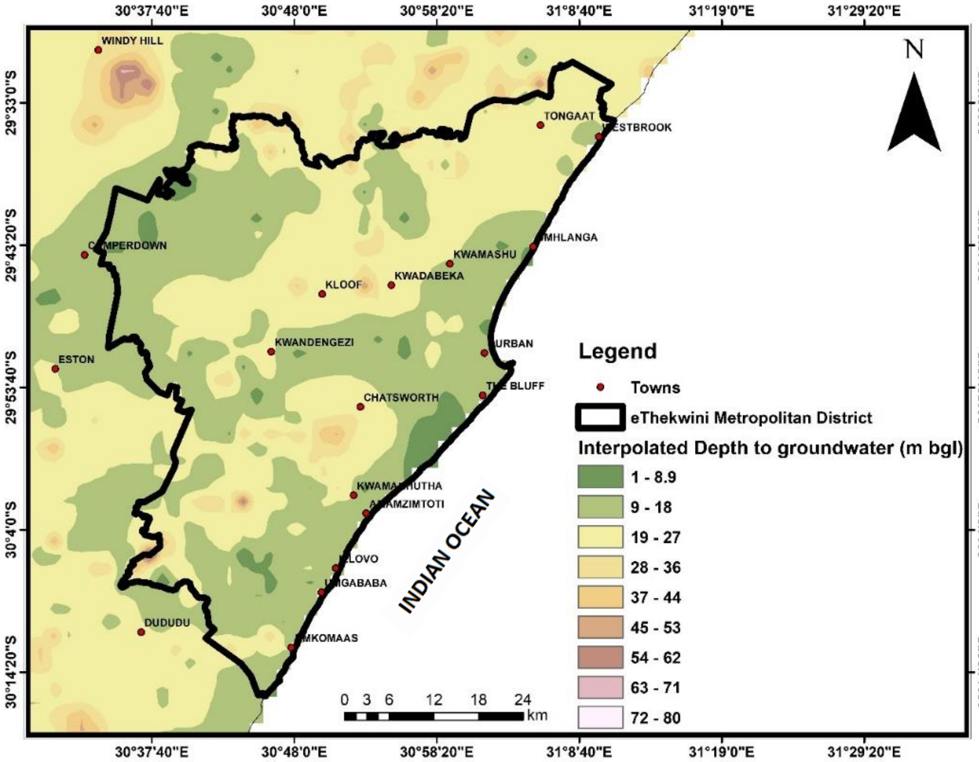

Figure 5. 7. Interpolated depth to groundwater level map of the study area**.**

The groundwater level map of Figure 5.8 shows the spatial distribution of groundwater flow direction in the study area. Groundwater flows from high hydraulic head to low hydraulic head, towards decreasing energy. The groundwater flow responds to differences in energy and groundwater recharges in high elevation areas and discharges to low elevation areas (Fetter, 2014). Similarly, groundwater in the study area flows from high elevated western region to the lower elevation eastern area, where it discharges along the coastline into the Indian Ocean, following a topographic gradient (Figure 5.8). Furthermore, it can also be observed that the groundwater flow converges at rivers and wetlands, indicating that groundwater discharges and contributes to flow in surface water bodies and sustaining wetlands. This in turn indicates groundwater-surface water interaction. On the other hand, the groundwater flow diverges at topographically elevated regions indicating recharge areas.

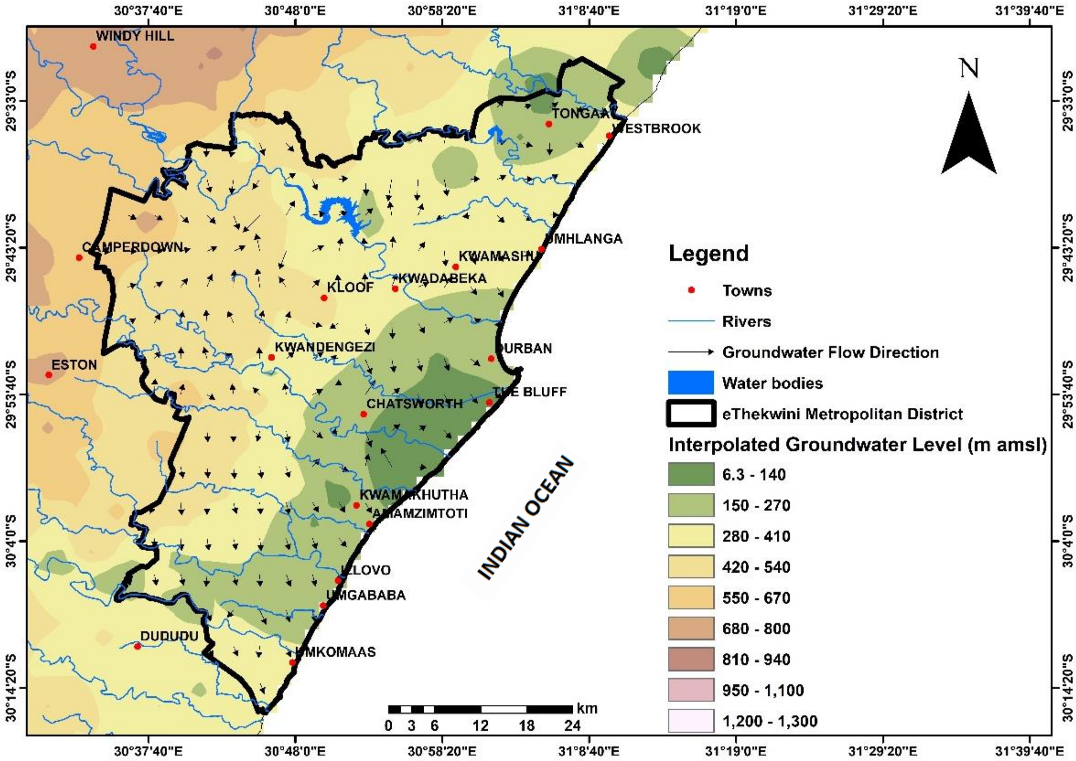

Figure 5. 8. Groundwater level contour map and groundwater flow directions across the study area.

5.2.3 Groundwater recharge, discharge and abstraction

The quantification of natural groundwater recharge and groundwater abstraction rates are prerequisite for efficient and sustainable groundwater resource management. Groundwater abstraction data were sourced from the Department of Water and Sanitation (2019). The total registered groundwater abstraction across the eThekwini Metropolitan region is about $1.9*10^6$ m^3/year, and it is mainly used for irrigation of golf courses and for industrial activities.

The amount of rainfall that turns into streamflow and groundwater recharge depends on several factors including the characteristics of land surface and the vegetation, as they both affect evaporation and infiltration (Brauman et al., 2007; Calder, 2005; Postel and Thompson Jr., 2005). The steepness of the slope increases run-off and so decreases potential recharge (Bell and Maud, 2000). In this study the Chloride Mass Balance (CMB) method was used to estimate groundwater recharge, based on an average rainfall chloride concentration of 7.8 mg/l sourced from DWAF (2006). The estimated recharge rate for the study area ranges from 10.2 mm/a to 253 mm/a with an average recharge rate of 143 mm/a or 14 % of MAP (Figure 5.9 and Table 5.3). The variation in the estimated rainfall recharge is due to a number of factors including urbanization, which brings significant changes in the physical properties of the land surface, modification of slopes, elevations, soils and vegetation coverage (McGrane, 2016).

Natural groundwater recharge is reported to decrease because of the transformation of pervious ground to impervious surfaces, compaction of soil that reduces infiltration of rainwater and engineered pipes that transfer water to the storm-water ways (Arnold and Gibbons, 1996). However, the results of groundwater recharge indicates that it increases from inland towards the coast due to the rate of rainfall and aquifer characteristics.

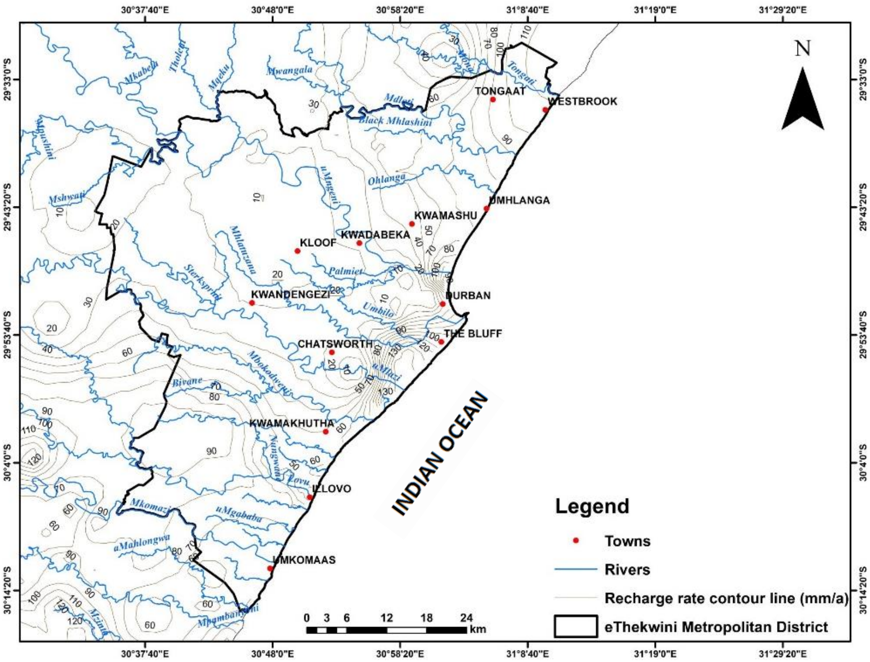

Figure 5. 9. Distribution of estimated groundwater recharge rate contour lines in the study area.

Table 5. 3. Results of groundwater recharge estimated using the chloride mass balance (Ndlovu et al., 2019 and DWS, 2019).

Site ID	Groundwater Cl (mg/L)	Rainfall Cl (mg/l)	Recharge (mm/year)	Recharge (%MAP)
ETM1	78.32	5.50	88.06	9.42
ETM3	28.52	5.50	241.78	25.87
ETM5	44.62	5.50	154.56	16.54
ETM6	36.45	5.50	189.56	20.24
ETM8	33.14	5.50	208.07	22.27
ETM11	108.98	5.50	63.28	6.77
ETM15	69.47	5.50	99.28	10.62
ETM19	52.95	5.50	130.25	13.94
ETM21	54.57	5.50	126.38	13.52
ETM25	102.90	5.50	67.02	7.17
BH1	62.00	5.50	111.23	11.90
BH2	40.00	5.50	172.41	18.45

BH3	94.00	5.50	73.37	7.85
BH4	86.00	5.50	80.19	8.58
BH5	67.80	5.50	101.72	10.88
BH6	192.60	5.50	35.81	3.83
BH7	86.00	5.50	80.19	8.58
BH8	192.00	5.50	35.92	3.84
BH9	82.60	5.50	83.49	8.93
BH20	65.59	5.50	105.14	11.25
BH11	105.60	5.50	65.31	6.99
Mean	80.20	5.50	110.13	11.78
Standard deviation	44.32	0	55.41	5.93
Coefficient of variation	55.26	0	50.31	50.31

5.3 Hydrochemical characteristics of the eThekiwni Metropolitan District

Several factors affect the chemical composition and characteristics of surface water and groundwater in urban and semi-urban areas. These factors include geology, climate, topography, soil, vegetation, aquifer characteristics, hydrological stresses and anthropogenic impacts. Understanding these factors helps in better understanding their contribution to the hydrochemistry of waters in the study area. Urbanization and industrialization and consequent environmental pollution is increasing day by day, so it is essential to assess the quality of water resources for safer use and better management. Therefore, the present study characterises the hydrochemistry of the greater eThekwini Municipality. Suitability of water is evaluated by comparing the value of different water quality parameters against the South African water quality (SAWQ) guidelines for domestic, agricultural and industrial water uses (DWAF, 1996), as well as the World Health Organization (WHO) guidelines for drinking water (WHO, 2017). The hydrochemistry, water quality and the interaction of groundwater and surface water within and around the study area are evaluated based on analyses of major ions, minor constituents and trace elements.

5.3.1 Surface water hydrochemistry

From the collected data, the pH of surface water varies within a range from 6.17 to 10.83 with an average of 6.93 (Table 5.4). This shows that the surface water of the study area is slightly acidic to slightly alkaline but largely neutral. Electrical conductivity (EC) is a function of the concentration of dissolved ions present in a solution and provides an estimate of the total dissolved solids (TDS) (Clark, 2015). The EC that measures the salinity of water, range from 248 µS/cm to 613 µS/cm, with an average of 387µS/cm. The TDS values of surface water range from 28 mg/l to 303 mg/l with an average of 176 mg/l, which indicate freshwater. The total hardness of surface water ranges from 33.74 mg/l to 261.79 mg/l as $CaCO_3$, regarded as soft to very hard (Durfer and Becker, 1964). As a result of diverse activities that takes place such as industrial, agricultural and domestic use. Oxidation –reduction rection (Eh) ranges from 42.6 mV to -45.9 mV and Oxidation reduction potential ranges from 22.8 mV to -16.6 mV. These chemical parameters control the behaviour of chemical constituents in the water as they transfer electrons and indicate free electron ready to be oxidised or reduced. The amount of Dissolved oxygen (DO) ranges from 1.24 mg/l to 4.33 mg/l. Urban land uses influence the hydrochemistry of the study area, where an overall increase in the concentration of Na^+, Cl^-, EC, DO is noted from suburban headwaters towards the developed urban areas in surface waters. The high concentration of Na^+, Cl^-, EC, DO indicate source of pollution, also the change in water color from clour to smoky green color and bad odor most likely as a result of fertilizer runoff (5.8). The pollution is attributed to the anthropogenic activities including industrial, urban and agricultural activities, where uncontrolled discharge of effluent and solid waste may have contributed to it (eThekwini Municipality, 2020). The concentration of the pollutant indicator such as DO, pH, TDS, affecting the salinity of water increase towards the south-eastern side of the study area, where rivers discharge into the Indian Ocean. The high pH value of 10.83 is from a spring located in a highly industrialised area that is exposed to various chemicals and pollutants. In summary, quality of surface water bodies continues to deteriorate at unprecedented rates due to human impact which include agricultural activities, urban and industrial development, mining and recreation.

Figure 5. 10. Photograph showing the Umbilo river with some indications of pollution.

Table 5. 4. Hydrochemical data generated in the course of this study for surface water sampling points (Concentration is in mg/l, EC is in µS/cm and Eh and ORP is in mV)

Sample No	EC	pH	Eh	ORP	Ca	K	Mg	Na	Cl	SO_4	HCO_3
DM01	385	6.17	42.6	22.8	14.5	4.3	10.2	34	0.97	0.63	85.43
DM02	368	7.19	-15.6	-16.6	15.8	4.09	10	30	2.02	1.55	90.31
DM03	197	7.06	-8.2	-0.8	13.3	3.95	4.51	12.6	407	0.78	58.66
DM04	308	6.89	1	16.5	11.2	2.61	8.35	25	0.65	1.29	66.51
DM05	595	6.82	5.8	5.3	25	6.88	14.5	52	2.39	3.61	184.89
DM06	566	6.4	28.1	10.5	15.6	6.91	13.9	60	1.15	0.25	141.57
DM07	613	6.17	42.6	22.8	77	7.33	16.9	45	45	15.4	275.32
DM08	248	7.27	-19.9	4.1	14.1	2.64	6.6	28	43	22	47.92
DM09	443	7.75	-45.9	8.8	24	3.74	8.54	54	47	38.6	118.66
DM10	259	7.16	-13.1	-3.1	10.4	3.87	7.36	29	41	17.3	42.31
DM11	276	7.37	-23.4	-7.6	6.1	1.19	9.67	50	62	17.6	64.07

5.3.2 Groundwater Hydrochemistry

The pH of groundwater in the study area ranges from 6.1 to 8.9 with an average value of 7.6 (Table 5.5). This shows that the groundwater of the study area varies from slightly acidic to slightly alkaline and falls within the normal range of natural groundwater and the permissible limit of the WHO water quality guideline (WHO, 2011). The EC range from 44.40 µS/cm to 1530 µS/cm, with an average of 378.1 µS/cm. The TDS value ranged from 22.53 mg/l to 806 mg/l with an average of 271.90 mg/l, which indicate freshwater. The total hardness of groundwater ranges from 10.08 mg/l to 604.48 mg/l as $CaCO_3$, regarded as soft to very hard water due to different constituent chemicals reaching groundwater including landfill leachate (Durfer and Becker, 1964).

Samples from groundwater, springs, streams, and wetlands in the study area have a similar chemical composition as they tend to plot together as a group (Figure 5.11). The piper trilinear plots in Figure 5.11a reveals that the study area is dominated by alkalis (Na^+ and K^+) over alkaline earth (Ca^{2+} and Mg^{2+}). On the other hand, weak acids (HCO_3^-) exceeds the strong acids (SO_4^{2-}), which reflects recent recharge (DWAF, 1995). The trilinear plot further indicates that all groundwater samples are characterised as Na-Cl-HCO_3 water. Surface water samples are dominated by Na-Mg-Ca-HCO_3 water type. The Durov diagram (Figure 5.11b) shows that the hydrochemical composition in the study area is influenced by dissolution and mixing processes. According to Lloyd and Heathcoast (1985), this trend can be attributed to fresh, recent recharge water dissolving simple salts and mixing with various water sources. The Schoeller diagram (Figure 5.11c) plots the groundwater, streams, springs, and wetlands samples parallel to each other indicating similar composition. The dominant cation is Na^+ with a nearly similar anion concentration of HCO_3^- and Cl^-. In summary, the distribution of hydrochemical parameters of groundwater and surface water within the study area have a similar chemical composition as most samples cluster as a group mixture of groundwater and surface water samples. This indicates groundwater and surface water interaction and probably have the same origin.

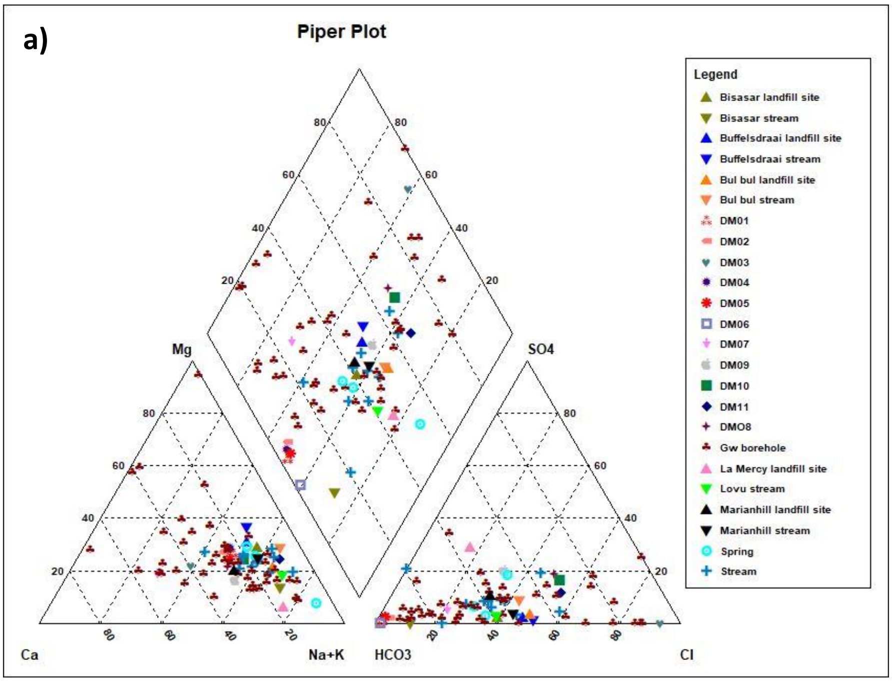

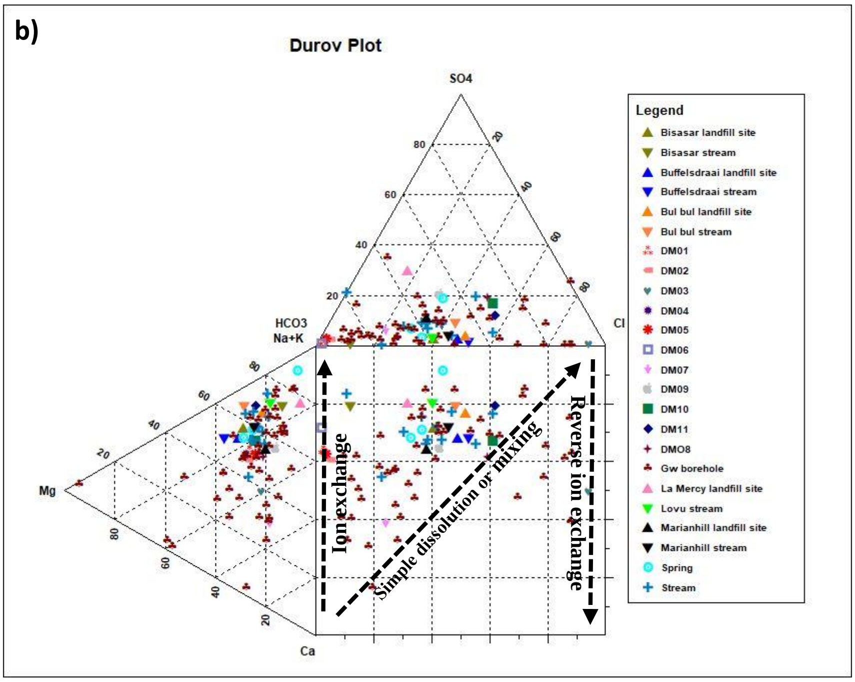

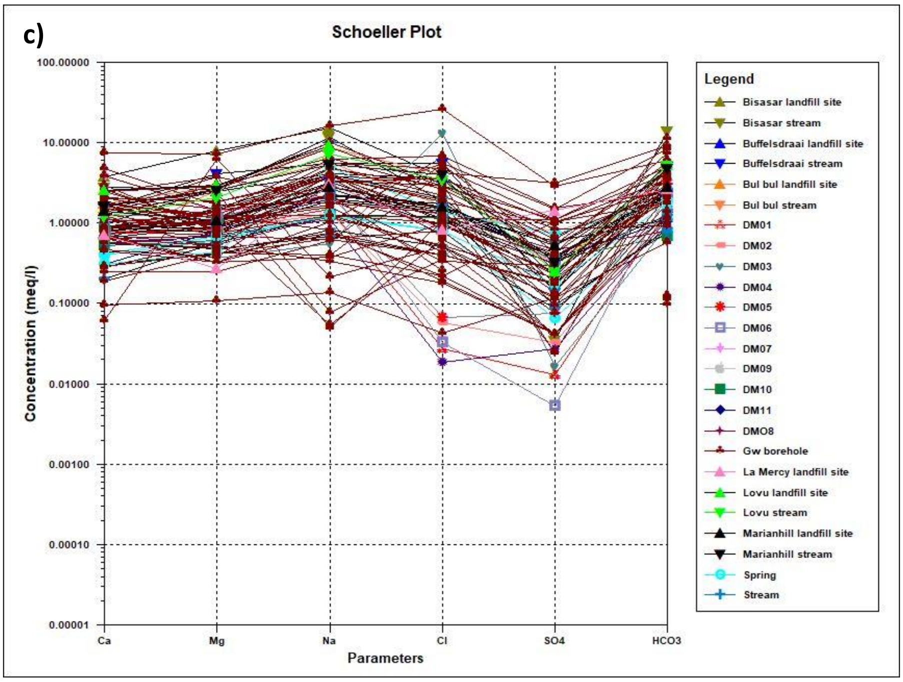

Figure 5. 11. Groundwater hydrochemical characteristics within the study area: (a) Piper trilinear diagram, (b) Durov diagrams and (c) Schoeller diagram (Original data generated in this study complimented with data from GRIP; Vorajee, 2017; Ndlovu, 2019; Ndlovu et al., 2019).

The Gibbs Diagram represent the processes controlling groundwater and surface water chemistry. These include three distinct field such as precipitation dominance, evaporation, and rock-water interaction (Gibbs, 1970). The influence of these processes is clear on the scatter plot, where the predominant surface water samples fall in the precipitation dominance field and the rock-water dominance, indicating that the main controls of surface water hydrochemical composition are precipitation and rock weathering respectively (Figure 5.12a&b). However, some water samples plot outside the solid line, which indicate other influencing factors, such as cation exchange, evaporation and human factors have influence on the major composition. The predominant process controlling the groundwater composition is also precipitation and rock-water interactions (Figure 5.12c&d). The rock-water interaction field of Figure 5.12d indicates that chemical weathering of rock forming minerals is the major driving force in controlling groundwater chemistry and the chemistry of the percolated water into the subsurface.

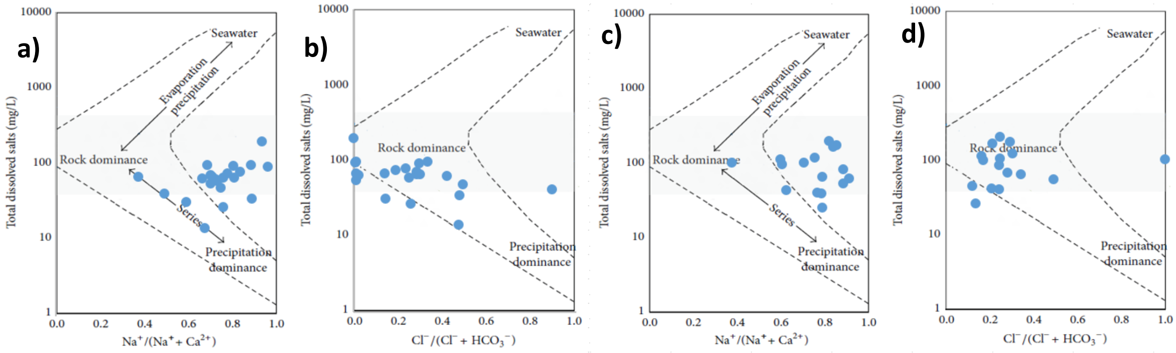

Figure 5. 12. Gibbs diagram indicating a&b) surface water and c&d) groundwater natural evolution mechanisms.

5.3.3 The distribution of water types across the study area

The dominant hydrochemical facies in the intergranular and fractured aquifer of the study area is Na-Mg-HCO_3-Cl (Figure 5.13). Marine influences and coastal hydrogeochemical processes within a predominantly sand to silty clay rock-water interaction that takes place during weathering, dissolution and mixing of minerals including ion exchange processes are attributed to the observed hydrochemical water types. Additionally, land-use changes extentified the discharge of inadequete treated industrial, agriculrural and domestic wastewater contributing to different hydrochemistry in the study area.

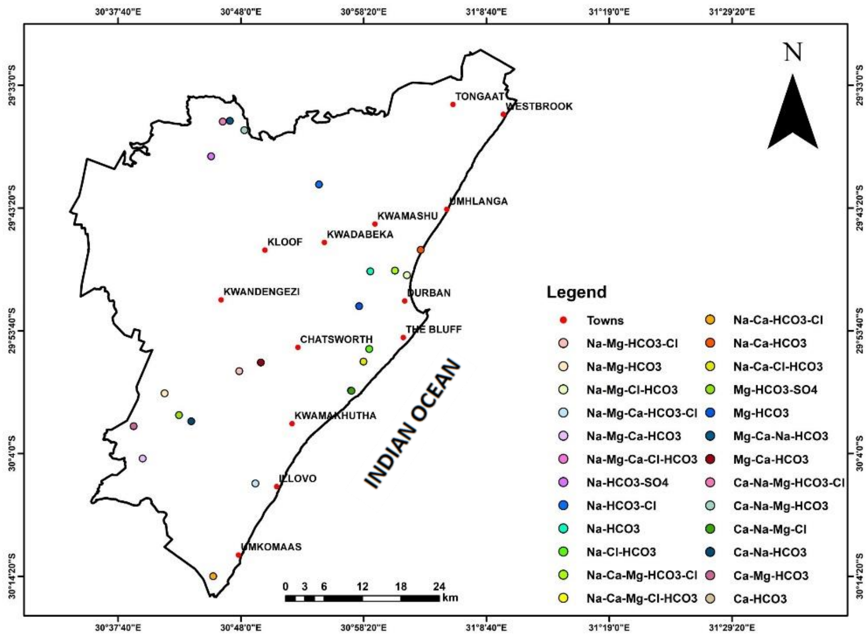

Figure 5. 13. Spatial distribution of groundwater hydrochemical facies in the study area**.**

5.3.4 Statistical analyses of hydrochemical data

Correlation matrix, principal component analysis (PCA) and hierarchical cluster analysis (HCA) were applied on the hydrochemical data to understand the hydrochemical processes controlling the hydrochemistry and the interrelationship between hydrochemical parameters. The hydrochemical data set is assessed based on 84 water samples from rivers, wetlands and groundwater. These water samples come from all hydrogeological units and surface water bodies. The descriptive statistics (Table 5.5) shows the pH range from 6.10 to 8.91, revealing slightly acidic to alkaline water. The Electrical conductivity (EC) varied widely from 4 µS/cm to 1530 µS/cm. Similar to EC, Total dissolve solids (TDS) also showed wide variation (28 mg/l-594 mg/l). The variation in EC and TDS reflected a considerable variation in the hydrochemical characteristics in the different parts of the study area with different types of hydrochemical facies. Considerable variation in the concentration of Na^+ (1.3-270.24), K^+ (1.22-86.37) and HCO_3^-(6.1-852.12) were also observed. These variations highlight that the groundwater chemistry is heterogeneous due to variation in aquifer mineralogy, hydrogeochemical processes and proximity to the coast. Additionally, the land use changes also contribute towards the varied hydrochemistry due to conversion of lands, increasing urban residence, surface runoff and dwelling along surface water bodies such as rivers and wetlands.

Table 5. 5. Description statistics for groundwater and surface water (all concentration in mg/l and EC in µS/cm) (* 0.00 values are due to the instrument limitation used).

Variables	**Range**	**Maximum**	**Minimum**	**Mean**	**Standard deviation**	**Coefficient variant**
Ca	146.37	147.60	1.23	26.25	23.04	530.71
K	86.37	86.37	0.00	5.26	10.30	106.10
Mg	94.25	95.55	1.30	17.26	17.03	289.90
Na	375.70	375.70	0.00	72.24	75.13	5645.12
Cl	928.20	928.20	0.00	76.23	118.61	14068.00
SO4	152.70	152.70	0.00	17.41	26.22	687.66
$HCO3^-$	852.13	852.13	0.00	181.91	148.69	22107.45
pH	2.81	8.91	6.10	7.48	0.60	0.26
EC	1911.50	1915.50	4.00	466.67	428.08	183249.58
Si	32.00	32.00	0.00	10.55	8.03	64.56
TDS	765.00	765.00	0.00	109.79	172.32	29693.45

Pearson's correlation coefficients

To understand the relationship between the various hydrochemical parameters, a bivariate Pearson's correlation matrix of the measured variables was undertaken. It is a simplified statistical tool to show the degree of dependency of one variable on the other (Belkhiri et al., 2010). It measures and establishes the strength of a linear dependence relationship between two variables, or two sets of data expressed as the covariance of the two variables divided by the product of their standard deviation. The resultant dimensionless r values range between +1 and -1, where 1 is perfect positive linear. In this study, correlation among variables with r ≥ 0.5 is regarded to have correlation. Pearson's correlation coefficient (r) is commonly classified as very strong when 0.8<r <1, strong when 0.70<r< 0.79), moderate when 0.5<r<0.69), and weak when r is between 0 and 0.49 (Borradaile, 2003).

The correlation coefficient r among various water quality parameters was calculated and the values are given in the Table 5.6. The results show that EC is moderately correlated to Na^+ (0.59) and HCO_3^- (0.52). $Ca^{2+}$is moderately correlated with Mg^{2+} (0.57) and Na^+ (0.54). K^+ is moderately correlated with Na^+ (0.51) and HCO_3^- (0.51). Mg^{2+} is moderately correlated with Na^+ (0.68). Na^+ is moderately correlated to Cl^- (0.50). Cl^- is moderately correlated with SO_4^{2-} (0.58). TDS, pH and silica shows weak correlation with other samples.

Table 5. 6. Pearson's correlation coefficients between major ions concentrations measured.

Variables	**pH**	**EC**	**TDS**	**Ca^{2+}**	**K^+**	**Mg^{2+}**	**Na^+**	**Cl^-**	**SO_4^{2-}**	**HCO_3^-**	**Si^+**
pH	1										
EC	-0.08	1									
TDS	-0.01	0.44	1								
Ca^{2+}	0.10	0.20	0.04	1							
K^+	-0.02	0.47	0.02	0.34	1						
Mg^{2+}	0.01	0.36	0.04	0.57	0.31	1					
Na^+	-0.02	0.59	0.28	0.54	0.51	0.68	1				
Cl^-	0.10	0.16	-0.11	0.47	0.24	0.44	0.50	1			.
SO_4^{2-}	0.19	0.12	-0.12	0.20	0.06	0.12	0.28	0.58	1		
HCO_3^-	0.18	0.52	-0.05	0.39	0.52	0.28	0.35	0.29	0.31	1	
Si^+	0.18	0.20	-0.01	0.11	0.10	0.14	0.13	0.15	0.08	0.38	1

Hierarchical Cluster Analysis

Hierarchical cluster analysis (HCA) was performed to classify groundwater and surface water hydrochemical data and understand their relationship and its controls. HCA was undertaken on the hydrochemical data of 84 sampling points using ward linkage method in Q-mode and based on the squared Euclidean distance between groups. HCA classifies the set of observed hydrochemical data within two or more groups based on combination of interval hydrochemical variables (Brown, 1998). The results of the cluster analysis for this study are shown as a Dendrogram in Figure 5.14. The water samples are grouped according to their similarities in terms of physiochemical characteristics. The variables cluster in 2 major groups (C1 and C2). The presence of two distinct clusters suggests that there may be two distinct sets of influences that are affecting water sample in the study. Cluster 1 is a combination of groundwater samples, springs, streams and wetlands which may be affected by factors such as pollution from landfill site and industrial activities, waste disposal along the rivers. Cluster 2 is dominated by groundwater sample and one river sample and are most likely affected by natural processes including mineral dissolution as the concentration of these elements increased with flow down the hydraulic gradient from west to the east of the study area. Both clusters have a combination of groundwater and surface water indicating the interaction processes taking place.

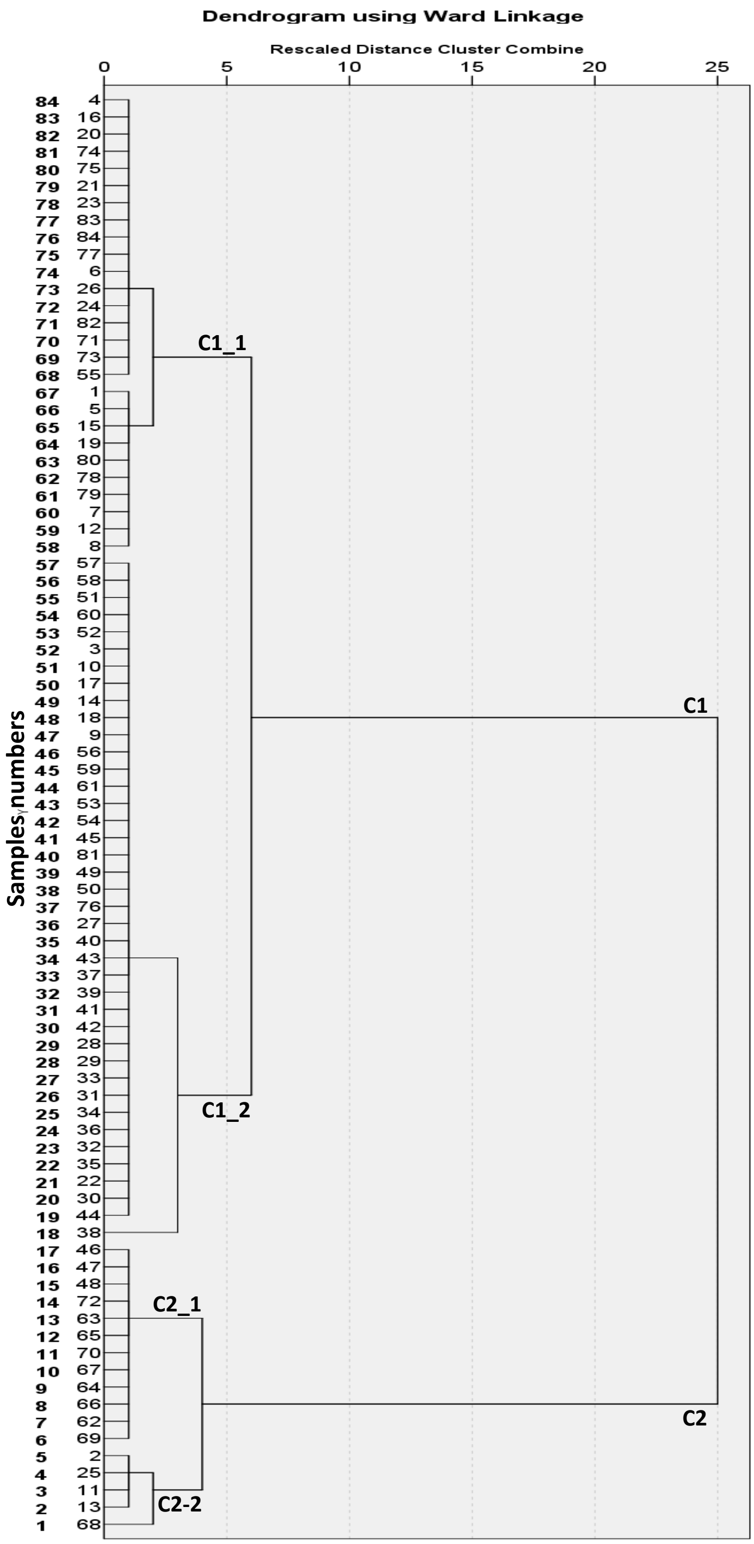

Figure 5. 14. Dendrogram of the HCA undertaken on 84 surface water and groundwater samples.

Factor Analysis

Factor analysis was undertaken using Kaiser-Metyer-Olkin Measure in the form of principal component analysis (PCA) with varimax rotation performed on 84 hydrochemical samples. PCA extract correlations and reduces the amount of data into components that explain a portion of the total variance between chemical parameters. The analysis was performed to identify the factor responsible for variation in groundwater and surface hydrochemistry in the study area**.** The main factors are determined using Catell's (1966) scree plot (Figure 5.15), which involves plotting the extracted component with the eigenvalue greater than 1. The components above the break before the plot become flat are retained as they contribute to the explanation of the variance. According to the scree plot (Figure 5.12), 4 components are identified. These four factors, with eigenvalues greater than 1, explain 69.8% of the hydrochemical variation (Table 5.7). These components can therefore be used to explain the hydrochemical processes without losing the most important characteristics. Component 1 contains most of the variance (28.7%) having high positive loading factors for Na^{+}, Mg^{2+}, Ca^{2+}, Cl^{-} and concentrations. Industrial effluent, sewer leakage, and wastewater could also be the source of these constituents as the study area is located in an urban to peri-urban environment. Component 2 account for 16.0 % of the explained variance in the hydrochemical data and shows high loading for HCO_3^{-}, Si^{+4}, K^{+} and EC. Component 3 accounts for 13.0% of the explained variance in the hydro-chemical data and shows high loading for TDS. Component 4 accounts for 12.1% of the explained variance in the hydro-chemical data and shows high loading for pH and SO_4^{2-}.

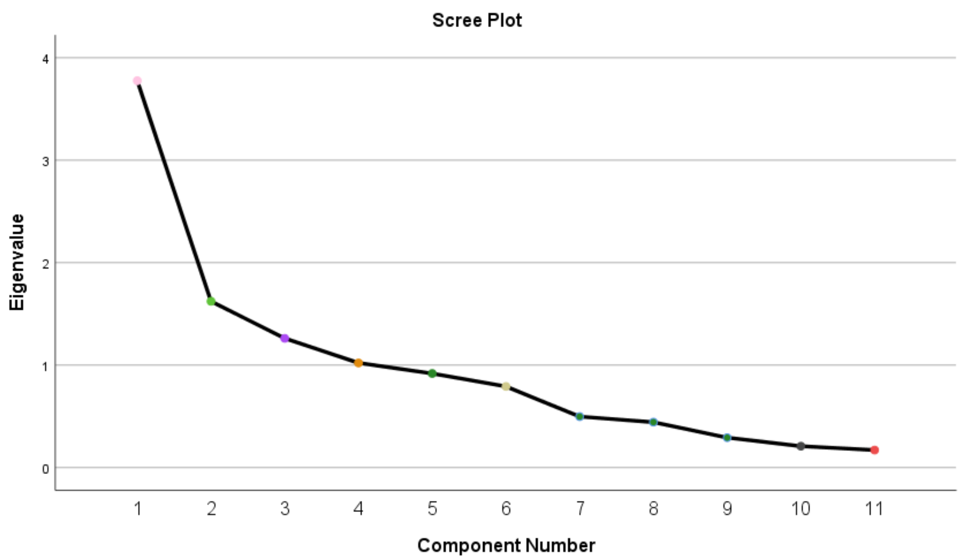

Figure 5. 15. Scree plots showing the four values that have eigenvalue greater than 1.

The relationship of various hydro-chemical variables relative to the dominant or principal components determined in Table 5.7 are illustrated in the varimax plot of Figure 5.16. Where most of the communalities were above 0.5, indicating a high communality of variables factor in the study area. Si^{+}

is derived from the weathering of granite, conglomerate and the dominant sandstone of the study area. Where SO_4^{2-}, Na^+, Mg^{2+}, Ca^{2+}, Cl^- are clustered together due to geogenic processes and EC, K^+, HCO_3^-, Si^{+4} is influenced by anthropogenic processes.

Table 5. 7. Results of principal components analysis of hydro-chemical data for all groundwater and surface water samples.

Variables	Communalities		Components			
			1	2	3	4
pH	1.00	0.60	-0.06	0.20	0.04	0.75
EC	1.00	0.78	0.39	0.51	0.13	-0.16
TDS	1.00	0.90	0.02	-0.07	0.95	0.01
Ca	1.00	0.57	0.75	0.11	-0.04	0.03
K	1.00	0.67	0.46	0.59	-0.00	-0.34
Mg	1.00	0.63	0.78	0.08	0.09	-0.11
Na	1.00	0.83	0.83	0.17	0.35	-0.07
Cl	1.00	0.75	0.77	-0.03	-0.18	0.36
SO4	1.00	0.62	0.47	-0.02	-0.15	0.61
HCO3	1.00	0.78	0.37	0.79	-0.05	0.12
Si	1.00	0.54	-0.01	0.66	0.02	0.32
Initial Eigenvalues	**Total explained**		3.16	1.76	1.43	1.33
	% of Variance		28.73	15.97	13.02	12.09
	Cumulative%		28.73	44.71	57.73	69.82

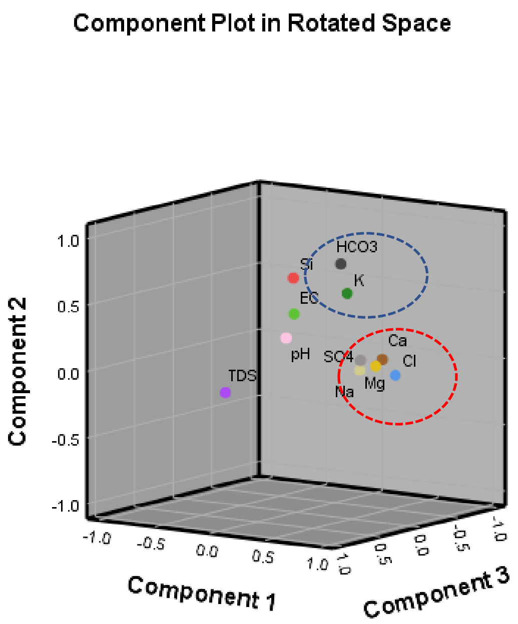

Figure 5. 16. Principal component plot of the variables in rotated space**.**

5.4 Environmental isotope characteristics of the eThekwini Metropolitan District

5.4.1 Stable environmental isotopes

Stable isotopes (Deuterium and ^{18}O) are naturally existing heavy isotopes of water that are conservative in nature (Kendall and McDonell, 1998). Stable isotopes provide information about water circulation, recharge and discharge and help identify the source of different recharge sources. The environmental isotopes are used to reveal the interrelationships between surface water and groundwater effectively. The stable isotopic compositions ($\delta^{18}O$ and δD) of groundwater and surface water samples within the study area are plotted along the Global Meteoric Water Line (GMWL) and Local Meteoric Water Line LMWL Figure 5.17 and the data is presented in Appendix 2.3. The samples plot along the LMWL indicating that groundwater and surface water originates from local precipitation and from meteotic sources. The samples that plot below the LMWL indicate that water was subjected to secondary fractionation before recharge, hence the slope is less than 8. The general isotopic values of all water samples in the study area range from -8.78 ‰ for δD, and from -4.18 ‰ to 2.22 ‰ for $\delta^{18}O$. The isotope samples plot along the global and local meteoric water lines (Craig, 1961), indicating that precipitation is the recharge source of water in the study area. These samples are clustered in 3 groups due to different hydrological processes, while samples within each cluster share the same rainfall source and or hydrological process. Groundwater samples have relatively depleted isotopic signal indicating some preferential recharge mechanisms without evaporation (Figure 5.17). Whereas surface water and some groundwater samples shift towards the heavy isotopic signature. The presence of groundwater samples in heavy isotopic signal gives a clue that, these samples may have undergone evaporation prior to infiltration and most likely to be recharged from surface water sources. This gives an indication of groundwater- surface water interaction. A highly enriched spring sample due to secondary evaporation

(Clark and Fritz, 2006), lie on the right side below the meteoric water lines is located in an highly urbanized area. It is recharged from highly evaporated water sources including water from various anthropogenic water use that have recirculated in the urban area.

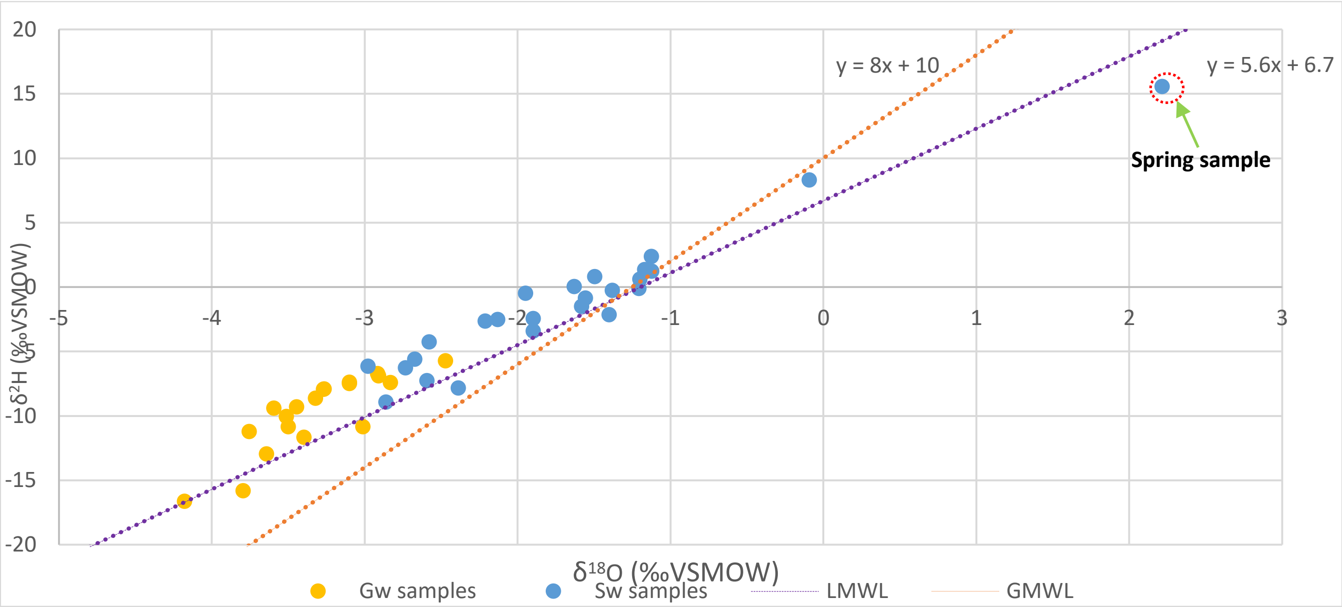

Figure 5. 17. Environmental isotopic ($\delta^{18}O$ and Deuterium) plot of data collected in 2018 and 2020 from groundwater, Streams, springs and wetlands samples along with GMWL (Craig, 1961) and LMWL.

5.4.2 Deuterium-excess

The deuterium excess (d-excess), which is defined by d-excess = δD - 8x$\delta^{18}O$ (Dansgaard, 1964), is one of the most useful tools to study the features of water vapour sources, such as the humidity of vapour source region or the evaporation effect during rainfall (Clark and Fritz, 1997). In the study area, the d-excess of water samples varied with a large scale from -7.9 ‰ to 18.85 ‰, with an average of 5.48 ‰. Appendix 2.3 shows that almost all the samples have high d-excess indicating recycled moisture during secondary evaporation (Clark and Fritz, 2006). As high temperatures induce kinetic effects causing water molecules to diffuse during evaporation, resulting in ^{18}O to be concentrated in a weak bond phase (vapour)and deuterium to be concentrate in strong bonds in a liquid phase (water bodies). D-excess was more significant than the intercept of GMWL (10‰) for most samples, which might indicate that the primary evaporation was controlled by the low humidity in the vapour source region (Kendall and McDonnell, 1998).

5.4.3 Environmental isotopes distribution in the eThekwini Metropolitan Region

The highly enriched samples were found in shallow groundwater level at approximately 8.5 m amsl and at lower elevation as the water is highly exposed to evaporation and recharged from urban recirculated waters. The highly depleted environmental isotopes samples are distributed across the study area, along the western, eastern and southern part of the study area. These samples are distributed mainly within the fractured aquifers (Figure 5.18). Where the stable isotope falls into a distinct group, providing information on the secondary processes acting on the water as it travels from precipitation to groundwater or surface water (Baskaran et al., 2009). Groundwater samples are mainly depleted due to recharge that takes place prior to evaporation and surface water samples are enriched as water is exposed to climatic variability including heat that increases evapotranspiration (Baskaran et al., 2009). This is also a case in the study area where stable isotope composition for groundwater samples close to the river is different from the isotopic composition of the groundwater that is farthest from the river. However, groundwater samples may be enriched to some extent when they evaporate before infiltration. The near stream groundwater samples have a relatively enriched isotopic signature, similar to that of river water.

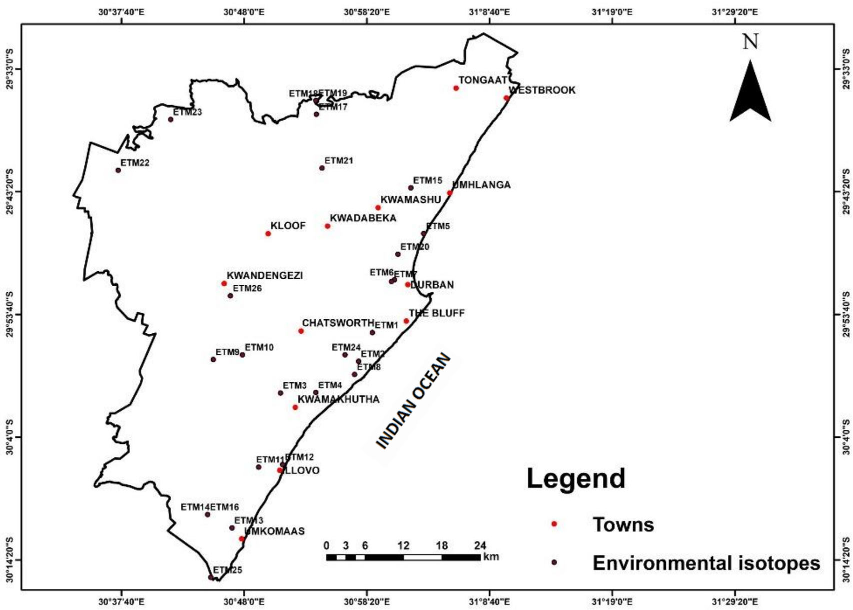

Figure 5. 18. Distribution of environmental isotopes sample points in the study area.

5.5 Land use and land cover changes in the eThekwini Metropolitan District

Land-use and land cover (LULC) are major drivers of water quality deterioration in many areas. These are mainly driven by anthropogenic activities such as over-exploitation of agricultural lands, the conversion of natural vegetation to commercial forestry and rapid urbanization (Namugize et al., 2018). The increase in population and consequence increase in built-up areas leads to a decline in urban greenery. This is the case in the study area where in-migration to urban centres expanded the urban land use due to better urban economic development and industrialization. The 1990, 2013 and 2018 LULC maps of the study area are interpreted to understand the changes over time based on six LULC classes (Figure 5.19a-c). These land use classes are water bodies, wetlands, forested areas, cultivated areas, mines/ bare land and Urban/ built-up areas. The land use classes varied from 1990 to 2018, where water bodies increased by 2.7% due to the building of dams, cultivated land decreased by 25.6% to accommodate built up areas, quarry sites increased by 0.43%, bare land increased by 1.54% and erosional land features decreased by 1.4 % and urban areas increased by 56.7% to accommodate the rapidly growing population. This increase in population has increased informal settlements thereby deteriorating the water quality across the urban and peri-urban catchment, which is also perpetuated by industrial activities and agricultural intensification.

The decline of natural vegetation has a direct impact on runoff and infiltration. Shrinkage of natural vegetation in favour of urban or built-up areas, i.e. the conversion of natural vegetation to resedential land uses increases impervious areas and consequently runoff. This is the case in the eThekwini Metropolitan region, where the urban and industrial sector, has resulted in land-use conversion and encroachment, dam's construction, irrigated agriculture and afforestation have reduced inflow of water to wetlands (UEP, 2016). The rapid economic development and increase in population trigger the expansion of urban-up areas and industrialization. This extensive urbanization has resulted in dramatic reduction and degradation of natural landscapes contributing to the loss of wetlands (Dickens, 2016). Wetlands occupy about 0.53% of the study area in 1990, however, extensive urbanization resulted in dramatic reduction and degradation of natural landscapes contributing to the loss of wetlands to 0.18% in 2018.

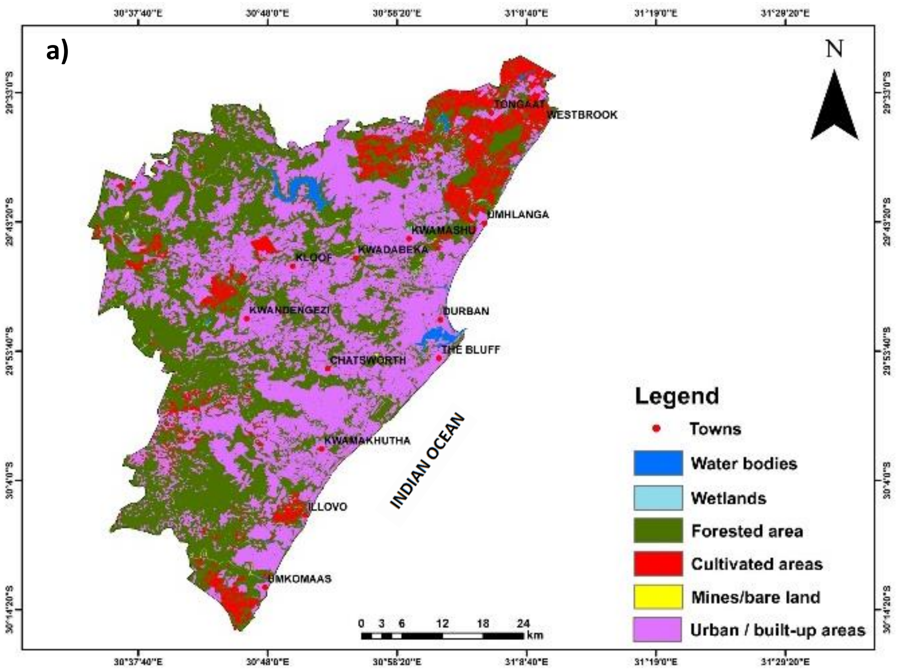

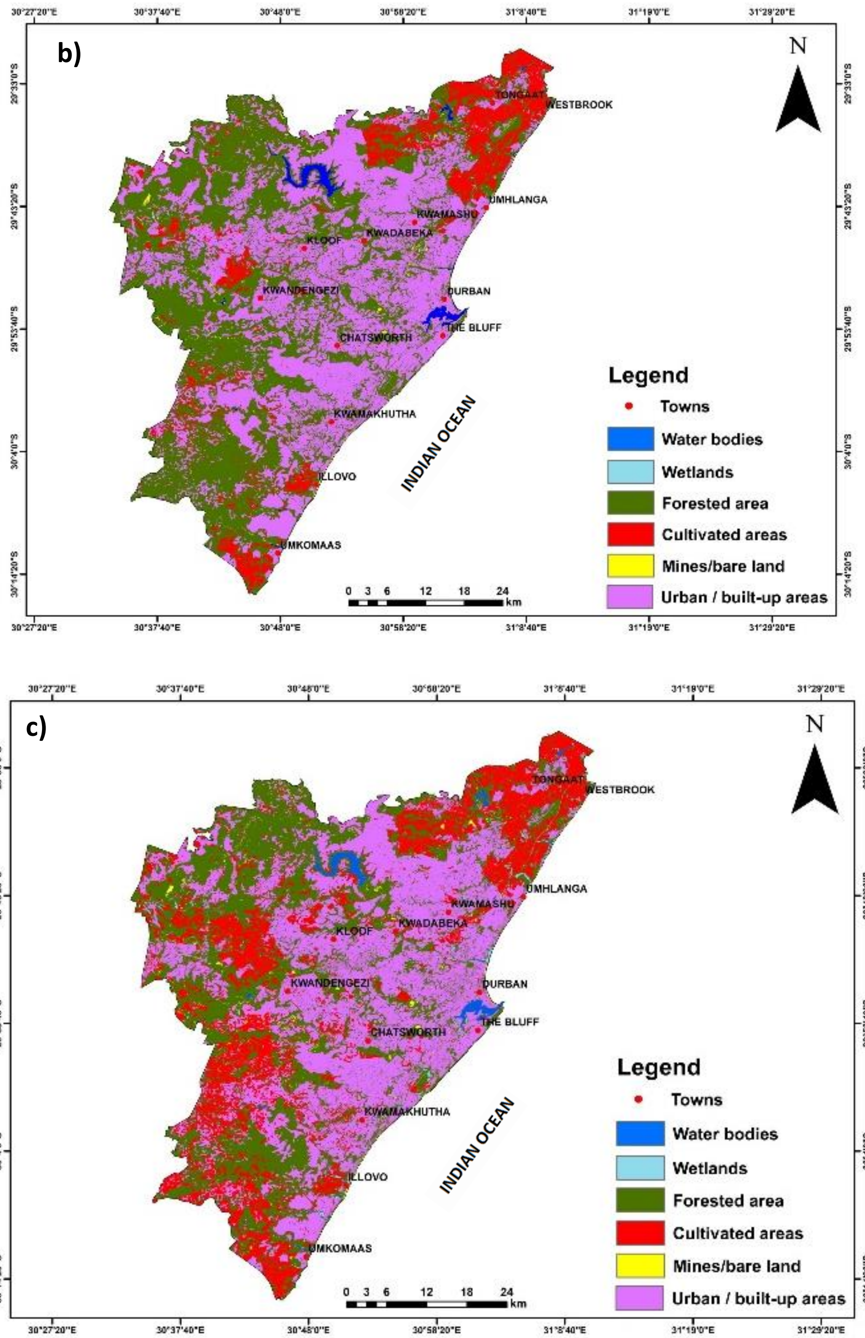

Figure 5. 19. Land use and land cover maps: a) 1990; b) 2013 and c) 2018.

5.6. Groundwater-surface water interaction in the eThekwini Metropolitan District

Groundwater and surface water are hydraulically connected in many landscapes, and a better understanding of their connectivity is critical for the effective management of water resources. Groundwater is known to maintaining surface water bodies such as rivers and wetlands during dry periods. The interaction of groundwater and surface water in the study area is identified using hydrogeological, hydrochemical and environmental isotope evidence which are presented in the preceding sections. Groundwater flows from high hydraulic head to low hydraulic head, in the direction of decreasing mechanical energy or potential, where it discharges to surface depression, wetlands and rivers (Fetter, 2014). This is why groundwater sustain river flows as base flow during the dry season. However, due to prevailing topographic, hydraulic and other conditions, rivers and streams also lose water along some reaches, to recharge the groundwater. Figure 5.20 indicates selected areas where groundwater-surface water interactions were identified in the study area.

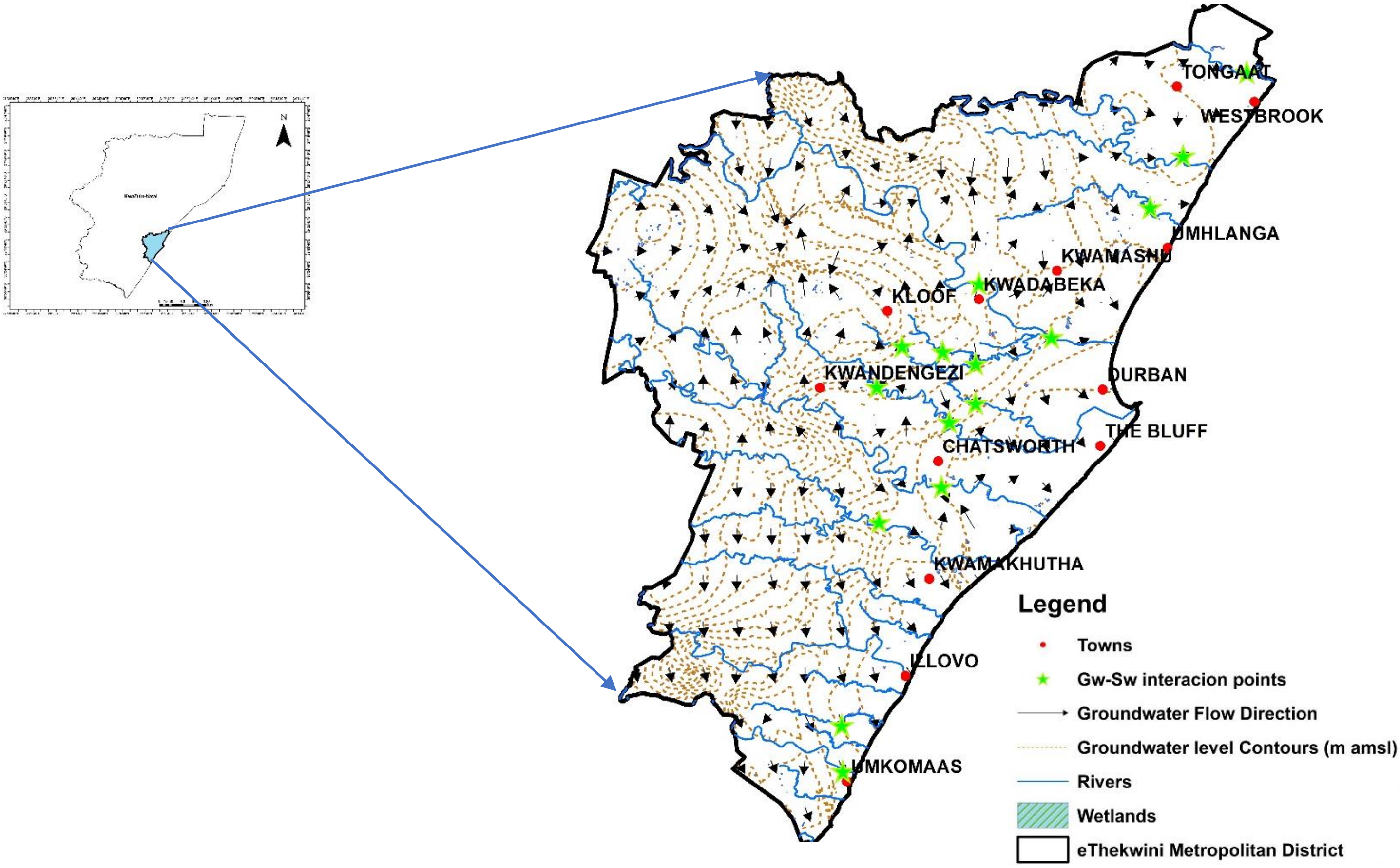

Figure 5. 20. Areas in the study area where groundwater -surface water interactions are identified to occur.

A conceptual model of groundwater-surface water interaction is proposed for selected areas identified based on evidence collected in this study (Figure 5.20). The conceptual models of the groundwater-surface water interactions are developed based on observation of topographical, seepages, groundwater levels, groundwater flow direction, hydrochemical and isotopic evidence. This data was analysed and interpreted using various softwares including Arc-gis, Surfer, Aquachem, Spss and Coral draw to formulate a coceptual model. In some sections, groundwater flows from high head to lower head and discharges to surface depression, wetlands and rivers and streams, where the prevailing hydraulic head difference between the surface water and groundwater levels is the controlling factor (Figure 5.21b). In these cases, a gaining or effluent stream occurs. In other sections, streams occur above the water table and effectively recharging the underlying aquifers, creating a losing stream or influent streams (Figure 5.21 a). Similarly, Figure 5.22b &a indicates a conceptual model of groundwater-wetland interaction in the study area. However, urbanization in the area means that the natural groundwater-surface water interactions has been believed to be changed or modified to a large extent.

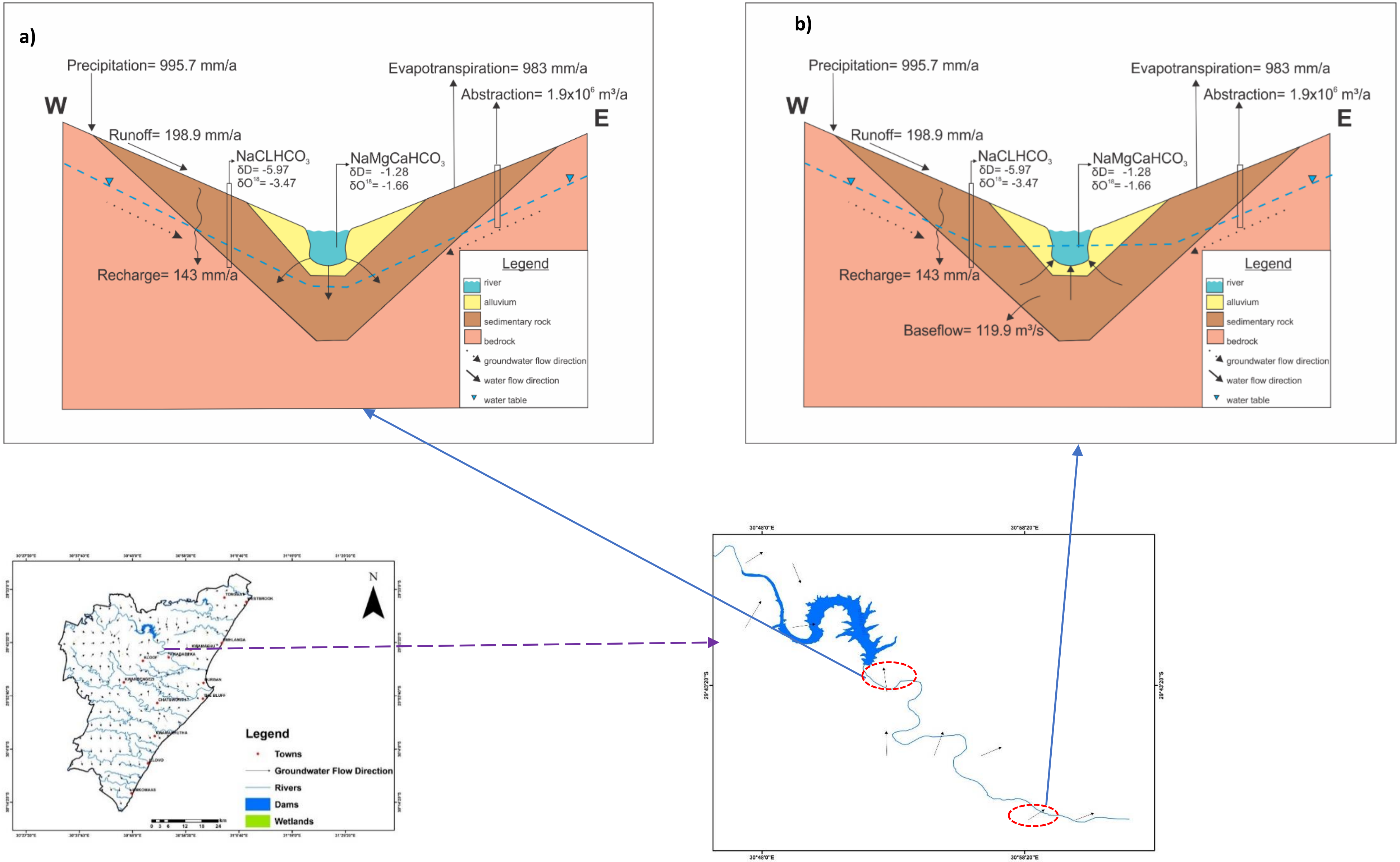

Figure 5. 21. a) Stream losing water to groundwater and b) groundwater flow direction towards rivers.

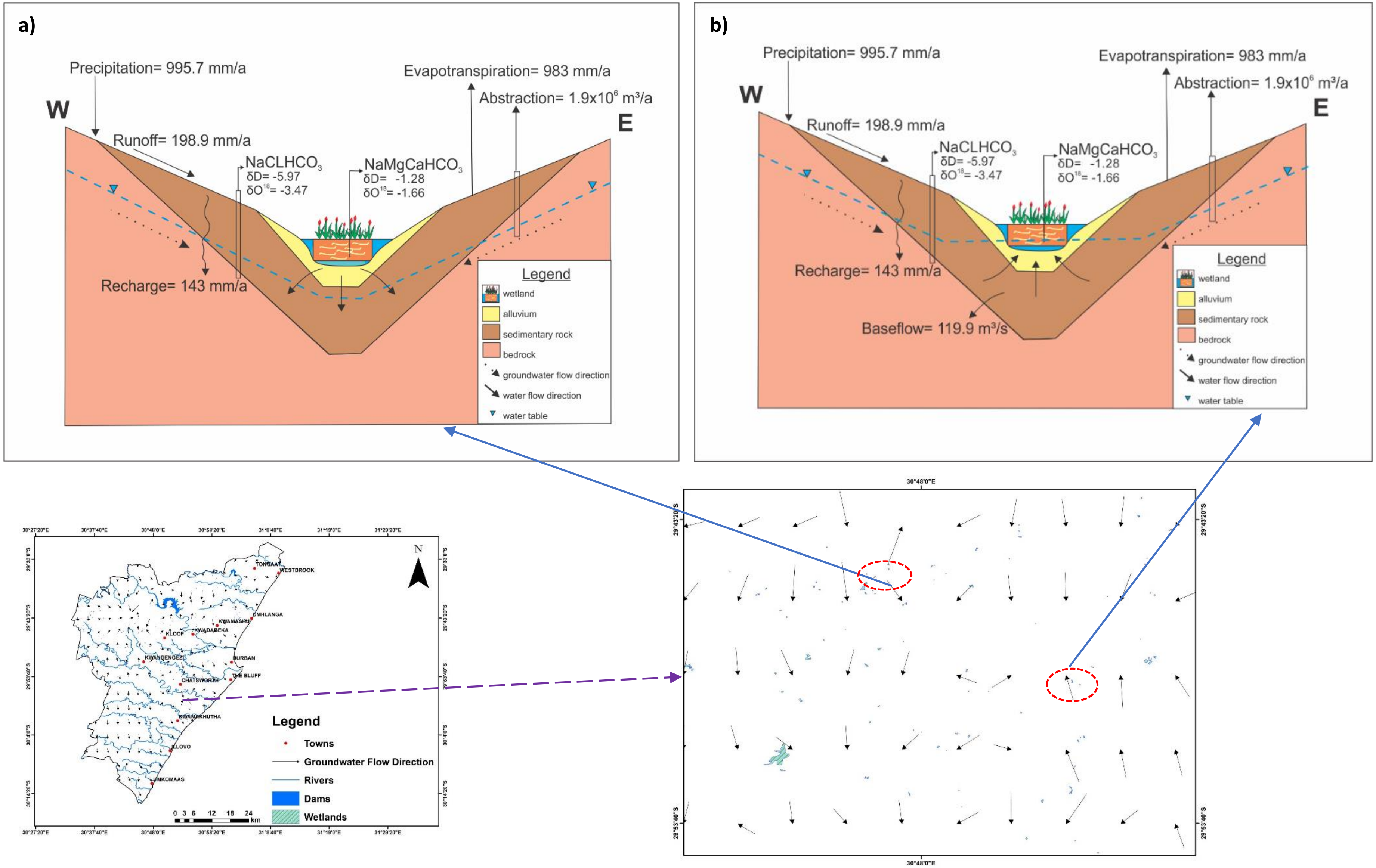

Figure 5. 22. a) Wetland losing water to groundwater and b) groundwater flow direction towards a wetland.

CHAPTER SIX: CONCLUSION AND RECOMMENDATIONS

The various secondary and field data collected, such as hydrometeorological, hydrological, geological, hydrogeological, hydrochemical and environmental isotope data were integrated and interpreted to understand and conceptualize groundwater-surface water interaction in the greater eThekwini region and understand the impact of urbanization. The study has shown that increase in certain LU/LC activities between 1990 and 2018 has resulted in a significant decline in water bodies such as wetlands. However, due to the construction of dams and related structures, water bodies have increased by about 2.7% in area. Urban/ built-up areas increased by about 56% to accommodate the rapidly growing population. The groundwater flow in the area is from west to the eastern side following the topographic gradient and discharges along the coastline into the Indian Ocean. Furthermore, groundwater flow converges at rivers and wetlands, indicating that groundwater sustains and contributes to the flow in surface water bodies and sustains wetlands. This, in turn, indicates groundwater-surface water interactions. On the other hand, the groundwater flow diverges at topographically elevated regions indicating recharge areas. Due to urbanization, the land surface is transformed to accommodate development, affecting the type of flows in some reaches, causing a disconnection between groundwater and surface water, threatening groundwater-dependent ecosystems. Baseflow separated from total stream discharge along the uMngeni River shows that it is relatively low upstream (at U2HO52 gauging stations) indicating a losing stream and increases downstream (at U2HO55 gauging stations) indicating a gaining stream where groundwater discharges and feeds surface water bodies along the reach. The baseflow again decreases further downstream (at U2HO54 gauging station) due to flow regulations by dams.

The estimated water balance components of the study area are such that annual evapotranspiration is about 983 mm/a, annual runoff rate is 199 mm/a, groundwater recharge rate ranges average at 143 mm/a. The spatial distributions of groundwater recharge indicate that it increases towards the coast from inland due to increase in the rate of rainfall and aquifer characteristics. Heterogeneity of the lithologies causes the transmissivity and hydraulic conductivity to vary significantly across the study area, bring about variable in groundwater occurrence: 1) the central region is dominated by fractured aquifers with borehole yields ranging between 0.1 and 0.5 l/s; 2) along the north-eastern sector, weathered and fractured aquifer occur with borehole yields that range from 0.5 to 2.0 l/s. These aquifer yields are indicative of poor to moderate productivity.

Water samples analysed from groundwater, springs, streams, and wetlands in the study area show similar hydrochemical composition indicating similar origin and influenced by dissolution and mixing processes. The dominant hydrochemical water type in the study area is Na-Mg-HCO_3-Cl. The similarity between the composition of groundwater and surface water indicates some degree of groundwater - surface water interactions.

Shallow groundwater levels and groundwater located at lower elevations are characterised by enriched heavy environmental isotopes indicating some degree of evaporation and recharged from urban recirculated waters and surface water bodies. On the other hand, samples with depleted heavy environmental isotope signatures are distributed across the study area, along the western, eastern and southern parts of the study area, mainly within the fractured aquifers indicating direct rainfall recharge without prior evaporation. The stable isotope composition of groundwater samples taken close to the rivers and streams have a relatively enriched isotopic signature, similar to that of the surface water samples indicating that surface water is the primary source of groundwater recharge close to the stream. The hydrochemical, environmental isotope and baseflow information converge to indicate linkage between groundwater and surface water.

Based on the preceding hydrological, hydrogeological, hydrogeochemical and environmental isotopes findings, the following are recommended:

- Continuous monitoring of stream flow and installation of new gauging stations along the main rivers are recommended to improve the baseflow estimation of the catchment.
- Continuous groundwater level monitoring and installation of new monitoring well in the urban centres are required to obtain groundwater flow and hydrochemical data.
- It is recommended that wetland including artificial wetlands be protected and promoted to improve the ecosystem services.
- Further research is recommended to define seasonal changes to groundwater-surface water connectivity and improve the understanding of the mode’s groundwater - surface water interaction.

REFERENCES

Acremen, M.C., and Miller, F. (2007). Practical approaches to hydrological assessment of wetlands lessons from the UK. In: Okruszko, T., Maltby, E., Szatyłowicz, J., Świątek, D., Kotowski, W. (eds) Wetlands; monitoring, modelling and management: Taylor and Francis, London.

Africa, S. (2017). Lithostratigraphy of the pietermaritzburg formation (Ecca group karoo Lithostratigraphy of the Pietermaritzburg Formation (Ecca Group Karoo Supergroup). South Africa', 120(January 2019). doi: 10.25131/gssajg.120.2.293.

Allen, R.G., Pereira, L.S., Raes, D. and Smith, M. (1998). Crop evapotranspiration: guidelines for computing crop water requirements. Irrigation and Drainage Paper, No. 56. Rome: Food and Agriculture Organization of the United Nations, 300p.

Allison, G.B., Barnes, C.J., Hughes, M.W. and Leaney, F.W.J. (1984). Effect of climate and vegetation on oxygen-18 and deuterium profiles in soils. In: Isotope Hydrology 1983, IAEA Symposium 270, September 1983, Vienna, 195-123. In: Clark, I.D. and Fritz, P. 1997. Environmental isotopes in hydrogeology. Lewis Publishers, New York, 328p.

Anderson, M., Woessner, W. W. and Hunt, R. (1990). Applied Groundwater Modelling, Second Edition: Simulation of Flow and Advective Transport. doi: 10.1016/B978-0-08-091638-5.00001-8.

Anderson, J. T. and Davis, C. A. (2013). Wetland techniques volume 2: Organisms, Wetland Techniques: Volume 2: Organisms. doi: 10.1007/978-94-007-6931-1.

Anderson , M.P., Woessner, W.M. and Hunt,R.J. (2015). Applied Groundwater Modelling: Simulation of flow and Advective Transport. Academic Press, San Diego, CA. 720p.

Anwari, M (2018). Modelling land use and land cover change in the western cape province (September), pp. 160–164.

Arnold Jr C. L, Gibbons C. J. (1996). Impervious surface coverage: the emergence of a key environmental indicator. J Am Plann Assoc. 62:243–258.

Baskaran, S., Ransley, T., Brodie, R. S., & Baker, P. (2009). Investigating groundwater-river interactions using environmental tracers. Australian Journal of Earth Sciences, 56(1), 13–19. https://doi.org/10.1080/08120090802541887.

Belkhiri, L., Boudoukha, A. and Mouni, L. (2010). Groundwater quality and its suitability for drinking and agricultural use in AinAzel plain, Algeria.Journal of Geography and Regional Planning Vol. 3(6), pp. 151-157, June 2010.

Bell, F.G. and Lindsay, P. (1999). The petrographic and geomechanical properties of some sandstones from the Newspaper Member of the Natal Group, near Durban, South Africa. Engineering Geology, 52, 57–81.

Bell, F. G. and Maud, R. R. (2000). A groundwater survey of the greater Durban area and environs, Natal, South Africa. Environmental Geology, 39(8), pp. 925–936. doi: 10.1007/s002549900076.

Bello-Schünemann, J. and Aucoin, C. (2016). African urban futures. (November). Available at: https://issafrica.s3.amazonaws.com/site/uploads/af20.pdf.

Bershaw, J. (2018). Controls on Deuterium Excess across Asia. doi: 10.3390/geosciences8070257.

Boone, C.G., Buckley, G.L., Grove, J.M. and Sister, C., (2009). Parks and people: An environmental justice inquiry in Baltimore, Maryland. *Annals of the Association of American Geographers*, *99*(4), pp.767-787.

Botai, C. M, Botai, J. O, Dlamini, L. C, Zwane, N. S. and Phaduli, E. (2016). Characteristics of droughts in South Africa: A case study of free state and North West provinces. Water (Switzerland), 8(10). doi.

Botes, W. (2011). Freshwater wetlands of eThekwini Municipality.

Botha, J. F., Verwey, J. P., Van der Voort, I., Vivier, J. J. P., Buys, J., Colliston, W. P. and Loock, J. C., (1998). Karoo Aquifers. Their Geology, Geometry and Physical Behaviour. WRC Report No 487/1/98. Water Research Commission, Pretoria

Botha, G. A., Bristow, C. S., Porat, N., Duller, G. A. T., Armitage, S. J., Roberts, H. M., Clarke, B. M., Kota, M. W., and Schoeman, P. (2003). Evidence for dune reactivation from ground penetrating radar (GPR) profiles on the Maputaland coastal plain, South Africa. In: Bristow, C.S. and Jol, H.M. (Eds.), Ground Penetrating Radar: Applications in Sedimentology. Geological Society, London, Special Publications 211: 26-46.

Borradaile, G. J. (2003). Statistics of earth science data; their distribution in time, space, and orientation. Springer, New York, 351 pp.

Boyer, T., & Polasky, S. (2004). Valuing Urban Wetlands: A Review of non material valuation Studies. Wetlands, 24(4), 744-755. https://doi.org/10.1672/0277-5212(2004)024[0744:VUWARO]2.0.CO;2

Brauman K.A, Daily G.C, Duarte T.K.E and Mooney H.A (2007). The nature and value of ecosystem services: an overview highlighting hydrologic services. Annu. Rev. Environ. Resour. 32 67–98. https://doi.org/10.1146/annurev.energy.32.031306.102758.10.3390/w8100439.

Braune, E. and Xu, Y. (2009). Groundwater management issues in Southern Africa - An Iwrm perspective. Water SA, 34(6), pp. 699–706.

Brodie R., Sundaram B., Tottenham R., Hostetler S. and Ransley T. (2007). An adaptive management framework for connected groundwater–surface water resources in Australia. Bureau of Rural Sciences, Canberra.

Brown, C.E. (1998). Applied multivariate statistics in geohydrology and related sciences. Springer, Berlin, 248p.

Brutsaert, W. (2005). Hydrology: An introduction. Cambridge University Press, New York.

Bucher, E.H., Bonetto, A., Boyle T., Canevari P., Castro G., Huszar P. and Stone, T., 1993. Hidrovia- an initial environmental examination of the Paraguay - Parana waterway. Wetlands for the Americas Publication No. 10, Manomet, MA, USA, 72pp.

Burden, R. J. (1982). Hydrochemical variation in a water-table aquifer be- neath grazed pastureland. J. Hydrol., 21, 61–75, 1982.

Buss, S.R., Cai, Z., Cardenas, B., Fleckenstein, J., Hannah, D.M., Hepell, K., Hulme, P., Ibrahim, T., Käser, D., Krause, S., Lawler, D.., Lerner, D., Mant, J., Malcolm, I., Old, G., Parkin, G., Pickup, R., Pinay, G., Porter, J., Rhoes, G., Richie, A., Riley, J., Robertson, A., Sear, D., Shields, B., Smith, J., Tellam, J., Wood, P. (2009). A Handbook on the Groundwater–Surface Water Interface and Hyporheic Zone for Environment Managers Integrated Catchment Science Programme. Programme. pp. 1–264 UK Environment Agency Science Report SC050070.

Calder, I.R. (2005). The Blue Revolution: Land Use and Integrated Water Resources Management, 2nd ed. Earthscan Publications, London.

Cattell, R. B. (1966). The scree test for the number of factors. Multivariate Behavioral Research, 1, 245-276.

Chapman, T.G. (1999). A Comparison of Algorithms for Stream Flow Recession and Baseflow Separation. Hydrological Process 13(5):701-714.

Changnon, S.A. (1976). Inadvertent weather modification 1. Journal of the American Water Resources Association, 12(4): 695-715.

Clark, I.D, Fritz, P. (1997). Environmental isotopes in Hydrogeology. Boca Raton, FL: CRC Press /Lewis Publishers.

Clarke, B. M. (2008). The geology of the Natal Metamorphic Province in the Durban area. South African Journal of Geology, 111(1), pp. 1–20. doi: 10.2113/gssajg.111.1.1.

Clark, B. M., Massie, V., Laird, M., Biccard, A., Hutchings, K., Harmer, R., Brown, E., Dun, a. O. O., Makunga, M. & Turpie, J. (2015). The State of Saldanha Bay and Langebaan Lagoon 2015. Anchor Environmental Consultants.

Clark, I. (2015). Groundwater geochemistry and isotopes. Boca Raton: Taylor & Francis Group.

Craig, H. (1961). Isotopic variations in meteoric waters. Science, 133, pp. 1702-03.

Craig, H., Gordon, L.I. and Horibe, Y., (1963). Isotopic exchange effects in the evaporation of water: 1. Low-temperature experimental results. Journal of Geophysical Research, 68(17), pp.5079-5087.

Collins, N.B. (2005). Wetlands: The basics and some more. Free State Department of Tourism, Environmental and Economic Affairs, Free State, South Africa.

Colvin, C, Maitre, D, Saayman, I, Hughes, S (2007). An Introduction to Aquifer Dependent Ecosystems in South Africa: Aquifer Dependent Ecosystems in Key Hydrogeological Type settings in South Africa.

Cornell, D.H., Thomas, R.J., Bowring, S.A., Armstrong, R.A. and Grantham, G. H. (1996). Protolith interpretation in metamorphic terranes: aback-arc environment with Besshi-type base metal potential for the Quha Formation , Natal Province, South Africa. Precambrian Research 77: 243-271.

Council for Geoscience. (1988a). 2930 Durban Geological map series 1: 250 000, South Africa.

Custodio, E. (2000). Utilización de la relación Cl/Br como trazador hidrogeoquímico en hidrología subterránea. Bol. Geolog. y Minero, Vol. 11, Madrid, pp. 49–68.

Dahm, C. N., Grimm, N. B., Marmonier, P., Valette, H. M., and Vervier, P (1998). Nutrient dynamics at the interface between sur- face waters and groundwaters. Freshwater Biology, 40, 427–451.

Dansgaard, W. (1964). Stable isotopes in precipitation. Tellus, 16(4), 436–468.

de Vries, J. J. and Simmers, I. (2002). Groundwater recharge: An overview of process and challenges. Hydrogeology Journal, 10(1), pp. 5–17. doi: 10.1007/s10040-001-0171-7.

Deventer, H. Smith-Adao, L, Petersen, C, Mbona, N, Skowno, A, Nel, J. L. (2018). Review of available data for a south african inventory of inland aquatic ecosystems (Saiiae). Water SA, 44(2), pp. 184–199. doi: 10.4314/wsa. v44i2.05.

Dickens, C. (2016). State of Rivers Report – uMngeni River and neighbouring rivers and streams. (January 2002).

Diouf, O.C, Weihermüller, L, Ba, K, Faye, S. C, Faye, S. and Vereecken, H. (2016). Estimation of Turc reference evapotranspiration with limited data against the Penman-Monteith Formula in Senegal. Journal of Agriculture and Environment for International Development, 110(1), pp. 117–137. doi: 10.12895/jaeid.20161.417.

Durfer, C. N, and Becker, E. (1964). Public water supplies of the 100 largest cities in the United States. U.S. Geological Survey Water Supply 1812, 372 pp.

Dussaillant, A., Galdames P., Sun, C. L.(2009) Water level fluctuations in a coastal lagoon: El Yali Ramsar wetland, Chile. Desalination, pp 202–214.

Department of Water and Sanitation (DWS). (2019). Annual Report: Department of Water and Sanitation - 2019/20 Financial Year. 396.

DWAF (1995). South African Law Review - A Call for Public Response. Department of Water Affairs and Forestry, Pretoria.

DWAF (1996). Water Quality Guidelines Volume 8 Field Guide South African Water Quality (Vol. 8).

41:367–377.

DWAF (1998). 1:500 000 hydrogeological map series of the Republic of South Africa. Durban Sheet 2928.

DWAF (2006). A Guideline for the Assessment, Planning and Management of Groundwater Resources within Dolomitic Areas in South Africa, Volumes 1-3. Department of Water Affairs and Forestry, Pretoria, South Africa.

Department of Water Affairs (DWA). (2010.) Groundwater Strategy 2010. Department of Water Affairs. Pretoria.

Economic Commission for Africa. (2000). United Nations. Economic Commission for Africa; United Nations. Economic and Social Council; United Nations. Economic Report on Africa 2000: Transforming Africa's Economies. Addis Ababa:. © UN. ECA,.

Elliott, H., Brooks, N.H. (1997). Transfer of nonsorbing solutes to a streambed with bed forms: theory. Water Resour. Res. 33 (1), 123–136.

Faller, R. F., Kallehauge, L., Sørensen, U., & Siohan, M. (2010). S Ustainable U Rban D Evelopment in the. January.

eThekwini Municipality (2008). Durban's sustainability best practice portfolio for Water. pp. 15–18.

eThekwini Municipality (2017). Municipal Spatial Development Framework. (January 2019). Available at: http://www.durban.gov.za/City_Services/development_planning_management/Documents/Final Report SDF 2017-2018 To 2021-2022 Main Doc 30 June 201.pdf.

eThekwini Municipality (2018). eThekwini Municipality: Integrated Development Plan (5 Year Plan): 2017/18 to 2021/22). doi: 10.1109/PLANS.2014.6851474.

eThekwini Municipality. (2020). DURBAN STRATEGIC ENVIRONMENTAL ASSESSMENT-Environmental Analysis Phase Environmental Status Quo, eThekwini Municipality, June 2020. September 2020.

Eriksson, E. and Khunakasem, V. (1969). Chloride Concentration in Groundwater, Recharge Rate and Rate of Deposition of Chloride in the Israel Coastal Plain. Journal of Hydrology, 7, 178-197. https://doi.org/10.1016/0022-1694(69)90055-9.

Fan, P., Ouyang , Z, Basnou, C., Pino, J., Park, H., Chen, J. (2017). Nature-based solution for urban landscapes under post-industrialization and globalization: Barcelona versus Shanghai. Environmental Research. Volume 156, July 2017, Page 272-283.

Farvolden, R. N. (1963). Geologic controls on ground-water storage and base flow. Journal of Hydrology, 1(3), 219– 249. https://doi.org/10.1016/0022-1694(63)90004-0.

Fetter, Jr. C, W. (2014). Applied Hydrogeology. Fourth Edition, Applied Hydrogeology Fourth Edition.

Fisher, D. K. and Pringle III, H. C. (2013). Evaluation of alternative methods for estimating reference evapotranspiration. Agricultural Sciences, 4(8A), pp. 51-60.

Ford, C. M. (2016). Characterizing Groundwater Recharge and Streamflow using Stable Isotopes of Oxygen and Hydrogen.

Freeze, R. A. and Cherry, J. A (1979). Groundwater, Prentice-Hall, New Jersey

Gardner, B.D., Pool, D.R., Tillman, F.D.and Forbes, B.T. (2013). Human Effects on the Hydrologic system of the Verde Valley. Central Arizona, 1910-2005 and 2005-2110, Using a Regional Groundwater Flow Model, U.S. Geological Survey Scientific Investigations Report 2013-5029., pp.47.

Gibbs, J.R. (1970). Mechanisms controlling world water chemistry. Science(80-), 170(1970), pp. 1088-1090.

Gillson, J., Suthers, I. and Scandol, J., (2012). Effect of flood and drought events on multi-species, multi-method estuarine and coastal fisheries in eastern Australia. Fisheries Management and Ecology, 2012, 19, 54-68.

Guan, H. Z, Xinping. S, Grzegorz. S. and Zhian X, X. (2013). Deuterium excess variations of rainfall events in a coastal area of South Australia and its relationship with synoptic weather systems and atmospheric moisture sources. 118, pp. 1123–1138. doi: 10.1002/jgrd.50137.

Guggenmos, M.R, Daughney, C. J. Jackson. B. M, and Morgenstern. U. (2011). Regional-scale identification of groundwater-surface water interaction using hydrochemistry and multivariate statistical methods. Wairarapa Valley, New Zealand.

G¨uler, C. and Thyne, G. D. (2004). Delineation of hydrochemical facies distribution in a regional groundwater system by means of fuzzy c-means clustering. Water Resour. Res., 40, 1–11.

Heeren, D. M., Fox, G. A., Fox, A. K., Storm, D. E., Miller, R. B., & Mittelstet, A. R. (2014). Divergence and flow direction as indicators of subsurface heterogeneity and stage-dependent storage in alluvial floodplains.Hydrological Processes, 28(3), 1307–1317. https://doi.org/10.1002/hyp.9674.

Hem, J.D. (1985). Study and Interpretation of the Chemical Characteristics of Natural Water. 3rd Edition, US Geological Survey Water-Supply Paper 2254, University of Virginia, Charlottesville, 263 p.

Hill, R.A. (1940). Geochemical patterns in Coachella Valley. Trans Am Geophys Union 21:46–49.

http://ga.water. Usgs.gov/ edu/watercycle.html.

Infrastructure Master Plan 2012. Umngeni water vol1.

Institute of Soil Climate and Weather (ISCW) (2004). soils formed under Mediterranean-type climate in South Africa

Jabareen, Y.R., (2006). Sustainable urban forms: Their typologies, models, and concepts. Journal of planning education and research, 26(1), pp.38-52.

Jansen, L.J. and Di Gregorio, A., (2003). Land-use data collection using the “land cover classification system”: results from a case study in Kenya. *Land Use Policy*, *20*(2), pp.131-148.

Johnson, M.R., Visser, J.N.J., Cole, D.I., de Wickens, H., Christie, A.D.M., Roberts, D.L. and Bradle, G. (2006). Sedimentary Rocks of the Karoo Supergroup, in "Johnson, M.R., Anhaeusser, C.R., and Thomas., R.J (eds). (2006). The Geology of South Africa. Geological Society of South Africa, Johannesburg/ Council for Geoscience, Pretoria, 691p".

Kaandorp, V. P, Molina-Navarro, E, Andersen, H. E, Bloomfield, J.P, Kuijper, M.J.M. and de Louw, P.G.B. (2018). A conceptual model for the analysis of multi-stressors in linked groundwater–surface water systems', Science of the Total Environment, 627, pp. 880–895. doi: 10.1016/j.scitotenv.2018.01.259.

Kalbus, E, Reinstorf, F, Schirmer, M. and Measuring, M.S. (2006). Measuring methods for groundwater? surface water interactions: a review To cite this version : Measuring methods for groundwater – surface water interactions : a review', Hydrology and Earth System Sciences, 10(6), pp. 873–887.

Kendall, C and McDonell. J.J. (1998). Isotope Tracers in Catchment Hydrology.

Kercival, N. (2015). Assessing Changes in Land Use and Land Cover using Remote Sensing: A Case Study of the Umhlanga Ridge Sub-Place', (December). Available at: https://researchspace.ukzn.ac.za/bitstream/handle/10413/13869/Kercival_Nadira_2015.pdf.

Khosravi, K., Mirzai, H. and Saleh, I. (2013). Assessment of Empirical Methods of Runoff Estimation by Statistical Test (Case Study: Banadak Sadat Watershed, Yazd Province). International Journal of Advanced Biological and Biomedical Research, 1(3), 285-301.

King, G.M. (1997). The Development Potential of KwaZulu-Natal Aquifers for rural water supply. Unpublished MSc. Disseration. Rhodes University.

King, G.M. (2002). An Explanation of the 1:500 000 General Hydrogeological Map, Durban 2928. Department of water and forestry. Pretoria, South Africa, 28p.

Kolm, K.E. (1996). Conceptualization and characterization of ground-water systems using Geographic Information Systems. Engineering Geology, 42(23): 111-118.

Kometa, S. S., Kimengsi, J. N. and Petiangma, D. M. (2017). Urban Development and its Implications on Wetland Ecosystem Services in Ndop, Cameroon. Environmental Management and Sustainable Development, 7(1), p. 21. doi: 10.5296/emsd. v7i1.12141.

Kopec, B. G. (2018). Seasonal Deuterium Excess Variations of Precipitation at Summit, Greenland, and their Climatological Signi fi cance. pp. 72–91. doi: 10.1029/2018JD028750.

Kotze, D., Marneweck, G.C., Batchelor, A.L., Lindley, D.S. and Collins, N.B. (2005). WET-EcoServices: A technique for rapidly assessing ecosystem services supplied by wetlands. Department Tourism, Environmental and Economic Affairs, Free State.

Kumar, M., Ramanathan, A., and Keshari, A. K. (2009). Understanding the extent of interactions between groundwater and surface water through major ion chemistry and multivariate statistical techniques. Hydrol. Process., 23, 297–310.

Kuusisto, E. (1996). A practical guide to the design and implementation of freshwater quality studies and monitoring programmes.

KwaZulu-Natal Provincial Planning Commission. (2016). KwaZulu-Natal situational overview. (April). Available at: http://www.kznppc.gov.za/images/downloads/KZN Situational Overview 2016 Final.pdf.

Lewis, R.R. and Gilmore, R.G., (2007). Important considerations to achieve successful mangrove forest restoration with optimum fish habitat. *Bulletin of Marine Science, 80*(3), pp.823-837.

Lloyd, J. A. and Heathcote, J.A. (1985). Natural inorganic hydrochemistry in relation to groundwater: An introduction. Oxford Uni. Press, New York p: 296.

Lim, K.J. and B.A. Engel, (2004). WHAT: Web-Based Hydrograph Analysis Tool. Available at http://pasture.ecn.purdue.edu/~what. Accessed in September 2005.

Lim, K. J., Engel, B. A., Tang, Z., & Choi, J. (2006). Automated Web GIS Based Hydrograph Analysis Tool, WHAT 1.1397, 1407-1416.

Linsley, R. K., Kohler, M.A. and Paulhus, J. L.H. (1975). Hydrology for engineers. McGraw- Hill, New York. 482p.

Liu, K.W. (2000). Deep-burial Diagenesis of the Siliciclastic Ordovician Natal Group, South Africa. Sedimentary Geology, (154) 177-189.

Maltby, E., and Barker, T. (2009). The wetland handbook volume 2, John Wiley & Sons.

Marshall, C.G.A. (1994). The stratigraphy of the Natal Group. Unpublished M.Sc. thesis, University of Natat, Pietermaritzburg.

Marshall, C. G.A. (2006). The Natal Group. In: Anhaeusser, C. R., Johnson, M.E., and Thomas, R. J. (Eds). The Geology of South Africa. The Geological Society of South Africa, Johannesburg, South Africa.

Matthews, P.E. (1972). Possible Precambrian obduction and plate tectonics in southeastern Africa. Nature Physical Science, 240(98): 37-39.\

Mazvimavi, P. D. (2017). Hydrological Characterization of wetlands: Understanding wetlands-catchment linkages.

McCarthy, K. A., Mcfarland, W. D., Wilkison, J. M. & White L. D. (1992). The dynamic relationship between ground water and the Columbia River: using deuterium and oxygen-18 as tracers. Journal ofHydrology 135, 1–12.

McEwan, K., Jolly, I., and Holland, K., (2006). Groundwater - surface water interactions in arid/semi-arid wetlands and the consequences of salinity for wetland ecology. CSIRO land and water science report No 53/06.

Mcgrane, S. J. (2016). Impacts of urbanisation on hydrological and water quality dynamics , and urban water management: a review water management : a review. Hydrological Sciences Journal. Taylor & Francis, 61(13), pp. 2295–2311. doi: 10.1080/02626667.2015.1128084.

McLachlan, P. J, Chambers, J. E, Uhlemann, S. S.and Binley, A. (2017). Geophysical characterisation of the groundwater–surface water interface. Advances in Water Resources. Elsevier, 109(August), pp. 302–319. doi: 10.1016/j.advwatres.2017.09.016.

Merlivat, L. and Jouzel, J. (1979). Global climatic interpretation of the deuterium-oxygen 18 relationship for precipitation, J. Geophys. Res., 84, 5029–5033.

Miller, M.P., Susong, D.D., Shope, C.L., Heilweil, V.M. and Stolp, B.J. (2014). Continuous estimation of baseflow in snowmelt-dominated streams and rivers in the Upper Colorado River Basin: a chemical hydrograph separation approach. Water Resour. Res. 50(8), 6986-6999, http://dx.dio.org/10.1002/2013WR014939.

Mitsch, W.J., and Gosselink, J.G., (1986). Wetlands. Van Nostrand Reinhold, New York. Mitsch.

Mitsch, W.J., Gosselink, J.G. (2007). Wetlands. Wiley. Müller.

MPCA. (2007). Water Chemistry Assessment Protocol for Depressional Wetland Monitoring Sites. February, 1–12.

Namugize, J.N., Jewitt, G.P.W. (2018). Sensitivity analysis of water quality monitoring frequency in the application of a water quality index for the uMngeni River and its Tributaries, KwaZulu-Natal, South Africa. Water S.A 3465 Accepted.

Ndlovu, M. S., Demlie, M. and Butler, M. (2019). Hydrogeological setting and hydrogeochemical characteristics of the Durban Metropolitan District, eastern South Africa. South African Journal of Geology, 122(3), pp. 299-316.

Ndlovu, V. (2019). Conceptual hydrogeological and steady-state numerical groundwater flow modelling of the Wentworth area, Durban, South Africa.

Nel, J.l, Driver, A, Strydom, W.f, Maherry, A, Petersen, C, Hill, L, Roux, D.J, Nienaber, S, Van Deventer, H, Swartz, E and Smith-Adao, L.b. (2011). Front Cover: Clanwilliam and Fiery redfins in the Rondegat River of Cederberg, South Africa atlas of freshwater ecosystem priority areas in South Africa: Maps to support sustainable development of water resources Water Research Commission.

Otunga, C., Odindi, J and Mutanga, O. (2014). Land Use , Land Cover change in the fringe of eThekwini Municipality: Implications for urban green spaces using remote sensing. South African Journal of Geomatics 3: 145-162.

Oumou, K.L., Bishop, J.T., Moran, D. and Dansokho, M. (2006). Estimating the value of ecotourism in the Djoudj National Bird Park in Senegal. IUCN, Gland, Switzerland. 34pp.

Ozesmi, S. L. and BAUER, M. E. (2002). Satellite remote sensing of wetlands. Wetl. Ecol. Manage. 10 381–402. https://doi. org/10.1023/A:1020908432489

Pfahl, S., and Sodemann, H. (2014) . What controls deuterium excess in global precipitation. (1), pp. 771–781. doi: 10.5194/cp-10-771-2014.

Phaduli, E. (2018). Drought characterization in South Africa under a changing climate. By Elelwani Phaduli Submitted in partial fulfillment of the requirements for the degree of master of science (meteorology) in the Faculty of Natural and Agricultural Sciences University Drought characterization in South Africa under a changing climate, (February), p. 112.

Plan, I. D. (2017). eThekwini Municipality.

Plan, I. D. (2019). eThekwini Municipality.

Paul, M.J. and Meyer, J.L. (2001). Streams in the urban landscape. Annu Rev Ecol Syst. 32:333–365.

Piper, A. M. (1944). A graphic procedure in the geochemical interpretation of water-analyses. Eos, Transactions American Geophysical Union, 25(6), pp.914–928.

Ponce, V.M. (1989). Engineering Hydrology: Principles and Practices: New Jersey, Prentice Prentice Hall, 640 p.

Postel, S.L. and Thompson Jr, B.H., (2005). May. Watershed protection: Capturing the benefits of nature's water supply services. In *Natural Resources Forum* (Vol. 29, No. 2, pp. 98-108). Oxford, UK: Blackwell Publishing, Ltd.

Pirastru, M. and Niedda, M. (2013). Evaluation of the soil water balance in an alluvial flood plain with a shallow groundwater table. Hydrol. Sci. J. 58 (4), 898-911.

Prince, K. (2011). Effects Of watershed topography, soils, land use, and climate on baseflow hydrology in humid regions: a review. Prog.Phys. Geogr.35 (4),465–492.

Price, K., Jackson, C.R, Parker, A.J, Reitan.T, Dowd, J. and Cyterski, M. (2011). Effects Of watershed land use and geomorphology on stream low flows during severe drought conditions in the southern Blue Ridge Mountains. Georgia And North Carolina, United States. Water Resour. Res. 47, http://dx.doi.org/10.1029/2010WR009340.

Ramsar Convention Secretariat. (2007). Wise use of wetlands: A conceptual framework for the wise use of wetlands. Ramsar handbooks for the wise use of wetlands, 3rd edition, volume 1. Ramsar Convention Secretariat, Gland, Switzerland.

Ramsay, P. and Cooper, A. (2002). Late Quaternary Sea-Level Change in South Africa. Quaternary Research, 57: 82-90.

Reid, M, Cheng, X, Banks, E, Jankowski, J, Jolly, I, Kumar, P, Lovell, D, Mitchell, M, Mudd, G, Richardson, S, Silburn, M. and Werner, A. (2009). Catalogue of conceptual models for groundwater – stream interaction in eastern Australia.

Renault, D., Molden, D., and Hemakumara, M. (2000). Importance of evaporative depletion by non-crop vegetation in irrigated areas of the humid tropics. In Davids, G. G.; Anderson, S. S. (Eds.), Benchmarking irrigation system performance using water measurement and water balances: Proceedings from the 1999 USCID Water Management Conference, San Luis Obispo, California, March 10-13, 1999. Denver, CO, USA: USCID, 259-274.

Riddell, E.S. (2011). Characterization of the hydrological processes and responses to rehabilitation of a headwater wetland of the Sand River, South Africa. Unpublished doctorate dissertation: University of KwaZulu Natal.

Rugel, K, Golladay, S. W, Jackson, C. R. and Rasmussen, T.C. (2016). Delineating groundwater/surface water interaction in a karst watershed: Lower Flint River Basin, southwestern Georgia, USA', Journal of Hydrology: Regional Studies. Elsevier B.V., 5, pp. 1–19. doi: 10.1016/j.ejrh.2015.11.011.

Rukundo, E. and Doğan, A. (2019). Dominant influencing factors of groundwater recharge spatial patterns in Ergene river catchment, Turkey. Water (Switzerland), 11(4). doi: 10.3390/w11040653.

Rumsey, C. A., Miller, M. P, Susong, D. D, Tillman, F. D, and Anning, D.W. (2015). Journal of Hydrology: Regional Studies Regional scale estimates of baseflow and factors influencing baseflow in the Upper Colorado River Basin. Elsevier B.V., 4, pp. 91–107.

Sadashivaiah. C, Ramakrishnaiah and Ranganna. G. (2008). Hydrochemical Analysis and Evaluation of Groundwater Quality in Tumkur Taluk, Karnataka State, India.

SANBI (South African National Biodiversity Institute), (2009). Further Development of a Proposed National Wetland Classification System for South Africa. Primary Project Report. Prepared by the Freshwater Consulting Group (FCG) for the South African National Biodiversity Institute (SANBI), Cape Town

SAWS, (2019). South African Weather Services, Durban Weather Office Climatic data.

Schoeller, H. (1955). Geochemie des eaux souterraines. Revue de L'Institute Francais du Petrole 10:230–44.

Schoeller, H. (1965). Qualitative Evaluation of Groundwater Resources. In Methods and Techniques of Groundwater Investigations and Developments. UNESCO.

Shone, R.W. and Booth, P.W.K. (2005). The Cape Basin , South Africa: a review. Journal of Africa Earth Sciences 43(1-3): 196-210

Soil Conservation Services (SCS). (1986). Urban Hydrology for Small Watersheds: Technical Release 55, Washington: United States Department of Agriculture.

Sophocleous, M. (2002). Interactions between groundwater and surface water: The state of the science. Hydrogeology Journal, 10(1), pp. 52–67. doi: 10.1007/s10040-001-0170-8.

Souch, C., Grimmond, C.S.B., and Wolfe, C.P. (1998). Evapotranspiration rates from wetlands with different disturbance histories: Indiana dunes national lakeshore. Wetlands, 18 (2): 216-229.

Soulis, K. X. and Valiantzas, J. D. (2012). SCS-CN parameter determination using rainfall-runoff data in heterogeneous watersheds – the two-CN system approach. Hydrology and Earth System Sciences, Volume 16, pp. 1001-1015.

Stephenson, B. and Barta, B. (2005). Impacts of stormwater and groundwater ingress on municipal sanitation services.

Stewart, M., Cimino, J. and Ross, M. (2007). Calibration of base flow separation methods with streamflow conductivity. Groundwater 45 (1), 17-27.

Subramanyanna, K. (2008). Engineering Hydrology, Third Edition, Tata McGraw Hill, 195-196.

Subyani, A., Sen, Z., (2005). Refined chloride mass balance method and its application in Saudi Arabia. King Abdulaziz University.Saudi Arabiya.

Taylor, C. B., Wilson, D. D., Brown, L. J., Stewart, M. K., Bur- den, R. J., and Brailsford, G. W., (1989). Sources and flow of North Canterbury Plains groundwater, New Zealand, J. Hydrol., 106, 311–340.

Tague, C. and Grant, G.E. (2009). Groundwater dynamics mediate low-flow response to global warming in snow-dominated alpine regions. Water Resour. Res., 45.

Tallaksen, L.M. (1995). A review of baseflow recession analysis. J. Hydrol. 165, 345-370.

Tanner, J. L., and Hughes, D. A. (2015). Understanding and Modelling Surface Water-Groundwater Interactions Water Research Commission (Issue 2056). http://www.wrc.org.za/Knowledge Hub Documents/Research Reports/2056 -2-14.pdf.

Thomas, R. J. (1988). The geology of the Port Shepstone area. Explanation of sheet 3030 Port Shepstone. Geological Survey of South Africa, Pretoria, 136p.

Thomas, B. F., Vogel, R. M. and Famiglietti, J. S. (2015). Objective hydrograph baseflow recession analysis. Journal of Hydrology. Elsevier B.V., 525, pp. 102–112. doi: 10.1016/j.jhydrol.2015.03.028.

Thornthwaite, C. W., and J. R. Mather. (1955). The Water Balance, Publications in Climatology VIII(1): 1-104, Drexel Institute of Climatology, Centerton, New Jersey.

Thornthwaite, C. W., and J. R. Mather. (1957). Instructions and Tables for the Computing Potential Evapotranspiration and the Water Balance, Publications in Climatology X (3): 311.

Ting, C. S., Kerh, T. and Liao, C. J. (1998). Estimation of groundwater recharge using the chloride mass-balance method, Pingtung Plain, Taiwan. Hydrogeology Journal, 6(2), pp. 282–292. doi: 10.1007/s100400050151.

Tockner, K., and Stanford, J. A. (2002). Riverine flood plains: present state and future trends. Environmental Conservation 29, 308–330. doi:10.1017/S037689290200022X.

Toran, L. (2017). Groundwater-Surface Water Interaction. Research gate.

Trajkovic, S. and Kolakovic, S. (2009). Wind-adjusted Turc equation for estimating reference evapotranspiration at humid European locations. Hydrology Research, 40(1), pp. 45-52.

Tripathi, R. P. and Singh, H.P (1998). Soil erosion and conservation. New Age International (P) LTD Publishers, pp316.

Umgeni Water. (2016). Infrastructure Master Plan 2015: 2016/2017– 2046/2047, Vol. 1, Planning Services, Engineering and Scientific Services Division, Umgeni Water, Pietermaritzburg.

United Nations. (1992). Report of the United Nations Conference on Environment and Development. Rio de Janeiro, l(June 1992), 3–14. http://legal.icsf.net/icsflegal/uploads/pdf/instruments/rio0201.pdf.

United Nations. (2014). World urbanization prospects: The 2014 revision.

Urban Environment Profile (UEP). (2016). Promoting Green Urban Development in African Cities. eThekwini, South Africa.

U.State. EPA. (2008). Methods for Evaluating Wetland Condition: Wetland Hydrodology. Office of Water, U.S. Environmental Protection Agency, Washington, DC. EPA-822-R-08-024.

Vega M, Pardo R, Barrado E. and Deban, L. (1998). Assessment of seasonal and polluting effects on the quality of river water byex ploratory data analysis. Water Res. 32:3581– 3592.

Vorajee, W. (2017). A hydrogeological investigation of the central eThekwini district landfills: Towards understanding the state of water resources in the area.

Vörösmarty, C.J., Green, P., Salisbury, J., Lammers R.B. (2000). Global water resources: Vulnerability from climate change and population growth. Science, 289(5477): 284-288.

Walsh, C.J. (2005). The urban stream syndrome: current knowledge and the search for a cure. Journal of the North American Benthological Society, 24 (3), 706–723. doi:10.1899/0887-3593(2005)024\ [0706:

TUSSCK\]2.0.CO;2.

Wanielista, M.P., Kersten. R and Eaglin. R. (1997). Hydrology: water quantity and quality control. John Wiley & Sons Inc. Wanielista.P. ISBN 0-471-07259-1.

WHO. (2011). Guidelines for drinking-water quality: fourth edition incorporating the first addendum. Geneva: World Health Organization. Licence: CC BY-NC-SA 3.0 IGO. 631p.

WHO. (2017). Guidelines for drinking-water quality: fourth edition incorporating the first addendum. Geneva: World Health Organization. Licence: CC BY-NC-SA 3.0 IGO. 631p.

Winograd, I.J., Riggs, A.C., Coplen, T.B. (1998). The relative contributions of summer and cool-season precipitation to groundwater recharge, Spring Mountains, Nevada, USA. Hydrogeol. J. 6 (1), 77–93.

Woodford, A. C. and Chevallier, L. (2002). Hydrogeology of the Main Karoo Basin: Current Knowledge and Future Research Needs. WRC Report No. TT 179/02, Pretoria: Water Research Commission.

Winter ,T. (1995). Recent advances in understanding the interaction of groundwater and surface water.

Winter, T. C, Harvey J.W, Franke, O.L and Alley, W. M. (1998). Groundwater and surface water: A single source. Denver, Colorado. ISBN 0–607–89339–7.

Xinyan. L, Hao. W, Hui. Q, and Yanyan. G. (2018). Groundwater chemistry regulated by hydrochemical processes and geological structures: A case study in Tongchuan, China.

Xu, Y., and Beekman, H.E. (2003). Review of groundwater recharge estimation in arid and semi-arid Southern Africa. Council for Scientific and Industrial Research (South Africa) and University of the Western Cape Report.

Zedler, J. B., and Leach, M. K. (1998). Managing urban wetlands for multiple use: research, restoration and recreation. Urban Ecosystems 2, 189–204. doi:10.1023/A:1009528505009.

Zhao, O. G., and Song, J. (2004). Wetland utilisation and protection in China. In Wong M.H. ed. (2004). Developments in ecosystems, volume 1: Wetlands ecosystems in Asia: Function and management, 27-34.

Zheng, C., Bennett, G.D., (2002). Applied contaminant transport modeling, 2nd EDN. New York.

APPENDICES

Appendix 1: Hydrometeorological parameters

Appendix 1.1: Monthly rainfall (mm) recorded at different weather station (SAWS, 2019)

LOUIS BOTHA – WK

Year	JAN	FEB	MAR	APR	MAY	JUN	JUL	AUG	SEP	OCT	NOV	DEC
1988	69.10	106.50	313.20	37.50	67.6	29.10	20.70	62.20	27.80	89.10	101.10	164.9
1989	51.20	255.90	17.80	168.30	10.30	20.10	48.00	5.10	86.10	96.90	246.30	27.00
1990	101.2	137.30	2380	39.60	20.40	10.20	1.20	115.40	51.60	123.90	53.70	116.90
1991	184.50	206.50	233.20	3.40	61.20	33.70	35.70	13.10	140.90	130.30	173.80	34.40
1992	99.80	76.90	40.90	11.10	0.20	2.80	7.50	12.70	13.00	14.23	76.95	43.65

DURBAN SOUTH AWS

Year	JAN	FEB	MAR	APR	MAY	JUN	JUL	AUG	SEP	OCT	NOV	DEC
1993	73.50	58.40	38.60	43.80	16.20	8.80	33.20	44.80	58.90	117.00	84.60	169.50
1994	69.60	37.00	165.00	16.20	2.00	13.60	91.60	49.00	15.30	112.30	24.70	79.60
1995	73.60	32.80	211.20	172.60	44.10	44.40	16.10	11.10	16.20	102.90	82.60	224.00
1996	448.20	247.50	106.40	36.90	18.70	1.10	261.40	12.70	22.90	120.80	72.70	72.70
1997	187.10	99.50	59.60	167.90	40.50	89.40	159.20	16.60	71.20	151.30	277.20	71.30
1998	93.30	158.30	83.80	237.40	52.20	0.00	22.90	69.40	25.50	64.50	106.40	132.60
1999	94.00	239.30	44.20	36.70	36.50	74.40	3.50	12.20	74.10	195.90	59.10	291.80
2000	181.70	157.30	148.80	63.20	167.50	3.80	20.20	17.70	62.80	60.20	142.00	124.50
2001	65.50	77.40	43.40	89.50	12.50	0.00	45.30	0.30	145.40	171.30	191.20	142.90
2002	155.80	154.70	21.30	162.60	3.30	23.80	151.50	53.90	43.60	32.40	64.20	113.30
2003	102.10	15.70	96.30	121.80	36.30	61.50	1.90	58.40	121.50	48.50	61.30	93.80
2004	231.70	126.00	39.50	23.70	2.10	5.30	111.30	12.60	56.40	64.60	51.70	74.20

2005	66.60	128.80	120.70	38.90	3.40	48.30	2.80	20.60	25.00	44.20	95.10	90.00
2006	110.80	188.80	77.50	81.60	110.40	5.40	0.00	71.90	67.40	109.10	178.80	201.90
2007	68.20	80.10	245.40	156.00	0.80	58.70	21.30	22.70	98.10	139.50	301.20	57.30
2008	133.80	78.70	196.20	122.10	28.40	171.20	3.50	1.80	99.30	81.60	80.50	184.90
2009	159.80	121.70	52.00	51.50	25.00	8.90	12.90	54.00	72.60	94.20	126.80	145.00
2010	94.30	104.20	28.40	8.50	54.00	24.60	1.60	0.40	18.20	82.80	100.00	169.80
2011	124.80	12.20	75.00	67.80	73.20	47.40	98.40	62.40	47.40	65.40	276.20	55.40
2012	50.60	33.40	282.40	17.00	18.20	28.40	5.80	80.80	265.00	209.80	125.60	124.20
2013	165.80	57.20	115.40	87.00	52.60	28.00	33.40	13.20	50.60	156.80	83.20	79.00
2014	69.00	89.20	65.20	35.00	17.80	10.40	4.40	0.00	5.2	86.2	119.6	83.8

DURBAN SOUTH MEREBANK

Year	JAN	FEB	MAR	APR	MAY	JUN	JUL	AUG	SEP	OCT	NOV	DEC
2015	56.00	96.80	79.40	25.80	0.80	6.60	199.40	10.80	75.80	39.20	61.40	102.00
2016	103.20	69.40	129.40	30.80	212.60	6.80	281.20	67.20	85.80	116.60	84.40	55.20
2017	62.40	137.00	47.80	60.60	217.40	0.00	34.40	40.80	77.60	166.60	129.00	119.60
2018	34.40	82.40	98.80	36.20	17.60	0.60	0.20	2.60				

Appendix 1.2 Daily mean monthly temperature recorded at different stations (SAWS, 2019).

(LOUIS BOTHA – WK, DURBAN SOUTH AWS, DURBAN SOUTH MEREBANK and DURBAN SOUTH ATHLONE PARK)

Year	JAN	FEB	MAR	APR	MAY	JUN	JUL	AUG	SEP	OCT	NOV	DEC
1988	22.00	22.50	22.00	17.70	14.60	11.40	12.00	14.60	16.10	17.10	18.30	20.00
1989	21.60	21.30	21.70	18.10	15.90	12.50	11.40	14.40	15.30	16.40	19.10	21.20
1990	21.40	21.20	19.80	19.00	14.80	11.10	12.10	13.90	14.90	17.60	18.40	20.20
1991	21.60	22.10	20.70	18.00	15.10	12.40	11.80	13.20	16.20	17.90	19.30	20.60
1992	21.20	22.60	20.70	19.60	12.60	10.10	9.60	12.10	14.60	17.50	18.20	20.60
1993	20.90	20.80	20.00	18.40	15.60	11.40	12.20	12.50	16.00	17.50	18.50	19.90
1994	20.40	20.60	20.20	18.00	13.40	9.80	9.90	12.50	15.50	16.00	18.50	19.80
1995	21.30	21.90	20.10	17.10	14.40	10.80	10.40	12.40	15.80	16.90	18.50	18.70
1996	21.20	21.30	19.40	16.50	13.30	9.00	10.00	11.40	14.60	17.10	18.50	21.10
1997	21.00	21.10	20.40	16.70	13.60	10.80	11.00	13.70	15.80	16.70	17.90	19.40
1998	20.90	21.60	20.50	18.70	13.40	9.70	11.40	12.90	15.40	16.80	18.80	20.10
1999	22.10	21.70	21.80	18.60	14.90	11.30	11.60	13.00	14.50	16.40	19.50	21.20
2000	20.20	22.50	21.30	16.70	13.70	11.70	10.40	13.80	15.00	16.80	18.40	20.40
2001	20.90	20.70	20.70	18.30	14.20	12.30	11.50	13.20	14.80	17.70	19.70	20.30
2002	21.50	20.40	20.90	18.10	14.00	11.30	10.30	14.30	15.70	17.20	17.10	20.70
2003	21.30	22.70	20.40	18.90	14.20	11.80	9.80	11.80	14.90	16.90	18.40	19.80
2004	21.20	21.90	19.90	17.60	13.40	9.70	10.00	13.90	13.80	16.50	19.60	20.90
2005	21.50	21.80	19.90	17.70	14.50	11.00	11.10	13.70	15.60	17.50	19.00	18.20
2006	21.60	22.20	18.70	17.90	13.00	10.00	10.90	12.60	15.80	18.70	19.30	20.60
2007	20.90	21.50	19.70	18.10	12.40	11.20	10.00	12.40	16.80	17.20	18.10	19.60
2008	21.10	21.50	20.00	16.20	15.10	12.20	10.80	13.30	13.30	16.50	18.90	20.40
2009	20.90	21.00	19.90	16.90	14.80	12.40	9.70	12.60	14.60	17.40	17.50	19.40
2010	21.30	22.30	21.00	18.60	16.20	11.40	11.50	12.40	16.30	17.40	18.70	19.60

2011	20.90	21.40	21.30	16.60	14.30	10.50	10.60	12.20	15.60	17.20	17.80	20.20
2012	22.50	22.60	20.90	16.10	15.20	10.70	10.30	13.30	14.70	16.80	17.70	20.70
2013	20.90	21.00	19.80	16.20	13.90	10.00	12.00	12.00	13.90	15.80	18.10	19.50
2014	21.20	21.30	20.10	16.80	14.20	10.40	9.60	14.20	16.00	16.20	18.00	20.20
2015	21.20	20.60	20.50	17.00	15.20	11.40	12.10	13.80	15.70	17.90	17.50	21.70
2016	22.20	21.80	21.80	19.40	15.20	12.10	10.70	12.60	16.00	16.30	18.80	20.50
2017	20.70	21.40	20.60	17.80	14.50	11.90	11.90	13.20	15.90	16.50	17.60	19.40
2018	21.00	21.70	20.00	19.30	16.10	14.40	11.10	13.50	15.70	15.50	16.90	19.80

Appendix 1.3. Location of hydrometeorological stations**.**

Station Name	**Latitude**	**Longitude**	**Time range**
Louis Botha -WK	-30.041	30.886	1988-1992
Durban South AWS	-29.918	30.958	1992-2014
Durban South Merebank	-29.944	30.959	2014-2018
Durban SouthAthlone	-30.012	30.922	2018

Appendix 1.4. River gauging stations

Site	**Latitude**	**Longitude**	**Catchment Area**	**Time range**
U2H052 Nagle Diversion (U2H052 - Mgeni River @ Inanda Loc)	-29.585	30.625	2535	1989-2018
U2R002 Nagle Dam (U2R002 - Mgeni River @ Inanda Loc.)	-29.591	30.627	2535	1989-2018
U2H059 Nagle Bypass(U2H059 - Mgeni River @ Inanda Location)	-29.587	30.623	2535	1989-2018
U2H055 Mgeni @ Inanda Loc.	-29.642	30.689	3771	1989-2018

U2H054 D/S river component (Mgeni River @ Inanda Mission Res)	-29.715	30.869	4084	1989-2018
U2R004 Inanda Dam (U2R004 - Mgeni River @ Inanda Mission Res)	-29.709	30.867	4079	1989-2018

Appendix 2: Hydrochemical data across the study area

Appendix 2.1: Secondary chemistry data (Concentration is in mg/l and EC is in μS/cm)

Sample No	pH	EC	TDS	Ca	K	Mg	Na	Cl	SO4	Si	HCO_3
Sample 1	6.78	807.00	403.00	36.12	2.72	14.04	113.46	78.32	25.79	18.54	179.23
Sample 2	7.20	1191.00	594.00	27.22	20.74	36.32	148.54	93.25	0.75	24.85	348.37
Sample 3	6.94	204.00	104.00	8.24	1.71	8.29	27.81	28.52	8.30	6.68	108.49
Sample 4	7.50	381.00	191.00	13.11	4.63	11.23	51.08	55.28	17.73	8.09	141.07
Sample 5	7.65	736.00	369.00	59.56	7.71	9.45	90.01	44.62	20.59	18.23	229.55
Sample 6	8.07	501.00	252.00	11.32	1.66	5.91	92.99	36.45	18.54	19.30	113.35
Sample 7	7.93	566.00	283.00	6.12	4.07	5.35	112.53	48.14	34.49	16.34	114.92
Sample 8	8.47	644.00	323.00	77.42	7.21	17.63	47.87	33.14	15.04	13.29	0.00
Sample 9	8.91	169.00	85.00	4.01	1.22	7.03	28.80	42.79	4.54	7.45	47.38
Sample 10	7.46	196.00	99.00	7.90	3.85	7.48	29.72	27.92	3.09	4.27	86.37
Sample 11	8.55	1530.00	765.00	49.20	2.04	34.79	233.41	108.98	1.15	4.03	331.05
Sample 12	7.89	605.00	303.00	13.04	1.34	18.67	90.33	72.42	7.25	9.17	145.27
Sample 13	6.92	1500.00	750.00	19.75	9.84	32.95	229.08	0.00	15.69	6.31	76.80
Sample 14	6.70	152.00	76.00	11.19	0.96	5.75	15.72	14.32	0.00	6.01	86.58
Sample 15	6.89	661.00	331.00	34.82	3.56	15.60	85.30	69.47	4.56	25.87	213.33
Sample 16	7.70	381.00	191.00	17.28	2.78	13.25	51.69	62.10	18.40	9.16	146.88
Sample 17	6.88	226.00	114.00	15.93	2.44	8.66	26.94	18.47	10.11	22.74	132.88
Sample 18	8.85	119.00	62.00	6.22	1.67	5.07	18.59	17.85	4.18	11.45	51.26
Sample 19	7.75	618.00	312.00	42.14	3.02	17.98	66.28	52.95	1.19	21.56	255.98

Sample 20	8.29	322.00	167.00	17.87	3.92	10.63	46.12	52.33	17.60	7.04	159.15
Sample 21	6.23	356.00	180.00	5.60	1.67	7.25	63.93	54.57	0.00	27.39	104.90
Sample 22	6.95	107.00	57.00	3.79	0.71	5.05	14.71	27.91	3.64	5.48	175.52
Sample 23	8.40	353.00	177.00	17.64	4.95	9.36	44.03	49.24	28.12	5.05	67.83
Sample 24	8.11	434.00	222.00	18.71	7.23	12.75	61.56	33.00	11.92	5.05	143.33
Sample 25	7.36	1267.00	634.00	32.64	2.71	31.99	199.82	102.90	30.26	15.59	247.09
Sample 26	7.55	478.00	240.00	16.09	8.99	12.17	74.36	40.68	14.84	1.08	132.51
Sample 27	7.79	75.10	0.00	32.20	3.80	11.80	110.20	100.70	52.90	12.36	253.40
Sample 28	7.80	47.60	0.00	19.20	0.00	23.30	0.00	40.00	0.00	0.00	312.00
Sample 29	7.80	44.40	0.00	37.60	0.00	10.20	0.00	30.00	0.00	32.00	335.81
Sample 30	7.10	57.80	0.00	20.80	0.00	11.70	0.00	86.00	0.00	0.00	135.10
Sample 31	7.80	12.70	0.00	5.80	0.70	5.10	9.30	7.90	2.00	16.91	108.61
Sample 32	8.25	25.60	0.00	24.80	0.65	5.60	17.00	14.30	8.50	15.68	213.27
Sample 33	8.24	33.90	0.00	17.00	2.85	12.20	36.80	11.90	14.20	6.07	279.25
Sample 34	7.59	18.70	0.00	12.80	0.76	6.40	7.80	6.40	2.00	13.23	132.99
Sample 35	8.18	19.90	0.00	12.80	0.83	8.30	14.40	14.00	8.40	15.76	170.60
Sample 36	7.28	4.00	0.00	1.90	2.03	1.30	3.10	1.50	5.60	8.63	34.88
Sample 37	7.77	64.10	0.00	18.10	5.82	17.40	86.30	125.80	49.90	9.48	160.58
Sample 38	8.18	343.00	0.00	147.60	29.00	88.80	375.70	928.20	137.00	14.71	372.60
Sample 39	7.45	60.60	0.00	26.33	5.37	8.46	74.64	129.19	33.20	13.28	144.65
Sample 40	7.82	57.50	0.00	15.05	3.13	10.72	85.35	65.59	46.73	8.70	218.26
Sample 41	6.75	50.40	0.00	9.28	4.55	4.50	76.57	105.60	40.68	7.67	57.06
Sample 42	6.93	94.60	0.00	16.33	1.29	17.04	143.79	245.07	73.14	13.93	147.48
Sample 43	8.04	94.20	0.00	40.84	2.58	13.72	127.37	167.69	52.32	16.37	253.37
Sample 44	7.98	78.10	0.00	96.16	4.54	20.27	40.92	46.83	6.50	14.56	701.43
Sample 45	6.90	190.00	0.00	53.00	3.80	11.00	52.00	9.00	0.00	0.00	6.90
Sample 46	7.96	1197.00	0.00	18.00	0.80	13.00	38.00	199.01	71.08	19.73	513.27
Sample 47	7.77	1241.00	0.00	5.80	0.70	5.10	9.30	148.00	152.70	8.00	563.98
Sample 48	7.31	1072.00	0.00	5.00	5.00	3.00	14.00	189.20	20.10	22.05	453.11
Sample 49	7.20	440.00	0.00	41.00	2.50	22.00	92.00	30.00	0.00	0.00	7.20

Sample 50	7.44	319.00	0.00	41.00	2.70	22.00	83.00	24.80	0.00	0.00	7.44
Sample 51	6.75	111.00	0.00	48.00	4.80	46.00	1.80	12.70	2.00	11.31	58.55
Sample 52	7.77	147.00	0.00	1.23	4.83	76.40	4.92	18.20	5.90	18.56	71.77
Sample 53	6.10	220.00	0.00	22.00	2.60	12.00	95.00	24.00	0.00	0.00	6.10
Sample 54	7.56	250.00	0.00	28.00	1.10	18.00	46.00	15.60	0.00	0.00	7.56
Sample 55	7.80	454.00	0.00	34.00	1.40	29.00	1.13	38.20	11.00	15.83	329.00
Sample 56	7.26	305.00	0.00	14.00	1.90	4.00	8.70	35.10	11.60	16.62	159.46
Sample 57	7.83	147.00	0.00	34.00	1.80	9.00	29.00	17.80	2.00	11.68	84.64
Sample 58	7.80	127.00	0.00	13.00	1.70	4.00	17.00	7.90	2.00	16.91	108.61
Sample 59	7.93	273.00	0.00	30.00	0.86	15.00	29.00	35.90	9.30	23.31	127.94
Sample 60	6.73	102.00	0.00	21.00	0.86	12.00	19.00	6.80	2.00	3.14	70.33
Sample 61	7.95	269.00	0.00	49.00	1.60	12.00	1.23	22.10	5.50	12.48	173.16
Sample 62	7.49	955.00	0.00	9.00	4.70	4.00	24.00	232.10	12.00	27.41	233.89
Sample 63	6.96	1017.71	0.00	34.59	5.09	34.84	200.49	143.17	14.42	13.75	235.54
Sample 64	6.63	890.00	0.00	11.99	5.21	31.14	130.07	58.41	16.02	18.28	111.55
Sample 65	7.39	1041.75	0.00	50.44	2.23	35.70	214.22	159.28	11.91	12.97	319.96
Sample 66	7.43	814.50	0.00	24.31	20.66	24.89	168.15	122.26	7.72	10.87	226.26
Sample 67	7.26	1084.60	0.00	75.26	6.87	95.55	348.26	131.47	10.19	15.92	337.59
Sample 68	7.49	1915.50	0.00	55.75	86.37	31.70	270.24	65.48	1.67	16.21	852.13
Sample 69	7.12	1099.20	0.00	27.79	2.85	13.11	64.72	56.46	24.78	10.67	169.00
Sample 70	7.16	1043.00	0.00	32.59	27.56	30.89	123.72	140.85	15.38	11.89	293.59
Sample 71	6.89	623.75	0.00	26.04	2.88	29.85	93.08	129.26	8.33	12.60	237.49
Sample 72	7.53	1330.67	0.00	30.92	4.15	49.77	125.79	193.84	6.58	10.99	306.73
Sample 73	7.35	576.00	0.00	14.16	5.89	3.31	70.71	29.09	68.37	5.84	161.25
Sample 74	6.17	385.00	195.00	14.50	4.30	10.20	34.00	0.97	0.63	0.00	85.43
Sample 75	7.19	368.00	185.00	15.80	4.09	10.00	30.00	2.02	1.55	0.00	90.31
Sample 76	7.06	197.00	105.00	13.30	3.95	4.51	12.60	470.00	0.78	0.00	58.66
Sample 77	6.89	308.00	152.00	11.20	2.61	8.35	25.00	0.65	1.29	0.00	66.51
Sample 78	6.82	595.00	303.00	25.00	6.88	14.50	52.00	2.39	3.61	0.00	184.89
Sample 79	6.40	566.00	294.00	15.60	6.19	13.90	60.00	1.15	0.25	0.00	141.57

Sample 80	6.17	613.00	195.00	77.00	7.33	16.90	45.00	45.00	15.40	0.00	275.32
Sample 81	7.27	248.00	28.00	14.10	2.64	6.60	28.00	43.00	22.00	0.00	47.92
Sample 82	7.75	443.00	208.00	24.00	3.74	8.54	54.00	47.00	38.60	0.00	118.66
Sample 83	7.16	259.00	128.00	10.40	3.87	7.36	29.00	41.00	17.30	0.00	42.31
Sample 84	7.37	276.00	145.00	6.10	1.19	9.67	50.00	62.00	17.60	0.00	64.07

Appendix 2.2. Environmental isotope data sourced from Sherhara (2019) , Vuyiswa (2019) , Ndlovu (2019) and Primary data.

Sample	**d D(‰)**	**d^{18}O(‰)**	**D - excess(‰)**	**Temp (°C)**
EM1	-10.04	-3.51	18.05	23.00
EM2	-11.19	-3.75	18.85	23.20
EM3	1.37	-1.16	10.73	20.49
EM4	-2.42	-1.89	12.76	17.72
EM5	-7.39	-2.83	15.26	22.50
EM6	-5.71	-2.47	14.06	22.66
EM7	-0.84	-1.55	11.61	22.62
EM8	-8.61	-3.32	17.96	21.01
EM9	-6.26	-2.73	15.60	18.03
EM10	15.59	2.215	-2.13	18.52
EM11	-9.29	-3.45	18.28	22.13
EM12	-2.62	-2.21	15.07	21.81
EM13	-7.24	-2.59	13.50	21.28
EM14	-7.82	-2.39	11.27	21.26
EM15	-10.82	-3.49	17.18	22.40

EM16	-3.38	-1.89	11.79	20.13
EM17	-11.64	-3.39	15.53	22.38
EM18	-8.92	-2.86	13.96	15.45
EM19	-10.83	-3.01	13.26	21.23
EM20	-0.11	-1.20	9.55	20.36
EM21	-12.95	-3.64	16.19	23.88
EM22	-15.80	-3.79	14.56	22.02
EM23	-2.13	-1.40	9.08	18.75
EM24	-0.24	-1.38	10.79	17.44
EM25	-9.37	-3.59	19.38	22.60
EM26	-1.48	-1.58	11.17	18.46
EM27	-7.48	-3.10	-7.48	0.00
EM28	-7.93	-3.27	-7.93	0.00
EM29	-6.87	-2.91	-6.87	0.00
EM30	-10.00	-3.30	16.40	0.00
EM31	-3.20	-2.49	16.72	0.00
EM32	-9.60	-3.20	16.00	0.00
EM33	3.10	-0.73	8.94	0.00
EM34	-1.90	-1.80	12.50	0.00
EM35	-0.10	-1.93	15.34	0.00
EM36	2.90	-1.38	13.94	0.00
EM37	-13.80	-4.00	18.20	0.00
EM38	-1.60	-1.64	11.52	0.00

EM39	-12.7	-3.81	17.78	0.00
EM40	0.60	-1.31	11.08	0.00
EM41	0.20	-1.44	11.72	0.00
EM42	0.50	-1.32	11.06	0.00
DM01	-2.51	-2.13	14.53	24.4
DM02	1.24	-1.12	10.22	24.80
DM03	8.32	-0.09	9.05	21.58
DM04	0.63	-1.20	10.23	25.64
DM05	2.38	-1.13	11.39	24.04
DM06	-0.46	-1.95	15.13	23.18
DM07	0.05	-1.63	13.09	24.40
DM08	-4.25	-2.58	16.38	23.19
DM09	0.82	-1.50	12.79	28.90
DM10	-5.58	-2.67	15.81	25.58
DM11	-6.14	-2.98	17.69	22.41
DM12	-16.62	-4.18	16.80	22.61

Appendix 2.3 Primary hydrochemical data

a. Onsite measured groundwater and surface water hydrochemical parameters in the study area.

Sample No	Source	Sample date	Latitude	Longitude	EC(µS/ cm)	pH	Eh (mV)	T (°C)	TDS (mg/l)	Salinity	DO (mg/l)	DO (%)	ORP
DM01	River	9/11/2020	-29.564	31.160	385.00	6.17	42.60	24.40	195.00	0.19	4.03	45.90	22.80
DM02	River	9/11/2020	-29.803	30.980	368.00	7.19	-15.60	24.8	185.00	0.18	4.16	50.80	-16.60
DM03	River	9/11/2020	-29.817	30.883	197.00	7.06	-8.20	21.58	105.00	0.1	4.33	51.40	-0.80
DM04	River	9/11/2020	-29.755	30.909	308.00	6.89	1.00	25.64	152.00	0.14	4.04	49.50	16.50
DM05	River	9/11/2020	-29.695	31.076	595.00	6.82	5.80	24.04	303.00	0.29	4.02	47.00	5.30
DM06	River	9/11/2020	-29.649	31.105	566.00	6.40	28.10	23.18	294.00	0.28	4.20	48.20	10.50
DM07	Wetland	23/11/2020	-29.829	30.983	613.00	6.17	42.60	24.40	195.00	0.19	4.03	45.90	22.80
DM08	River	23/11/2020	-29.824	30.856	248.00	7.27	-19.90	23.19	28.00	0.12	2.24	27.70	4.10
DM09	Wetland	23/11/2020	-29.895	30.975	443.00	7.75	-45.90	28.90	208.00	0.20	1.42	17.30	8.80
DM10	River	23/11/2020	-29.839	30.818	259.00	7.16	-13.10	25.58	128.00	0.12	1.24	15.60	-3.10
DM11	River	25/11/2020	-30.155	30.793	276.00	7.37	-23.40	22.41	145.00	0.14	1.62	18.20	-7.60
DM12	borehole	25/11/2020	-29.794	30.667	361.00	6,68	14.10	22.61	188.00	0.18	1.99	23.70	-16.10
DM13	Spring	02/3/2021	-30.004	30.852	422.00	10.83	-212.00	25.90	207.00	0.20	2.16	27.20	57.10
DM14	Spring	02/3/2021	-29.523	30.797	748.00	8.75	-100.60	28.54	350.00	0.34	1.65	22.20	22.10
DM15	Spring	02/3/2021	-29.933	30.800	137.00	7.51	-32.90	27.56	65.00	0.06	1.40	18.50	43.60
DM16	Spring	02/3/2021	-29.812	30.665	688.00	8.75	-99.60	24.82	345.00	12.50	0.78	9.70	12.50

b. Laboratory measured groundwater and surface water Major ions (Concentration is in mg/l and Ec is in µS/cm).

Sample ID	pH	EC	TDS	Ca	K	Mg	Na	Cl	SO4	HCO3
DM01	6.17	385	195	14.5	4.3	10.2	34	0.97	0.63	85.42
DM02	7.19	368	185	15.8	4.09	10	30	2.02	1.55	90.31
DM03	7.06	197	105	13.3	3.95	4.51	12.6	470.00	0.78	58.66
DM04	6.89	308	152	11.2	2.61	8.35	25	0.65	1.29	66.51
DM05	6.82	595	303	25	6.88	14.5	52	2.39	3.61	184.89
DM06	6.4	566	294	15.6	6.19	13.9	60	1.15	0.25	141.57

DM07	6.17	613	195	77	7.33	16.9	45	45	15.4	275.32
DM08	7.27	248	28	14.1	2.64	6.6	28	43	22	47.92
DM09	7.75	443	208	24	3.74	8.54	54	47	38.6	118.66
DM010	7.16	259	128	10.4	3.87	7.36	29	41	17.3	42.31
DM011	7.37	276	145	6.1	1.19	9.67	50	62	17.60	64.07

Appendix 2.4: Discharge rate at three gauging stations along the Umngeni River (U2H052, U2H055, U2H054) (Department of water and Sanitation, 2021).

a. UMngeni river at Inanda Location (U2H052) (m^3/s).

Day	1993	1994	1995	1996	1997	1998	1999	2001	2002	2003	2004	2005	2006	2007	2008	2009	2010	2011	2012	2013	2014	2015	2016	2017	2018	Average
1	0.92	1.70	0.00	0.00	0.01	0.36	0.00	0.01	0.00	0.01	0.00	0.00	0.01	0.02	0.00	0.01	0.05	0.07	0.00	0.00	0.03	0.02	0.00	0.00	0.00	0.13
2	0.92	1.76	0.00	0.00	0.03	0.04	0.00	0.01	0.00	0.01	0.00	0.00	0.01	0.07	0.01	0.01	0.02	0.02	0.00	0.00	0.04	0.01	0.00	0.00	0.00	0.12
3	0.92	1.91	0.00	0.00	0.00	0.04	0.10	0.01	0.01	0.01	0.00	0.01	0.01	0.03	0.01	0.01	0.28	0.02	0.00	0.00	0.04	0.01	0.00	0.00	0.00	0.14
4	0.92	1.92	0.00	0.00	0.05	0.04	0.00	0.01	0.00	0.02	0.00	0.00	0.04	0.02	0.00	0.00	0.25	0.07	0.00	0.00	0.05	0.01	0.00	0.00	0.00	0.14
5	0.89	1.91	0.00	0.00	0.02	0.10	0.00	0.03	0.00	0.02	0.00	0.00	0.02	0.02	0.03	0.00	0.05	0.05	0.00	0.00	0.05	0.01	0.00	0.00	0.00	0.13
6	0.90	1.99	0.00	0.00	0.05	0.23	0.00	0.05	0.00	0.02	0.00	0.00	0.01	0.02	0.01	0.00	0.02	0.04	0.00	0.00	0.07	0.00	0.00	0.00	0.00	0.14
7	1.20	2.08	0.00	0.00	0.08	0.20	0.00	0.06	0.00	0.02	0.00	0.00	0.01	0.01	0.00	0.00	0.03	0.04	0.00	0.00	0.05	0.00	0.01	0.00	0.00	0.15
8	1.10	1.76	0.00	0.00	0.07	0.16	0.00	0.06	0.00	0.00	0.00	0.00	0.01	0.01	0.00	0.00	0.19	0.05	0.00	0.00	0.03	0.00	0.00	0.00	0.00	0.14
9	1.09	1.94	0.00	0.00	0.05	0.09	0.00	0.05	0.00	0.00	0.00	0.00	0.01	0.01	0.00	0.00	0.11	0.05	0.00	0.00	0.04	0.00	0.00	0.00	0.00	0.14
10	1.14	1.74	0.00	0.00	0.05	0.07	0.00	0.04	0.00	0.01	0.00	0.00	0.01	0.01	0.00	0.00	0.06	0.04	0.00	0.00	0.03	0.00	0.00	0.00	0.00	0.13
11	1.11	3.37	0.00	0.00	0.05	0.06	0.00	0.03	0.00	0.04	0.00	0.00	0.01	0.01	0.00	0.00	0.04	0.03	0.00	0.00	0.03	0.00	0.00	0.00	0.00	0.19
12	1.04	1.67	0.00	0.00	0.06	0.05	0.00	0.03	0.01	0.03	0.00	0.00	0.01	0.01	0.00	0.00	0.08	0.02	0.00	0.00	0.03	0.00	0.00	0.00	0.00	0.12
13	0.99	1.44	0.00	0.00	0.06	0.05	0.00	0.02	0.02	0.03	0.00	0.00	0.01	0.02	0.00	0.05	0.13	0.02	0.00	0.00	0.04	0.00	0.00	0.01	0.00	0.12
14	0.93	1.72	0.00	0.00	0.05	0.04	0.00	0.02	0.01	0.03	0.00	0.00	0.01	0.02	0.00	0.01	0.11	0.02	0.00	0.00	0.08	0.00	0.00	0.00	0.00	0.12
15	0.95	1.64	0.00	0.00	0.04	0.04	0.00	0.01	0.01	0.03	0.00	0.00	0.01	0.02	0.00	0.00	0.08	0.03	0.00	0.00	0.02	0.00	0.00	0.00	0.01	0.12
16	0.95	1.72	0.00	0.00	0.04	0.05	0.00	0.01	0.01	0.03	0.00	0.00	0.01	0.02	0.00	0.02	0.07	0.03	0.00	0.00	0.11	0.00	0.00	0.00	0.03	0.12
17	0.97	1.58	0.00	0.00	0.04	0.06	0.00	0.02	0.01	0.00	0.00	0.00	0.00	0.01	0.00	0.01	0.08	0.03	0.00	0.00	0.12	0.00	0.00	0.01	0.01	0.12
18	1.04	1.52	0.00	0.00	0.02	0.20	0.00	0.03	0.02	0.00	0.00	0.00	0.00	0.02	0.00	0.00	0.20	0.02	0.00	0.00	0.14	0.01	0.00	0.00	0.01	0.13
19	1.02	1.31	0.00	0.00	0.01	0.36	0.00	0.04	0.02	0.00	0.00	0.00	0.00	0.02	0.00	0.00	0.37	0.03	0.00	0.00	0.13	0.05	0.00	0.00	0.00	0.14
20	1.00	1.15	0.00	0.00	0.04	0.40	0.00	0.04	0.02	0.00	0.00	0.00	0.00	0.03	0.00	0.00	0.20	0.03	0.00	0.00	0.32	0.07	0.00	0.00	0.00	0.13

21	0.99	1.30	0.00	0.00	0.03	0.66	0.00	0.03	0.01	0.03	0.00	0.00	0.00	0.02	0.03	0.00	0.31	0.02	0.00	0.00	0.26	0.06	0.00	0.01	0.00	0.15
22	1.02	1.50	0.00	0.00	0.04	0.49	0.00	0.04	0.01	0.01	0.00	0.00	0.01	0.02	0.02	0.00	0.27	0.03	0.00	0.01	0.18	0.04	0.00	0.00	0.00	0.15
23	1.42	1.19	0.00	0.00	0.07	0.00	0.00	0.04	0.01	0.01	0.00	0.00	0.01	0.02	0.02	0.00	0.10	0.03	0.00	0.00	0.15	0.03	0.00	0.00	0.01	0.12
24	1.28	1.11	0.00	0.00	0.04	0.01	0.00	0.03	0.00	0.06	0.00	0.00	0.02	0.02	0.01	0.00	0.02	0.04	0.00	0.00	0.09	0.01	0.00	0.00	0.01	0.11
25	1.15	1.22	0.00	0.00	0.00	0.12	0.00	0.01	0.00	0.02	0.00	0.00	0.01	0.03	0.01	0.00	0.03	0.04	0.00	0.00	0.05	0.01	0.00	0.00	0.01	0.11
26	1.15	1.67	0.00	0.00	0.00	0.60	0.00	0.01	0.00	0.02	0.00	0.00	0.01	0.03	0.00	0.00	0.08	0.05	0.00	0.00	0.03	0.01	0.00	0.00	0.00	0.15
27	1.14	1.53	0.00	0.00	0.00	0.55	0.00	0.02	0.00	0.02	0.00	0.00	0.01	0.03	0.00	0.00	0.04	0.24	0.00	0.00	0.04	0.01	0.00	0.00	0.00	0.15
28	1.14	2.06	0.00	0.00	0.00	0.40	0.00	0.14	0.01	0.00	0.00	0.00	0.00	0.02	0.01	0.00	0.09	0.01	0.01	0.01	0.04	0.02	0.00	0.00	0.00	0.16
29	1.22	0.77	0.00	0.00	0.00	0.03	0.00	0.04	0.00	0.01	0.00	0.00	0.01	0.02	0.00	0.00	0.04	0.01	0.00	0.03	0.02	0.03	0.00	0.00	0.00	0.09
30	1.22	0.81	0.00	0.00	0.01	0.04	0.00	0.01	0.00	0.01	0.00	0.00	0.02	0.02	0.01	0.00	0.05	0.06	0.00	0.01	0.02	0.03	0.00	0.00	0.00	0.09
31	0.60	0.72	0.00	0.00	0.00	0.06	0.00	0.01	0.00	0.00	0.00	0.00	0.01	0.01	0.00	0.00	0.03	0.03	0.00	0.00	0.01	0.02	0.00	0.00	0.00	0.06

b. UMngeni river at Inanda Location (U2H055) (m^3/s).

Day	1988	1989	1990	1991	1992	1993	1994	1995	1996	1997	1998	1999	2000	2001	2002	2003	2004	2005	2006	2007	2008	2009	2010	2011	2012	2013	2014	2015	2016	2017	2018	Average
1	20.29	15.26	3.85	2.05	3.40	2.36	15.71	12.63	3.05	19.55	8.33	6.65	12.74	3.20	2.03	4.18	5.01	3.27	5.01	22.58	8.98	3.95	4.47	10.97	5.80	3.18	0.16	2.61	3.79	3.73	0.88	7.09
2	18.75	11.85	5.44	1.90	3.14	2.44	14.50	15.81	3.34	17.91	7.36	7.28	16.16	2.69	2.12	6.23	5.98	3.76	7.67	18.07	7.61	4.04	5.18	10.10	5.48	3.15	0.16	2.57	4.23	3.50	0.96	7.08
3	13.46	12.69	5.73	1.80	3.96	2.39	17.72	13.88	8.33	16.26	7.04	7.72	11.40	2.56	4.32	4.53	7.20	4.57	4.89	13.46	7.19	4.11	4.79	9.02	5.06	2.71	0.16	2.77	3.48	3.01	0.86	6.68
4	11.40	11.94	5.02	2.26	3.33	2.29	21.71	15.29	4.46	15.40	9.72	6.51	10.43	2.87	2.69	9.25	8.61	3.49	4.34	15.50	6.89	4.91	4.34	8.92	5.15	3.43	0.16	2.81	3.16	2.99	0.98	6.78
5	11.39	10.81	4.46	2.53	3.31	2.19	24.20	13.80	5.41	11.51	9.80	5.67	11.11	2.63	2.48	5.55	6.57	5.23	4.64	13.39	8.22	4.46	3.59	9.58	4.70	2.66	0.21	2.66	6.21	3.04	1.01	6.55
6	10.10	10.97	3.97	2.05	3.47	2.09	21.56	8.21	2.98	10.84	9.59	4.76	12.30	3.03	2.80	4.24	5.20	3.50	4.34	12.35	6.68	4.21	3.92	9.29	4.84	3.37	0.18	2.81	4.71	2.74	0.94	5.87
7	13.36	15.13	3.52	1.85	3.59	2.00	22.39	9.84	3.98	12.32	9.98	4.21	10.74	3.31	2.61	4.30	4.82	3.13	4.41	10.43	5.89	5.22	8.86	13.01	4.53	3.03	0.17	3.02	3.65	2.57	0.90	6.35
8	12.52	14.47	3.27	1.91	3.32	2.35	20.15	9.62	2.98	11.36	9.08	4.35	14.23	2.86	2.82	6.38	4.20	3.04	5.12	7.70	5.21	5.40	7.31	11.81	4.08	2.43	0.17	3.11	3.27	2.52	0.94	6.06
9	13.79	19.72	3.73	2.29	3.26	2.20	23.26	9.26	3.33	11.52	8.22	5.08	12.17	2.60	3.11	6.62	4.34	3.00	5.68	7.52	5.14	4.67	6.43	9.12	4.61	2.72	0.15	3.07	3.76	2.75	1.01	6.26
10	13.34	19.34	4.42	2.32	4.58	2.30	22.19	8.84	3.28	11.75	7.48	5.78	10.77	2.72	2.56	5.06	5.39	3.59	5.50	7.22	7.26	4.58	4.77	8.96	4.80	2.41	0.16	2.44	3.31	3.32	1.42	6.19
11	11.32	19.89	4.87	3.18	5.90	2.30	21.43	8.91	3.83	10.15	7.92	5.74	10.76	2.59	2.15	5.36	5.41	3.12	4.41	7.80	5.92	5.07	4.43	10.25	4.44	2.46	0.16	2.32	3.36	3.56	2.75	6.18
12	10.56	17.67	4.99	2.59	5.06	2.30	20.59	8.44	6.77	9.67	11.43	8.94	9.02	3.83	2.02	4.82	5.10	2.86	5.12	7.71	5.74	4.99	4.13	10.44	4.53	2.60	0.18	3.47	3.38	5.96	3.08	6.39
13	8.17	15.74	5.94	2.88	4.33	2.15	20.78	8.70	3.78	9.69	7.83	9.00	9.42	4.30	1.99	4.43	5.23	2.76	7.39	8.03	5.77	4.19	3.92	9.66	5.82	2.73	0.17	3.18	4.21	4.24	3.06	6.11
14	7.72	14.39	10.09	4.06	3.40	2.40	16.88	10.47	3.64	9.05	7.40	9.23	13.31	4.93	2.12	3.98	4.89	3.09	5.30	8.96	5.23	4.55	3.85	10.15	4.78	2.47	0.21	2.96	3.52	3.95	4.36	6.17
15	7.94	14.81	6.77	3.13	3.49	6.65	33.91	11.62	2.91	8.51	7.03	8.16	12.00	4.03	3.46	3.62	4.37	2.94	8.35	7.43	4.76	4.63	3.84	11.63	4.82	2.29	0.24	3.55	3.84	3.96	2.64	6.69
16	7.16	18.69	6.80	2.63	4.37	4.59	38.47	11.07	2.76	9.21	8.21	6.61	11.48	3.37	3.41	4.84	4.34	3.28	5.95	6.84	4.64	5.61	4.63	10.26	3.95	2.07	0.19	3.84	4.90	3.71	1.47	6.75

17	7.54	15.66	5.30	2.36	3.36	2.88	30.87	10.62	2.76	10.83	12.65	6.32	10.55	3.62	3.25	3.98	4.52	3.02	6.24	6.39	4.97	6.16	5.74	11.27	4.48	2.86	0.19	3.28	4.45	3.58	1.16	6.48
18	8.63	13.85	3.68	2.10	2.79	2.64	32.66	9.61	2.82	12.29	10.88	6.40	10.35	3.56	3.02	4.05	5.27	3.90	6.40	8.07	5.05	7.04	4.19	10.98	5.98	2.20	0.24	3.00	4.08	3.55	1.21	6.47
19	8.82	15.22	4.60	2.12	2.80	3.04	28.86	8.10	3.05	12.75	9.74	10.18	10.35	3.80	2.76	5.47	6.58	6.15	5.06	8.98	4.84	4.29	3.73	11.15	5.07	1.92	0.33	2.63	4.68	3.97	0.97	6.52
20	8.42	17.43	5.13	2.14	2.53	2.86	25.38	9.32	3.22	12.38	10.89	8.95	13.81	3.69	2.95	4.33	7.71	3.34	4.58	10.98	5.12	4.14	3.49	12.07	7.12	2.18	0.25	2.61	4.06	3.33	0.88	6.62
21	6.36	15.79	4.56	2.00	2.87	2.69	22.39	21.94	3.32	12.77	10.24	11.08	15.93	3.90	2.46	3.84	5.77	3.16	4.92	11.64	6.25	4.21	3.34	16.66	7.06	1.76	0.22	2.73	3.55	3.22	0.94	7.02
22	6.36	15.31	4.48	2.51	2.49	2.63	21.10	20.01	3.76	23.26	14.40	9.74	11.49	3.44	3.64	4.37	5.01	5.38	6.78	12.55	6.75	3.89	3.22	14.25	6.30	1.91	0.21	4.38	3.76	3.24	1.89	7.37
23	6.47	14.47	6.71	2.47	3.25	2.41	26.09	21.10	3.16	15.89	12.90	9.15	9.98	3.44	3.36	5.54	5.57	3.64	5.04	15.29	4.73	3.99	3.82	12.80	5.69	1.91	0.20	3.93	6.24	4.59	1.25	7.26
24	6.53	22.02	6.56	2.99	3.41	2.73	22.94	21.06	2.74	12.07	11.72	7.98	9.67	3.39	3.73	5.82	5.08	3.59	4.45	14.56	4.20	4.39	4.50	12.33	6.50	1.90	0.53	3.33	5.50	5.42	1.06	7.18
25	8.67	17.17	4.60	2.86	3.25	3.05	18.96	13.50	2.65	13.00	10.34	6.39	12.77	3.28	2.76	5.02	4.77	4.02	4.16	15.80	4.81	4.11	4.75	11.59	5.03	2.22	0.54	3.11	4.82	3.98	1.15	6.55
26	10.52	15.80	3.89	2.30	3.03	2.84	24.20	11.30	2.88	12.04	8.65	5.97	11.44	3.05	2.36	5.91	4.92	3.07	4.70	12.46	5.17	4.86	4.34	10.58	5.56	2.06	0.45	3.06	4.69	3.68	0.80	6.34
27	9.98	13.52	3.75	2.15	3.23	2.52	28.26	12.77	3.04	15.49	9.90	5.98	12.02	3.00	2.97	4.82	5.26	3.50	4.46	13.66	11.31	5.10	4.37	10.09	5.36	2.05	0.42	2.93	3.68	3.81	0.76	6.78
28	10.10	12.91	3.60	2.33	3.08	2.88	27.97	12.93	3.65	16.63	14.56	6.10	11.87	2.78	2.72	5.29	5.05	3.94	4.13	17.15	14.65	4.94	5.01	8.96	6.32	2.12	0.41	2.80	3.71	4.31	0.97	7.22
29	9.90	12.75	3.99	2.21	4.69	2.73	19.59	14.50	2.80	10.36	19.97	3.94	11.07	2.71	2.64	5.97	4.26	3.42	4.22	7.55	10.03	4.50	5.33	6.90	5.59	1.79	0.40	2.52	2.97	3.50	0.81	6.24
30	26.36	20.68	3.53	1.90	2.74	2.80	11.86	12.73	2.98	9.88	11.48	3.75	17.12	2.49	1.81	4.78	4.21	3.04	8.04	8.45	9.01	4.52	4.07	10.72	6.15	1.68	0.38	2.32	2.67	2.99	0.76	6.64
31	7.53	20.67	2.53	1.09	2.12	1.97	9.11	10.34	1.59	5.90	5.99	2.65	11.62	1.78	1.07	3.04	2.78	2.19	2.23	5.49	8.09	2.77	2.46	5.45	5.83	1.08	0.17	1.57	3.14	1.80	0.51	4.34

c. UMngeni river at Inanda Missiona Res (U2H054) (m^3/s).

Day	1989	1990	1991	1992	1993	1994	1995	1996	1997	1998	1999	2001	2002	2003	2004	2005	2006	2007	2008	2009	2010	2011	2012	2013	2014	2015	2016	2017	2018	2019	Average
1	6.81	24.73	10.73	2.76	4.47	2.26	13.31	13.06	20.54	4.92	6.81	9.21	15.91	4.98	0.91	2.30	3.53	3.60	4.41	18.09	7.98	2.75	9.10	5.22	2.37	0.60	0.60	0.33	0.51	0.48	6.78
2	5.47	20.94	9.37	2.82	4.40	2.25	11.12	12.87	19.85	5.09	5.47	8.90	15.13	4.76	0.84	2.19	3.37	5.14	3.41	17.86	7.28	3.38	9.63	3.83	2.14	0.60	0.60	0.34	0.53	0.49	6.34
3	4.79	19.07	9.50	2.85	4.52	2.65	11.11	13.60	19.31	7.03	4.79	9.65	16.49	4.49	0.80	2.56	4.21	5.70	2.72	14.15	6.47	2.95	8.81	2.97	1.92	0.60	0.60	0.33	0.57	0.49	6.19
4	5.24	18.14	8.07	2.91	4.61	2.69	14.83	14.88	16.99	7.55	5.24	9.77	13.64	5.00	0.79	2.26	5.76	3.12	2.31	10.89	5.71	3.22	7.93	2.80	1.75	0.61	0.61	0.31	0.56	0.49	5.96
5	5.20	19.35	7.07	3.06	4.60	2.20	20.22	16.11	17.57	8.45	5.20	10.09	11.56	4.99	0.82	1.85	2.90	3.33	2.57	10.67	5.67	3.10	7.46	2.98	1.58	0.61	0.61	0.31	0.54	0.49	6.04
6	4.15	18.13	7.35	2.96	4.65	2.21	16.86	13.35	15.13	7.27	4.15	10.24	11.55	4.47	0.88	1.59	3.01	3.58	2.69	9.82	5.79	2.15	7.14	3.21	2.14	0.61	0.61	0.26	0.55	0.48	5.57
7	3.88	18.88	7.38	2.87	4.66	2.19	16.21	12.12	13.95	5.75	3.88	9.91	11.44	5.17	1.65	1.38	3.26	3.01	2.17	8.33	4.69	1.97	8.40	3.58	1.27	0.61	0.61	0.27	0.55	0.48	5.35
8	3.85	20.37	6.44	3.00	4.65	2.18	15.19	12.38	13.80	6.80	3.85	9.64	13.67	4.90	0.83	1.68	3.83	2.10	2.75	6.83	4.22	2.17	12.56	3.41	1.13	0.61	0.61	0.26	0.56	0.48	5.49
9	3.50	22.24	6.43	3.05	4.64	2.17	13.64	16.26	13.85	6.63	3.50	10.08	14.12	4.00	0.86	2.89	2.88	2.05	3.35	6.02	3.95	2.22	10.63	3.04	1.05	0.61	0.61	0.26	0.57	0.49	5.52

10	**3.01**	**24.13**	**6.45**	**2.86**	**4.63**	**2.16**	**12.27**	**18.29**	**14.13**	**4.29**	**3.01**	**9.43**	**12.64**	**3.47**	**0.83**	**3.25**	**3.30**	**1.91**	**2.67**	**5.46**	**3.67**	**2.15**	**9.38**	**3.42**	**0.94**	**0.60**	**0.60**	**0.26**	**0.60**	**0.48**	**5.34**
11	**2.71**	**22.26**	**6.37**	**2.85**	**4.62**	**2.16**	**13.38**	**16.42**	**14.24**	**4.29**	**2.71**	**8.53**	**11.69**	**3.56**	**0.82**	**2.87**	**3.96**	**1.93**	**2.50**	**5.05**	**2.98**	**2.18**	**9.74**	**3.89**	**0.85**	**0.59**	**0.59**	**0.27**	**0.63**	**0.44**	**5.17**
12	**2.68**	**20.15**	**6.30**	**2.78**	**4.65**	**2.15**	**14.02**	**14.56**	**13.49**	**4.67**	**2.68**	**9.12**	**11.70**	**3.35**	**0.88**	**2.85**	**3.99**	**2.04**	**2.27**	**4.99**	**3.57**	**2.21**	**9.85**	**4.03**	**0.80**	**0.58**	**0.58**	**0.27**	**0.66**	**0.44**	**5.08**
13	**3.03**	**18.57**	**6.55**	**2.72**	**4.74**	**2.12**	**15.26**	**13.17**	**13.38**	**4.99**	**3.03**	**10.77**	**12.72**	**3.42**	**1.41**	**2.74**	**3.72**	**2.27**	**2.83**	**5.00**	**2.53**	**2.23**	**9.37**	**4.20**	**0.74**	**0.57**	**0.57**	**0.28**	**0.65**	**0.44**	**5.13**
14	**6.46**	**15.73**	**9.57**	**2.79**	**4.80**	**2.13**	**19.62**	**12.37**	**13.31**	**4.74**	**6.46**	**10.05**	**14.13**	**3.94**	**1.55**	**2.55**	**3.33**	**2.50**	**4.12**	**5.01**	**3.13**	**2.12**	**9.14**	**5.24**	**0.71**	**0.57**	**0.57**	**0.31**	**0.63**	**0.46**	**5.60**
15	**5.93**	**14.92**	**11.39**	**2.66**	**4.84**	**2.13**	**32.08**	**12.17**	**13.11**	**4.32**	**5.93**	**9.15**	**14.25**	**6.28**	**1.80**	**2.33**	**2.98**	**2.52**	**4.26**	**4.93**	**3.43**	**2.09**	**10.93**	**4.96**	**0.70**	**0.56**	**0.56**	**0.31**	**0.65**	**0.47**	**6.09**
16	**5.70**	**19.77**	**9.79**	**2.66**	**4.80**	**2.13**	**31.68**	**12.69**	**13.34**	**3.90**	**5.70**	**8.56**	**13.16**	**6.19**	**1.70**	**2.18**	**2.64**	**2.60**	**5.27**	**4.77**	**3.46**	**2.03**	**9.50**	**3.62**	**0.73**	**0.55**	**0.55**	**0.45**	**0.63**	**0.46**	**6.04**
17	**8.29**	**19.28**	**9.41**	**2.62**	**4.70**	**2.17**	**28.54**	**12.61**	**14.40**	**3.71**	**8.29**	**8.08**	**12.31**	**7.29**	**1.43**	**2.43**	**2.42**	**2.72**	**4.66**	**5.66**	**3.57**	**2.92**	**10.24**	**3.47**	**0.74**	**0.56**	**0.56**	**0.53**	**0.62**	**0.45**	**6.16**
18	**10.99**	**16.47**	**9.28**	**2.58**	**4.72**	**2.18**	**21.69**	**12.36**	**15.51**	**3.32**	**10.99**	**7.84**	**12.00**	**7.07**	**1.25**	**2.82**	**2.34**	**2.96**	**5.17**	**4.65**	**3.49**	**3.24**	**10.17**	**3.96**	**0.73**	**0.59**	**0.59**	**0.31**	**0.61**	**0.45**	**6.01**
19	**9.77**	**16.72**	**9.44**	**2.56**	**4.72**	**2.03**	**19.95**	**11.31**	**16.07**	**2.94**	**9.77**	**9.97**	**11.13**	**5.62**	**1.20**	**2.20**	**2.59**	**4.76**	**4.39**	**5.58**	**3.36**	**2.11**	**10.16**	**4.33**	**0.73**	**0.61**	**0.61**	**0.32**	**0.60**	**0.44**	**5.87**
20	**9.67**	**20.55**	**9.36**	**2.62**	**4.72**	**2.56**	**18.51**	**10.58**	**15.77**	**2.89**	**9.67**	**10.99**	**11.52**	**8.50**	**2.44**	**2.47**	**3.81**	**5.28**	**4.10**	**6.36**	**3.22**	**1.81**	**10.30**	**5.03**	**1.13**	**0.67**	**0.67**	**0.33**	**0.58**	**0.44**	**6.22**
21	**9.33**	**22.13**	**8.76**	**2.71**	**5.16**	**2.64**	**16.55**	**12.19**	**18.86**	**3.06**	**9.33**	**12.03**	**12.25**	**14.24**	**0.90**	**2.82**	**4.16**	**4.04**	**3.37**	**7.79**	**3.09**	**1.60**	**11.90**	**6.69**	**1.76**	**0.58**	**0.58**	**0.33**	**0.57**	**0.43**	**6.66**
22	**14.38**	**20.42**	**6.72**	**3.34**	**4.91**	**1.96**	**15.11**	**16.78**	**25.93**	**4.10**	**14.38**	**13.06**	**11.41**	**11.81**	**0.84**	**2.80**	**3.39**	**5.44**	**3.51**	**9.28**	**4.13**	**1.44**	**12.66**	**7.50**	**0.70**	**0.57**	**0.57**	**0.33**	**0.56**	**0.43**	**7.28**
23	**18.31**	**18.97**	**6.40**	**3.20**	**4.75**	**2.00**	**13.66**	**19.73**	**24.72**	**4.02**	**18.31**	**12.35**	**10.18**	**9.15**	**1.19**	**2.67**	**3.23**	**5.70**	**3.93**	**10.45**	**4.06**	**1.34**	**11.13**	**7.54**	**0.67**	**0.57**	**0.57**	**0.33**	**0.54**	**0.43**	**7.34**
24	**13.83**	**21.94**	**8.16**	**2.62**	**4.73**	**2.04**	**12.45**	**20.90**	**20.88**	**2.57**	**13.83**	**11.53**	**10.03**	**7.06**	**1.74**	**3.32**	**2.87**	**4.94**	**3.30**	**12.63**	**3.08**	**1.44**	**9.83**	**7.75**	**0.65**	**0.58**	**0.58**	**0.32**	**0.53**	**0.43**	**6.88**
25	**11.92**	**23.47**	**7.83**	**2.43**	**4.72**	**2.09**	**12.06**	**19.57**	**18.48**	**2.65**	**11.92**	**10.03**	**11.04**	**6.12**	**0.88**	**3.72**	**2.74**	**5.27**	**2.78**	**12.19**	**2.88**	**1.94**	**9.02**	**7.41**	**0.73**	**0.58**	**0.58**	**0.32**	**0.51**	**0.43**	**6.54**
26	**9.04**	**18.21**	**7.47**	**2.28**	**4.71**	**2.14**	**16.80**	**15.48**	**16.03**	**3.27**	**9.04**	**8.56**	**12.53**	**5.93**	**1.01**	**3.46**	**3.24**	**5.19**	**2.57**	**11.87**	**3.13**	**1.91**	**8.29**	**6.54**	**0.67**	**0.57**	**0.57**	**0.31**	**0.50**	**0.43**	**6.06**
27	**7.90**	**15.19**	**7.68**	**2.36**	**4.76**	**2.13**	**23.36**	**13.78**	**17.75**	**2.09**	**7.90**	**8.00**	**11.43**	**5.60**	**1.75**	**3.23**	**3.28**	**4.16**	**2.70**	**10.89**	**4.84**	**2.07**	**7.63**	**6.45**	**0.66**	**0.56**	**0.56**	**0.30**	**0.48**	**0.43**	**6.00**
28	**8.74**	**15.15**	**5.90**	**2.36**	**4.77**	**2.12**	**30.25**	**13.16**	**19.58**	**2.06**	**8.74**	**7.50**	**12.45**	**5.43**	**0.93**	**3.08**	**3.19**	**3.92**	**2.65**	**11.50**	**10.14**	**2.79**	**7.04**	**7.34**	**0.64**	**0.55**	**0.55**	**0.30**	**0.47**	**0.43**	**6.46**
29	**13.34**	**10.42**	**6.31**	**2.23**	**4.34**	**2.02**	**28.03**	**12.98**	**12.83**	**2.09**	**13.34**	**5.59**	**10.79**	**5.35**	**0.89**	**2.54**	**1.63**	**3.49**	**2.42**	**1.89**	**9.38**	**2.90**	**4.94**	**5.99**	**0.58**	**0.56**	**0.56**	**0.26**	**0.45**	**0.43**	**5.62**
30	**11.48**	**15.25**	**7.35**	**2.31**	**4.34**	**1.93**	**17.43**	**14.56**	**13.70**	**2.02**	**11.48**	**6.29**	**14.72**	**5.24**	**0.80**	**2.31**	**1.99**	**3.15**	**3.01**	**2.26**	**7.88**	**2.96**	**6.31**	**6.23**	**0.56**	**0.55**	**0.55**	**0.26**	**0.44**	**0.43**	**5.59**
31	**9.01**	**15.52**	**5.73**	**1.37**	**2.73**	**1.04**	**12.73**	**11.77**	**7.02**	**1.07**	**9.01**	**3.94**	**12.66**	**3.54**	**0.38**	**2.22**	**1.70**	**1.38**	**1.04**	**3.07**	**7.04**	**2.14**	**6.18**	**3.41**	**0.33**	**0.37**	**0.37**	**0.14**	**0.23**	**0.27**	**4.25**

Appendix 3: Groundwater level, depth to groundwater and borehole yield (DWS, 2016; NGA, 2020).

Site ID	Latitude	longitude	Altitude (m)	Depth to Water (m bgl)	Water lvl (a msl)	Yield (l/s)
BH1	-29.716	30.249	1198.00	31.61	1166.39	0.11
BH2	-29.442	30.207	1271.00	8.00	1263.00	0.19
BH3	-29.439	30.208	1290.00	15.00	1275.00	6.31
BH4	-29.404	30.169	1194.00	10.53	1183.47	0.76
BH5	-29.429	30.168	1122.00	22.37	1099.63	0.50
BH6	-29.467	30.155	1058.00	2.00	1056.00	1.51
BH7	-29.341	30.215	1108.00	43.00	1065.00	10.00
BH8	-29.347	30.213	1129.00	14.00	1115.00	0.95
BH9	-29.347	30.224	1114.00	37.16	1076.84	1.51
BH10	-29.337	30.237	1097.00	1.67	1095.33	0.76
BH11	-29.373	30.459	759.00	24.81	734.19	0.76
BH12	-29.368	30.462	782.00	6.97	775.03	1.01
BH13	-29.332	30.460	813.00	17.00	796.00	0.83
BH14	-29.344	30.466	786.00	12.60	773.40	2.16
BH15	-29.334	30.425	794.00	7.13	786.87	0.34
BH16	-29.417	30.440	701.00	7.05	693.95	0.61
BH17	-29.419	30.438	689.00	9.11	679.89	1.67
BH18	-29.417	30.439	699.00	6.54	692.46	2.02
BH19	-29.415	30.440	705.00	5.77	699.23	0.56
BH20	-29.343	30.296	1091.00	3.66	1087.34	2.50
BH21	-29.343	30.296	1092.00	15.00	1077.00	0.25
BH22	-29.350	30.254	1086.00	0.85	1085.15	2.00
BH23	-29.477	30.346	725.00	8.28	716.72	0.33
BH24	-29.442	30.294	815.00	47.68	767.32	3.19
BH25	-29.362	30.330	1062.00	30.00	1032.00	1.94
BH26	-29.371	30.316	1156.00	10.46	1145.54	2.15
BH27	-29.382	30.462	719.00	17.00	702.00	1.51
BH28	-29.390	30.468	750.00	9.21	740.79	0.56
BH29	-29.422	30.478	715.00	15.96	699.04	0.08
BH30	-29.404	30.440	786.00	32.88	753.12	0.39
BH31	-29.417	30.371	679.00	18.28	660.72	0.14
BH32	-29.416	30.395	718.00	70.00	648.00	2.50
BH33	-29.424	30.366	713.00	9.70	703.30	4.00
BH34	-29.485	30.358	806.00	17.47	788.53	0.22
BH35	-29.468	30.492	674.00	20.85	653.15	0.22
BH36	-29.483	30.447	696.00	6.60	689.40	0.01
BH37	-29.490	30.441	724.00	9.06	714.94	1.00
BH38	-29.477	30.441	680.00	15.00	665.00	0.19
BH39	-29.448	30.429	679.00	6.00	673.00	2.86
BH40	-29.496	30.288	1039.00	9.26	1029.74	0.14
BH41	-29.443	30.551	890.00	26.48	863.52	0.50

BH42	-29.394	30.607	845.00	14.07	830.93	0.50
BH43	-29.463	30.594	894.00	27.47	866.53	1.30
BH44	-29.350	30.492	786.00	21.00	765.00	0.05
BH45	-29.364	30.540	813.00	27.47	785.53	0.20
BH46	-29.466	30.569	910.00	30.26	879.74	0.11
BH47	-29.344	30.640	1019.00	12.81	1006.19	0.50
BH48	-29.434	30.640	948.00	4.48	943.52	0.13
BH49	-29.418	30.668	1034.00	21.24	1012.76	1.17
BH50	-29.446	30.732	918.00	24.26	893.74	0.33
BH51	-29.488	30.665	950.00	1.14	948.86	0.33
BH52	-29.491	30.733	897.00	1.40	895.60	0.30
BH53	-29.492	30.702	904.00	1.00	903.00	0.20
BH54	-29.459	30.742	912.00	20.00	892.00	0.22
BH55	-29.407	30.542	790.00	11.55	778.45	0.42
BH56	-29.355	30.699	983.00	46.60	936.40	0.42
BH57	-29.353	30.685	990.00	66.00	924.00	0.42
BH58	-29.358	30.694	990.00	4.70	985.30	0.28
BH59	-29.474	30.970	514.00	1.00	513.00	2.52
BH60	-29.367	30.979	529.00	45.30	483.70	0.36
BH61	-29.427	30.888	916.00	63.10	852.90	0.17
BH62	-29.434	30.879	896.00	9.40	886.60	0.36
BH63	-29.494	30.991	542.00	57.39	484.61	0.33
BH64	-29.380	30.893	862.00	46.90	815.10	0.17
BH65	-29.321	30.894	963.00	31.40	931.60	0.22
BH66	-29.410	30.939	681.00	57.40	623.60	0.39
BH67	-29.374	30.762	1006.00	23.66	982.34	0.25
BH68	-29.458	30.865	726.00	31.32	694.68	0.24
BH69	-29.458	30.853	619.00	25.00	594.00	0.06
BH70	-29.455	30.965	660.00	6.81	653.19	0.08
BH71	-29.472	30.978	611.00	9.38	601.62	0.22
BH72	-29.493	30.991	541.00	57.39	483.61	0.36
BH73	-29.455	30.965	660.00	6.81	653.19	0.01
BH74	-29.448	30.824	783.00	49.65	733.35	0.14
BH75	-29.450	30.942	614.00	17.48	596.52	0.45
BH76	-29.441	30.957	562.00	51.32	510.68	0.67
BH77	-29.441	30.930	608.00	44.64	563.36	0.70
BH78	-29.426	30.903	858.00	11.27	846.73	11.00
BH79	-29.431	30.879	887.00	3.62	883.38	2.22
BH80	-29.435	30.859	673.00	34.25	638.75	1.40
BH81	-29.451	30.796	951.00	43.00	908.00	2.50
BH82	-29.440	30.933	588.00	33.45	554.55	0.77
BH83	-29.410	30.939	676.00	57.93	618.07	0.80
BH84	-29.413	30.912	861.00	51.03	809.97	0.70
BH85	-29.473	30.989	557.00	0.18	556.82	2.50
BH86	-29.448	30.824	778.00	49.65	728.35	0.42
BH87	-29.450	30.942	609.00	17.48	591.52	1.70

BH88	-29.441	30.957	557.00	51.32	505.68	0.44
BH89	-29.441	30.930	603.00	44.64	558.36	2.00
BH90	-29.426	30.903	853.00	11.27	841.73	0.17
BH91	-29.431	30.879	882.00	3.62	878.38	2.00
BH92	-29.435	30.859	668.00	34.25	633.75	0.67
BH93	-29.451	30.796	946.00	43.00	903.00	1.00
BH94	-29.440	30.933	583.00	33.45	549.55	2.00
BH95	-29.440	30.822	809.00	22.00	787.00	2.60
BH96	-29.331	30.895	918.00	21.10	896.90	1.89
BH97	-29.344	30.891	934.00	63.00	871.00	4.42
BH98	-29.407	30.853	1033.00	44.41	988.59	0.14
BH99	-29.483	30.879	514.00	22.53	491.47	1.67
BH100	-29.438	30.876	917.00	27.80	889.20	2.00
BH101	-29.449	30.878	722.00	15.79	706.21	0.52
BH102	-29.388	30.930	693.00	37.35	655.65	2.50
BH103	-29.388	30.930	693.00	40.98	652.02	2.22
BH104	-29.339	30.958	712.00	49.99	662.01	0.56
BH105	-29.413	30.839	799.00	5.10	793.90	0.56
BH106	-29.396	30.844	863.00	1.97	861.03	0.42
BH107	-29.374	30.944	552.00	15.34	536.66	0.60
BH108	-29.337	30.955	708.00	46.18	661.82	1.00
BH109	-29.373	30.870	973.00	13.00	960.00	1.10
BH110	-29.398	30.843	879.00	0.63	878.37	0.44
BH111	-29.328	30.894	880.00	12.82	867.18	6.67
BH112	-29.416	30.838	753.00	5.52	747.48	4.17
BH113	-29.387	30.847	886.00	3.90	882.10	2.78
BH114	-29.356	30.910	746.00	2.35	743.65	0.88
BH115	-29.466	30.865	666.00	30.00	636.00	2.78
BH116	-29.496	30.893	505.00	45.30	459.70	0.33
BH117	-29.497	30.891	489.00	17.00	472.00	0.83
BH118	-29.497	30.892	510.00	37.00	473.00	0.83
BH119	-29.467	30.866	675.00	27.56	647.44	0.22
BH120	-29.531	30.221	1106.00	6.00	1100.00	0.31
BH121	-29.528	30.224	1110.00	10.00	1100.00	0.61
BH122	-29.548	30.194	1080.00	28.35	1051.65	0.67
BH123	-29.714	30.479	754.00	15.00	739.00	1.67
BH124	-29.745	30.424	888.00	27.00	861.00	0.28
BH125	-29.535	30.456	888.00	10.00	878.00	1.39
BH126	-29.534	30.456	883.00	21.20	861.80	1.11
BH127	-29.590	30.453	696.00	12.76	683.24	1.14
BH128	-29.587	30.465	701.00	24.17	676.83	2.78
BH129	-29.585	30.468	679.00	15.70	663.30	0.50
BH130	-29.534	30.456	881.00	19.92	861.08	0.76
BH131	-29.569	30.451	861.00	8.42	852.58	0.01
BH132	-29.565	30.449	855.00	10.47	844.53	2.00
BH133	-29.521	30.252	1079.00	43.68	1035.32	0.01

BH134	-29.513	30.259	1063.00	18.00	1045.00	3.30
BH135	-29.514	30.259	1059.00	16.64	1042.36	3.30
BH136	-29.750	30.282	1024.00	62.71	961.29	6.39
BH137	-29.576	30.280	1191.00	11.36	1179.64	1.94
BH138	-29.526	30.254	1067.00	1.40	1065.60	1.00
BH139	-29.516	30.310	1143.00	10.25	1132.75	4.00
BH140	-29.519	30.306	1120.00	14.06	1105.94	6.39
BH141	-29.667	30.380	804.00	15.23	788.77	20.00
BH142	-29.668	30.382	787.00	9.55	777.45	0.67
BH143	-29.677	30.382	870.00	36.51	833.49	6.67
BH144	-29.721	30.376	932.00	24.92	907.08	3.05
BH145	-29.716	30.449	848.00	46.75	801.25	1.73
BH146	-29.707	30.469	790.00	46.00	744.00	1.50
BH147	-29.608	30.460	660.00	26.27	633.73	0.45
BH148	-29.708	30.397	804.00	17.61	786.39	0.45
BH149	-29.709	30.398	794.00	13.11	780.89	0.45
BH150	-29.610	30.458	648.00	18.29	629.71	0.45
BH151	-29.607	30.457	638.00	27.43	610.57	0.10
BH152	-29.601	30.461	667.00	19.94	647.06	0.56
BH153	-29.501	30.311	1118.00	1.50	1116.50	5.00
BH154	-29.621	30.447	610.00	12.00	598.00	5.00
BH155	-29.621	30.447	610.00	5.50	604.50	6.67
BH156	-29.945	30.222	661.00	5.50	655.50	11.00
BH157	-29.808	30.173	1091.00	5.00	1086.00	4.17
BH158	-29.811	30.167	1146.00	18.00	1128.00	0.64
BH159	-29.946	30.204	813.00	4.70	808.30	0.14
BH160	-29.887	30.234	983.00	33.00	950.00	0.56
BH161	-29.881	30.248	874.00	0.76	873.24	0.56
BH162	-29.886	30.241	897.00	1.20	895.80	1.11
BH163	-29.872	30.232	920.00	10.19	909.81	22.00
BH164	-29.885	30.233	980.00	14.30	965.70	0.56
BH165	-29.883	30.245	877.00	5.04	871.96	2.78
BH166	-29.989	30.410	714.00	9.00	705.00	1.11
BH167	-29.990	30.400	795.00	9.00	786.00	2.78
BH168	-29.977	30.391	763.00	9.00	754.00	19.00
BH169	-29.876	30.311	859.00	5.40	853.60	0.61
BH170	-29.877	30.313	859.00	5.00	854.00	2.70
BH171	-29.944	30.370	783.00	25.00	758.00	11.00
BH172	-29.961	30.454	734.00	30.00	704.00	0.07
BH173	-29.956	30.460	748.00	6.00	742.00	1.60
BH174	-29.761	30.478	723.00	40.00	683.00	1.40
BH175	-29.773	30.471	797.00	6.00	791.00	1.40
BH176	-29.793	30.489	672.00	1.27	670.73	0.08
BH177	-29.793	30.489	672.00	1.20	670.80	0.70
BH178	-29.845	30.460	853.00	5.00	848.00	13.00
BH179	-29.817	30.464	663.00	1.00	662.00	2.00

BH180	-29.806	30.459	700.00	25.00	675.00	0.01
BH181	-29.894	30.461	830.00	5.00	825.00	8.33
BH182	-29.882	30.412	838.00	5.80	832.20	0.01
BH183	-29.840	30.297	954.00	25.00	929.00	0.06
BH184	-29.841	30.298	936.00	10.00	926.00	5.00
BH185	-29.885	30.261	860.00	0.70	859.30	6.94
BH186	-29.873	30.364	842.00	6.37	835.63	0.14
BH187	-29.873	30.265	841.00	21.43	819.57	0.83
BH188	-29.874	30.264	845.00	7.46	837.54	0.12
BH189	-29.874	30.264	843.00	6.38	836.62	1.11
BH190	-29.877	30.264	852.00	5.55	846.45	1.67
BH191	-29.889	30.290	840.00	6.73	833.27	10.00
BH192	-29.742	30.501	742.00	7.00	735.00	0.69
BH193	-29.730	30.500	776.00	12.00	764.00	1.11
BH194	-29.534	30.608	910.00	47.00	863.00	0.61
BH195	-29.516	30.590	908.00	78.00	830.00	0.33
BH196	-29.532	30.623	903.00	93.00	810.00	1.94
BH197	-29.532	30.623	902.00	78.00	824.00	1.82
BH198	-29.508	30.606	838.00	69.00	769.00	8.33
BH199	-29.508	30.689	852.00	12.00	840.00	0.56
BH200	-29.552	30.699	811.00	30.00	781.00	5.56
BH201	-29.559	30.703	693.00	1.08	691.92	1.11
BH202	-29.511	30.720	810.00	6.00	804.00	0.74
BH203	-29.532	30.662	899.00	1.02	897.98	0.23
BH204	-29.544	30.682	740.00	4.00	736.00	0.23
BH205	-29.568	30.677	605.00	10.00	595.00	0.20
BH206	-29.656	30.591	566.00	9.00	557.00	0.72
BH207	-29.592	30.679	620.00	1.02	618.98	1.25
BH208	-29.693	30.632	804.00	39.61	764.39	2.78
BH209	-29.694	30.623	805.00	3.76	801.24	3.06
BH210	-29.583	30.575	700.00	31.22	668.78	5.00
BH211	-29.631	30.689	400.00	11.90	388.10	5.55
BH212	-29.618	30.693	410.00	26.00	384.00	8.33
BH213	-29.614	30.683	415.00	26.50	388.50	2.50
BH214	-29.604	30.746	320.00	7.49	312.51	2.78
BH215	-29.600	30.735	223.00	6.60	216.40	4.17
BH216	-29.599	30.738	215.00	8.40	206.60	11.00
BH217	-29.507	30.900	484.00	10.00	474.00	3.33
BH218	-29.518	30.866	511.00	28.00	483.00	2.22
BH219	-29.518	30.940	607.00	19.00	588.00	8.89
BH220	-29.570	30.976	334.00	30.10	303.90	5.00
BH221	-29.591	30.933	237.00	49.50	187.50	0.14
BH222	-29.540	30.950	472.00	53.60	418.40	0.14
BH223	-29.507	30.964	498.00	65.90	432.10	0.02
BH224	-29.554	30.916	533.00	39.40	493.60	0.11
BH225	-29.546	30.885	333.00	13.70	319.30	0.08

BH226	-29.591	30.876	377.00	50.70	326.30	0.14
BH227	-29.605	30.854	517.00	50.60	466.40	0.12
BH228	-29.551	30.876	391.00	46.90	344.10	0.08
BH229	-29.518	30.807	777.00	10.00	767.00	0.15
BH230	-29.604	30.869	429.00	49.22	379.78	0.44
BH231	-29.586	30.843	488.00	20.85	467.15	0.02
BH232	-29.623	30.983	188.00	17.26	170.74	0.66
BH233	-29.626	30.988	226.00	59.20	166.80	0.17
BH234	-29.627	30.983	203.00	10.14	192.86	0.22
BH235	-29.626	30.976	270.00	62.73	207.27	0.68
BH236	-29.632	30.979	239.00	34.15	204.85	0.50
BH237	-29.626	30.983	194.00	3.05	190.95	0.40
BH238	-29.626	30.983	193.00	1.59	191.41	0.40
BH239	-29.626	30.983	193.00	10.14	182.86	0.61
BH240	-29.625	30.988	227.00	59.23	167.77	0.08
BH241	-29.567	30.762	630.00	40.14	589.86	0.01
BH242	-29.574	30.792	400.00	54.02	345.98	1.50
BH243	-29.576	30.791	460.00	38.30	421.70	0.30
BH244	-29.579	30.762	630.00	55.38	574.62	0.17
BH245	-29.609	30.773	500.00	40.46	459.54	0.29
BH246	-29.646	30.793	180.00	10.80	169.20	0.67
BH247	-29.691	30.892	220.00	19.00	201.00	0.33
BH248	-29.657	30.895	340.00	9.00	331.00	0.14
BH249	-29.645	30.892	400.00	51.00	349.00	0.17
BH250	-29.631	30.884	405.00	23.94	381.06	0.17
BH251	-29.627	30.889	430.00	20.40	409.60	0.25
BH252	-29.621	30.893	440.00	10.50	429.50	2.00
BH253	-29.621	30.888	450.00	22.40	427.60	0.33
BH254	-29.614	30.888	450.00	26.63	423.37	0.01
BH255	-29.614	30.893	450.00	21.30	428.70	1.00
BH256	-29.614	30.902	405.00	19.70	385.30	1.33
BH257	-29.597	30.891	270.00	12.61	257.39	1.00
BH258	-29.600	30.893	320.00	46.40	273.60	0.33
BH259	-29.594	30.901	250.00	5.15	244.85	0.33
BH260	-29.595	30.888	273.00	3.38	269.62	0.17
BH261	-29.591	30.886	367.00	35.69	331.31	0.33
BH262	-29.581	30.866	392.00	35.10	356.90	1.66
BH263	-29.562	30.903	261.00	6.98	254.02	0.07
BH264	-29.608	30.855	486.00	5.08	480.92	0.24
BH265	-29.605	30.860	515.00	6.55	508.45	1.50
BH266	-29.592	30.866	452.00	48.50	403.50	3.30
BH267	-29.711	30.890	314.00	85.94	228.06	12.00
BH268	-29.572	30.756	693.00	52.75	640.25	0.24
BH269	-29.602	30.788	371.00	3.65	367.35	0.07
BH270	-29.600	30.784	407.00	4.18	402.82	1.66
BH271	-29.601	30.774	466.00	44.49	421.51	0.66

BH272	-29.613	30.805	488.00	27.96	460.04	0.25
BH273	-29.615	30.807	527.00	5.80	521.20	2.00
BH274	-29.654	30.886	299.00	19.92	279.08	2.30
BH275	-29.631	30.858	502.00	2.92	499.08	1.10
BH276	-29.658	30.888	293.00	56.70	236.30	0.80
BH277	-29.636	30.865	449.00	7.12	441.88	0.10
BH278	-29.649	30.876	313.00	49.80	263.20	0.55
BH279	-29.669	30.888	247.00	23.65	223.35	0.50
BH280	-29.688	30.886	183.00	12.50	170.50	0.70
BH281	-29.642	30.874	422.00	34.40	387.60	0.10
BH282	-29.658	30.885	243.00	4.74	238.26	0.60
BH283	-29.671	30.879	188.00	42.25	145.75	0.20
BH284	-29.535	30.880	404.00	47.50	356.50	0.30
BH285	-29.521	30.896	366.00	27.70	338.30	0.20
BH286	-29.505	30.862	534.00	1.00	533.00	0.20
BH287	-29.539	30.912	609.00	0.50	608.50	0.11
BH288	-29.505	30.901	495.00	28.00	467.00	0.13
BH289	-29.539	30.872	395.00	49.00	346.00	10.00
BH290	-29.505	30.902	497.00	76.00	421.00	0.12
BH291	-29.508	30.902	475.00	9.00	466.00	0.01
BH292	-29.514	30.939	640.00	20.00	620.00	0.41
BH293	-29.969	30.748	421.00	10.00	411.00	0.16
BH294	-29.999	30.712	498.00	3.00	495.00	0.23
BH295	-29.780	30.501	723.00	1.40	721.60	0.11
BH296	-29.785	30.507	679.00	1.29	677.71	0.08
BH297	-29.846	30.661	576.00	15.00	561.00	1.94
BH298	-29.786	30.505	696.00	1.36	694.64	3.06
BH299	-29.853	30.523	713.00	6.00	707.00	6.67
BH300	-29.860	30.523	731.00	15.00	716.00	1.17
BH301	-29.862	30.523	738.00	6.00	732.00	5.69
BH302	-29.812	30.518	639.00	35.00	604.00	1.17
BH303	-29.865	30.506	772.00	13.00	759.00	1.94
BH304	-29.872	30.504	819.00	32.00	787.00	1.39
BH305	-29.933	30.511	739.00	12.00	727.00	1.81
BH306	-29.936	30.559	679.00	30.00	649.00	0.13
BH307	-29.971	30.505	780.00	69.00	711.00	2.78
BH308	-29.997	30.548	668.00	25.00	643.00	2.78
BH309	-29.882	30.721	492.00	47.00	445.00	0.50
BH310	-29.956	30.642	692.00	17.90	674.10	0.70
BH311	-29.957	30.646	672.00	19.85	652.15	0.37
BH312	-29.961	30.646	660.00	8.80	651.20	0.69
BH313	-29.958	30.653	655.00	13.50	641.50	3.79
BH314	-29.958	30.657	695.00	94.50	600.50	0.70
BH315	-29.961	30.746	427.00	5.07	421.93	0.88
BH316	-29.828	30.748	503.00	2.77	500.23	0.44
BH317	-29.833	30.739	453.00	4.60	448.40	0.01

BH318	-29.795	30.668	575.00	16.41	558.59	0.25
BH319	-29.793	30.670	547.00	37.43	509.57	0.17
BH320	-29.794	30.673	523.00	49.10	473.90	0.17
BH321	-29.793	30.670	547.00	8.22	538.78	0.07
BH322	-29.831	30.746	548.00	14.93	533.07	0.25
BH323	-29.824	30.747	563.00	46.88	516.12	0.20
BH324	-29.841	30.748	491.00	41.74	449.26	0.40
BH325	-29.885	30.716	520.00	23.00	497.00	0.08
BH326	-29.975	30.703	555.00	23.00	532.00	0.09
BH327	-29.940	30.698	518.00	0.53	517.47	0.10
BH328	-29.950	30.698	524.00	13.77	510.23	1.43
BH329	-29.936	30.701	558.00	11.12	546.88	0.80
BH330	-29.876	30.723	446.00	46.70	399.30	2.78
BH331	-29.947	30.722	576.00	54.61	521.39	0.03
BH332	-29.952	30.737	484.00	41.36	442.64	0.67
BH333	-29.928	30.708	535.00	36.45	498.55	1.40
BH334	-29.939	30.693	574.00	23.78	550.22	3.50
BH335	-29.959	30.701	547.00	22.76	524.24	0.40
BH336	-29.952	30.702	519.00	0.27	518.73	42.00
BH337	-29.952	30.702	519.00	35.48	483.52	14.00
BH338	-29.939	30.693	574.00	30.20	543.80	4.22
BH339	-29.939	30.693	574.00	42.53	531.47	6.94
BH340	-29.999	30.701	478.00	2.95	475.05	2.14
BH341	-29.971	30.696	500.00	25.00	475.00	1.75
BH342	-29.942	30.674	650.00	34.50	615.50	2.33
BH343	-29.944	30.730	565.00	57.03	507.97	12.00
BH344	-29.884	30.714	580.00	22.68	557.32	1.51
BH345	-29.893	30.709	561.00	30.92	530.08	0.75
BH346	-29.896	30.673	668.00	9.92	658.08	1.34
BH347	-29.902	30.682	630.00	8.80	621.20	0.67
BH348	-29.947	30.722	570.00	55.88	514.12	0.10
BH349	-29.948	30.711	521.00	23.71	497.29	0.03
BH350	-29.898	30.670	705.00	1.25	703.75	1.00
BH351	-29.897	30.666	710.00	4.04	705.96	1.67
BH352	-29.950	30.764	284.00	3.00	281.00	0.72
BH353	-29.904	30.755	561.00	1.80	559.20	0.04
BH354	-29.990	30.847	188.00	18.00	170.00	0.23
BH355	-29.987	30.840	168.00	41.00	127.00	0.80
BH356	-29.986	30.831	254.00	45.60	208.40	2.00
BH357	-29.986	30.802	320.00	40.96	279.04	1.50
BH358	-29.982	30.819	251.00	33.00	218.00	2.50
BH359	-29.984	30.814	282.00	37.00	245.00	1.30
BH360	-29.986	30.800	331.00	39.50	291.50	0.20
BH361	-30.422	30.573	199.00	11.00	188.00	0.22
BH362	-30.239	30.684	242.00	29.50	212.50	1.94
BH363	-29.987	30.805	307.00	12.00	295.00	1.40

BH364	-29.985	30.813	294.00	15.00	279.00	0.15
BH365	-29.987	30.781	375.00	25.00	350.00	0.70
BH366	-29.981	30.788	349.00	18.00	331.00	0.33
BH367	-30.000	30.795	346.00	6.00	340.00	1.20
BH368	-29.999	30.846	122.00	17.00	105.00	10.00
BH369	-29.996	30.806	317.00	4.00	313.00	0.40
BH370	-29.993	30.802	311.00	5.40	305.60	0.15
BH371	-29.998	30.805	318.00	5.00	313.00	0.17
BH372	-29.998	30.772	384.00	27.00	357.00	0.30
BH373	-29.993	30.790	339.00	8.00	331.00	0.01
BH374	-29.931	30.841	150.00	27.00	123.00	0.56
BH375	-29.943	30.811	323.00	17.00	306.00	2.22
BH376	-29.955	30.806	307.00	72.50	234.50	0.66
BH377	-29.957	30.837	249.00	75.00	174.00	2.50
BH378	-29.959	30.849	193.00	67.00	126.00	1.11
BH379	-29.947	30.803	307.00	7.00	300.00	0.07
BH380	-29.954	30.814	295.00	77.00	218.00	0.18
BH381	-29.950	30.837	247.00	48.00	199.00	0.01
BH382	-29.939	30.828	214.00	48.00	166.00	0.01
BH383	-29.939	30.818	332.00	62.50	269.50	0.83
BH384	-29.952	30.846	176.00	55.00	121.00	0.06
BH385	-29.939	30.823	258.00	2.90	255.10	0.01
BH386	-29.981	30.840	140.00	29.00	111.00	4.00
BH387	-29.980	30.825	207.00	32.00	175.00	1.50
BH388	-29.980	30.836	160.00	33.00	127.00	1.00
BH389	-29.974	30.824	132.00	22.00	110.00	14.00
BH390	-29.974	30.793	241.00	30.00	211.00	4.00
BH391	-29.851	30.933	175.00	2.20	172.80	2.50
BH392	-29.851	30.933	175.00	1.60	173.40	6.00
BH393	-29.824	30.834	363.00	16.00	347.00	10.00
BH394	-29.815	30.847	349.00	14.00	335.00	5.00
BH395	-29.821	30.880	324.00	8.00	316.00	6.00
BH396	-29.775	30.808	576.00	76.00	500.00	2.50
BH397	-29.833	30.928	244.00	3.41	240.59	7.00
BH398	-29.800	30.828	540.00	15.40	524.60	3.50
BH399	-29.800	30.830	528.00	10.60	517.40	0.17
BH400	-29.795	30.829	530.00	1.30	528.70	0.14
BH401	-29.799	30.825	547.00	54.00	493.00	0.25
BH402	-29.794	30.828	535.00	12.30	522.70	0.33
BH403	-29.846	30.825	315.00	3.89	311.11	0.33
BH404	-29.848	30.821	276.00	3.50	272.50	2.26
BH405	-29.954	30.910	67.00	52.32	14.68	2.00
BH406	-29.958	30.910	61.00	32.10	28.90	0.63
BH407	-29.956	30.912	50.00	19.50	30.50	6.60
BH408	-29.979	30.954	4.00	1.91	2.09	0.58
BH409	-29.962	30.963	10.00	5.11	4.89	1.10

BH410	-29.962	30.963	10.00	5.48	4.52	1.11
BH411	-29.963	30.963	9.00	0.93	8.07	9.80
BH412	-29.963	30.964	9.00	3.80	5.20	19.00
BH413	-29.963	30.964	9.00	3.01	5.99	0.83
BH414	-29.963	30.967	7.00	2.93	4.07	13.00
BH415	-29.963	30.967	7.00	2.41	4.59	26.00
BH416	-29.965	30.964	6.00	0.83	5.17	10.00
BH417	-29.965	30.964	6.00	0.90	5.10	6.31
BH418	-29.963	30.968	7.00	0.45	6.55	8.33
BH419	-29.963	30.968	7.00	0.48	6.52	25.00
BH420	-29.969	30.964	6.00	1.05	4.95	25.00
BH421	-29.969	30.964	6.00	1.08	4.92	5.56
BH422	-29.963	30.966	6.00	2.06	3.94	4.44
BH423	-29.963	30.965	7.00	0.84	6.16	1.06
BH424	-29.963	30.965	7.00	0.88	6.12	0.28
BH425	-29.963	30.965	7.00	0.64	6.36	1.00
BH426	-29.963	30.965	7.00	0.41	6.59	3.79
BH427	-29.963	30.965	7.00	0.94	6.06	0.13
BH428	-29.963	30.965	7.00	0.62	6.38	0.81
BH429	-29.963	30.962	4.00	1.05	2.95	1.30
BH430	-29.958	30.963	14.00	1.05	12.95	0.15
BH431	-29.958	30.963	14.00	4.10	9.90	1.82
BH432	-29.959	30.964	12.00	4.80	7.20	1.25
BH433	-29.959	30.964	12.00	3.88	8.12	0.10
BH434	-29.953	30.964	10.00	4.35	5.65	0.25
BH435	-29.985	30.958	13.00	4.74	8.26	0.23
BH436	-29.971	30.971	16.00	1.43	14.57	0.57
BH437	-29.971	30.971	16.00	1.44	14.56	0.39
BH438	-29.961	30.971	8.00	0.63	7.37	0.47
BH439	-29.960	30.971	11.00	0.44	10.56	0.50
BH440	-29.985	30.958	13.00	4.34	8.66	0.56
BH441	-29.983	30.963	19.00	3.05	15.95	0.30
BH442	-29.983	30.963	19.00	2.92	16.08	1.40
BH443	-29.975	30.969	53.00	1.41	51.59	0.34
BH444	-29.975	30.969	53.00	1.76	51.24	0.09
BH445	-29.975	30.969	53.00	1.54	51.46	0.10
BH446	-29.966	30.967	6.00	1.44	4.56	0.20
BH447	-29.969	30.967	7.00	1.45	5.55	1.66
BH448	-29.967	30.972	10.00	1.33	8.67	0.33
BH449	-29.973	30.969	11.00	1.56	9.44	0.53
BH450	-29.972	30.967	8.00	1.27	6.73	0.15
BH451	-29.971	30.966	9.00	1.99	7.01	0.22
BH452	-29.976	30.963	9.00	1.86	7.14	0.08
BH453	-29.984	30.961	13.00	1.87	11.13	0.50
BH454	-29.982	30.961	14.00	4.53	9.47	0.07
BH455	-29.875	30.756	291.00	75.90	215.10	1.00

BH456	-29.870	30.776	212.00	50.20	161.80	1.00
BH457	-29.948	30.761	323.00	0.61	322.39	6.30
BH458	-29.952	30.753	410.00	27.78	382.22	0.51
BH459	-29.993	30.796	321.00	15.26	305.74	0.51
BH460	-29.860	30.966	63.00	29.04	33.96	1.39
BH461	-29.982	30.789	370.00	9.36	360.64	4.44
BH462	-29.952	30.753	410.00	29.00	381.00	7.58
BH463	-29.875	30.756	337.00	75.04	261.96	0.14
BH464	-29.904	30.756	558.00	4.86	553.14	0.14
BH465	-29.938	30.804	325.00	5.10	319.90	0.67
BH466	-29.941	30.828	251.00	36.88	214.12	5.00
BH467	-29.931	30.842	150.00	27.36	122.64	1.11
BH468	-29.946	30.789	345.00	42.83	302.17	0.17
BH469	-29.355	31.028	523.00	54.00	469.00	0.17
BH470	-29.408	31.146	234.00	3.29	230.71	0.50
BH471	-29.411	31.057	417.00	1.28	415.72	0.09
BH472	-29.423	31.056	404.00	17.50	386.50	0.55
BH473	-29.460	31.048	376.00	42.10	333.90	0.40
BH474	-29.461	31.049	366.00	41.30	324.70	0.10
BH475	-29.325	31.010	370.00	16.50	353.50	0.06
BH476	-29.447	31.015	537.00	12.15	524.85	0.08
BH477	-29.496	31.031	329.00	21.98	307.02	0.08
BH478	-29.447	31.015	532.00	12.15	519.85	0.03
BH479	-29.420	31.003	621.00	31.84	589.16	0.03
BH480	-29.331	31.109	468.00	32.90	435.10	0.02
BH481	-29.377	31.038	635.00	27.44	607.56	0.08
BH482	-29.347	31.110	506.00	51.34	454.66	0.02
BH483	-29.497	31.082	235.00	3.62	231.38	0.10
BH484	-29.519	31.059	103.00	1.19	101.81	0.08
BH485	-29.534	31.062	204.00	55.40	148.60	0.05
BH486	-29.596	31.058	80.00	52.30	27.70	0.01
BH487	-29.546	31.083	95.00	1.31	93.69	0.10
BH488	-29.546	31.068	188.00	16.30	171.70	0.34
BH489	-29.553	31.095	123.00	32.30	90.70	3.79
BH490	-29.549	31.103	114.00	2.92	111.08	3.33
BH491	-29.555	31.087	101.00	52.80	48.20	0.40
BH492	-29.560	31.088	133.00	12.00	121.00	0.08
BH493	-29.555	31.089	101.00	25.00	76.00	2.00
BH494	-29.521	31.048	195.00	54.05	140.95	2.48
BH495	-29.534	31.057	193.00	35.00	158.00	0.34
BH496	-29.531	31.081	95.00	30.24	64.76	0.20
BH497	-29.543	31.047	219.00	47.00	172.00	0.88
BH498	-29.502	31.020	345.00	12.98	332.02	1.25
BH499	-29.526	31.098	80.00	58.24	21.76	1.25
BH500	-29.521	31.048	190.00	54.05	135.95	0.05
BH501	-29.534	31.057	188.00	35.00	153.00	5.55

BH502	-29.531	31.081	90.00	30.24	59.76	2.75
BH503	-29.543	31.047	214.00	47.00	167.00	0.66
BH504	-29.502	31.020	340.00	12.98	327.02	0.43
BH505	-29.505	31.218	56.00	4.80	51.20	10.00
BH506	-29.507	31.228	23.00	52.45	-29.45	0.56
BH507	-29.506	31.216	65.00	21.70	43.30	0.03
BH508	-29.943	30.187	76.00	1.81	74.19	0.01
BH509	-30.184	30.170	900.00	18.00	882.00	0.02
BH510	-30.164	30.153	964.00	12.00	952.00	0.02
BH511	-30.149	30.183	778.00	10.00	768.00	0.03
BH512	-30.057	30.236	493.00	13.00	480.00	0.02
BH513	-30.037	30.241	599.00	40.00	559.00	0.50
BH514	-30.097	30.245	692.00	20.00	672.00	0.02
BH515	-30.066	30.232	496.00	20.00	476.00	0.01
BH516	-30.185	30.169	920.00	10.00	910.00	0.02
BH517	-30.216	30.175	1035.00	10.00	1025.00	0.40
BH518	-30.218	30.152	1050.00	20.00	1030.00	0.01
BH519	-30.216	30.183	1044.00	15.00	1029.00	0.40
BH520	-30.163	30.153	958.00	30.00	928.00	0.08
BH521	-30.061	30.166	808.00	21.38	786.62	0.03
BH522	-30.064	30.164	838.00	28.90	809.10	0.10
BH523	-30.326	30.228	943.00	12.84	930.16	0.10
BH524	-30.064	30.163	1258.00	28.90	1229.10	0.01
BH525	-30.061	30.167	800.00	21.38	778.62	0.03
BH526	-30.064	30.164	857.40	42.75	814.65	0.10
BH527	-30.119	30.404	352.00	7.60	344.40	0.02
BH528	-30.166	30.398	537.00	22.00	515.00	0.30
BH529	-30.183	30.397	551.07	81.00	470.07	0.08
BH530	-30.101	30.400	228.00	17.00	211.00	0.20
BH531	-30.169	30.437	405.68	49.00	356.68	0.38
BH532	-30.147	30.310	901.00	1.10	899.90	0.31
BH533	-30.076	30.305	769.00	62.70	706.30	0.14
BH534	-30.090	30.257	714.00	10.00	704.00	0.14
BH535	-30.110	30.252	862.00	50.00	812.00	2.50
BH536	-30.111	30.359	785.00	18.00	767.00	0.17
BH537	-30.113	30.262	865.00	11.00	854.00	0.20
BH538	-30.114	30.264	852.00	50.00	802.00	1.40
BH539	-30.115	30.266	845.00	60.00	785.00	0.50
BH540	-30.220	30.340	672.08	12.00	660.08	0.30
BH541	-30.240	30.375	674.82	22.00	652.82	0.01
BH542	-30.211	30.455	445.00	40.00	405.00	0.08
BH543	-30.219	30.490	416.00	61.00	355.00	0.39
BH544	-30.232	30.472	421.00	25.00	396.00	0.19
BH545	-30.012	30.394	870.00	6.00	864.00	0.14
BH546	-30.023	30.393	847.00	30.00	817.00	1.00
BH547	-30.118	30.402	353.00	88.00	265.00	20.00

BH548	-30.170	30.390	593.44	1.33	592.11	0.08
BH549	-30.145	30.314	902.00	1.10	900.90	0.34
BH550	-30.147	30.307	895.00	1.03	893.97	0.71
BH551	-30.076	30.305	780.00	2.70	777.30	0.13
BH552	-30.176	30.390	637.94	0.90	637.04	1.00
BH553	-30.175	30.375	715.00	0.10	714.90	0.50
BH554	-30.117	30.345	930.00	76.69	853.31	0.30
BH555	-30.366	30.179	851.61	30.50	821.11	0.30
BH556	-30.128	30.438	776.00	38.00	738.00	2.50
BH557	-30.132	30.463	665.00	23.50	641.50	2.22
BH558	-30.323	30.233	945.18	7.00	938.18	0.03
BH559	-30.300	30.223	892.00	7.62	884.38	0.01
BH560	-30.276	30.240	946.00	31.64	914.36	0.04
BH561	-30.335	30.229	976.00	68.64	907.36	0.01
BH562	-30.325	30.229	940.00	12.60	927.40	0.10
BH563	-30.387	30.175	720.00	0.09	719.91	0.01
BH564	-30.375	30.175	775.00	0.10	774.90	0.01
BH565	-30.164	30.375	740.00	2.40	737.60	0.03
BH566	-30.374	30.151	880.00	42.80	837.20	0.02
BH567	-30.305	30.158	885.00	17.86	867.14	0.01
BH568	-30.320	30.236	982.06	60.61	921.45	0.02
BH569	-30.320	30.235	1082.65	1.01	1081.64	0.03
BH570	-30.305	30.158	889.40	17.86	871.54	0.02
BH571	-30.296	30.294	929.33	11.40	917.93	0.08
BH572	-30.327	30.266	961.00	28.00	933.00	0.50
BH573	-30.259	30.402	746.00	3.00	743.00	0.03
BH574	-30.317	30.273	911.00	69.00	842.00	0.10
BH575	-30.345	30.282	906.00	60.00	846.00	0.02
BH576	-30.271	30.349	754.00	14.00	740.00	0.05
BH577	-30.288	30.321	965.00	26.00	939.00	0.02
BH578	-30.263	30.329	772.00	54.00	718.00	0.02
BH579	-30.257	30.423	769.00	63.00	706.00	0.20
BH580	-30.266	30.357	757.12	23.00	734.12	0.50
BH581	-30.356	30.485	485.00	7.00	478.00	0.03
BH582	-30.341	30.460	552.00	15.00	537.00	0.02
BH583	-30.371	30.444	527.00	8.00	519.00	1.00
BH584	-30.373	30.447	499.00	6.00	493.00	0.60
BH585	-30.373	30.462	501.00	14.00	487.00	0.30
BH586	-30.369	30.466	497.00	14.00	483.00	0.02
BH587	-30.382	30.476	507.00	40.00	467.00	0.03
BH588	-30.380	30.493	461.00	54.00	407.00	0.02
BH589	-30.396	30.474	446.00	22.00	424.00	0.01
BH590	-30.386	30.368	798.00	80.00	718.00	0.02
BH591	-30.286	30.348	784.00	45.00	739.00	0.06
BH592	-30.258	30.423	773.00	63.00	710.00	0.20
BH593	-30.356	30.484	485.00	7.00	478.00	0.05

BH594	-30.267	30.357	759.00	23.00	736.00	0.10
BH595	-30.340	30.251	943.00	11.60	931.40	0.30
BH596	-30.332	30.286	924.00	71.22	852.78	0.08
BH597	-30.340	30.251	945.00	14.42	930.58	0.20
BH598	-30.343	30.278	938.00	39.20	898.80	4.11
BH599	-30.343	30.250	920.00	1.30	918.70	0.14
BH600	-30.273	30.488	575.00	2.38	572.62	0.72
BH601	-30.274	30.491	500.00	20.75	479.25	0.57
BH602	-30.106	30.654	266.00	24.49	241.51	0.34
BH603	-30.124	30.744	270.00	18.00	252.00	0.56
BH604	-30.136	30.738	276.00	2.00	274.00	0.22
BH605	-30.172	30.641	329.00	8.50	320.50	0.22
BH606	-30.193	30.521	344.00	12.00	332.00	1.00
BH607	-30.227	30.667	276.00	8.00	268.00	0.17
BH608	-30.104	30.605	142.00	4.20	137.80	0.20
BH609	-30.012	30.714	506.00	30.00	476.00	10.00
BH610	-30.074	30.571	655.00	3.40	651.60	0.20
BH611	-30.075	30.552	654.00	7.00	647.00	2.90
BH612	-30.131	30.652	115.00	24.00	91.00	0.30
BH613	-30.226	30.648	383.00	38.00	345.00	1.50
BH614	-30.028	30.649	631.00	4.00	627.00	0.10
BH615	-30.045	30.625	640.00	30.00	610.00	1.00
BH616	-30.069	30.686	337.00	9.00	328.00	0.27
BH617	-30.086	30.530	177.00	6.20	170.80	1.00
BH618	-30.206	30.515	315.00	19.00	296.00	0.20
BH619	-30.177	30.580	492.00	15.00	477.00	0.71
BH620	-30.046	30.520	350.00	6.00	344.00	0.10
BH621	-30.053	30.666	484.00	6.00	478.00	0.60
BH622	-30.135	30.698	360.00	8.00	352.00	0.60
BH623	-30.111	30.654	482.00	3.00	479.00	0.08
BH624	-30.107	30.588	222.00	1.13	220.87	1.50
BH625	-30.035	30.681	581.00	96.00	485.00	0.10
BH626	-30.210	30.662	358.00	41.50	316.50	1.20
BH627	-30.195	30.510	409.00	40.00	369.00	0.66
BH628	-30.002	30.530	705.00	22.00	683.00	1.00
BH629	-30.004	30.528	700.00	19.00	681.00	2.00
BH630	-30.025	30.545	642.00	12.00	630.00	4.00
BH631	-30.112	30.572	207.00	25.45	181.55	0.76
BH632	-30.116	30.646	413.00	8.18	404.82	4.00
BH633	-30.113	30.610	253.00	69.53	183.47	0.42
BH634	-30.142	30.682	98.00	45.00	53.00	0.70
BH635	-30.095	30.502	185.00	0.79	184.21	0.50
BH636	-30.109	30.599	136.00	3.27	132.73	0.50
BH637	-30.110	30.673	275.00	25.34	249.66	7.00
BH638	-30.098	30.535	198.00	40.40	157.60	0.14
BH639	-30.168	30.517	450.00	8.63	441.37	0.27

BH640	-30.112	30.572	202.00	25.45	176.55	0.40
BH641	-30.110	30.673	270.00	25.34	244.66	0.27
BH642	-30.116	30.646	408.00	8.18	399.82	0.02
BH643	-30.113	30.610	248.00	69.53	178.47	0.28
BH644	-30.095	30.502	180.00	0.79	179.21	0.28
BH645	-30.087	30.639	249.00	15.85	233.15	0.28
BH646	-30.109	30.599	131.00	3.27	127.73	1.39
BH647	-30.097	30.549	263.00	13.27	249.73	0.31
BH648	-30.081	30.511	309.00	46.76	262.24	0.14
BH649	-30.091	30.525	152.00	14.35	137.65	1.00
BH650	-30.103	30.621	265.00	13.87	251.13	0.54
BH651	-30.117	30.684	140.00	6.38	133.62	3.33
BH652	-30.081	30.643	377.00	29.15	347.85	0.61
BH653	-30.086	30.643	326.00	38.75	287.25	1.40
BH654	-30.089	30.656	165.00	56.73	108.27	0.53
BH655	-30.104	30.616	238.00	2.97	235.03	0.42
BH656	-30.109	30.624	322.00	43.08	278.92	0.63
BH657	-30.100	30.668	164.00	12.30	151.70	0.19
BH658	-30.107	30.639	349.00	1.99	347.01	0.69
BH659	-30.049	30.520	369.00	60.33	308.67	0.13
BH660	-30.036	30.589	711.00	6.13	704.87	0.89
BH661	-30.039	30.524	443.00	10.80	432.20	0.13
BH662	-30.075	30.568	646.00	8.24	637.76	0.25
BH663	-30.075	30.581	633.00	11.95	621.05	0.72
BH664	-30.102	30.670	160.00	60.33	99.67	0.06
BH665	-30.132	30.683	138.00	6.38	131.62	0.24
BH666	-30.128	30.693	199.00	26.70	172.30	0.30
BH667	-30.122	30.694	137.00	11.70	125.30	2.03
BH668	-30.114	30.694	103.00	8.18	94.82	0.20
BH669	-30.135	30.697	359.00	8.71	350.29	0.47
BH670	-30.133	30.697	373.00	40.55	332.45	0.19
BH671	-30.102	30.634	391.00	21.23	369.77	0.06
BH672	-30.118	30.718	178.00	48.77	129.23	0.69
BH673	-30.118	30.602	146.00	4.95	141.05	0.13
BH674	-30.089	30.524	179.00	16.10	162.90	0.89
BH675	-30.077	30.554	753.00	18.60	734.40	0.25
BH676	-30.101	30.589	237.00	1.58	235.42	0.11
BH677	-30.112	30.568	264.00	55.75	208.25	0.72
BH678	-30.105	30.609	158.00	3.65	154.35	0.26
BH679	-30.112	30.659	400.00	26.14	373.86	0.19
BH680	-30.014	30.516	620.00	35.09	584.91	0.69
BH681	-30.116	30.753	251.00	5.00	246.00	0.07
BH682	-30.026	30.788	307.00	54.00	253.00	0.31
BH683	-30.001	30.773	382.00	6.00	376.00	0.18
BH684	-30.021	30.817	233.00	13.00	220.00	0.02
BH685	-30.009	30.808	306.00	6.00	300.00	0.69

BH686	-30.001	30.805	325.00	8.00	317.00	0.17
BH687	-30.004	30.853	151.00	8.00	143.00	1.25
BH688	-30.009	30.826	198.00	36.00	162.00	0.16
BH689	-30.000	30.834	158.00	40.00	118.00	0.17
BH690	-30.045	30.818	146.00	64.00	82.00	0.28
BH691	-30.039	30.818	124.00	11.50	112.50	0.66
BH692	-30.035	30.829	156.00	62.00	94.00	0.68
BH693	-30.016	30.854	77.00	31.00	46.00	1.43
BH694	-30.019	30.844	83.00	24.00	59.00	0.22
BH695	-30.000	30.844	144.00	32.00	112.00	0.80
BH696	-30.024	30.796	288.00	33.00	255.00	0.95
BH697	-30.035	30.821	126.00	5.00	121.00	0.02
BH698	-30.000	30.807	325.00	7.00	318.00	0.08
BH699	-30.050	30.841	120.00	12.00	108.00	0.44
BH700	-30.027	30.832	140.00	30.00	110.00	2.00
BH701	-30.019	30.832	114.00	10.00	104.00	0.24
BH702	-30.012	30.808	292.00	10.00	282.00	0.05
BH703	-30.139	30.786	138.00	5.00	133.00	0.04
BH704	-30.124	30.765	195.00	6.00	189.00	0.28
BH705	-30.130	30.760	210.00	5.27	204.73	0.14
BH706	-30.102	30.798	158.00	11.00	147.00	1.43
BH707	-30.100	30.790	187.00	1.20	185.80	0.08
BH708	-30.109	30.813	95.00	22.70	72.30	0.55
BH709	-30.102	30.798	155.00	13.00	142.00	0.28
BH710	-30.034	30.821	142.00	0.80	141.20	0.34
BH711	-30.009	30.789	323.00	3.62	319.38	0.30
BH712	-30.025	30.787	299.00	7.53	291.47	6.60
BH713	-30.027	30.816	160.00	10.35	149.65	0.33
BH714	-30.042	30.809	139.00	4.02	134.98	0.44
BH715	-30.002	30.783	357.00	0.30	356.70	0.15
BH716	-30.004	30.853	140.00	4.26	135.74	0.20
BH717	-30.267	30.639	250.00	15.00	235.00	0.10
BH718	-30.343	30.646	74.00	1.00	73.00	0.10
BH719	-30.301	30.537	435.00	78.00	357.00	0.30
BH720	-30.261	30.510	578.00	30.00	548.00	1.30
BH721	-30.317	30.556	436.00	1.00	435.00	10.00
BH722	-30.315	30.555	418.00	80.00	338.00	0.75
BH723	-30.293	30.510	564.00	30.00	534.00	0.42
BH724	-30.347	30.516	330.00	1.41	328.59	0.38
BH725	-29.956	30.975	8.09	10.43	-2.33	0.00
BH726	-29.953	30.986	19.90	10.44	9.46	0.00
BH727	-29.947	30.990	44.00	10.45	33.55	0.00
BH728	-29.950	30.987	37.60	10.45	27.15	0.00
BH729	-29.956	30.983	23.90	0.94	22.96	0.00
BH730	-29.963	30.987	4.80	0.57	4.23	0.00
BH731	-29.964	30.987	5.60	1.18	4.42	0.00

BH732	-29.940	30.968	12.44	1.80	10.64	0.00
BH733	-29.961	30.971	4.30	0.63	3.67	0.00
BH734	-29.960	30.971	5.60	0.44	5.16	0.00
BH735	-29.959	30.964	9.10	4.80	4.30	0.00
BH736	-29.959	30.964	9.10	3.88	5.22	0.00
BH737	-29.958	30.963	9.50	0.00	9.50	0.00
BH738	-29.958	30.963	9.50	1.05	8.45	0.00
BH739	-29.958	30.963	9.50	4.10	5.40	0.00
BH740	-29.955	30.975	9.60	0.68	8.92	0.00
BH741	-29.953	30.961	5.00	0.00	5.00	0.00
BH742	-29.953	30.964	9.90	4.35	5.55	0.00
BH743	-29.920	30.980	6.60	0.81	5.79	0.00
BH744	-29.851	30.933	175.00	2.20	172.80	0.00
BH745	-29.851	30.933	175.00	1.60	173.40	0.00
BH746	-29.833	30.933	244.00	3.41	240.59	0.00
BH747	-29.954	30.910	67.00	52.32	14.68	0.00
BH748	-29.958	30.910	61.00	32.10	28.90	0.00
BH749	-29.956	30.912	50.00	19.50	30.50	0.00
BH750	-29.979	30.954	4.00	1.91	2.09	0.00
BH751	-29.962	30.963	10.00	5.11	4.89	0.00
BH752	-29.962	30.963	10.00	5.48	4.52	0.00
BH753	-29.963	30.963	9.00	0.93	8.07	0.00
BH754	-29.963	30.964	9.00	3.80	5.20	0.00
BH755	-29.963	30.964	9.00	3.01	5.99	0.00
BH756	-29.963	30.967	7.00	2.93	4.07	0.00
BH757	-29.963	30.967	7.00	2.41	4.59	0.00
BH758	-29.965	30.964	6.00	0.83	5.17	0.00
BH759	-29.963	30.964	6.00	0.90	5.10	0.00
BH760	-29.963	30.968	7.00	0.45	6.55	0.00
BH761	-29.963	30.968	7.00	0.48	6.52	0.00
BH762	-29.969	30.964	6.00	1.05	4.95	0.00
BH763	-29.969	30.964	6.00	1.08	4.92	0.00
BH764	-29.963	30.966	6.00	2.06	3.94	0.00
BH765	-29.956	30.966	7.00	0.84	6.16	0.00
BH766	-29.956	30.966	7.00	0.88	6.12	0.00
BH767	-29.956	30.966	7.00	0.64	6.36	0.00
BH768	-29.956	30.966	7.00	0.41	6.59	0.00
BH769	-29.956	30.966	7.00	0.94	6.06	0.00
BH770	-29.956	30.966	7.00	0.62	6.38	0.00
BH771	-29.956	30.962	4.00	1.05	2.95	0.00
BH772	-29.963	30.963	14.00	1.05	12.95	0.00
BH773	-29.958	30.964	14.00	4.10	9.90	0.00
BH774	-29.958	30.964	12.00	4.80	7.20	0.00
BH775	-29.959	30.964	12.00	3.88	8.12	0.00
BH776	-29.959	30.958	10.00	4.35	5.65	0.00
BH777	-29.985	30.971	13.00	4.74	8.26	0.00

BH778	-29.971	30.971	16.00	1.43	14.57	0.00
BH779	-29.971	30.971	16.00	1.44	14.56	0.00
BH780	-29.961	30.971	8.00	0.63	7.37	0.00
BH781	-29.960	30.971	11.00	0.44	10.56	0.00
BH782	-29.985	30.958	13.00	4.34	8.66	0.00
BH783	-29.983	30.963	19.00	3.05	15.95	0.00
BH784	-29.983	30.969	19.00	2.92	16.08	0.00
BH785	-29.975	30.969	53.00	1.41	51.59	0.00
BH786	-29.975	30.967	53.00	1.76	51.24	0.00
BH787	-29.975	30.967	53.00	1.54	51.46	0.00
BH788	-29.966	30.972	6.00	1.44	4.56	0.00
BH789	-29.969	30.969	7.00	1.45	5.55	0.00
BH790	-29.967	30.967	10.00	1.33	8.67	0.00
BH791	-29.973	30.969	11.00	1.56	9.44	0.00
BH792	-29.972	30.963	8.00	1.27	6.73	0.00
BH793	-29.971	30.975	9.00	1.99	7.01	0.00
BH794	-29.976	30.961	9.00	1.86	7.14	0.00
BH795	-29.984	30.961	13.00	1.87	11.13	0.00
BH796	-29.961	30.961	14.00	4.53	9.47	0.00
BH797	-29.966	30.966	63.00	29.04	33.96	0.00
BH798	-29.794	30.668	555.00	16.41	538.59	0.58
BH799	-29.793	30.667	559.00	37.43	521.57	1.70
BH800	-29.793	30.673	517.00	0.00	517.00	10.00
BH801	-29.793	30.672	517.00	8.22	508.78	0.00
BH802	-29.794	30.677	486.00	0.00	486.00	0.00
BH803	-29.754	30.940	239.00	11.50	227.50	0.00
BH804	-29.754	30.940	239.00	34.00	205.00	0.70
BH805	-29.623	30.863	610.00	85.00	525.00	0.05
BH806	-29.629	30.869	606.00	61.00	545.00	0.11
BH807	-29.874	30.790	197.00	0.00	197.00	0.00
BH808	-29.660	30.891	270.00	44.00	226.00	0.03
BH809	-29.629	30.924	507.00	0.00	507.00	0.08
BH810	-29.671	30.888	236.00	0.00	236.00	0.00
BH811	-29.623	30.891	426.00	24.00	402.00	3.89
BH812	-29.618	30.893	422.00	20.00	402.00	0.69
BH813	-29.660	30.888	275.00	112.00	163.00	0.08
BH814	-29.622	30.892	430.00	20.00	410.00	0.08
BH815	-30.192	30.776	38.00	2.30	35.70	0.00
BH816	-30.195	30.776	83.00	56.00	27.00	0.00
BH817	-30.192	30.774	80.00	63.00	17.00	0.00
BH818	-30.192	30.777	7.00	2.60	4.40	1.00
BH819	-29.815	30.983	53.00	14.30	38.70	0.00
BH820	-29.816	30.982	59.00	14.30	44.70	0.44
BH821	-29.819	30.993	98.00	23.70	74.30	0.56
BH822	-29.822	30.982	131.00	15.70	115.30	5.00
BH823	-29.822	30.978	133.00	30.70	102.30	0.00

BH824	-29.816	30.976	73.00	18.60	54.40	0.00
BH825	-29.815	30.977	81.00	22.70	58.30	0.00
BH826	-29.813	30.980	39.00	25.65	13.35	0.00
BH827	-29.814	30.980	47.00	22.00	25.00	0.00
BH828	-29.813	30.982	18.00	0.80	17.20	0.00
BH829	-29.830	30.978	148.00	16.00	132.00	4.00
BH830	-29.818	30.984	106.00	28.50	77.50	0.83
BH831	-29.831	30.746	531.00	0.00	531.00	0.00
BH832	-29.820	30.747	575.00	44.63	530.37	0.30
BH833	-29.819	30.747	575.00	34.52	540.48	0.00
BH834	-29.827	30.750	504.00	40.20	463.80	0.05
BH835	-29.829	30.751	467.00	26.43	440.57	0.00
BH836	-29.784	30.917	246.00	17.40	228.60	0.00
BH837	-29.784	30.917	246.00	20.75	225.25	0.00
BH838	-29.790	30.843	508.00	33.45	474.55	2.08
BH839	-29.788	30.910	197.00	45.48	151.52	6.25
BH840	-29.556	31.044	199.00	5.10	193.90	0.00
BH841	-29.841	30.748	496.00	41.47	454.53	0.08
BH842	-29.824	30.747	559.00	46.88	512.12	1.30
BH843	-29.833	30.756	386.00	4.60	381.40	0.40
BH844	-29.827	30.748	509.00	2.77	506.23	0.20
BH845	-30.058	30.805	185.00	9.66	175.34	0.06
BH846	-30.061	30.802	186.00	42.56	143.44	0.00
BH847	-29.621	31.134	97.00	43.65	53.35	0.17
BH848	-29.618	31.137	113.00	50.00	63.00	0.13
BH849	-29.616	31.134	96.00	0.00	96.00	0.00
BH850	-29.619	31.133	82.00	11.90	70.10	0.40
BH851	-29.615	31.136	111.00	35.60	75.40	0.50
BH852	-30.022	30.790	315.00	19.80	295.20	0.97
BH853	-30.027	30.787	294.00	26.40	267.60	1.24
BH854	-30.033	30.818	143.00	33.90	109.10	0.80
BH855	-30.053	30.805	181.00	7.63	173.37	0.38
BH856	-30.100	30.791	190.00	60.20	129.80	0.03
BH857	-30.104	30.787	164.00	55.70	108.30	0.03
BH858	-30.031	30.679	578.00	17.20	560.80	0.14
BH859	-30.009	30.679	575.00	35.00	540.00	0.07
BH860	-30.031	30.686	556.00	27.00	529.00	0.18
BH861	-30.031	30.686	566.00	55.00	511.00	0.05
BH862	-29.974	30.722	505.00	43.30	461.70	0.13
BH863	-29.952	30.768	356.00	52.08	303.92	1.67
BH864	-29.949	30.767	3616.00	0.00	3616.00	0.00
BH865	-29.971	30.684	515.00	29.80	485.20	0.19
BH866	-30.143	30.709	330.00	87.25	242.75	0.63
BH867	-30.142	30.709	315.00	0.00	315.00	0.00
BH868	-30.117	30.688	130.00	3.40	126.60	1.22
BH869	-30.111	30.659	429.00	28.00	401.00	0.87

BH870	-30.109	30.569	249.00	24.40	224.60	0.72
BH871	-30.109	30.653	397.00	22.90	374.10	0.42
BH872	-30.095	30.637	368.00	55.20	312.80	0.52
BH873	-30.096	30.625	266.00	112.56	153.44	1.11
BH874	-30.121	30.583	108.00	18.40	89.60	1.25
BH875	-30.112	30.569	285.00	106.00	179.00	0.24
BH876	-29.994	30.718	470.00	25.60	444.40	0.11
BH877	-29.993	30.717	484.00	24.34	459.66	0.42
BH878	-30.012	30.714	511.00	39.90	471.10	0.03
BH879	-30.020	30.723	467.00	39.30	427.70	1.05
BH880	-30.020	30.723	467.00	38.20	428.80	0.08
BH881	-30.033	30.736	431.00	48.60	382.40	0.16
BH882	-30.033	30.736	431.00	88.70	342.30	0.00
BH883	-30.129	30.756	221.00	3.85	217.15	1.43
BH884	-30.134	30.762	215.00	33.70	181.30	0.41
BH885	-30.131	30.762	205.00	0.00	205.00	0.00
BH886	-30.131	30.763	201.00	0.00	201.00	0.00
BH887	-30.059	30.756	230.00	46.50	183.50	0.02
BH888	-30.067	30.772	265.00	14.20	250.80	0.00
BH889	-30.104	30.787	170.00	0.00	170.00	0.00
BH890	-30.071	30.675	469.00	0.00	469.00	0.00
BH891	-30.035	30.632	644.00	0.00	644.00	0.56
BH892	-30.032	30.631	651.00	0.00	651.00	0.17
BH893	-29.958	30.647	679.00	0.00	679.00	1.94
BH894	-29.993	30.796	331.00	0.00	331.00	0.00
BH895	-29.993	30.796	333.00	0.00	333.00	0.00
BH896	-29.986	30.801	332.00	0.00	332.00	0.00
BH897	-29.940	30.694	583.00	0.00	583.00	0.00
BH898	-29.928	30.709	548.00	0.00	548.00	0.08
BH899	-29.988	30.657	677.00	0.00	677.00	0.00
BH900	-30.000	30.783	366.00	0.00	366.00	0.00
BH901	-30.137	30.796	136.00	0.00	136.00	0.00
BH902	-30.137	30.792	137.00	0.00	137.00	0.00
BH903	-30.070	30.564	669.00	0.00	669.00	1.39
BH904	-30.082	30.549	750.00	0.00	750.00	0.42
BH905	-30.077	30.553	752.00	0.00	752.00	0.00
BH906	-30.035	30.551	599.00	0.00	599.00	0.14
BH907	-30.121	30.585	110.00	0.00	110.00	0.00
BH908	-30.034	30.554	561.00	0.00	561.00	0.33
BH909	-30.034	30.554	561.00	0.00	561.00	2.03
BH910	-30.040	30.806	153.00	6.00	147.00	2.78
BH911	-30.042	30.809	133.00	5.00	128.00	0.00
BH912	-30.041	30.821	125.00	2.00	123.00	0.22
BH913	-30.023	30.821	166.00	4.00	162.00	2.50
BH914	-30.005	30.822	178.00	51.00	127.00	0.22
BH915	-30.024	30.821	163.00	32.00	131.00	0.22

BH916	-30.014	30.832	146.00	0.00	146.00	0.02
BH917	-30.028	30.828	122.00	15.00	107.00	0.22
BH918	-30.022	30.838	122.00	25.00	97.00	0.22
BH919	-30.042	30.805	145.00	6.00	139.00	1.83
BH920	-30.002	30.797	327.00	1.00	326.00	0.33
BH921	-30.109	30.594	146.00	3.00	143.00	0.56
BH922	-30.104	30.616	241.00	18.00	223.00	0.19
BH923	-30.103	30.623	275.00	0.00	275.00	0.02
BH924	-30.103	30.633	406.00	15.00	391.00	0.10
BH925	-30.080	30.643	372.00	72.00	300.00	0.25
BH926	-30.088	30.655	180.00	26.00	154.00	0.08
BH927	-30.085	30.643	330.00	48.00	282.00	0.08
BH928	-30.107	30.641	356.00	3.00	353.00	0.19
BH929	-30.099	30.608	196.00	18.00	178.00	0.69
BH930	-30.102	30.668	177.00	14.00	163.00	0.22
BH931	-30.097	30.671	142.00	0.00	142.00	0.02
BH932	-30.123	30.689	183.00	0.00	183.00	0.02
BH933	-30.132	30.653	123.00	0.00	123.00	0.00
BH934	-30.113	30.695	103.00	7.00	96.00	0.83
BH935	-30.129	30.723	240.00	20.00	220.00	0.11
BH936	-30.103	30.622	269.00	6.00	263.00	0.83
BH937	-30.122	30.694	148.00	13.00	135.00	0.24
BH938	-30.127	30.694	206.00	25.00	181.00	0.11
BH939	-30.127	30.669	113.00	45.00	68.00	0.11
BH940	-30.113	30.645	476.00	0.00	476.00	0.00
BH941	-30.099	30.675	195.00	17.00	178.00	0.19
BH942	-30.129	30.650	105.00	34.00	71.00	800.00
BH943	-30.128	30.683	164.00	0.00	164.00	0.00
BH944	-30.074	30.580	643.00	20.00	623.00	800.00
BH945	-30.074	30.568	649.00	11.00	638.00	800.00
BH946	-30.131	30.683	153.00	42.00	111.00	1500.00
BH947	-30.016	30.665	631.00	0.00	631.00	0.00
BH948	-30.044	30.626	365.00	27.00	338.00	2500.00
BH949	-30.040	30.623	637.00	18.00	619.00	4000.00
BH950	-30.034	30.623	620.00	1.00	619.00	800.00
BH951	-30.058	30.653	389.00	66.00	323.00	0.25
BH952	-30.042	30.657	596.00	0.00	596.00	0.00
BH953	-30.013	30.676	585.00	0.00	585.00	0.02
BH954	-30.013	30.688	519.00	10.00	509.00	0.67
BH955	-30.007	30.695	516.00	26.00	490.00	0.19
BH956	-30.002	30.709	500.00	18.00	482.00	0.22
BH957	-30.056	30.707	413.00	68.00	345.00	0.11
BH958	-30.020	30.783	343.00	30.00	313.00	0.33
BH959	-30.015	30.789	338.00	0.00	338.00	6.67
BH960	-30.012	30.799	308.00	4.00	304.00	6.67
BH961	-29.982	30.744	459.00	66.00	393.00	0.17

BH962	-29.985	30.664	631.00	18.00	613.00	0.14
BH963	-29.983	30.667	612.00	22.00	590.00	0.17
BH964	-29.946	30.722	577.00	60.00	517.00	0.14
BH965	-29.935	30.701	563.00	14.00	549.00	0.18
BH966	-29.924	30.718	528.00	32.00	496.00	0.22
BH967	-29.948	30.711	526.00	22.00	504.00	0.14
BH968	-29.976	30.743	348.00	28.00	320.00	0.19
BH969	-30.017	30.795	320.00	12.00	308.00	8.89
BH970	-29.903	30.736	588.00	16.00	572.00	0.08
BH971	-29.903	30.751	577.00	0.00	577.00	0.02
BH972	-29.914	30.763	434.00	0.00	434.00	0.00
BH973	-29.971	30.758	358.00	0.00	358.00	0.00
BH974	-29.916	30.751	334.00	0.00	334.00	0.02
BH975	-29.901	30.750	582.00	0.00	582.00	0.02
BH976	-30.036	30.701	481.00	0.00	481.00	0.00
BH977	-30.038	30.696	516.00	50.00	466.00	0.07
BH978	-30.040	30.678	548.00	0.00	548.00	0.02
BH979	-30.039	30.677	559.00	80.00	479.00	0.28
BH980	-29.972	30.761	332.00	0.00	332.00	0.08
BH981	-30.023	30.700	533.00	0.00	533.00	0.02
BH982	-30.027	30.684	562.00	21.00	541.00	0.14
BH983	-30.046	30.714	436.00	60.00	376.00	0.71
BH984	-30.029	30.813	200.00	12.00	188.00	0.56
BH985	-29.947	30.823	258.00	4.00	254.00	0.95
BH986	-30.019	30.660	665.00	0.00	665.00	0.04
BH987	-30.021	30.652	673.00	10.00	663.00	0.15
BH988	-30.040	30.655	616.00	19.00	597.00	0.04
BH989	-30.050	30.667	516.00	20.00	496.00	0.17
BH990	-30.019	30.682	574.00	5.30	568.70	0.10
BH991	-30.015	30.678	599.00	12.30	586.70	0.56
BH992	-30.038	30.684	554.00	49.00	505.00	0.33
BH993	-30.018	30.684	559.00	10.00	549.00	0.14
BH994	-30.038	30.625	649.00	18.00	631.00	0.22
BH995	-30.034	30.639	571.00	23.30	547.70	0.42
BH996	-30.028	30.636	604.00	20.00	584.00	0.44
BH997	-29.921	30.723	493.00	1.00	492.00	0.17
BH998	-29.923	30.708	513.00	9.40	503.60	0.22
BH999	-29.943	30.681	580.00	11.40	568.60	0.33
BH1000	-29.962	30.699	546.00	23.00	523.00	0.39
BH1001	-29.945	30.730	559.00	53.00	506.00	0.15
BH1002	-29.950	30.724	571.00	0.00	571.00	0.00
BH1003	-29.950	30.723	573.00	0.00	573.00	0.00
BH1004	-29.950	30.724	571.00	0.00	571.00	0.00
BH1005	-30.034	30.588	735.00	6.00	729.00	0.10
BH1006	-30.165	30.814	63.00	30.00	33.00	0.22
BH1007	-30.130	30.784	160.00	13.00	147.00	0.22

BH1008	-29.886	30.714	546.00	78.00	468.00	2.00
BH1009	-29.886	30.714	546.00	47.00	499.00	0.25
BH1010	-29.992	30.802	308.00	16.00	292.00	1.20
BH1011	-29.993	30.804	306.00	19.00	287.00	0.83
BH1012	-29.998	30.839	129.00	30.00	99.00	0.47
BH1013	-29.935	30.794	279.00	0.00	279.00	0.09
BH1014	-30.038	30.806	176.00	0.00	176.00	0.00
BH1015	-30.042	30.804	145.00	0.00	145.00	0.00
BH1016	-30.103	30.799	162.00	0.00	162.00	0.00
BH1017	-30.115	30.744	276.00	0.00	276.00	0.00
BH1018	-30.118	30.746	268.00	0.00	268.00	0.00
BH1019	-30.132	30.698	380.00	0.00	380.00	0.00
BH1020	-30.134	30.699	365.00	0.00	365.00	0.00
BH1021	-30.138	30.784	159.00	0.00	159.00	0.00
BH1022	-30.136	30.795	124.00	0.00	124.00	0.00
BH1023	-30.183	30.784	79.00	0.00	79.00	0.00
BH1024	-30.180	30.784	80.00	0.00	80.00	0.00
BH1025	-30.018	30.821	219.00	0.00	219.00	0.00
BH1026	-30.006	30.805	318.00	0.00	318.00	0.00
BH1027	-29.992	30.797	327.00	0.00	327.00	0.00
BH1028	-29.993	30.804	317.00	0.00	317.00	0.00
BH1029	-29.993	30.810	291.00	0.00	291.00	0.00
BH1030	-30.017	30.887	81.00	0.00	81.00	0.00
BH1031	-29.939	30.806	335.00	0.00	335.00	0.00
BH1032	-29.941	30.820	311.00	0.00	311.00	0.00
BH1033	-29.949	30.823	252.00	0.00	252.00	0.00
BH1034	-29.947	30.826	298.00	0.00	298.00	0.00
BH1035	-29.952	30.823	242.00	0.00	242.00	0.00
BH1036	-29.882	30.709	529.00	0.00	529.00	0.00
BH1037	-30.136	30.697	369.00	16.00	353.00	0.00
BH1038	-30.108	30.657	423.00	87.00	336.00	0.00
BH1039	-30.119	30.586	93.00	0.00	93.00	1.43
BH1040	-30.101	30.796	183.00	13.00	170.00	0.00
BH1041	-30.052	30.813	155.00	0.00	155.00	1.54
BH1042	-30.048	30.819	197.00	0.00	197.00	1.00
BH1043	-30.019	30.803	287.00	0.00	287.00	0.17
BH1044	-30.018	30.797	302.00	0.00	302.00	0.00
BH1045	-30.158	30.813	43.00	0.00	43.00	0.00
BH1046	-30.156	30.797	43.00	13.00	30.00	0.00
BH1047	-30.156	30.797	43.00	16.00	27.00	0.17
BH1048	-30.181	30.783	80.00	23.00	57.00	0.22
BH1049	-30.138	30.785	152.00	51.00	101.00	0.00
BH1050	-30.131	30.767	200.00	0.00	200.00	0.17
BH1051	-30.130	30.764	197.00	0.00	197.00	0.00
BH1052	-30.133	30.764	194.00	0.00	194.00	0.00
BH1053	-30.131	30.767	205.00	0.00	205.00	0.17

BH1054	-30.143	30.705	327.00	0.00	327.00	0.00
BH1055	-30.143	30.705	335.00	0.00	335.00	0.00
BH1056	-30.142	30.704	343.00	0.00	343.00	0.00
BH1057	-30.007	30.803	310.00	10.00	300.00	0.00
BH1058	-30.042	30.554	495.00	0.00	495.00	0.00
BH1059	-30.039	30.553	518.00	0.00	518.00	0.00
BH1060	-30.037	30.547	612.00	0.00	612.00	0.00
BH1061	-30.037	30.552	593.00	40.00	553.00	0.14
BH1062	-30.035	30.546	613.00	32.00	581.00	0.14
BH1063	-29.986	30.703	550.00	9.00	541.00	0.42
BH1064	-29.990	30.711	521.00	27.00	494.00	0.00
BH1065	-30.133	30.699	373.00	14.80	358.20	0.28
BH1066	-30.021	30.813	213.00	7.00	206.00	6.94
BH1067	-30.018	30.797	302.00	16.00	286.00	0.36
BH1068	-30.018	30.785	325.00	24.66	300.34	0.68
BH1069	-30.021	30.813	202.00	28.80	173.20	1.08
BH1070	-30.168	30.781	61.00	0.55	60.45	0.67
BH1071	-29.986	30.713	488.00	0.00	488.00	0.00
BH1072	-29.941	30.691	569.00	0.00	569.00	0.00
BH1073	-29.946	30.852	58.00	55.00	3.00	8.06
BH1074	-29.950	30.846	158.00	60.00	98.00	0.10
BH1075	-29.944	30.842	75.00	27.00	48.00	0.33
BH1076	-29.948	30.835	292.00	7.00	285.00	0.40
BH1077	-29.948	30.839	233.00	64.00	169.00	0.04
BH1078	-29.947	30.836	275.00	26.50	248.50	0.00
BH1079	-29.956	30.819	268.00	45.10	222.90	1.67
BH1080	-29.948	30.823	252.00	42.00	210.00	0.13
BH1081	-29.957	30.826	236.00	0.00	236.00	0.02
BH1082	-29.957	30.844	215.00	75.00	140.00	1.00
BH1083	-29.957	30.842	239.00	67.00	172.00	1.67
BH1084	-29.948	30.850	91.00	51.00	40.00	0.67
BH1085	-29.949	30.836	272.00	48.00	224.00	0.72
BH1086	-29.986	30.833	244.00	0.00	244.00	0.03
BH1087	-29.894	30.693	524.00	0.00	524.00	0.00
BH1088	-29.894	30.707	540.00	20.00	520.00	1.94
BH1089	-29.877	30.743	429.00	27.00	402.00	1.88
BH1090	-29.869	30.775	249.00	0.00	249.00	0.00
BH1091	-29.876	30.759	305.00	0.00	305.00	0.00
BH1092	-29.877	30.743	429.00	0.00	429.00	0.00
BH1093	-29.882	30.702	545.00	29.00	516.00	0.19
BH1094	-29.883	30.694	585.00	14.00	571.00	0.44
BH1095	-29.878	30.736	443.00	0.00	443.00	0.00
BH1096	-29.871	30.736	304.00	0.00	304.00	0.01
BH1097	-29.987	30.780	374.00	25.00	349.00	0.67
BH1098	-29.980	30.793	350.00	30.00	320.00	0.67
BH1099	-30.039	30.816	121.00	11.50	109.50	0.33

BH1100	-30.020	30.844	91.00	24.00	67.00	1.00
BH1101	-30.016	30.854	82.00	31.00	51.00	1.27
BH1102	-30.046	30.818	169.00	64.00	105.00	0.05
BH1103	-29.957	30.806	313.00	72.50	240.50	2.78
BH1104	-29.954	30.816	290.00	77.00	213.00	0.36
BH1105	-30.027	30.833	148.00	30.00	118.00	1.67
BH1106	-30.023	30.824	152.00	0.00	152.00	0.00
BH1107	-29.974	30.824	140.00	22.00	118.00	2.50
BH1108	-30.018	30.832	117.00	10.00	107.00	1.00
BH1109	-30.013	30.808	280.00	10.00	270.00	0.15
BH1110	-30.012	30.842	124.00	0.00	124.00	0.00
BH1111	-30.034	30.841	158.00	12.00	146.00	0.11
BH1112	-30.034	30.821	126.00	5.00	121.00	2.22
BH1113	-30.019	30.788	326.00	6.00	320.00	0.56
BH1114	-29.993	30.790	341.00	8.00	333.00	1.11
BH1115	-29.998	30.736	450.00	32.00	418.00	0.14
BH1116	-30.007	30.779	338.00	0.00	338.00	0.22
BH1117	-29.857	30.711	388.00	0.00	388.00	0.13
BH1118	-29.998	30.772	389.00	27.00	362.00	0.67
BH1119	-29.952	30.703	522.00	0.00	522.00	0.22
BH1120	-29.975	30.703	563.00	51.00	512.00	0.17
BH1121	-29.952	30.756	351.00	21.00	330.00	5.00
BH1122	-29.952	30.739	488.00	42.00	446.00	0.17
BH1123	-29.990	30.713	510.00	32.00	478.00	0.17
BH1124	-29.991	30.710	530.00	38.00	492.00	0.14
BH1125	-29.992	30.708	536.00	24.00	512.00	0.21
BH1126	-30.043	30.661	590.00	0.00	590.00	0.00
BH1127	-30.010	30.790	336.00	5.00	331.00	2.50
BH1128	-30.018	30.784	335.00	72.00	263.00	2.50
BH1129	-30.018	30.802	296.00	21.00	275.00	0.14
BH1130	-29.999	30.700	473.00	15.00	458.00	0.11
BH1131	-30.003	30.690	477.00	1.00	476.00	0.21
BH1132	-29.988	30.700	523.00	9.00	514.00	0.14
BH1133	-29.998	30.840	126.00	15.00	111.00	5.00
BH1134	-29.999	30.804	323.00	18.00	305.00	3.06
BH1135	-30.124	30.764	196.00	6.00	190.00	0.28
BH1136	-30.126	30.716	264.00	10.00	254.00	0.08
BH1137	-30.139	30.706	330.00	0.00	330.00	0.00
BH1138	-30.110	30.725	117.00	20.00	97.00	0.78
BH1139	-30.136	30.737	273.00	2.00	271.00	0.17
BH1140	-30.116	30.776	134.00	3.00	131.00	0.08
BH1141	-30.132	30.792	98.00	4.00	94.00	0.51
BH1142	-30.104	30.768	152.00	0.00	152.00	0.33
BH1143	-30.104	30.799	157.00	11.00	146.00	0.87
BH1144	-30.117	30.711	138.00	11.00	127.00	0.07
BH1145	-30.118	30.684	144.00	10.00	134.00	0.07

BH1146	-30.101	30.788	177.00	0.00	177.00	0.00
BH1147	-30.107	30.799	126.00	57.00	69.00	1.73
BH1148	-30.096	30.768	194.00	0.00	194.00	0.00
BH1149	-30.097	30.738	70.00	0.00	70.00	0.00
BH1150	-30.129	30.753	225.00	24.00	201.00	0.28
BH1151	-30.118	30.748	267.00	1.00	266.00	0.13
BH1152	-30.137	30.763	176.00	0.00	176.00	0.00
BH1153	-30.146	30.750	156.00	4.00	152.00	0.22
BH1154	-30.124	30.745	266.00	18.00	248.00	0.33
BH1155	-30.124	30.755	228.00	10.00	218.00	0.28
BH1156	-30.108	30.750	247.00	2.00	245.00	0.11
BH1157	-30.135	30.713	256.00	5.00	251.00	0.67
BH1158	-30.130	30.823	19.00	4.00	15.00	0.56
BH1159	-30.127	30.733	272.00	12.00	260.00	0.67
BH1160	-30.028	30.817	155.00	9.00	146.00	4.17
BH1161	-30.138	30.796	127.00	0.00	127.00	0.00
BH1162	-30.025	30.805	280.00	3.00	277.00	0.67
BH1163	-30.144	30.818	62.00	15.00	47.00	0.17
BH1164	-30.012	30.793	326.00	0.00	326.00	0.67
BH1165	-30.029	30.824	149.00	0.00	149.00	0.00
BH1166	-30.133	30.826	30.00	7.00	23.00	0.83
BH1167	-30.025	30.754	306.00	12.00	294.00	20.00
BH1168	-30.015	30.826	136.00	7.00	129.00	3.33
BH1169	-30.120	30.843	49.00	0.00	49.00	0.28
BH1170	-30.135	30.831	52.00	18.00	34.00	0.17
BH1171	-30.019	30.818	237.00	3.00	234.00	0.44
BH1172	-30.133	30.825	55.00	0.00	55.00	1.94
BH1173	-30.121	30.844	24.00	0.00	24.00	1.39
BH1174	-30.013	30.831	149.00	9.00	140.00	0.56
BH1175	-30.008	30.811	290.00	0.00	290.00	0.50
BH1176	-29.984	30.812	276.00	15.00	261.00	3.06
BH1177	-29.985	30.805	297.00	12.00	285.00	1.94
BH1178	-30.018	30.799	306.00	12.00	294.00	0.28
BH1179	-29.982	30.789	349.00	18.00	331.00	1.00
BH1180	-30.003	30.729	433.00	11.00	422.00	0.17
BH1181	-29.995	30.725	433.00	22.00	411.00	0.08
BH1182	-29.971	30.700	523.00	0.00	523.00	0.14
BH1183	-29.990	30.709	532.00	0.00	532.00	0.33
BH1184	-29.979	30.700	543.00	0.00	543.00	0.56
BH1185	-29.957	30.662	708.00	0.00	708.00	0.00
BH1186	-29.983	30.656	631.00	15.00	616.00	0.31
BH1187	-29.978	30.665	597.00	18.00	579.00	0.08
BH1188	-29.970	30.697	484.00	12.00	472.00	0.56
BH1189	-29.949	30.698	535.00	12.00	523.00	0.08
BH1190	-29.938	30.722	474.00	0.00	474.00	0.00
BH1191	-30.003	30.654	673.00	47.00	626.00	0.28

BH1192	-29.992	30.658	673.00	12.00	661.00	0.17
BH1193	-29.995	30.693	541.00	44.00	497.00	0.11
BH1194	-29.995	30.693	541.00	15.00	526.00	0.17
BH1195	-29.976	30.684	583.00	25.00	558.00	0.17
BH1196	-29.945	30.741	540.00	69.00	471.00	0.14
BH1197	-29.949	30.740	523.00	0.00	523.00	0.00
BH1198	-29.998	30.804	319.00	30.00	289.00	1.17
BH1199	-29.859	30.808	327.00	0.00	327.00	0.00
BH1200	-30.035	30.681	580.00	96.00	484.00	1.00
BH1201	-29.869	30.749	389.00	0.00	389.00	0.00
BH1202	-29.873	30.746	403.00	0.00	403.00	0.00
BH1203	-29.869	30.776	235.00	50.00	185.00	0.14
BH1204	-29.982	30.693	561.00	0.00	561.00	3.00
BH1205	-30.052	30.666	479.00	6.00	473.00	4.00
BH1206	-30.028	30.649	630.00	4.00	626.00	0.50
BH1207	-30.034	30.628	649.00	0.00	649.00	0.00
BH1208	-30.044	30.625	638.00	30.00	608.00	0.30
BH1209	-30.045	30.657	521.00	20.00	501.00	3.00
BH1210	-29.981	30.730	403.00	7.00	396.00	6.60
BH1211	-29.996	30.731	430.00	0.00	430.00	0.00
BH1212	-29.960	30.746	440.00	7.00	433.00	0.11
BH1213	-30.013	30.713	515.00	30.00	485.00	0.66
BH1214	-30.116	30.600	106.00	6.00	100.00	1.60
BH1215	-30.121	30.635	285.00	0.00	285.00	0.00
BH1216	-30.087	30.820	91.00	0.00	91.00	0.00
BH1217	-30.085	30.809	75.00	8.00	67.00	0.95
BH1218	-30.113	30.793	77.00	0.00	77.00	0.00
BH1219	-29.982	30.693	561.00	26.00	535.00	0.12
BH1220	-29.942	30.741	565.00	0.00	565.00	0.00
BH1221	-30.021	30.730	448.00	0.00	448.00	10.00
BH1222	-30.139	30.779	158.00	0.00	158.00	0.00
BH1223	-30.142	30.764	171.00	0.00	171.00	0.00
BH1224	-30.128	30.779	160.00	8.00	152.00	0.02
BH1225	-30.116	30.753	251.00	5.00	246.00	0.08
BH1226	-30.036	30.678	575.00	0.00	575.00	0.00
BH1227	-30.033	30.704	462.00	37.00	425.00	0.27
BH1228	-29.968	30.748	426.00	10.00	416.00	0.08
BH1229	-29.903	30.755	563.00	0.00	563.00	0.10
BH1230	-29.924	30.777	416.00	0.00	416.00	0.00
BH1231	-29.999	30.713	492.00	3.00	489.00	0.05
BH1232	-30.072	30.678	438.00	0.00	438.00	0.00
BH1233	-30.059	30.660	387.00	0.00	387.00	1.00
BH1234	-29.950	30.764	274.00	3.00	271.00	0.40
BH1235	-30.051	30.700	399.00	0.00	399.00	0.30
BH1236	-29.920	30.714	533.00	0.00	533.00	0.00
BH1237	-30.035	30.682	582.00	0.00	582.00	0.00

BH1238	-30.130	30.652	116.00	3.00	113.00	0.14
BH1239	-29.902	30.687	567.00	9.00	558.00	1.00
BH1240	-30.036	30.666	563.00	0.00	563.00	0.00
BH1241	-29.935	30.794	279.00	12.00	267.00	0.00
BH1242	-29.874	30.633	667.00	0.00	667.00	0.00
BH1243	-29.896	30.671	690.00	0.00	690.00	0.00
BH1244	-29.857	30.803	362.00	0.00	362.00	0.00
BH1245	-29.844	30.792	413.00	0.00	413.00	0.00
BH1246	-29.854	30.676	476.00	0.00	476.00	0.00
BH1247	-29.579	30.554	821.00	60.00	761.00	0.00
BH1248	-29.643	30.671	376.00	0.00	376.00	0.00
BH1249	-29.650	30.674	374.00	0.00	374.00	0.00
BH1250	-29.654	30.654	416.00	0.00	416.00	0.00
BH1251	-29.656	30.653	397.00	0.00	397.00	0.00
BH1252	-29.636	30.658	362.00	12.00	350.00	0.00
BH1253	-29.653	30.647	373.00	0.00	373.00	0.00
BH1254	-29.725	30.630	752.00	0.00	752.00	0.56
BH1255	-29.846	30.661	582.00	15.00	567.00	0.50
BH1256	-29.844	30.658	532.00	45.00	487.00	0.14
BH1257	-29.534	30.608	914.00	47.00	867.00	0.11
BH1258	-29.537	30.589	843.00	78.00	765.00	0.12
BH1259	-29.833	30.646	622.00	0.00	622.00	0.02
BH1260	-29.882	30.683	421.00	0.00	421.00	0.00
BH1261	-29.896	30.671	688.00	0.00	688.00	0.00
BH1262	-29.612	30.708	439.00	22.00	417.00	0.56
BH1263	-29.612	30.708	432.00	5.00	427.00	1.39
BH1264	-29.607	30.716	499.00	56.00	443.00	0.14
BH1265	-29.616	30.693	393.00	30.00	363.00	0.67
BH1266	-29.864	30.781	276.00	0.00	276.00	0.00
BH1267	-30.222	30.717	140.00	20.00	120.00	0.10
BH1268	-30.237	30.726	127.00	6.00	121.00	4.00
BH1269	-30.239	30.734	113.00	4.00	109.00	0.22
BH1270	-30.216	30.724	191.00	55.00	136.00	5.00
BH1271	-29.604	30.949	417.00	37.00	380.00	0.08
BH1272	-29.604	30.930	469.00	64.00	405.00	1.66
BH1273	-29.614	30.893	420.00	22.00	398.00	2.00
BH1274	-29.599	30.893	319.00	50.00	269.00	0.58
BH1275	-29.626	30.889	428.00	19.00	409.00	0.50
BH1276	-29.642	30.876	377.00	5.00	372.00	1.06
BH1277	-29.632	30.841	640.00	39.00	601.00	0.28
BH1278	-29.609	30.773	489.00	44.00	445.00	0.14
BH1279	-29.917	30.843	206.00	0.00	206.00	0.56
BH1280	-29.847	30.837	292.00	37.70	254.30	1.00
BH1281	-29.846	30.838	298.00	0.00	298.00	0.00
BH1282	-29.844	30.839	331.00	0.00	331.00	0.00
BH1283	-29.797	30.832	525.00	76.05	448.95	0.10

BH1284	-30.029	30.823	157.00	0.00	157.00	0.00
BH1285	-30.034	30.821	127.00	0.00	127.00	5.00
BH1286	-29.864	30.781	276.00	0.00	276.00	0.00
BH1287	-29.662	30.913	303.00	0.00	303.00	0.11
BH1288	-29.597	30.890	265.00	0.00	265.00	1.11
BH1289	-29.632	30.885	391.00	0.00	391.00	0.17
BH1290	-29.664	30.881	181.00	0.00	181.00	0.78
BH1291	-29.667	30.889	285.00	0.00	285.00	0.00
BH1292	-29.658	30.883	240.00	0.00	240.00	0.56
BH1293	-29.631	30.884	407.00	0.00	407.00	0.83
BH1294	-29.627	30.895	411.00	0.00	411.00	0.17
BH1295	-29.617	30.918	572.00	0.00	572.00	0.11
BH1296	-29.577	30.887	342.00	0.00	342.00	0.00
BH1297	-29.652	30.918	370.00	0.00	370.00	2.50
BH1298	-29.658	30.875	205.00	0.00	205.00	0.17
BH1299	-29.717	31.048	110.00	4.50	105.50	2.50
BH1300	-29.601	30.959	361.00	0.00	361.00	0.42
BH1301	-29.604	30.942	411.00	0.00	411.00	0.00
BH1302	-29.609	30.909	371.00	0.00	371.00	0.00
BH1303	-29.616	30.915	565.00	0.00	565.00	0.00
BH1304	-29.731	31.072	118.00	0.00	118.00	0.00
BH1305	-29.686	30.931	300.00	0.00	300.00	0.40
BH1306	-29.686	30.931	300.00	0.00	300.00	0.00
BH1307	-29.686	30.927	291.00	24.30	266.70	0.30
BH1308	-29.686	30.927	266.00	0.00	266.00	0.00
BH1309	-29.687	30.928	266.00	0.00	266.00	6.00
BH1310	-29.687	30.928	266.00	0.00	266.00	0.00
BH1311	-29.830	30.978	148.00	16.05	131.95	4.50
BH1312	-30.106	30.621	257.00	32.00	225.00	0.08
BH1313	-30.107	30.617	219.00	0.00	219.00	0.00
BH1314	-29.849	30.839	269.00	0.67	268.33	0.50
BH1315	-29.846	30.843	322.00	0.00	322.00	0.00
BH1316	-29.592	30.894	265.00	0.00	265.00	0.46
BH1317	-29.649	30.953	317.00	0.00	317.00	1.33
BH1318	-29.644	30.794	186.00	0.00	186.00	0.28
BH1319	-29.664	30.819	170.00	0.00	170.00	0.67
BH1320	-29.598	30.888	281.00	0.00	281.00	0.25
BH1321	-29.596	31.058	86.00	0.00	86.00	0.25
BH1322	-29.546	31.083	91.00	0.00	91.00	0.33
BH1323	-29.604	30.930	469.00	0.00	469.00	1.66
BH1324	-29.598	30.773	433.00	0.00	433.00	0.00
BH1325	-29.643	30.904	344.00	0.00	344.00	0.00
BH1326	-30.025	30.821	160.00	0.00	160.00	20.00
BH1327	-29.872	30.759	286.00	0.00	286.00	2.00
BH1328	-29.950	30.719	593.00	0.00	593.00	0.00
BH1329	-30.109	30.821	24.00	0.00	24.00	0.14

BH1330	-30.114	30.815	73.00	0.00	73.00	6.60
BH1331	-30.109	30.813	93.00	22.70	70.30	0.34
BH1332	-30.115	30.809	96.00	28.00	68.00	0.33
BH1333	-30.113	30.813	76.00	0.00	76.00	0.21
BH1334	-30.108	30.814	105.00	0.00	105.00	0.00
BH1335	-29.693	30.632	803.00	0.00	803.00	0.40
BH1336	-29.701	30.621	810.00	0.00	810.00	10.55
BH1337	-29.692	30.623	801.00	0.00	801.00	5.00
BH1338	-29.706	30.628	811.00	0.00	811.00	0.00
BH1339	-30.084	30.718	323.00	0.00	323.00	0.14
BH1340	-30.081	30.679	299.00	0.00	299.00	0.14
BH1341	-30.115	30.715	171.00	0.00	171.00	0.27
BH1342	-30.084	30.719	323.00	47.35	275.65	0.08
BH1343	-29.943	30.738	572.00	0.00	572.00	0.00
BH1344	-29.626	30.983	197.00	0.00	197.00	0.00
BH1345	-29.626	30.983	197.00	3.05	193.95	0.00
BH1346	-29.626	30.983	197.00	1.59	195.41	0.00
BH1347	-29.626	30.983	197.00	10.14	186.86	0.24
BH1348	-29.625	30.988	232.00	59.23	172.77	0.07
BH1349	-29.623	30.983	182.00	17.26	164.74	1.66
BH1350	-29.628	30.980	220.00	0.00	220.00	3.30
BH1351	-29.632	30.979	249.00	34.15	214.85	11.76
BH1352	-29.626	30.976	277.00	62.73	214.27	1.50
BH1353	-29.553	31.049	184.00	0.00	184.00	0.00
BH1354	-29.564	31.050	190.00	53.37	136.63	0.00
BH1355	-29.556	31.044	199.00	5.10	193.90	0.40
BH1356	-29.564	31.036	141.00	8.41	132.59	1.60
BH1357	-29.997	30.944	48.00	0.00	48.00	3.00
BH1358	-29.711	30.890	305.00	85.94	219.06	0.26
BH1359	-29.705	30.886	349.00	0.00	349.00	0.00
BH1360	-29.817	30.755	583.00	0.00	583.00	10.00
BH1361	-29.813	30.750	578.00	0.00	578.00	1.33
BH1362	-29.817	30.755	583.00	0.00	583.00	13.33
BH1363	-29.774	30.975	44.00	0.00	44.00	0.17
BH1364	-30.110	30.821	24.00	68.50	-44.50	1.33
BH1365	-29.838	30.752	421.00	3.34	417.66	0.28
BH1366	-29.834	30.751	452.00	1.67	450.33	0.00
BH1367	-29.843	30.758	421.00	105.42	315.58	0.00
BH1368	-29.836	30.759	349.00	2.05	346.95	2.80
BH1369	-29.848	30.836	292.00	17.14	274.86	0.60
BH1370	-29.849	30.839	269.00	0.00	269.00	0.10
BH1371	-29.726	31.051	99.00	0.00	99.00	0.64
BH1372	-29.615	30.914	562.00	0.00	562.00	0.00
BH1373	-29.594	30.901	235.00	5.15	229.85	0.95
BH1374	-29.626	30.889	428.00	0.00	428.00	0.39
BH1375	-29.629	30.845	657.00	0.00	657.00	0.00

BH1376	-29.604	30.746	213.00	7.45	205.55	1.33
BH1377	-29.662	30.698	348.00	0.00	348.00	0.00
BH1378	-29.727	31.052	108.00	15.06	92.94	0.83
BH1379	-29.623	31.133	94.00	0.00	94.00	0.00
BH1380	-29.623	31.133	94.00	0.00	94.00	0.00
BH1381	-29.727	30.584	753.00	0.00	753.00	0.00
BH1382	-29.727	30.584	753.00	0.00	753.00	0.00
BH1383	-29.729	30.583	740.00	0.00	740.00	0.00
BH1384	-29.729	30.583	740.00	0.00	740.00	0.00
BH1385	-29.720	31.090	20.00	6.40	13.60	0.97
BH1386	-29.992	30.939	7.00	0.00	7.00	0.00
BH1387	-29.909	30.986	10.00	0.00	10.00	0.00
BH1388	-29.833	30.898	307.00	0.00	307.00	0.00
BH1389	-29.826	30.890	375.00	0.00	375.00	0.00
BH1390	-29.590	31.154	60.00	2.01	57.99	0.58
BH1391	-29.590	30.985	150.00	30.00	120.00	4.20
BH1392	-30.120	30.744	291.00	0.00	291.00	0.07
BH1393	-30.119	30.744	288.00	22.80	265.20	0.31
BH1394	-30.102	30.798	160.00	13.00	147.00	0.88
BH1395	-29.849	31.009	17.00	0.00	17.00	1.39
BH1396	-29.738	30.645	684.00	13.37	670.63	1.28
BH1397	-30.130	30.642	155.00	0.00	155.00	0.00
BH1398	-30.129	30.641	159.00	0.00	159.00	0.00
BH1399	-29.728	31.087	18.00	8.10	9.90	0.56
BH1400	-29.691	30.752	602.00	5.44	596.56	0.55
BH1401	-29.692	30.756	636.00	1.43	634.57	0.27
BH1402	-29.714	30.736	581.00	6.00	575.00	0.22
BH1403	-29.705	30.754	646.00	19.00	627.00	0.56
BH1404	-29.727	30.737	586.00	20.58	565.42	0.17
BH1405	-29.743	30.733	590.00	0.00	590.00	0.14
BH1406	-29.899	30.665	677.00	95.90	581.10	0.56
BH1407	-29.895	30.680	365.00	0.00	365.00	0.14
BH1408	-29.895	30.671	687.00	0.00	687.00	0.14
BH1409	-29.768	30.887	385.00	69.60	315.40	0.17
BH1410	-29.775	30.749	651.00	33.48	617.52	0.33
BH1411	-29.885	30.708	552.00	39.80	512.20	0.00
BH1412	-29.649	30.740	198.00	9.65	188.35	0.17
BH1413	-29.646	30.744	186.00	9.22	176.78	0.28
BH1414	-29.634	30.747	194.00	0.00	194.00	0.11
BH1415	-29.936	30.910	102.00	45.06	56.94	0.17
BH1416	-29.940	30.908	79.00	26.77	52.23	2.85
BH1417	-29.942	30.908	72.00	0.00	72.00	0.00
BH1418	-29.862	30.886	242.00	7.86	234.14	1.39
BH1419	-29.936	30.873	115.00	38.56	76.44	0.28
BH1420	-29.824	31.030	10.00	0.00	10.00	0.00
BH1421	-29.777	30.810	582.00	0.00	582.00	0.00

BH1422	-29.951	30.774	370.00	0.00	370.00	0.00
BH1423	-29.950	30.774	355.00	90.00	265.00	0.03
BH1424	-29.940	30.695	591.00	20.16	570.84	0.00
BH1425	-29.948	30.766	316.00	24.15	291.85	0.06
BH1426	-30.256	30.768	13.00	2.62	10.38	6.67
BH1427	-29.923	30.988	19.00	2.11	16.89	1.39
BH1428	-29.956	30.946	13.00	3.23	9.77	0.69
BH1429	-29.743	31.078	18.00	7.12	10.88	2.86
BH1430	-29.924	30.969	44.00	20.84	23.16	0.00
BH1431	-29.952	30.979	15.00	10.35	4.65	0.00
BH1432	-29.954	30.980	12.00	9.68	2.32	0.00
BH1433	-29.951	30.981	19.00	8.40	10.60	0.00